

LOMBARD C

FURTHER REFINEMENTS AND A NEW EFFICIENT SOLUTION  
OF A NOVEL MODEL FOR PREDICTING INDOOR CLIMATE

MIng

UP

1990

FURTHER REFINEMENTS AND A NEW  
EFFICIENT SOLUTION OF A NOVEL MODEL  
FOR PREDICTING INDOOR CLIMATE

Presented by:

CHRISTOFFEL LOMBARD

In Partial Fulfillment of the Requirements for the Degree:

Master of Engineering

In

The Faculty of Engineering

Department of Mechanical Engineering

of the

UNIVERSITY OF PRETORIA

Promotors:

Prof. E.H. Mathews

Dr. J.D. Wentzel

December 1990

## ABSTRACT

In the first two chapters of this thesis, the novel method, developed by Mathews and Richards<sup>1</sup>, for predicting the thermal performance of buildings is introduced. The further enhancement and theoretical clarification of this method is the objective of this thesis. The method is based on a very simple thermo-flow network which models only the most important aspects of heat-flow in buildings. While Mathews and Richards based their network on analysis of the primary aspects of heat-flow in buildings, this thesis derives the simplified model by reduction from a comprehensive model. In this way, the assumptions and limitations is illuminated and the theoretical foundation of the method can be established. As a result of the investigation, a new simplified model with certain theoretical benefits is suggested. In later chapters, the method is extended and refined. Also, a new calculation procedure for finding solutions of the model is presented. In particular the method is extended to include multi-zone heat-flow, structural storage- and variable thermal systems. The new solution method is powerful, simple and efficient. This thesis contributes to the establishment of a viable tool for thermal analysis of buildings.

---

<sup>1</sup>See reference [10] on page 13.

## ACKNOWLEDGEMENTS

The author is indebted to Prof. E.H. Mathews who instigated, guided and encouraged this study.

The author gratefully acknowledges the financial contribution from the National Energy Council which made this study possible. The following bodies have also contributed to the Thermal Performance of Buildings project: Department of Public Works and Land Affairs, Department of Finance, Laboratory for Advanced Engineering, University of Pretoria.

The Division for Building Technology at the Council for Scientific and Industrial Research generously made their test facilities available.

The author wishes to express his gratitude to Mr. P G Richards and many other colleagues for many fruitful discussions. It is our hope that this study will be of benefit to all.

## TABLE OF CONTENTS

Abstract.....	i
Acknowledgements.....	ii
Table of Contents.....	iii
Summary of the Chapters.....	xi
Notation, Abbreviations and Nomenclature.....	xiv
Main Contents	
<hr/>	
1 INTRODUCTION: BUILDING THERMAL ANALYSIS.....	1
1.1 Historical Perspective.....	2
1.2 A Design Tool for Building Thermal Analysis.....	3
1.3 The Objectives and Scope of this Study.....	7
1.4 The Contributions of this Study.....	8
1.5 The Contents of this Thesis.....	11
References Chapter 1.....	13
<hr/>	
2 A NEW THEORETICAL FOUNDATION FOR THE THERMAL ANALYSIS METHOD OF MATHEWS AND RICHARDS.....	15
2.1 Background and Objective of this Chapter.....	15
2.1.1 The Variety of Available Methods for Building Thermal Analysis.....	15

2.1.2	The Objective of this Chapter.....	22
2.2	The Method of Mathews and Richards.....	23
2.3	Assumptions, Limitations and Possible Extensions of the Method.....	24
2.4	A More Comprehensive Theoretical Model.....	26
2.4.1	The Building Shell.....	27
2.4.2	The Floor.....	30
2.4.3	Heat Exchange Between Internal Surfaces..	30
	a) Radiative Exchange.....	31
	b) Convective Exchange.....	33
	c) Combined Film Coefficient for Interior Surfaces.....	34
2.4.4	The Forcing Functions.....	40
	a) External Surfaces.....	40
	b) Ventilation.....	42
	c) Internal Loads.....	44
2.4.5	A Comprehensive Model.....	44
2.4.6	Solution of the Comprehensive Model.....	46
2.5	Derivation of the Model of Mathews and Richards from the Comprehensive Model.....	47
2.5.1	Single Zone Approximation.....	47
2.5.2	The Assumption of Isothermal Mass.....	49
2.5.3	Lumping the Distributed Parameter Structures.....	56

a)	Lumping for Walls with Small Biot Numbers.....	58
b)	Exact Solution of the Heat Conduction Equation with Matrices.....	62
c)	Theoretical Values for the Lumped Elements.....	66
d)	Laminated Structures.....	73
e)	Combining the Surfaces.....	81
f)	Lumping of Interior Mass.....	87
2.5.4	The Definition of the Mean Sol–Air Temperature.....	90
2.5.5	Interior Heat Transfer.....	94
2.6	A Refined Simple Model.....	102
2.7	Conclusion, Chapter 2.....	104
References	Chapter 2.....	107
Symbols	Chapter 2.....	110
Appendices	Chapter 2	
2A	– Table: Accuracy of Lumping for Walls	
2B	– Table: Fourier Moduli for Layers	
2C	– Detailed Results for Office	

3	EXTENSION OF THE MODEL TO INCLUDE A FORCING FUNCTION FOR STRUCTURAL STORAGE.....	113
3.1	Introduction.....	113

3.2	The Principles of Structural Storage.....	116
3.3	The Equivalent Electrical Circuit with Structural Storage.....	121
3.3.1	The Definition of the Heat Transfer Coefficient.....	121
3.3.2	Incorporating Structural Storage in the Method.....	123
3.4	Implementation.....	124
3.4.1	The Daily Cycle.....	125
3.4.2	Verification of Software Implementation..	126
3.4.3	Measured Heat Transfer Coefficient in a Test Hut.....	128
3.5	Some Typical Results.....	128
3.5.1	Massive Structure.....	129
3.5.2	Lightweight Structure.....	132
3.6	Conclusion, Chapter 3.....	132
	References Chapter 3.....	134
	Symbols Chapter 3.....	135
<hr/>		
4	INTER-ZONE HEAT FLOW.....	136
4.1	Background and Objective of this Chapter.....	136
4.2	Multi-Zone Extension.....	138
4.3	Solution of the Multi-Zone Network.....	142

4.3.1	The Zone Circuit Operators and Thevenin Sources.....	144
4.3.2	The Partition Circuit Operators.....	147
4.3.3	Solution.....	150
	a) Finding the Admittance Matrix.....	150
	b) Calculating Interior Temperature.....	151
	c) Calculating Heat Load.....	152
4.4	Computer Implementation.....	153
	4.4.1 Time invariant system.....	153
	4.4.2 Time variant system.....	154
4.5	Verification of the New Inter-Zone Heat-Flow Method.....	156
	4.5.1 Experimental Results.....	156
	4.5.2 Application of Multi-Zone Procedure to Experimental Model.....	157
4.7	Conclusion, Chapter 4.....	161
	References Chapter 4.....	163
	Symbols Chapter 4.....	164
Appendices Chapter 4		
	4A - Derivation of the Impedance Operator	
	4B - Demonstration of the Multi-Zone Solution Procedure	
	4C - Estimation of Interior Surface Coefficient	
	4D - Multi-Zone Verification Calculation	

---

5 SOLUTION OF THE THERMAL NETWORK WITH TIME DEPENDENT	
PARAMETERS.....	166
5.1 Introduction, Solution of the Model with Constant	
Parameters: A Systems Approach.....	168
5.1.1 Solution for Calculating Indoor	
Temperature.....	169
5.1.2 Load Calculation.....	171
5.1.3 The Governing Equation.....	173
5.1.4 Proportionally Controlled Active Systems.	176
5.2 Variable Network.....	177
5.2.1 Indoor Temperature.....	179
5.2.2 System Load.....	180
5.2.3 The General First Order Differential	
Equation.....	181
5.3 Methods for Solving the Variable Parameter	
System.....	185
5.3.1 Solutions for Periodic Coefficients.....	186
a) Constant segments.....	187
b) Sinusoidal Variations of the Coefficient.	188
5.3.2 Solution of the Volterra Integral	
Equation.....	190
5.3.3 The Substitution Theorem.....	192
5.3.4 A Recursive Solution.....	193

5.3.5	Fourier Methods and The Modulation	
	Function Equation.....	195
a)	Phasor Representation of Sinusoidal	
	Signals.....	195
b)	Expansions for the Transfer Function.....	197
c)	Separate Treatment of Mean- and Swing	
	Components.....	201
5.4	A New Efficient Numerical Algorithm.....	204
a)	A First Difference Equation.....	205
b)	A Closed Form Solution for the Initial	
	Value.....	206
c)	Stability.....	207
d)	Accuracy of the Method.....	208
e)	More Accurate Algorithms.....	212
f)	Extension to Higher Order Systems.....	213
g)	Implementation.....	213
h)	Verification Measurements.....	214
5.7	Conclusion, Chapter 5.....	216
	References Chapter 5.....	218
	Symbols Chapter 5.....	220
	Appendices Chapter 5	
	5A – Evaluation of Numerical Solution	

---

6 CLOSURE.....	222
6.1 The Theoretical Underpinnings of the Method of Mathews and Richards.....	222
6.2 Structural Storage.....	224
6.3 Multi-Zone Thermo-Flow.....	224
6.4 Numerical Solution of a System with Time Dependent Parameters.....	224
6.5 Suggestions for the Future.....	225
6.6 The Utility of Highly Simplified Models.....	227
References Chapter 6.....	228

---

Appendix A – Synopses

Appendix B – Papers to which this study contributed.

C. Lombard, E.H. Mathews – Efficient Steady State Solution of a Time Variable RC Network, for Building Thermal Analysis.

E.H. Mathews, P.G. Rousseau, P.G. Richards, C. Lombard – A Procedure to Estimate the Effective Heat Storage Capability of a Building.

## SUMMARY of the CHAPTERS

In the **first chapter** of this thesis an overview of the current status and future prospects of building thermal analysis is given. Within this perspective; the objectives, scope and contributions of this study is presented.

In the **second chapter**, the origins of the method of building thermal analysis of Mathews and Richards, it's current status and future prospects are discussed, with emphasis on the basic assumptions on which the method is based. The simplified mathematical model of heat flow in buildings, which forms the foundation, is derived from a more comprehensive theory. The original derivation of the method by Mathews and his co-workers was based on apt reasoning about the critical aspects of heat-flow in buildings. It was not derived from first principles. In this thesis, it is attempted to derive this model by reduction from a more extensive and refined model. A relatively simple structure is used in the discussion, in an attempt to reduce the many complications of building thermo-flow to the essentials. The most important aspect of this discussion is the modelling of the storage effect of the massive structures of the building, since this aspect was previously most heavily based on empirical considerations. The validity of the various simplifying assumptions are investigated. Some possible refinements of the model are also pointed out.

In **chapter three**, the model is extended to include structural storage. The practical application of structural storage systems in buildings is first briefly touched. It is shown that the usual definition of the convective coefficient, for heat transfer from and to flat surfaces, can not be applied since the thermal model of Mathews and Richards makes no provision for surface temperatures. This problem is easily circumvented by defining the

convective coefficient with respect to the bulk wall temperature. With this definition of the heat transfer coefficient the inclusion of structural storage in the model is straightforward. This chapter concludes with a demonstration of the viability of structural cooling in two actual buildings, an office block and a shop.

In **chapter four**, a new method for extending the thermal model to cater for inter-zone heat flow is proposed. The main idea is to first obtain the thermal response of each individual zone, under the assumption that partitions between zones are adiabatic. This can be done with the present method of analysis without any alterations. In a second phase of the calculation, the various zones are combined, the actual heat flow between zones are determined and the final temperatures or loads in each zone are evaluated. This procedure forms a very natural extension of the present single zone method. It can be easily implemented in the case of time-invariant thermo-systems, but it requires the inversion of a complex matrix, the size of which is given by the number of zones. The method is verified by comparing measured temperatures in a two-zone experimental setup with predicted values.

In the introductory sections of **chapter five**, the solution of the thermal network for buildings is discussed from a systems point of view. In particular, it is shown that the various forcing functions can be effectively combined into one. This leads to considerable simplification in the solution of the network and facilitates easy introduction of new forcing functions. In this chapter, a new method of solution for the equivalent thermal network is given. This new method extends the applicability of the model to time variable ventilation of buildings, time variable shell conductance etc. The new calculation method is very efficient and simple. It is based on a first order numerical algorithm but it can be easily extended to higher order numerical methods. The periodicity of the parameters and forcing functions are exploited to derive a closed form solution for the initial value, so that the lengthy period of integration, which is usually

required to get rid of initial transients, is circumvented. In addition to the numerical method, various other methods for solving the time variable network are discussed. In particular, Fourier methods are also treated in some depth and an alternative method, based on Fourier series expansions, is discussed.

The last chapter, **chapter six**, concludes by summarizing the main results–, suggestions for the future–, and utility of this thesis.

## NOTATION, ABBREVIATIONS and NOMENCLATURE

### Notation

Generally, the following conventions are adhered to, although exceptions exist:

- (...) equation numbers
- [...] references (given at the end of each chapter), or units in SI system

A decimal point is used and not a comma.

Variables are written in *italics*.

**Boldface** symbols indicate a vector or a matrix.

Operators are written in *script* font.

### Often used symbols [SI units]

- $C$  Thermal capacitance [kJ/K]
- $H$  System transfer function.
- $h$  Heat transfer coefficients in [W/m<sup>2</sup>·K].
- $q$  Heat flow in [W], sometimes per unit area [W/m<sup>2</sup>].
- $Q$  Building loads in [W].
- $R$  Thermal resistance [K/W].
- $T$  Usually temperature [°C], sometimes the period of a periodic function [h].
- $t$  Time [h].
- $x$  A spatial dimension [m], or system input function.
- $y$  System output function.

A list of symbols is provided at the end of each chapter.

### Abbreviations

- ASHRAE American Society of Heating, Refrigerating and Air-Conditioning Engineers.
- CENT Centre for Experimental and Numerical Thermo-Flow.
- CIBS Chartered Institute Building Services.

CSIR	Council for Scientific and Industrial Research.
HVAC	Heating Ventilating and Air-Conditioning.
LGI	Laboratory for Advanced Engineering.
RC	Resistor-Capacitor lumped model.
RCR	Lumped section consisting of 2 resistors and a capacitor as in figure 2.14 page 67, also called T-section.
TTC	Thermal Time-Constant.
TTTCB	Total Thermal Time-Constant.
UP	University of Pretoria.

### **Nomenclature**

cascade matrix	A two-port (see below) model as in figure 2.12 page 64. Also called a cascade matrix.
load	Heating or cooling load to be supplied by a thermal control system, e.g. air-conditioning cooling load.
model of Mathews and Richards	Refers to the model presented by Mathews and Richards in reference [10] of chapter 2.
network	A graphic model of thermo-flow in buildings (thermal network), usually in terms of thermal resistances and capacitances.
shell	The structural part of a building which separates interior and exterior.
thermal response	The temperature in a building and heat flow into-and out of a building.
transmission matrix	See 'cascade matrix' above.
T-section	See 'RCR' above, also RCR T-sections, RCR-section etc.
two-port	A black box model of a particular structure with two boundaries or ports, e.g. a wall where the two flat surfaces form the boundaries. A two-port model

usually employs a 2x2 matrix as a mathematical model of the structure.

partition Refers to a partition between two thermal zones in a building, as opposed to a wall which divides interior and exterior.

zone A region in building which is thermally well connected so that the temperature in the region will always be uniform.

## INTRODUCTION: BUILDING THERMAL ANALYSIS

# CHAPTER 1

---

## 1 INTRODUCTION: BUILDING THERMAL ANALYSIS

Despite the fact that buildings are, in the first instance, erected to provide shelter and comfort from the outdoor climate, many designers of new buildings are often predominantly interested in the aesthetic and functional aspects of the building. The indoor environment is relegated to the consulting engineer who, supposedly, will contrive whatever is required to establish and maintain an acceptable level of indoor comfort. However, the design of the facade of the building, to a large extent, determines the economics of the air-conditioning system, which forms a significant part of both the building construction and operating cost. According to Bevington and Rosenfeld [1] the fragmentation of the building industry is a serious impediment to greater efficiency: "A commercial building project, for example, typically involves a series of handoffs: an architect designs the building but then hands it over to the engineer, who in turn specifies materials, systems and components, before passing the responsibility to a contractor. Eventually the finished building is turned over to a maintenance and operations staff, who had virtually no say in the design process but probably know most about the buildings day-to-day performance." If the thermal characteristics of the building are not given sufficient attention during the whole design process and, especially, at the very early design stages, it leads to the erection of thermally inefficient buildings. In South Africa and other countries a significant fraction of the total energy consumption is wasted on the maintenance of a comfortable indoor climate, in thermally inefficient buildings [2].

According to Carroll [2] energy consumption in buildings account for 23% of the total primary energy usage in South Africa. While this figure is reasonably low when compared to other countries – probably because of our moderate climate – it still represents a substantial national expenditure. In a recent American article it is predicted that the efficiency of buildings could double by the year 2010 [2]. German measurements in a

## INTRODUCTION: BUILDING THERMAL ANALYSIS

number of energy efficient houses suggest that as much as 40% reduction in heating energy requirements can be realized [3]. Some researchers even suggest that savings as high as 75% in new buildings and 50% in existing buildings are possible [1]. Local studies [4,5] indicate, that in the moderate South African climate, it is often feasible to provide acceptable indoor comfort without any mechanical refrigeration at all, provided sufficient care is taken with the thermal design of the envelope. In [2] it is claimed that by clever exploitation of the the capacity of buildings to store heat in massive structures, air-conditioning costs can be reduced by from 30 to 70 percent.

### 1.1 Historical Perspective

In the first six decades of this century, energy costs were insignificant and played virtually no role in the design of buildings and air-conditioning systems. With the oil-crisis in the seventies, and the subsequent escalations in the cost of energy, a very heavy emphasis was placed on energy efficiency measures. This emphasis on reducing energy consumption sometimes lead to the installation of inadequate conditioning systems. According to Sun [6] many buildings erected in the seventies and eighties were equipped with under-designed air-conditioning systems which have resulted in many complaints and the prevalent investigations in the literature of the so-called *sick building syndrome*. Thornley [7] states: "Of course the HVAC industry isn't blameless either; often we haven't understood the complicated interaction of system performance. Often our very resolve to save space, to save energy, and to save cost, has resulted in systems which fail to satisfy."

The continuing increase in the cost of energy will doubtless increase the pressure on the building industry to design energy efficient buildings. Thornley [7]: "The catch 'Can we afford to save energy?' has a peculiar connotation for air conditioned buildings, for although the cost of energy in recent years has outstripped the general rate of inflation, the cost of operating an air conditioning installation can still be a small proportion of

## INTRODUCTION: BUILDING THERMAL ANALYSIS

the total owning and operating cost of the building. It is therefore still argued that there is little inducement to refine designs and install additional energy saving equipment. I prefer the contrary argument that energy saved is money saved, although I recognize that we cannot rely wholly upon conscience and that some form of cost effectiveness must prevail." A new approach in building design is called for. Building and air-conditioning system must be designed together, as a complete indoor climate conditioning unit. Increasing the efficiency of buildings requires extensive co-operation between architect, engineer and developer. The air-conditioning system and passive thermal response of the building must match the local climate to ensure adequate comfort. The architect must carefully consider the thermal implications of his design, the engineer must optimize the design of the air-conditioning system but without sacrificing comfort. Building developers and owners must be provided with the means to enforce comfort prescriptions. Thornley [7] states the situation in the United Kingdom: "A great deal has been said and written in the last quarter-century on multidisciplinary co-ordination and the integration of buildings and their services; this is never more important than when a building is to be air-conditioned. While much has been achieved in this area, honestly successful solutions will depend on an even finer understanding between building owners, architects, and engineers than seems to exist at this time."

### 1.2 A Design Tool for Building Thermal Performance

It is clear that in future the thermal aspects of a particular design should be high on the priority list of designers of new buildings. To aid them, A friendly and easy to use computer program is required which will facilitate evaluation of the thermal response of a building, without the need for detailed technical knowledge of thermo-flow. The program must cater for analysis of the passive response of the building, the air-conditioning system, comfort criteria and total design evaluation. Such a program, commercially known as QUICK, was developed by the Centre for Experimental and Numerical Thermo-flow (CENT) at the Department of

## INTRODUCTION: BUILDING THERMAL ANALYSIS

Mechanical Engineering, University of Pretoria, under the leadership of Prof. E.H. Mathews. The project received support from the Department of Public Works and Land Affairs, Department of Finance, Laboratory for Advanced Engineering, University of Pretoria as well as the National Energy Council. Although this program was developed for South African conditions, it also generated a fair amount of overseas interest and won a prize at the International Congress on Building Energy Management (ICBM) at Laussane Switzerland in 1987 [8].

The program was designed to run on an inexpensive personal computer and to facilitate rapid and accurate evaluation of building thermal characteristics at sketch design stage. The user interface is extremely friendly, consisting of a pull down menu structure with many help screens, while a database of building materials is available on-line. The program, which has now gone through it's third revision, succeeds admirably in relieving all the tedium of performing a thermal analysis and is suitable for use both by engineers and architects. It provides for the determination of the passive response of a building i.e. interior temperature as well as load estimation. In the latest version it is also possible to obtain comfort criteria [9].

The thermal model on which the program is based was developed by Mathews and co-workers [10,11] with the philosophy that a design tool should place greater emphasis on ease of use than absolute accuracy and detailed thermal modelling. The program is capable of predicting the hourly indoor temperature as well as the energy load required to maintain a comfortable indoor climate; for given meteorological conditions. The method caters for multi-layered constructions, shaded windows and solar penetration, interior heat generation and extraction and natural and mechanical ventilation [9].

However, like all other thermal prediction programs, the method also has limitations [10]. It is a highly simplified method which essentially estimates

## INTRODUCTION: BUILDING THERMAL ANALYSIS

the heat conductance of the building shell and the total amount of stored heat in the massive structures. Since these limitations are the main topics of this thesis we state them explicitly:

- a) The most important limitation, from a theoretical point of view, is probably the restriction to single zones. This means the program can not handle heat flow between adjacent rooms at different interior temperatures. This assumption implies that all internal zones in a buildings are assumed to be at more or less the same temperature, or alternatively, that the partitions between zones do not allow heat transfer between the zones. This limitation is in practice seldom a big constraint. Conditioned buildings normally have all zones controlled at nearly the same temperature, and in passive buildings it is the heat flow through the shell which is the most important.
- b) It is also assumed that the thermal response of the building can be characterized with a single pole thermo-flow network. This approach employs a single heat storage capacitor to account for all the storage in the massive elements of the building. The method leads to a highly simplified model which is easily understood and can be solved quickly. It's use is justified by the very reasonable comparison of the predictions with measured results [10]. Obviously, with such a simplified method, the accuracy depends largely on the methodology for estimating the *active thermal capacitance of the building*, or rather, the instantaneous quantity of stored heat.
- c) Another assumption is that the interior air is well mixed and at a uniform temperature. Also the interior surfaces of the walls are assumed to be at the same temperature; so that radiative exchange between the walls can be ignored. This last assumption is closely coupled to the previous assumption of well mixed interior air. When the indoor air is agitated, temperature differences between the surfaces of the walls are reduced by convection as well as radiation.

## INTRODUCTION: BUILDING THERMAL ANALYSIS

Note that the assumption is not that radiation plays no part, rather, it is assumed that interior conditions are such that radiation and convective heat transfer are highly efficient in reducing temperature differences between interior surfaces.

- d) A further limitation is the restriction to fixed ventilation rates. In many naturally ventilated buildings the ventilation rate varies considerably due to diurnal and seasonal wind patterns. In buildings with mechanical ventilation, the ventilation rates may also vary: a high ventilation rate may be used during the night to cool the building in summer and a low ventilation rate during the day for comfort. This restriction to constant ventilation rates is different to the other limitations, in that it is not an inherent limitation of the mathematical model of the thermo-flow, but is simply an assumption to expedite the numerical solution of the model. In the second part of this thesis a method is described whereby this restriction is circumvented with no sacrifice in computation speed.

The indoor temperature prediction of the method was extensively evaluated by Mathews and Richards [10] by comparing predicted indoor temperatures with measured temperatures in more than 60 existing buildings of various types. These included office blocks, shops, schools, residential buildings, town houses, medium and high mass experimental buildings, low mass well insulated structures with ground contact such as factories and low mass poorly insulated structures e.g. agricultural buildings. For details of the validation see [10]. The accuracy proved to be satisfactory for the stated objective, i.e. to be a thermal analysis tool at sketch design stage of buildings, when many of the details are still unavailable and rapid results and ease of use, rather than absolute accuracy, is important. The program was also instrumental in establishing thermal design norms for the Department of Finance [12].

## INTRODUCTION: BUILDING THERMAL ANALYSIS

One of the objectives of this thesis is to determine the theoretical validity of the method from first principles. In chapter 2 the method of Mathews and Richards [10] is thoroughly investigated from a theoretical point of view. It is shown that the simple thermo-flow network they use (see figure 2.1) can be approximately derived from a more comprehensive model, by appropriate assumptions and reductions. From this analysis, a discussion of the theoretical validity of the original assumptions of Mathews and Richards<sup>1</sup> is possible. In the process, a somewhat more refined model, which incorporates the basic simplicity of the original model but which is more attractive from a theoretical point of view, is also presented. In later chapters some possible extensions of the method are investigated, and a new method of solution, which incorporates time variable parameters, is given.

### 1.3 The Objectives and Scope of this Study

The objective of this study is fourfold:

- A To investigate the theoretical underpinnings of the method of Mathews and Richards with emphasis on the active thermal storage capacitance of buildings.
- B To extend the method to buildings incorporating structural storage systems.
- C To extend the model to also cater for inter-zone heat flow in a convenient manner.
- D To obtain an efficient solution for the model when the parameters are time variable.

It is not in the scope of this study to substitute for the method of Mathews and Richards, a new method, although a new method with certain advantages is presented in chapter 2. A substitute method will require

---

<sup>1</sup>We shall from now on frequently refer to the method of [10] and [11] as the method of Mathews and Richards without further reference.

## INTRODUCTION: BUILDING THERMAL ANALYSIS

implementation in a computer program and extensive validation studies; tasks which were not attempted. We are also not so much concerned with the accuracy of the method *per se* as with the assumptions which are required by the method. This study is mainly concerned with theoretical considerations, and the implementation of solutions.

### 1.4 The Contributions of this Study

This study contributed to building thermo-flow research the following original results:

It is shown that the method of Mathews and Richards can indeed be derived from first principles with certain assumptions. The nature of these assumptions are illuminated and their validity is discussed. In particular, it is shown that the basic assumption required to derive the model of Mathews and Richards is; that the bulk temperatures of all the massive elements of the zone must be approximately equal. This is a more accurate formulation of the basic assumption, it replaces the assumption of equal interior surface temperatures as given by Mathews and Richards.

The simplification of interior thermo-flow networks is discussed in some depth. It is indicated that various assumptions about interior temperatures will lead to different definitions of interior surface heat transfer coefficients. Although effective film-coefficients are often discussed in the literature, the author could find no coherent and reasonably complete treatment of their definition and validity.

The lumping of distributed elements is treated from first principles. Many others have discussed this aspect, and methods for obtaining lumped representations, as well as criteria for accurate lumping, are well known. However, no complete study of the applicability of lumped representations to common building elements could be found. By calculating the accuracy of the lumped representation of more than 100 existing building elements, it is shown that the lumping of

## INTRODUCTION: BUILDING THERMAL ANALYSIS

distributed thermal elements can often be justified. Formulae for determining lumped parameters from the physical properties of the materials are obtained from first principles. It is shown that the pre-condition for accurate lumping of building elements is, in the first place, on the thickness of the walls with respect to the wavelength of the thermal wave propagating through the wall. These results are known in the literature but their physical interpretation, as stated above, is often misunderstood and obscured by statements about the thermal conductivity of the material.

The concepts of active stored heat and active thermal capacitance are clarified.

The definition of the mean external forcing function (mean sol-air temperature), as used by Mathews and Richards, is clarified.

In the method of Mathews and Richards it is necessary to apply an empirical correction to the phase shift of the interior temperature. It is shown that this phase shift can be attributed to two sources: the lumping of thick walls and the definition of the mean sol-air temperature.

It is shown that the technique of combining the heat storage capacitance of interior massive elements with those of the shell, as given by Mathews and Richards, can not be justified. It requires the assumption that the mean temperature of the interior mass is equal to the mean temperature of the massive parts of the shell. This can not be since the interior mass is driven by the interior temperature, and the shell mass by the difference between interior and exterior temperatures.

## INTRODUCTION: BUILDING THERMAL ANALYSIS

A revised simple thermo-flow model is presented. The method requires further investigation, implementation and also verification. The method is conceptually very similar to the method of Mathews and Richards but is theoretically better founded and has certain other advantages.

The method of Mathews and Richards is extended to cater for thermal control systems which utilize heat storage in the structure of the building directly.

The method is extended to allow effective multi-zone thermal performance predictions. It is shown that the proposed multi-zone method is a natural extension of the existing single-zone method.

A new numerical method for the solution of the thermo-flow network is proposed which allows efficient predictions with cyclic, time-variable parameters. An explicit formulation for the initial value, which is required to obtain periodic solutions, is derived. The new method allows the prediction of variable parameter thermal response, without the need for Fourier analysis or a long initial integration period to get rid of transients. It is applicable to any system of discrete cyclic equations with cyclic forcing functions. Besides this numerical method, an alternative approximate method is demonstrated which is based on a complex Fourier series representation with time dependent coefficients.

These contributions are not all original to the same extent. The method for numerical solution of time dependent heat flow is, to the authors knowledge, completely original. In other contributions the work of others have been either applied to the thermo-flow model of Mathews and Richards, or it was attempted to find a clearer or more comprehensive description and understanding, or the results were interpreted in a different way.

## INTRODUCTION: BUILDING THERMAL ANALYSIS

We have endeavoured to indicate, by way of reference, all authors which we feel directly influenced this study. There are also many others who have indirectly contributed; by enhancing our understanding and moulding our perception.

### 1.5 The Contents of this Thesis

Besides the objectives mentioned in §1.3, this study is also an attempt to unify the theory and techniques useful for constructing simple thermo-flow networks for buildings. In this thesis, we have accordingly not strictly confined ourselves to the above stated contributions and objectives, but we also discuss other well known relevant matters, such as the method for linearizing the radiation heat transfer coefficient, the solution of periodic thermoflow problems through walls with the aid of matrices, the definition of the sol-air temperature, the definition of the ventilation resistance etc. We hope in this way to make this thesis useful for those encountering these matters for the first time.

In addition we have gone to some pains in chapter 5 to describe the literature on time variable systems, since this literature is not widely known and often somewhat obscure. In this regard it is also important that the techniques we investigated, but found lacking, be documented.

The presentation of this thesis closely follows objectives A to D in §1.3 above, with each chapter (chapters 2 to 5) devoted to a theme. References, symbols and short appendices are given after each chapter. The final chapter is a summary of all the results, conclusions and recommendations of chapters 2 to 5.

Computer programs and other calculations are not given in full detail in the thesis and appendices. Programs are written in FORTRAN 77,

## INTRODUCTION: BUILDING THERMAL ANALYSIS

Turbo C, Turbo C++ and MATHCAD. Instead, a floppy-disk (MS-DOS formatted) is attached to the backcover which contains all the programs, input data and detailed results. In case further analyses are required for future investigations, the files on the floppy-disk contain sufficient descriptive comments that they can be used and modified<sup>2</sup>.

---

<sup>2</sup>This thesis was compiled with the T<sup>3</sup> Scientific Wordprocessor and printed on a HP Laserjet. Figures were drawn with HP Drawing Gallery on the Laserjet, most graphs were compiled with Quattro Professional.

INTRODUCTION: BUILDING THERMAL ANALYSIS

REFERENCES Chapter 1

- [1] D. Carrol, Energy Consumption and Conservation in Buildings An International Comparison, *Proc. 3rd Int. Symp. Energy Conservation in the Built Environment*, Vol. 1A, CIB/An Foras Forbartha, Dublin, 1982, pp. 190 –203.
- [2] R. Bevington, A.H. Rosenfeld, Energy for Buildings and Homes, *Scientific American*, Sept. 1990, pp. 39 – 45.
- [3] H. Erhorn, Solarenergiehäuser in der Praxis Welche Energieeinsparergebnisse erbringen sie wirklich? *Bauphysik 11(1989), H, 1*, pp. 70 –73.
- [4] G. van Aarle, T Herman, Potential for the air-conditioning of office buildings without mechanical refrigeration, *The South African Mechanical Engineer*, Vol. 36, June 1986, pp. 192 – 197.
- [5] W. Kruger, M. Kleingeld, Design Guidelines and Norms for Evaporative Cooling, Ventilation, Daylighting, *Final Report, CENT*, Dept. of Mech. Eng., UP, Oct 1990.
- [6] T.-S. Sun, A reflection on 30 years in air-conditioning design and energy conservation, *Plenary Paper, ASHRAE-FRIGAIR 90*, 23 – 25 April 1990, Pretoria, Vol 1.
- [7] D. L. Thornley, The Case for Air Conditioning—a Keynote Discourse, *Air Conditioning System Design for Buildings*, Editor A.F.C. Sherrat, McGraw-Hill, pp. 1 – 16.
- [8] **Proc. 3rd Int. Congress on Building Energy Managment**, Lausanne, 1987, *Presses Polytechniques Romandes*, Lausanne
- [9] **QUICK user's and reference manual**, Release 3 of 1990, *CENT*, Department of Mechanical Engineering, University of Pretoria.
- [10] E. H. Mathews, P.G. Richards, A Tool for Predicting Hourly Air Temperatures and Sensible Energy Loads in Buildings at Sketch Design Stage, *Energy and Buildings*, 14(1989), pp.61 – 80.

INTRODUCTION: BUILDING THERMAL ANALYSIS

- [11] **E. H. Mathews, P.G. Rousseau, P.G. Richards, C. Lombard**, A Procedure to Estimate the Effective Heat Storage Capability of a Building, *Energy and Buildings*, accepted for publication, 1990.
- [12] **W. Kruger**, Thermal Norms for Buildings on South Africa, *Master of Engineering Thesis, Dept. of Mech. Eng., University of Pretoria.*

## CHAPTER 2

---

### 2 A THEORETICAL FOUNDATION FOR THE THERMAL ANALYSIS METHOD OF MATHEWS AND RICHARDS

#### 2.1 Background and Objective of this Chapter

In this chapter we aim to examine the theoretical underpinnings of the highly simplified thermal model of Mathews and Richards [10]. Before we do so, we first motivate why we chose this method, from many others, for further investigation.

##### 2.1.1 The Variety of Available Methods for Building Thermal Analysis

A large variety of computer programs and methods for building thermal analysis are available today. Most popular (in English speaking countries) are certainly the *response factor* [1] method promulgated by ASHRAE in Northern America and the *admittance* [2] method of CIBS in the United Kingdom. Other prominent methods are the method of Muncey [3] as extended by Walsh and Delsante [4] in Australia, the *Total Thermal Time-Constant* method of Givoni and Hoffman [5], and in South Africa, the *CR* method of Wentzel, Page-Shipp and Venter [6]. Some of these methods are discussed and compared by Tuddenham [7], Walsh and Delsante [4], Athienitis [8,9] and Mathews and Richards [10]. According to Tuddenham [7]:

1. There is a wide range of theories and program types in use.
2. The degree of variation in results between various programs is high – the degree of accuracy is largely unknown.
3. There is strong evidence that the largest factor in the difference between program results is engineering interpretation.
4. There is no evidence that more complex engineering models give more accurate results."

Tuddenham also remarks that: "The most remarkable feature of computer load estimation work today is the continuing paucity of

## THEORETICAL FOUNDATION OF A NOVEL METHOD

supporting work to validate the calculation theories, although some work is now being undertaken, notably in the USA."

The method of Mathews and Richards<sup>1</sup> has the considerable advantage of using an extremely simple thermo-flow network with a clear interpretation in terms of the main thermal components of the building. Furthermore, the lumping of shell conductance and heat capacitance effectively circumvents the need for solving partial differential equations. Despite this simplicity of the network – or perhaps on account of this simplicity – extensive validation measurements in existing buildings indicate that all the essentials are adequately represented [10,11] and the observed error against measurements is below 2 °C in more than 80% of the cases. The simplicity of the method allows very efficient numerical solution, and the clear physical interpretation enables ready extension of the method. Recently the method has been extended to include simulation of active systems of various complexity and such exotic systems as evaporative cooling, structural cooling and night cooling [12].

But whatever the merits of a new method may be, general acceptance by the building industry is not something which will come about automatically. The old methods are well-known and consultants have learned their quirks, they are firmly established. Tuddenham observes [7]: "In more recent years, programs in the commercial field have tended to adopt a theory which is underwritten by the UK or American establishment, notably the CIBS 'admittance' method or the ASHRAE 'response factor' method. However, it may be that this trend is based more on their apparent respectability than on their proven excellence."

A large number of computer programs for building thermal analysis is available. According to Tuddenham [7] there are more than one hundred in the United Kingdom and many hundreds more elsewhere. Most of

---

<sup>1</sup>See footnote page 7.

## THEORETICAL FOUNDATION OF A NOVEL METHOD

these methods are based on the above mentioned admittance method of the CIBS [2], or the response factor method of ASHRAE [1]. The CIBS method was originally developed for manual calculations [13]. It employs pre-calculated tables of decrement- and other factors for building materials. The response factor method was originally developed for computer implementation [14] although it also employs pre-calculated 'response factors'. It does seem, however, that the method was severely influenced by the very crude computer hardware and software available at the time and the central theme of the method appears to be an attempt to alleviate the problem of evaluating the convolution integral, as required to obtain the forced response [15]. In view of the undreamt of growth in computer technology and numerical techniques in the last 30 years, both these methods appear outdated. The Fast Fourier Transform has made the evaluation of convolution integrals a very simple and computationally efficient exercise [16]. Consequently, frequency domain techniques are now predominant in numerical implementations in diverse scientific disciplines.

Both the CIBS and the ASHRAE method (and others e.g. [3,4]) employ the exact analytical solution of the diffusion equation in the form of matrices [15]. These matrices are then used to obtain the response\decrement factors from which the thermal response is obtained. In the admittance procedure the factors are used to obtain amplitude and phase-shift values for the internal temperature. The response factor method obtains the solution by superimposing the response to a series of triangular pulses. Strictly speaking, both methods are only applicable to linear time-invariant thermal systems. (Note, in [17] invariability is erroneously stated as a requirement for using the method of superposition; linearity is sufficient. Invariability is only required for the Laplace transform method to be tractable [18].)

Since the exact matrix solution for heat conduction is simple and amendable to computer implementation, and standard two port theory

## THEORETICAL FOUNDATION OF A NOVEL METHOD

can be used to combine the matrices of various elements, it is unnecessary that computer programs still employ response factors which have to be pre-calculated. Certainly, the matrices are more suited to time invariant systems, but so are the response factors, since they are derived from the matrices. For the time invariant case, it seems that a modern comprehensive method would compute the matrices for the various elements at a number of frequencies, combine the matrices with two port theory, and compute the exact solution via the superpositioning of the responses to the various frequencies (See chapter 5) as suggested by Athienitis [9]. Computationally this is certainly feasible and practical on modern desktop computers. The method can be used to obtain both transient and steady state solutions by employing either the Laplace or the Fourier domain; although the availability of the Fast Fourier Transform considerably increases the computational speed in the Fourier domain. Later in this chapter we use this comprehensive matrix method to derive a simple model for thermo-flow in buildings.

In [14] some emphasis is placed on the response factor method being applicable to non-steady state conditions. To simulate non-steady conditions one would have to specify initial conditions which can only be guessed or become known by measurements. Therefore, simulation of non-steady conditions seems rather academic. In practice one is confronted with continuous variables which can be described as quasi-periodic; there is no clearly defined initial state. One should therefore rather attempt to find the quasi-periodic solutions which are often sufficiently accurately represented by periodic solutions [9]. This is especially true if the principle of a design day is adhered to, where a single day is specifically chosen, and used to evaluate the building under the further assumption that all other days are similar. If results are required for e.g. one extraordinary day in a series of ordinary days, the periodicity can be assumed to extend to a number of days, e.g. 7 days or a design week. Computationally this approach is probably at least just as efficient as a time-domain non-steady analysis, where integration

## THEORETICAL FOUNDATION OF A NOVEL METHOD

would have to extend over at least 5 thermal time-constants to get rid of the initial transient.

In view of the availability of the practical, exact matrix solution to the heat conduction equation with steady excitation, it is also surprising to find many programs employing finite difference or finite element techniques. It is often stated that these numerical methods facilitate solution of a time variable, fully non-linear model [8]. In fact the powerful but often tedious numerical techniques are essentially employed to solve the time invariant, linear, heat conduction equation. The time variability and non-linearities in thermal models of buildings do not arise from heat conduction but from other heat transfer modes. The advantage of the finite difference\element techniques is rather that they allow a unified treatment of all aspects of thermo-flow in buildings. However, they are not the most efficient techniques, they are also quite remote from the physical structure, and, they often require careful fine-tuning to ensure convergence, accuracy etc.

One could use the matrix solution for the conduction equation and combine it with time variable non-linear two ports. The complete solution is then obtained from non-linear network methods which were extensively developed in recent years [19]. Athienitis in an important contribution [9] remarks that "Discrete frequency analysis, although virtually ignored in passive solar design, is computationally efficient and easy to program."

A central theme in the above discussion and in the literature is the use of matrices to obtain exact solutions for heat transmission through walls with sinusoidal boundary conditions. Matrices were first applied to heat transfer problems by Pipes [20], but many others, *viz.* [21-23,3,4,13,17], have also used the matrix solutions. For a description of the method refer to §2.5.3, see also Givoni [5] and Kimura [15]. This method has the clear distinction – from the many numerical methods – in that it is

## THEORETICAL FOUNDATION OF A NOVEL METHOD

an exact solution of the heat diffusion equation. However, it is based on Fourier analysis and therefore awkward when extended to time variable systems. Nevertheless, in many programs based on the matrix method, one disconcertingly finds that the extreme power of the matrix (two-port) theory for combining various elements is not appreciated. This is inexplicable, especially since these methods are ideally suited for computer implementation. For example, in the program described by Walsh and Delsante [4], which is based on the work of Muncey [3], one finds that the final result is evaluated, not from a final matrix description of the the total system, but rather, in terms of the response of the various elements of the building to certain types of input functions.

The modelling of thermal response with two-ports was extensively developed by Athienitis [8]. He has shown that the frequency domain matrix techniques can be extended to include time-varying parameters such as night insulation and variable ventilation. In this thesis, use is made of this fairly exact method to illuminate the assumptions and limitations of the simplified method of Mathews and Richards.

An important point we wish to clear-up at this stage, is that some present thermal analysis methods attempt to be extremely accurate, with emphasis on exact simulation, e.g. [24]. Highly refined numerical analysis techniques are used. The result is that these techniques need large mainframe computers and detailed specification of the construction, consequently, they are mostly of academic value. The established simplified methods of ASHRAE and CIBS on the other hand, are outdated. A design tool for use at sketch design stage should be sufficiently accurate with a design philosophy (e.g. design day) in mind – and practical. In this thesis we are interested in design tools and it is evident that there is scope for new methods and further developments in

## THEORETICAL FOUNDATION OF A NOVEL METHOD

this regard [10]. For such a new method to be acceptable, the following points warrant consideration:

- a) A complete description of the thermo-flow in real buildings requires many details, some of which (e.g. ventilation rates) are wholly unknown or only partly known. This is even more true if the objective is a design tool, since the thermal properties of a building are largely determined in the very early design stages when no details at all are available.
- b) Many studies and empirical models [25,26] indicate that a few essential parameters of buildings, such as heat storage capacity and shell admittance, are crucial and should be emphasized rather than details. It is also crucial that the assumptions underlying the model be clear, easy to explain and to understand. The model must have a very clear physical connection.
- c) A successful computer design tool must employ a very simple model with a straightforward physical explanation to allow the designer's good judgment and experience to play its essential part. Highly refined models and exact solutions are better employed in research laboratories for verification purposes and the extension of knowledge and understanding.
- d) For a design tool, extreme numerical accuracy – at the cost of computing time – is detrimental. Certain essential parameters of thermo-flow in buildings, such as ventilation rates, are largely unknown. The emphasis should be on establishing the relative merit of various designs, rather than absolute predictive accuracy. It must be remembered that the probability that the weather conditions, used for the simulation, will actually occur in practice, is small. The tool must endeavour to be indicative of the response of the building, rather than predictive.
- e) A design tool should allow innovation and easy extension to

## THEORETICAL FOUNDATION OF A NOVEL METHOD

cater for creative ideas and new techniques.

- f) A computer procedure should not be based on 'established' techniques which were developed for hand calculations and which are overly simplified or unnecessarily rigid.
- g) A design tool should follow a total approach. Both the passive response of the building and the HVAC system must receive due attention, but of the two, the passive response is probably the more important factor, since it essentially determines the required HVAC system and therefore the installation and running costs.

The method of Mathews and Richards was initially developed with these considerations in mind [10] and is therefore an excellent vehicle for further study and improvement.

### 2.1.2 The Objective of this Chapter

In the next sections of this chapter a theoretical foundation for the simple model of Mathews and Richards for thermo-flow in buildings is derived. This further establishes the validity of the method and will promote its general acceptance. The point is exemplified by other methods, which appear theoretically unsound, although they may have empirical merit, e.g. the TTTC method [27] where time-constants are averaged<sup>2</sup>.

Here we endeavour to illuminate the method of Mathews and Richards. The procedure we follow is to model a simple building, consisting of only two surfaces, comprehensively, and to deduce from this comprehensive model the parameters of the simplified model. The comprehensive model is constructed in terms of the exact frequency domain matrix method discussed above. This procedure enables investigation of the effect and validity of each simplifying assumption in

---

<sup>2</sup>See discussion of TTTC method in §2.5.3 e.

## THEORETICAL FOUNDATION OF A NOVEL METHOD

turn. The simple two surface building we use is approximated by a large flat building where one surface may be the roof and the other the floor. Although the quantitative results are limited to this theoretical building, the procedure we follow is applicable to any building. The building merely serves to provide quantitative results for evaluating the thermal response of typical building structures. The advantage of using only two surfaces is that the complexity of the comprehensive model is greatly reduced, so that the essential physical mechanisms of heat transfer are not obscured by detail. We begin the discussion by first introducing the simple thermal model of Mathews and Richards.

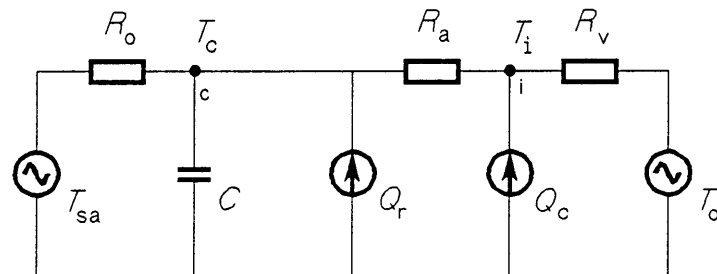


**FIGURE 2.1** The simple electrical analog of Mathews and Richards for thermo-flow in buildings. Symbols are defined above. From [10].

### 2.2 The Method of Mathews and Richards

In figure 2.1 the electrical network equivalent of Mathews and Richards for the heat flow problem in buildings is shown [10]. In this figure  $T_{sa}$  is the averaged sol-air temperature (for definition see §2.4.4 a),  $T_o$  is the outside air temperature,  $T_i$  is the indoor air temperature,  $Q_r$  is the radiative heat source and  $Q_c$  is the convective heat source. The shell resistance and thermal capacity of the building is represented by  $R_o$  and  $C$  respectively,  $R_a$  is the heat transfer coefficient of the internal surfaces

## THEORETICAL FOUNDATION OF A NOVEL METHOD

and  $R_v$  is the ventilation resistance. The most notable aspect of the circuit is the extreme simplicity, a single capacitor is used to represent all the mass available for heat storage. The conductance through the shell is modelled with a single resistance  $R_o$ , and a single exterior forcing function,  $T_{sa}$ , is used.

### 2.3 Assumptions, Limitations and Possible Extensions of the Method

In the development of the thermal model of Mathews and Richards they found it expedient to simplify the network to a single zone thermal system. It is assumed that the temperatures in adjacent rooms are equal, so that no exchange of heat occurs between them [10]. A more important assumption is that the interior surfaces are at the same temperature. Radiation between interior surfaces can therefore be completely ignored. It is also assumed that the surface heat transfer coefficients can be fixed. In the development of the model, a higher priority was assigned to speed of calculation and ease of use, than absolute accuracy. These assumptions will be discussed shortly.

Mathews and Richards stress that it is important to bear in mind that some important contributions to the heat flow, such as ventilation rates, are highly uncertain. These parameters can only be guessed so that there is a definite upper limit to the theoretical achievable accuracy for any thermal response model. In practice, it turns out that useful answers can be obtained with the single zone and other assumptions, and that a significant improvement in thermal performance of new buildings, designed with this model, is obtained. These conclusions are fully in accordance with points a) to g) of §2.1. The successful verification of the method [10], and the ready acceptance by some consultants, fully justifies further investment in the improvement- and promotion of the method.

Further enhancement will be beneficial since the simplified model was originally conceived as a design tool for architects, but lately, the

## THEORETICAL FOUNDATION OF A NOVEL METHOD

engineering fraternity has also shown considerable interest. Their objective is rather different; primarily, they desire to use the program to determine the required capacity of new air conditioning installations, and, to optimize these systems. The program is helpful for estimating the future running costs of a proposed new building. There exists a further possibility that, by improving the control systems used for maintaining the indoor climate at prescribed settings, the program may significantly decrease the running costs of existing buildings. For these engineering applications the accuracy obtained via the single zone approach and the other assumptions may sometimes be insufficient and a more refined model is called for. The logical approach to an extension of the applicability of the method is to remove the limitation to single zone analysis, fixed ventilation rates and to provide for active systems. These extensions must be incorporated without sacrificing the extensive base of understanding, knowledge and technique that has been proved in practice. The extension of the model of Mathews and Richards to include multi-zone thermal response, structural storage systems and variable parameters is treated in later chapters.

This chapter of the thesis is, in the first instance, an attempt to investigate theoretically the validity of the assumptions. Besides that, this thesis is also concerned with refining the model if the validity of some of the assumptions can not be substantiated. A theoretical study will in this way enhance the understanding of the implications of the assumptions and the behaviour of the method under various conditions.

A very important assumption of Mathews and Richards, which leads to great simplification, is the assumption that the essentially distributed massive elements comprising the walls, floors and interior masses, can be adequately represented with a single lumped capacitor. This is a very fundamental assumption, it enables the analysis method to obtain predictions for room thermal response without the need for obtaining first solutions to the heat diffusion equation. The validity of this assumption (and the others) must be based on measurements in actual

## THEORETICAL FOUNDATION OF A NOVEL METHOD

buildings. Many such verification experiments have been carried out [11], and the results indicate that adequate accuracy is obtained with the indoor temperature predictions. It does appear, however, that the correct time delay between peak exterior forcing temperature and peak interior temperature is not always obtained [11].

In the next two sections an attempt is made to elucidate these assumptions of Mathews and Richards by examining their validity in the light of a more refined model. As stated already, a very simple building structure, consisting of two infinite walls, often serves as butt of the discussion.

### 2.4 A More Comprehensive Theoretical Model

We model the thermal attributes of buildings along the same lines as Athienitis [8]. The model of Walsh and Delsante [4] also has close parallels, as well as the model presented by ASHRAE [28]. This comprehensive model we present here, is a refinement of the model of Mathews and Richards particularly in the following aspects:

1. The assumption that the internal air is well mixed is retained but the assumption that the interior wall surfaces are at the same temperature is dropped. In this model, heat transfer between the surfaces via both convection and radiation is incorporated. The objective of this part of the study is to determine the difference in temperature between the various internal surfaces and the accuracy of the assumption of isothermal interior surfaces.
2. The lumping of conductance and heat storage of the building shell in a single resistor and single capacitor network is avoided. Instead, the exact matrix solution of the diffusion equation is employed. The accuracy of the lumped model can be investigated in this way. In addition, the method of lumping, especially for laminated surfaces, as well as the

## THEORETICAL FOUNDATION OF A NOVEL METHOD

combination of the surfaces in a single RC network, is investigated.

3. Besides the lumping of the shell capacitance, the model of Mathews and Richards also combines the storage capability of internal masses with those of the shell in a single capacitor. In the refined model these internal masses are treated separately.
4. The external surfaces are treated individually. Mathews and Richards assume that it is possible to obtain a mean sol-air temperature which applies to all external surfaces. In the comprehensive model external surfaces are given individual boundary conditions.

### 2.4.1 The Building Shell

The walls forming the enclosure, as well as the roof, are modelled as laminae of various materials. The heat flow through these laminae are adequately described by the one-dimensional diffusion equation, with radiative and convective boundary conditions. This approach ignores two dimensional edge effects at the corners. It is easily shown, in the steady state case, that the effects of the edges are negligible<sup>3</sup>; solutions for steady state heat conduction are tabulated in Holman [29] for various geometries in the form of:

$$q = k \cdot S \cdot \nabla T$$

with  $q$  heat flow [W],  $k$  conductivity in [W/m<sup>2</sup>·K],  $S$  the *shape factor* in [m] and  $\nabla T$  the temperature difference forcing the heat flow in [K].

The shape factor for a wall is [29]:  $S_w = A/\ell$ , with  $A$  the area of the wall in [m<sup>2</sup>] and  $\ell$  the thickness of the wall in [m]. The shape factor for the edge between two walls is:  $S_e = 0.54 \cdot D$  where  $D$  is the length of the edge. For the corners where three surfaces meet the shape factor is  $S_c = 0.15 \cdot \ell$  with  $\ell$  the thickness of the surfaces. For a simple

---

<sup>3</sup>These results are well known. We include it for the sake of completeness and to aid newcomers to the science of building thermal response.

## THEORETICAL FOUNDATION OF A NOVEL METHOD

cubicle of  $3 \times 3 \times 2.75 \text{ m}^3$  with wall thickness 250 mm these factors are:  $S_w = 33 \text{ m}$ ,  $S_e = 1.62 \text{ m}$  and  $S_c = 0.0375 \text{ m}$ . For steady state conditions the contribution of the heat flow through the edges is clearly negligible and the one dimensional approach is very accurate. This conclusion is valid for all thin walled buildings. Only when the thickness of the wall is a sizable fraction of the cubic root of the internal volume will the assumption be erroneous.

The roof can be treated as just another surface. The presence of air-space between ceiling and roof must be accounted for by assigning an effective conduction coefficient to account for the radiative and convective heat exchange, which is in general dependent on the temperatures of the surfaces in contact with the air. It is not really necessary to resort to effective conductances to model ceiling space; the air gap can be treated from first principles. This will entail using a multi-zone approach to model the roof where one zone is the ceiling space and the other the interior space [28]. For the purposes of this study this is not necessary. The principle of an effective conductance is quite adequately established experimentally [5] and the extra detail will obscure more important aspects.

The solution of the heat diffusion equation for each surface must be determined with the appropriate boundary conditions for each surface. This will normally mean the sol-air temperature and the associated film coefficient must be determined for each external surface. The internal surfaces are coupled to each other via radiative exchange and to the internal air node via internal film coefficients. The solution of the diffusion equation is determined for steady periodic conditions in the form of a transmission matrix (two port) as set out in §2.5.3. We therefore have for each surface of the shell a two port and the two ports are driven from the outside by the sol-air temperatures. Internally, the two-ports are connected with a radiative exchange

THEORETICAL FOUNDATION OF A NOVEL METHOD

network between the internal surfaces and convection coefficients to the internal air. The model is shown schematically in figure 2.2.

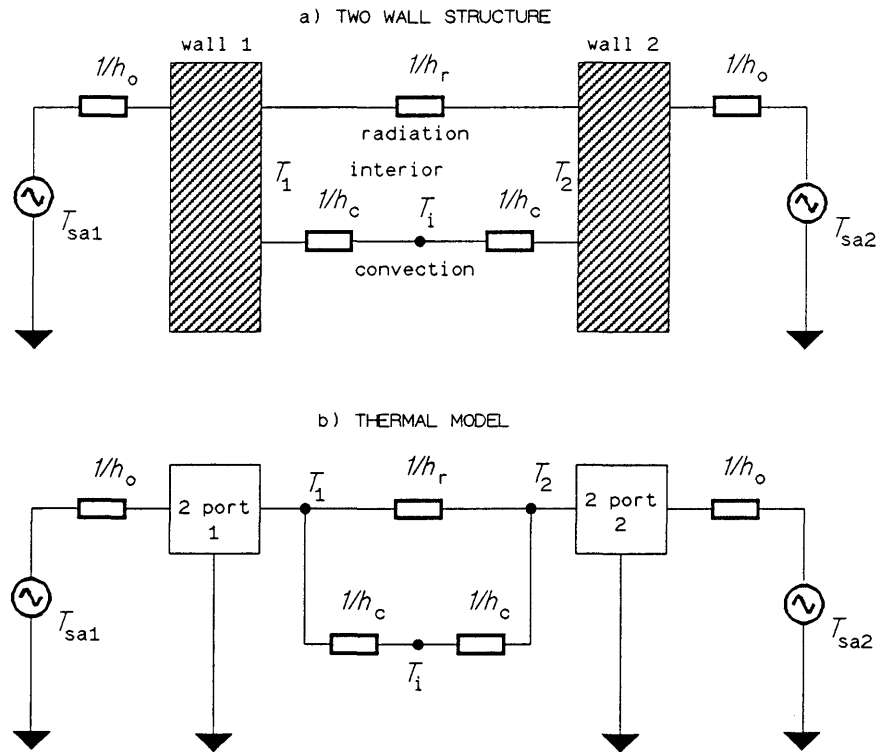


**FIGURE 2.2** Model of simple two wall structure with sol-air forcing function on external surfaces, internally interconnected via a radiation coefficient  $h_r$  and via the convective coefficient  $h_c$  to the interior air-node. The walls are represented by two-port networks. The outside surface coefficient  $h_o$  is the effective film coefficient to the sol-air which includes convection to the outside air, shortwave radiation from the sun as well as long wave radiation to the sky.

Ventilation (see §2.4.4) can be included by simply adding another forcing function  $T_o$  to the internal air node, via the ventilation resistance  $R_v$  as in figure 2.1. Ventilation is further discussed in §2.4.4 b.

## THEORETICAL FOUNDATION OF A NOVEL METHOD

### 2.4.2 The Floor

The model of the floor of a building presents no additional complication if the floor is a suspended floor of a multi-storey building. However, if the floor is in contact with the ground, as is frequently the case, considerable complication arises. The ground underneath the building is not insulated from the floor slab and heat will be exchanged between the soil and the interior air through the slab. This exchange is essentially three dimensional in nature [3]. The problem of ground contact receives considerable attention in the literature. According to [11], the soil can be introduced as another layer underneath the concrete slab up to a depth of 75 mm, at which point the temperature is essentially the (seasonally) mean outdoor air temperature. Delsante [30] recently published an analytical solution for the heat flow in the soil underneath the building. He indicates that a considerable heat flow exists between interior air and exterior air along a path through the soil underneath the foundations. The model of the floor is of minor importance for this study, since we are mainly concerned with the lumped representation of the walls.

### 2.4.3 Heat Exchange Between Internal Surfaces

One of the most important simplifying assumptions inherent in the model of Mathews and Richards, is the assumption of isothermal interior surfaces. In effect, this assumption ignores all heat exchange between the interior surfaces. This does not mean that the method assumes no heat exchange takes place, but rather, that it is very effective so that dynamic equilibrium is soon attained and little temperature differences will be observed. Two modes of heat exchange between interior surfaces evidently occur; direct radiation between the surfaces and indirect convection with internal air. A temperature difference between two walls will cause radiative transfer of heat directly from the hot to the cold surface. In addition, if the interior surface temperatures differ, they can not all be equal to the interior air temperature. Consequently, a natural

## THEORETICAL FOUNDATION OF A NOVEL METHOD

convection current will be set up so that heat will be transferred from the hot surfaces to the air and then from the air to the cold surfaces.

Indoor comfort are dependent on both the air temperature and the temperature of the interior surfaces [1]. Muncey [3] indicates that the interior heat flow network may be simplified from delta to star ( $\nabla$  to Y) form. It is then possible to find a single node representation of the interior temperature, although it is difficult to give a physical interpretation of this, so called, effective- or environment temperature. In the absence of ventilation and infiltration, the temperature of the interior air must equal the mean temperature of the internal surfaces, provided the air is well mixed and the convection coefficients of all the internal surfaces are the same. In this section we examine the radiative and convective exchange of heat between interior surfaces in some detail.

### a) Radiative Heat Exchange

Radiative heat exchange between interior surfaces is intrinsically a non-linear phenomenon. The basic law of heat exchange via radiation is the Stefan-Boltzman law [1,5,8,15,29,31], which can be put in the following form [15] for two parallel surfaces of area  $A$ :

$$q = F_{12} \cdot A_1 \cdot \epsilon_1 \cdot \epsilon_2 \cdot \sigma \cdot (T_1^4 - T_2^4) \quad (2.1)$$

with  $q$  the radiative heat flux [W]

$F_{12}$  a geometric form factor

$A_1$  the area of surface 1 [m<sup>2</sup>]

$\sigma$  Boltzman's constant =  $5.669 \cdot 10^{-8}$  W/m<sup>2</sup>·K<sup>4</sup>

$\epsilon_1$  and  $\epsilon_2$  the emissivities of the respective surfaces and

$T_1$  and  $T_2$  are the absolute temperatures of the respective surfaces in Kelvin.

If it is assumed that the temperature difference between the surfaces are small compared to the mean absolute temperature, the equation can be

## THEORETICAL FOUNDATION OF A NOVEL METHOD

linearized. It is a well known procedure [15] but for completeness it is again included here. Write (2.1) in the form<sup>4</sup>:

$$q = F_{12} \cdot A_1 \cdot \epsilon_1 \cdot \epsilon_2 \cdot \sigma \cdot (T_1^2 + T_2^2) \cdot (T_1 + T_2) \cdot (T_1 - T_2), \quad (2.2)$$

and define a radiative coefficient:

$$h_r = F_{12} \cdot A_1 \cdot \epsilon_1 \cdot \epsilon_2 \cdot \sigma \cdot (T_1^2 + T_2^2) \cdot (T_1 + T_2). \quad (2.3)$$

With  $\Delta T = (T_1 - T_2)$  and  $(T_1 + T_2)/2 = T_m$  (2.3) becomes:

$$\begin{aligned} h_r &= F_{12} \cdot A_1 \cdot \epsilon_1 \cdot \epsilon_2 \cdot \sigma \cdot (4 \cdot T_m^3 + \Delta T^2 \cdot T_m) \\ &= F_{12} \cdot A_1 \cdot \epsilon_1 \cdot \epsilon_2 \cdot \sigma \cdot T_m^3 \cdot (4 + [\Delta T/T_m]^2). \end{aligned} \quad (2.4)$$

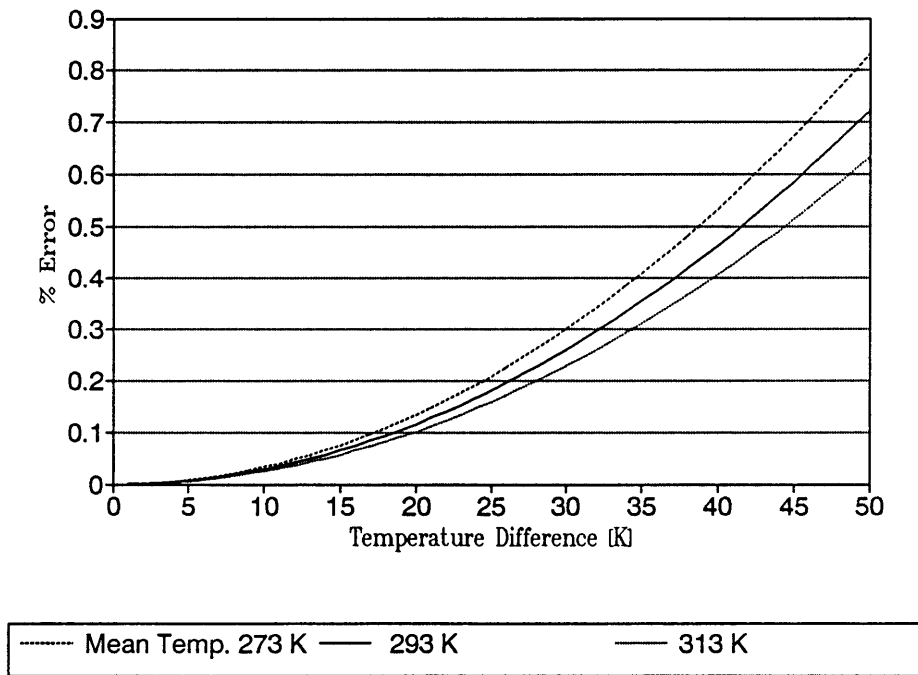


**FIGURE 2.3** Percentage error of linearized  $h_r$ , as a function of temperature difference of the radiating surfaces at a mean temperature of 20°C.

<sup>4</sup>These results are well known. We include it for the sake of completeness and to aid newcomers to the science of building thermal response.

## THEORETICAL FOUNDATION OF A NOVEL METHOD

In buildings, conditions are such that  $\Delta T/T_m$  is a very small fraction. (With  $T_m = 20^\circ\text{C}$  and  $\Delta T = 20^\circ\text{C}$ ,  $\Delta T/T_m = 20/(293) = 0.068$ .) Consequently, the second term in (2.4) is very much smaller than 4 and we find approximately:

$$h_r \approx 4 \cdot F_{12} \cdot A_1 \cdot \epsilon_1 \cdot \epsilon_2 \cdot \sigma \cdot T_m^3. \quad (2.5)$$

We see that with this definition of  $h_r$ , radiant heat transfer can be written in the same form as convective heat transfer:

$$q = h_r \cdot A \cdot (T_1 - T_2)$$

One can also define a radiant heat transfer resistance:

$$R_r = \frac{T_1 - T_2}{q} = 1/h_r A.$$

The error in using (2.5) instead of (2.4) is shown in figure 2.3 where the percentage error is given as a function of  $\Delta T$  with  $T_m = 20^\circ\text{C}$ . Even at  $\Delta T = 50^\circ\text{C}$  the error is below 1 %. Linearizing the radiative coefficient is seen to be extremely accurate for building thermal applications.

In the thermal model of the building each interior surface must be connected to every other interior surface with a radiation coefficient as in figure 2.2 [8,1,28]. For more than just two surfaces, a very complicated thermo-flow network is obtained<sup>5</sup>.

### b) Convective Heat Exchange

Convective heat exchange on interior surfaces have been the subject of many papers and is discussed in [1,3,5,15] and elsewhere. Convection is usually treated by defining a mean convection coefficient  $h_c$  as in

---

<sup>5</sup>For examples of realistic interior heat transfer networks see [8] and [28 p101].

## THEORETICAL FOUNDATION OF A NOVEL METHOD

Newton's law of cooling<sup>6</sup>:

$$q = h_c \cdot A \cdot (T_w - T_\infty)$$

with  $q$  the convective heat flux [W]

$h_c$  the convection (film) coefficient [W/m<sup>2</sup>·K]

$A$  the area of the surface [m<sup>2</sup>]

$T_w$  the temperature of the surface [°C]

$T_\infty$  the free temperature of the air [°C].

Although it is possible to derive theoretical values for convection coefficients from boundary layer theory<sup>7</sup>, in practice, convection coefficients are usually based on empirical correlations between non-dimensional groups [29]. Various authorities have published indoor convection coefficients for buildings [1,5,31].

In the model of thermo-flow in buildings each interior surface must be connected to the interior air-node with a convective resistance given by  $R_c = 1/h_c$  (for surfaces of unit area), as in figure 2.2.

### c) Combined Film Coefficient for Interior Surfaces

The combined radiative and convective heat exchange network for an enclosure consisting of only two surfaces is given in figure 2.4a. In general, buildings will consist of more than just two surfaces. If all these surfaces are connected to each other via radiation resistances, and to the interior air via convection resistances, a very complicated circuit arises [8,28 p101]. Athienitis [8] has shown that these complicated networks can be solved efficiently.

It is possible to simplify the internal heat flow network by introducing the concept of a combined film coefficient,  $h_i$ , which incorporates both

---

<sup>6</sup>These results are well known. We include it for the sake of completeness and to aid newcomers to the science of building thermal response.

<sup>7</sup>See appendix C of chapter 4 for an example of a theoretical calculation of the interior convection coefficient.

## THEORETICAL FOUNDATION OF A NOVEL METHOD

convective and radiative heat exchange. The definition of the combined coefficient is not unique and depends on certain simplifying assumptions. The procedure will be demonstrated for four distinct assumptions with the aid of the simple two surface structure of figure 2.2.

### Method 1: Airtight Enclosure

In the circuit of figure 2.2 the interior air node  $T_i$  is not connected to the exterior air which would be the case if infiltration or ventilation is included. In this case it is possible to determine a unique and accurate definition of the combined coefficient. First apply a  $\nabla$  to Y transform to the interior heat transfer network which translates the interior network of figure 2.2, reproduced as figure 2.4a, to the equivalent network of figure 2.4b. (It was assumed that convection from both interior surfaces are equal.)

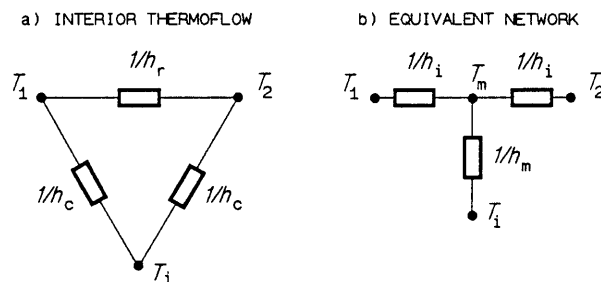


**FIGURE 2.4** Simplification of interior heat exchange for two wall structure via  $\nabla$  to Y transform of interior network.

The result is that the surfaces are inter-connected with conductances  $h_i = h_c + 2 \cdot h_r$  and via conductance  $h_m = h_c/h_r \cdot h_i$  to the interior air, for surfaces of unit area. The artificial node,  $T_m$ , which results from the transformation is non-physical. It represents an *environment temperature*. In the absence of ventilation and infiltration, no heat flows through  $h_m$  and the temperatures on both sides of  $h_m$  are the same, i.e.

## THEORETICAL FOUNDATION OF A NOVEL METHOD

the air-temperature is equal to the environment temperature. In this case, we see that the surfaces are effectively connected via  $h_i$  to the air temperature node  $T_i$ , and an equivalent film coefficient which incorporates both convection and radiation is:

$$h_i = h_c + 2 \cdot h_r. \quad (2.6)$$

For three surfaces one finds from figure 2.5:

$$h_i = h_c + 3 \cdot h_r. \quad (2.7)$$

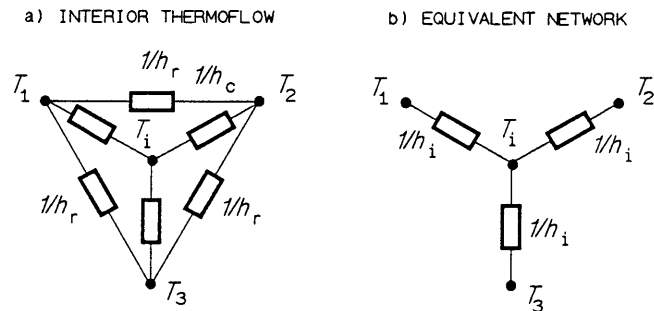


**FIGURE 2.5** Interior thermo-flow network for a 3 wall structure.

For  $n$  surfaces accordingly<sup>8</sup>:

$$h_i = h_c + n \cdot h_r \quad (2.8)$$

It is seen that each additional surface increases the effective coefficient to the interior air for all other surfaces, since it provides additional area for convection via the radiation. Note that (2.8) assumes the radiation resistances and convection resistances are equal for all the surfaces. Obviously this will not be so in practice. Besides differences in area the

---

<sup>8</sup>Equation (2.8) is only valid when the convection coefficients of all the surfaces are equal. If the convection coefficients differ, one can follow a similar procedure but it is a little more involved. E.g. in figure 2.5 the coefficients  $h_c$  are first converted to  $\nabla$  format, which places them in parallel to  $h_r$ . The combined coefficients are then obtained by transforming once more, this time from  $\nabla$  to  $Y$ . For more surfaces the procedure is obviously complicated and requires the simultaneous solution of a set of equations.

## THEORETICAL FOUNDATION OF A NOVEL METHOD

orientations of the surfaces and emissivities will affect the radiative exchange. Furthermore, we have neglected the resistance  $h_m$  in figure 2.4. Actual buildings are also very seldom airtight, in which case the effect of  $h_m$  on the interior air temperature will not be negligible and this definition of  $h_i$  can not be sustained.

### Method 2: Adiabatic surfaces

If it is assumed that the second surface is an interior partition, that is, when there is no net flow of heat through it, the interior effective convection coefficient for two walls can be defined as:

$$h_i^a = h_c / (h_c + h_r) \cdot h_i \quad (2.9)$$

from figure 2.4b with no net flow of heat through the conductance  $h_i$  connected to  $T_2$ . For multiple surfaces, it is clear that in the adiabatic case (all other walls regarded as partitions), the combined coefficient must represent the total coefficient for transportation of heat from the relevant surface, directly to the interior air, and via radiation to the other surfaces, and then by convection from the other surfaces indirectly to the interior air. Therefore, if the enclosure is made up of many surfaces the combined coefficient of each surface includes the following heat flows: a) convection from surface to air, b) radiation from the surface to every other surface, and from that surface, via convection, to the air. Heat flow a) for the surface is given by  $h_c$ , and heat flow b) from surface  $n$  to  $m$  by  $h_c \cdot h_{rnm} / (h_c + h_{rnm})$ , where  $h_c$  is the convective coefficient from the surface, and  $h_{rnm}$  the radiative coefficient from surface  $n$  to surface  $m$ . The combined adiabatic coefficient for the surface is thus given by:

$$h_i^a = h_c + \sum_j h_{cj} \cdot h_{rj} / (h_{cj} + h_{rj}) \quad (2.10)$$

where the summation extends over all surfaces, except the current surface for which the combined coefficient is being defined.

### Method 3: Surface temperatures equal to air-temperature

Kimura [15] gives typical values for a combined coefficient  $h_i$  under the

## THEORETICAL FOUNDATION OF A NOVEL METHOD

assumption that "all inside surfaces of the room enclosure elements, other than that of the exterior wall concerned, stay at the same temperature as the room air". In this case the convection from the other surfaces are neglected and the combined coefficient is found to be the sum of the convective and radiative coefficients, which follows immediately from figure 2.4a if  $T_2 = T_1$ :

$$h_i^i = h_c + h_r. \quad (2.11)$$

For  $n$  surfaces, each of unit area, one correspondingly finds:

$$h_i^i = h_c + (n-1) \cdot h_r. \quad (2.12)$$

These results are clearly similar to that of method 1 given by (2.8).

### Method 4: Isothermal surfaces

Another assumption which yields a combined coefficient is the assumption that all the interior surfaces are at the same temperature. This assumption will be realized in the circuit of figure 2.4a when the radiative coefficient is very large compared to the convective coefficient.

Condition	Combined Coefficients [W/m <sup>2</sup> ·K]		
	2	4	6
1) Airtight enclosure	11.5	19.5	27.5
2) Adiabatic surfaces	5.4	9.1	12.8
3) Surfaces equal to air	7.5	15.5	23.5
4) Isothermal surfaces	7.0	14.0	21.0

**TABLE 2.1** Numerical values for various definitions of the combined heat transfer coefficient, with  $h_c$  assumed  $3.5 \text{ W/m}^2 \cdot \text{K}$ , and  $h_r$   $4 \text{ W/m}^2 \cdot \text{K}$ .

In this case, radiation is so effective that heat conducted from an exterior surface, and arriving at an interior surface, is radiated immediately to all other interior surfaces, and then convected from all

## THEORETICAL FOUNDATION OF A NOVEL METHOD

surfaces to the interior air. The combined coefficient for  $n$  surfaces of unit area is in this case:

$$h_i^c = n \cdot h_c \quad (2.13)$$

In table 2.1 we show the combined interior coefficients for 2 and 6 surfaces of unit area, as obtained from the various definitions. A typical value for  $h_c$  is  $3.5 \text{ W/m}^2 \cdot \text{K}$ , and for  $h_r$ ,  $4 \text{ W/m}^2 \cdot \text{K}$ . The table was constructed with these values and under the assumption all areas are  $1 \text{ m}^2$ .

At this stage it is clear that the concept of a combined heat transfer coefficient is highly dependent on certain assumptions and that various assumptions lead to different definitions of the combined coefficient. Mitalas [32] has assessed the influence of the convection coefficient and the combined coefficient by extensive simulation on an analog computer. He comes to these conclusions: "...the cooling load required to maintain the room air temperature constant is quite insensitive to changes in the inside surface convection coefficients." On the combined coefficient he remarks: "The results show that it is not possible to select a particular value of the combined heat coefficient ( $h_i$ ) which would approximate the radiant heat interchange by the inside room surfaces equally well in all situations." He also remarks: "The other disadvantage of the combined coefficient ( $h_i$ ) is that the value of ( $h_i$ ), which gives a good approximation of the cooling load, introduces large errors in the calculation of the surface temperatures." This last remark is of great importance; it indicates that one should not expect a single circuit to be equally applicable to temperature predictions and load estimation.

Mathews and Richards [10] state that they assume the interior surfaces are isothermal. Their combined coefficient should therefore correspond to  $h_i^c = n \cdot h_c$  above. In practice, one can determine empirical values of interior surface coefficients for a specific thermal model by selecting values for a best fit of the predictions with measured data. The values

## THEORETICAL FOUNDATION OF A NOVEL METHOD

of the internal film coefficients, as given by Mathews and Richards, were presumably determined in this manner to suit the preceding CR-method [6].

It must be borne in mind that the convection coefficient is dependent on air flow speed, and therefore, in the case of natural convection, also on the temperature differences between the surfaces which drive the convection. Obviously, it is also dependent on ventilation rates. The radiation coefficient is to the third power dependent on the mean absolute surface temperatures (2.5). The use of constant empirical film coefficients can only be justified by verification experiments. The excellent results obtained by Mathews and Richards are therefore in agreement with the above quoted statement of Mitalas that the thermal response is fairly insensitive to these coefficients.

### 2.4.4 The Forcing Functions

The various forcing functions which influence the indoor environment have been described by Mathews and Richards [10] and also by many others. We restate them here for sake of completeness.

#### a) Sol-Air Temperature

The primary thermal forcing function on earth is radiation from the sun. The exterior surfaces of the building will both receive electromagnetic energy from the sun, as well as reradiate some of this energy to deep space and other surrounding surfaces<sup>9</sup>. The irradiation consists of both direct radiation from the sun and indirect or *diffuse* radiation from other hot surfaces. The radiation from the sun is mostly in the spectral range with wavelength 0.1 to 3  $\mu\text{m}$  while the *longwave* emissions are at wavelengths of around 10  $\mu\text{m}$  [29]. The radiation exchange is in accordance with the Stefan-Boltzman law given in §2.4.3.

---

<sup>9</sup>These results are well known. We include it for the sake of completeness and to aid newcomers to the science of building thermal response.

## THEORETICAL FOUNDATION OF A NOVEL METHOD

The dominant physical features of the exterior surface which determines the radiation is the shape factor  $F$ , which in this case can be taken as a shading factor, and the emissivity  $\epsilon_w$  of the surface.

Besides radiation, the temperature of the exterior surface is determined also by convective heat exchange with the surrounding air. This convective exchange is highly dependent on the movement of air over the external surfaces and the air temperature. This convection is also governed by Newton's law of cooling, see §2.4.3., with an external convection coefficient,  $h_{ce}$ .

To enable a unified treatment of radiation and convection Mackey and Wright [33] introduced the concept of sol-air temperature. The effects of convection, as well as direct and indirect radiation, are combined by defining an equivalent forcing function, the sol-air temperature  $T_{sa}$ , together with an appropriate film coefficient  $h_o$ .  $T_{sa}$  is a fictitious temperature which together with the film coefficient, will give the same rate of heat transfer to the surface, as would result from convection and radiation combined. (In electrical terminology, it represents a Thevenin equivalent source.)  $T_{sa}$  is defined by consideration of the external wall surface temperature when no heat flows through the wall (adiabatic surface). In this case a heat balance at the wall surface gives:

$$q_s = q_l + q_c \quad (2.14)$$

where  $q_s = \alpha I_s$  is the incident radiation from the sun and other hot objects,  $\alpha$  is the absorptivity,  $I_s$  is the irradiance on the surface,  $q_l = \epsilon \cdot (T_w^4 - T_s^4)$  is longwave re-radiation to cooler objects and the sky,  $\epsilon$  is the emissivity,  $T_w$  is the wall surface temperature,  $T_s$  the mean surrounding (sky) temperature, and  $q_c = h_{ce} \cdot (T_w - T_o)$  is convective heat losses to the air,  $h_{ce}$  is the external convection coefficient and  $T_o$  the ambient air temperature. The longwave radiative heat transfer can be represented with an equivalent radiation coefficient  $h_{re}$  in the manner described in §2.4.3. If we define the external film

## THEORETICAL FOUNDATION OF A NOVEL METHOD

coefficient  $h_o = h_{ce} + h_{re}$  the sol-air temperature equals  $T_w$  as defined above:

$$T_{sa} = \frac{\alpha \cdot I_s + h_{re} \cdot T_s + h_{ce} \cdot T_o}{h_o} \quad (2.15)$$

Some authorities which published lists of external heat transfer coefficients are [1,2,6,15,31].

The external coefficient  $h_o$  is obviously determined by exterior radiant temperatures and flow-rates. Nevertheless, many researchers [10,8 and references just cited] indicate that a constant value between 15 and 25 W/m<sup>2</sup>·K is often adequate.

The sol-air temperature will differ from one external surface element to another. (E.g. the intensity of sun light on northern and southern walls is different). In a general model, each element of the shell which is subject to a different sol-air temperature, must receive individual treatment, and be individually represented in the thermal model (see figure 2.7). The reduction of the various sol-air forcing functions of the model to one effective forcing function is discussed in §2.5.4.

### b) Ventilation

The most problematic aspect of the prediction of thermal performance of buildings is natural ventilation. Ventilation will significantly affect the thermal interior temperature by direct convection of interior heat to and from the outside air. The problem is not that the physical mechanism of heat transport is unknown, but rather, the accurate prediction of ventilation rates. Ventilation is a strong function of local outdoor air flow, placing and type of windows, occupant behavior etc. Kimura [15] reviews existing models for infiltration. In [1] various procedures for the estimation of ventilation rates are given. These models can only be used if adequate meteorological data are available. Fortunately, for a design tool, the problem can be circumvented by assuming 'standard' conditions or worst case conditions. Nevertheless, it is important to have some idea

## THEORETICAL FOUNDATION OF A NOVEL METHOD

of typical ventilation rates in order to be able to specify standard conditions. In this study we are interested in the mathematical modelling of heat flow in buildings and will not investigate ventilation in detail. It suffices to state that provided ventilation rates are known, ventilation is easily included in the two port model of the simple building by adding another *ventilation resistance*, and a temperature source, as in the model of Mathews and Richards (figure 2.1). The new temperature source is equal to the entry temperature of the ventilating air, which will normally be the outdoor air temperature  $T_o$ . The resistance through which  $T_o$  acts is the ventilation resistance  $R_v$  which is determined by the rate of heat transport by ventilation, which is again directly related to the air change rate per hour *ach* via (from [10])<sup>10</sup>:

$$R_v = 3.6/Vol \cdot \rho \cdot c_p \cdot ach \quad (2.16)$$

where *Vol* is the volume of the zone in [m<sup>3</sup>], *ach* the air change rate per hour [/h],  $\rho$  is the air density [kg/m<sup>3</sup>], and  $c_p$  the specific heat of the air at constant pressure [kJ/kg·K].

The main problem is clearly the determination of the air change rate as a function of the exterior wind, windows, building orientation etc. This problem is also discussed in [10]. ASHRAE [1] has published some estimates of air infiltration which take the form of power laws with respect to the pressure difference across the building, but states: "Unfortunately it is very difficult to determine accurate values of flow opening area and pressure difference for actual buildings, which consist of complex air leakage passages."

Although ventilation is a very important aspect in the thermal performance of buildings (it may constitute as much as 30% of the heating load [1, 28 p140]), it is, as we have stated, outside the scope of this thesis. More relevant here is the uncertainty which unknown

---

<sup>10</sup>These results are well known. We include it for the sake of completeness and to aid newcomers to the science of building thermal response.

## THEORETICAL FOUNDATION OF A NOVEL METHOD

ventilation rates enforce on thermal models of buildings. Even 'air-tight' conditioned buildings are still subject to unknown infiltration rates of outside air through the pores of the structure. It makes little sense to attempt to predict all other aspects of heat transfer in buildings with extreme accuracy, when a very basic component is largely unknown, and will in all probability never be completely known [10]. It follows that the accuracy of the simple model of Mathews and Richards should not be judged in absolute terms, but rather, in terms of the usefulness of the method as a design tool. It is, accordingly, not the objective of this thesis to express a final judgment on the accuracy of the method, but rather, to investigate the theory behind the method to gain a better understanding of the method and its limitations.

### c) Internal Loads

Besides ventilation, other internal loads may influence the interior temperature. Electrical equipment, people, air conditioning etc. adds to the internal load. The most important component is usually the rays of sunlight penetrating through windows. All these effects are easily included in the thermal model by adding the necessary sources and resistances (see [10] and figure 2.1). It is a major benefit of the simple thermal model of Mathews and Richards that it allows such easy extension. In chapter 3 of this thesis the ease with which the method is extended to include – in this case – structural storage is demonstrated.

### 2.4.5 A Comprehensive Model

We have modelled the walls of a rudimentary building, consisting of just two opposing walls, with two ports which are exact solutions of the diffusion equation for sinusoidal forcing functions. The only assumption for heat flow through the walls is that the one dimensional treatment is adequate. Our chief aim with this model is to investigate a) the lumping of conductance and capacitance of the massive parts of the building, and b) the temperatures of the interior surfaces. Obviously, the floor and earth underneath will contribute to the total heat storage capacitance of a building in contact with the ground, and, the roof may

## THEORETICAL FOUNDATION OF A NOVEL METHOD

introduce further complications. However, these issues fall outside the scope of this study.

We use the simple structure, consisting of only two opposing surfaces, to demonstrate comprehensive modelling of thermo-flow in buildings. In figure 2.6 the complete model for the simple building structure is shown. This model is directly related to figure 2.2 but includes separate internal mass. We only include the sol-air sources since the others are not needed for this investigation. This thermo-flow model is very similar to the model of Athienitis [8] and also to the 'room' model of ASHRAE [28], but it is highly simplified and unrealistic because of the presence of only two walls. It is, however, adequate for demonstrating the general points we wish to investigate.

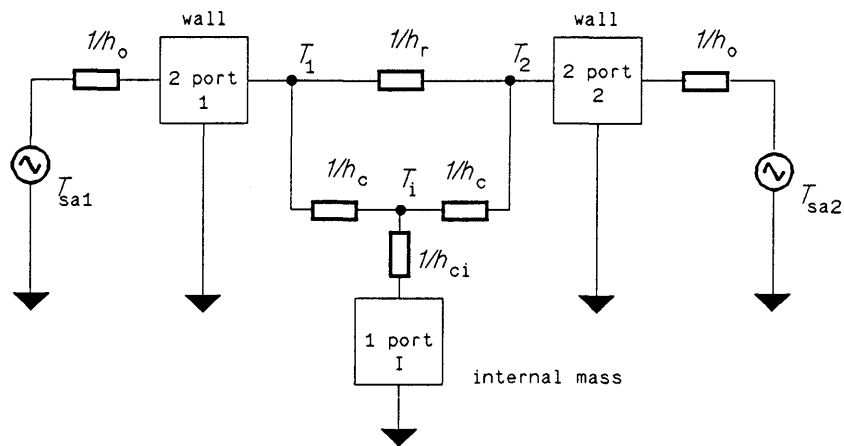


**FIGURE 2.6** Comprehensive thermo-flow model for a simple single zone structure, with only two external surfaces, and no infiltration or ventilation.

## THEORETICAL FOUNDATION OF A NOVEL METHOD

The interior surfaces of the two walls in figure 2.6 are inter-connected with radiative coefficients to each other and with convective coefficient to the interior air as discussed previously in §2.4.3. The interior air and other interior massive elements are represented by the one port  $I$ , which can also include contributions from partitions separating neighbouring zones (see chapter 4). One conspicuous omission of the model of Mathews and Richards is the absence of an explicit capacitance for internal mass. It is an important assumption inherent in the model of figure 2.1 that interior mass can be combined with the mass of the shell, "in order to provide an economical description of empirical facts" [11]. This assumption is discussed in more detail in §2.6.1.

As said before, the only forcing functions we take into consideration are the sol-air temperatures on each external surface. We have not included the intricacies of ventilation, interior loads, floors with ground contact etc. since the objective with the comprehensive model is not accurate modelling *per se*, but rather the investigation of certain critical assumptions of the model of Mathews and Richards.

It is fairly easy to extend the comprehensive model to include interconnected zones. Normally, in the single zone approach, a fraction of the storage capacitance of the partitions between the zones is included as internal mass in each zone; since it is assumed that the temperatures in adjacent zones are approximately equal. If this is not the case, then, instead of including the partitions between the zones in the internal mass, they should be used as connections between the various zones, as described in chapter 4.

### 2.4.6 Solution of the Comprehensive Model

The solution of the model of figure 2.6 involves standard two port theory as discussed in §2.5.3. The two ports for laminated walls are

## THEORETICAL FOUNDATION OF A NOVEL METHOD

evaluated by multiplying the individual cascade matrices of the laminae<sup>11</sup>, and the two ports for surfaces in parallel are obtained by converting to the admittance matrix representation and adding the individual matrices of the surfaces. Surfaces with different external forcing functions are combined into an admittance matrix, which gives the interior temperature and heat-flows through the surfaces by matrix inversion. The procedure was described by Athienitis [8].

We shall not solve the model of figure 2.6 here. We are not really interested in results for this highly simplified two wall structure. Our objective is to derive the simple model of Mathews and Richards from this comprehensive thermal model.

### 2.5 Derivation of The Model of Mathews and Richards from the Comprehensive Model

We have described a rather comprehensive two-port model for thermo-flow in the simple building structure. In this section, it is attempted to derive the parameters of the simple model of Mathews and Richards, from this comprehensive model, by suitable assumptions and simplifications. The assumptions of Mathews and Richards were stated in §2.3. It is the objective of this section to assess the validity of these assumptions, and to present possible alternatives for determining the circuit parameters of figure 2.1.

#### 2.5.1 Single Zone Approximation

The most basic assumption of Mathews and Richards is the single zone assumption, which enables ignoring the effect of neighbouring zones. The assumption boils down to assuming interior surface temperature differences, in- and between the zones, are far smaller than external-internal temperature differences. It is obviously not an assumption which can be substantiated by theoretical arguments or even

---

<sup>11</sup>Two-ports, cascade- and admittance matrices are defined in §2.5.3 b and e.

## THEORETICAL FOUNDATION OF A NOVEL METHOD

empirical considerations. Interior surfaces which are e.g. irradiated through windows, will obviously experience similar temperatures as external surfaces. According to [8] air temperature differences between 1 K and 3 K will exist between two rooms, even though they may be connected through an open doorway.

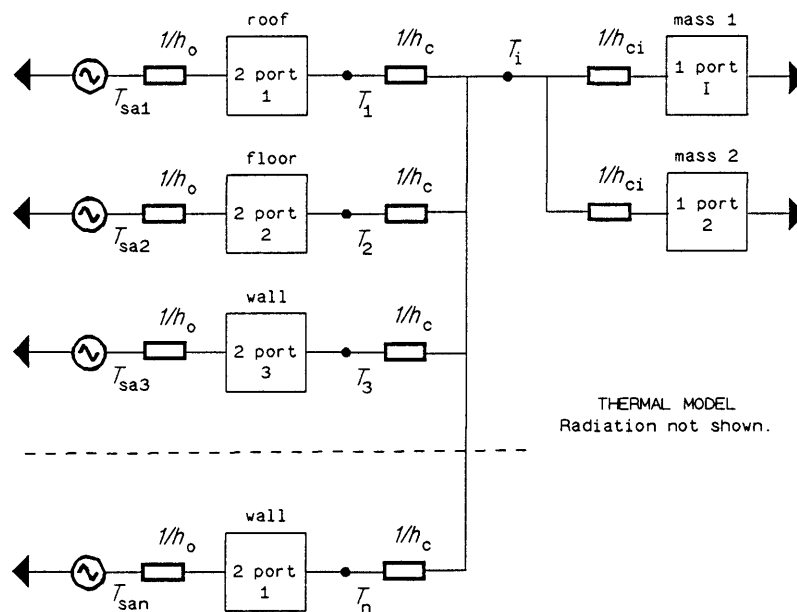


**FIGURE 2.7** Two port model for enclosure with more than just two walls. The interior radiative heat flow between surfaces are not shown. It is assumed the film coefficients are equal for all the surfaces.

The single zone assumption is satisfied when all the zones are subject to active climate control, with identical set point temperatures. It is also justified when the partitions between the zones are insulators, so that no inter-zone heat flow occurs. In passive buildings, it can not be

## THEORETICAL FOUNDATION OF A NOVEL METHOD

justified as an *a priori* assumption. In [10] it is indicated that the utility of the multizone approach lies in its simplicity, and that its use is justified solely by the useful results obtained with this assumption; as testified by validation studies. In this chapter, we shall confine ourselves to a single zone treatment. Extensions to more zones are discussed in chapter 4.

### 2.5.2 The Effective Heat Storage Capacitance

In the comprehensive model of the two surface structure, figure 2.6, the massive walls are represented by a two port. Similarly, actual structures with more than just two walls, require a two port descriptor for each wall as in figure 2.7.

In the simple model of figure 2.1 a single capacitor with associated resistances are used to describe all the walls as well as internal mass. In the reduction of the network of figure 2.7 to that of figure 2.1, two alternative sets of assumptions can be used. They are:

- i) the surfaces of the massive parts contributing to the stored heat in the building are always approximately at the same temperature,
- ii) the distributed elements can be approximated with a lumped single resistance–capacitance network.

Alternatively, the following assumption can be invoked:

- iii) it is possible to find a single resistance–capacitance network which will adequately describe the thermal response of the building.

These assumptions lead to considerable reduction in the complexity of the network. It enables a description of the thermo–flow with a simple, first order, ordinary differential equation instead of a system of partial differential equations.

With the first alternative of the two sets of assumptions, a simple network is derived by progressively simplifying the comprehensive model.

## THEORETICAL FOUNDATION OF A NOVEL METHOD

Assumption i) enables all the different masses to be combined in a single large mass and assumption ii) allows an RC representation. With this method one would try to couple the elements directly to certain characteristics of the physical construction, e.g.  $R_0$  in figure 2.1 represents the shell resistance,  $C$  represents the massive elements etc. The second alternative, iii), leads to an interpretation of the model which is less physical. With this assumption, one simply assumes the network of figure 2.1 can be used as an abstract representation of the thermo-flow, and attempts to find values for the elements which yields a good fit of the network to the theoretical or empirical response of the structure. In this case one does not try to give physical substance to the elements. (This latter alternative is often employed in empirical methods where the values of the parameters are determined by regression e.g.[6,36]). Since Mathews and Richards give a physical interpretation of their parameters, and this physical interpretation is considered a decided advantage, the first method through assumptions i) and ii) will be followed.

We have indicated above how assumptions i) and ii) may be used to derive the circuit of figure 2.1. The procedure will be discussed in more detail shortly. But first, let us deal with the second alternative, assumption iii). The various film resistances in figure 2.7 can be absorbed in the two ports describing the walls. Athienitis [8] has shown that this model can be transformed into one where the various forcing functions are combined in one effective source, which together with the effective admittance matrix of all the walls, determine the interior temperature. Exactly the same procedure can then be carried out with the simple circuit of figure 2.1. The correct resistances and capacitance for the simple network can now be determined by matching the two versions of the admittance matrix, since the simple network and the comprehensive network must yield similar results. In general, it will not be possible to select values for the resistances and capacitances for an exact match. It will be necessary to determine the best values for an

THEORETICAL FOUNDATION OF A NOVEL METHOD

optimum fit [21,36]. The procedure is very similar to the method described in §2.5.3 d and will be omitted here. Suffice to say that, in principle, it is possible to obtain any sort of circuit description for the thermo-flow problem in this way. The most general method requires the analytic solution of the comprehensive thermal network, and then obtains an approximate RC network for this comprehensive network by means of network synthesis [34].

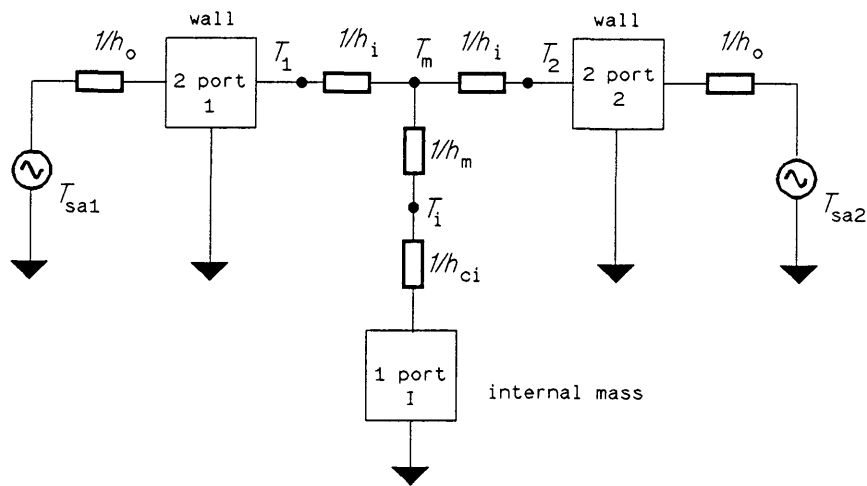


**FIGURE 2.8a** Model of figure 2.6 with internal heat flow simplified via  $\bar{V} - Y$  transform.

Assumptions i) and ii) allow the determination of an equivalent network in a less abstract manner. If the surface temperatures of the massive elements are approximately equal, the network of figure 2.6, reduces to that of figure 2.8b after first applying the  $\bar{V}$ - $Y$  transform, to obtain the circuit of figure 2.8a. The exact condition required is: the temperatures on both sides of the two port must be equal for all the elements, that is, all the external surfaces must be at one temperature and all the internal surfaces at another. The masses are then combined by

## THEORETICAL FOUNDATION OF A NOVEL METHOD

transforming to the admittance representation and adding the matrix elements as described in §2.5.3 d. The forcing functions on the exterior walls are combined in a single effective forcing function, and the interior resistor network is simplified as in figure 2.8c. This circuit is now very close to the model of Mathews and Richards, when the internal sources and ventilation in their model (figure 2.1) is ignored. The final step is the simplification of the two port representation of the masses in figure 2.8c to the single RC representation in figure 2.1. It will be discussed later. Note that the procedure is also applicable to zones with any number of surfaces.

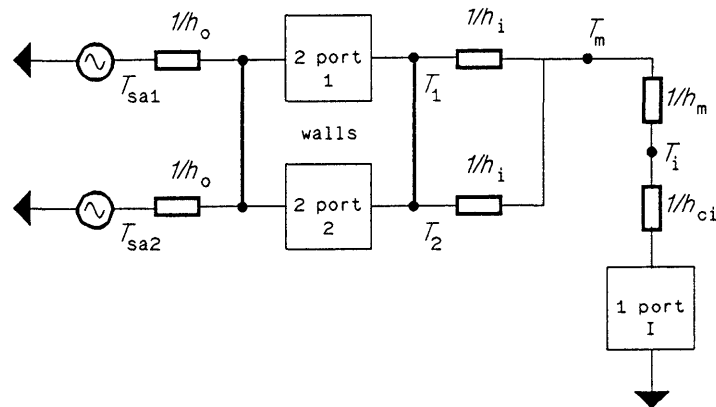


FIGURE 2.8b Circuit with surface temperatures assumed equal.

Another method of reduction, in complexity and accuracy more or less in between the exact method of Athienitis [8], and the method of the previous paragraph, is given in figures 2.9 a and b, starting again with the circuit of figure 2.8a. In this method, it is only assumed that the internal surfaces are isothermal. The only difference between this third method and the method in [8] is the treatment of interior heat flow. The combined two port for the walls, and effective exterior forcing function, is obtained by finding the equivalent Thevenin representation

THEORETICAL FOUNDATION OF A NOVEL METHOD

of all heat flows, incident from the exterior surfaces, on the – assumed isothermal – interior surfaces.

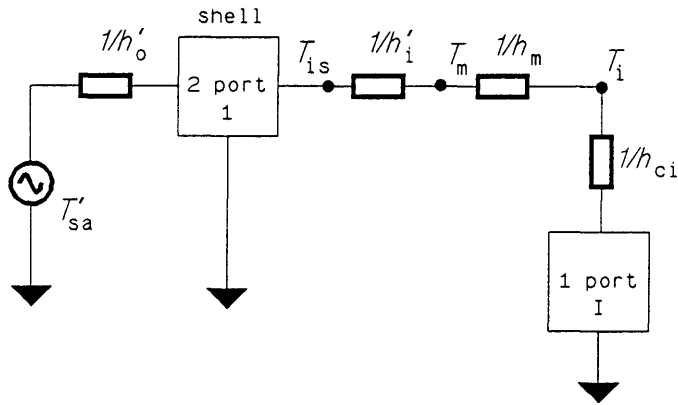


FIGURE 2.8c Final simplified circuit.

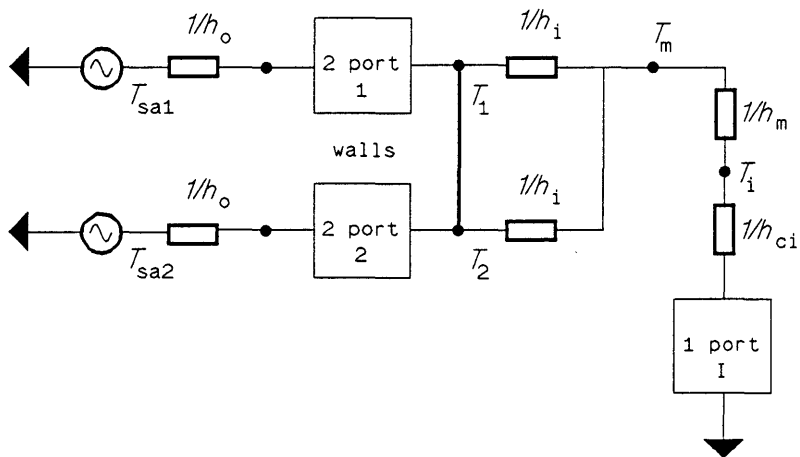
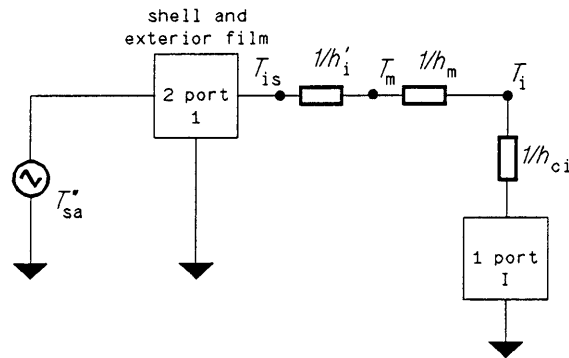


FIGURE 2.9a Reduction with isothermal interior surfaces.

## THEORETICAL FOUNDATION OF A NOVEL METHOD



**FIGURE 2.9b** Final simplified circuit with isothermal interior surfaces.

Clearly all three methods yield equivalent circuit topologies. The parameters of the three methods will however be different and will reflect the different assumptions. Obviously, the first method will be the most accurate and the second the least. Mathews and Richards state that their method assumes isothermal interior surfaces and it should therefore be equivalent to the last method. In fact, it is not so easy to determine which method is actually approximated by them. The topologies are the same, so the formulas employed to obtain numerical values for the different network elements must be compared. If this is done, (see §2.5.3e) it is found that their method corresponds more to the second method than the third. This indicates that inherent in the model of figure 2.1 is also the assumption that the temperatures of the external surfaces are approximately equal. In fact, since the internal mass is also included in the single  $C$  in figure 2.1, the best expression of the basic assumption is probably: the bulk temperatures of all the massive elements of the buildings is assumed fairly equal.

## THEORETICAL FOUNDATION OF A NOVEL METHOD

In the circuits of figures 2.8 and 2.9 the massive elements are still modelled with two ports. It was indicated above, that one method for determining an RC lumped equivalent for a two port, is to assume a certain RC form, e.g. the single R and C form used by Mathews and Richards, and then to obtain the two port representation for this assumed form. The definitions of elements are then obtained by matching the two port of the assumed form with the exact two port obtained from the solution of the diffusion equation. Another alternative is to derive an RC equivalent via RC network synthesis techniques. Penman [35] shows that the values of the model parameters can also be obtained from parameter estimation techniques, through measurement of the thermal response. This empirical method has, together with other empirical methods such as [6], the drawback that they can only with confidence be applied to those buildings which were originally included in the empirical studies. It is also possible to find an equivalent lumped circuit representation under the assumption that the frequency of variation of the thermo-flow is small. This technique will be used here and is described in the next section.

In order for the lumped representation to be useful, it is required that the parameters of the circuit be determined in terms of the physical properties of the building elements. The only method which yields an obvious connection between the parameters and the physical properties is when it is assumed that all the massive elements are always at the same temperature. In this case the quantity of stored heat is given by the total available heat capacitance multiplied by the temperature of the massive elements. In other methods the capacitance is not directly related to the physical properties, but theoretically represents the *active heat* stored in the structure. The concept can be clarified by noting that heat stored in a massive wall, which is thoroughly insulated on its interior surface, can not influence the interior temperature. In this case, although the amount of stored heat may be substantial, the active heat is small. The concept is further clarified by figures 2.10 a and b. In

## THEORETICAL FOUNDATION OF A NOVEL METHOD

figure 2.10 a the total amount of stored heat in the wall is given by  $Q_1 = T_w \cdot \rho \cdot c_p$  J/m<sup>3</sup>, where  $T_w$  is the uniform temperature distribution across the wall. If, at a later instant, the temperature distribution changes to the linear profile given by figure 2.10 b, the active stored heat is the heat which took part in the change, it is thus given by the change in the amount of stored heat  $Q_a = \Delta T \cdot \rho \cdot c_p / 2$  J/m<sup>3</sup>. In the next section it is shown that the matrix solutions of the heat conduction equation provides a very useful definition of the active capacitance of a layered structure; if it is assumed that the temperature distribution in each layer remains almost uniform.

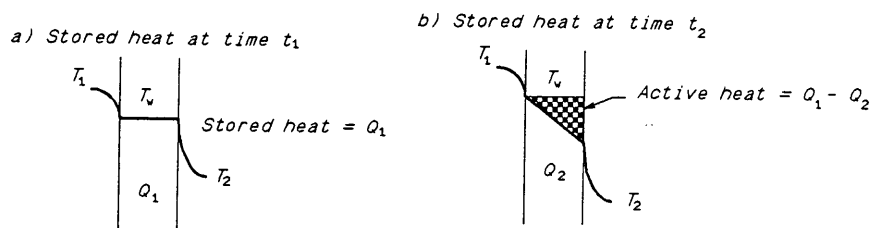


**FIGURE 2.10** The active stored heat is the change in stored heat which accompanies changes in the temperature distribution across the wall.

### 2.5.3 Lumping the Distributed Parameter Structures

One of the most obvious simplifications of the model of Mathews and Richards, figure 2.1, from the comprehensive model of figure 2.6, is the representation of distributed parameter elements with lumped elements. It is highly desirable to obtain a lumped representation of the heat flow

## THEORETICAL FOUNDATION OF A NOVEL METHOD

since the lumped circuit circumvents the problem of solving the partial differential equation for heat conduction. This allows a much simpler solution process and facilitates further extensions of the method to include more complicated active systems.

According to Muncey [3]: "The whole subject (lumping of elements) requires further study to define reasonable limitations within which lumped circuit calculations may be used confidently." In this section, the lumping of distributed parameter networks for 1 dimensional heat flow problems is discussed. The approximations and conditions for accurate lumping are derived. It is shown that the heat flow through the walls of typical building constructions can be modelled with reasonable accuracy with a lumped thermal resistance-capacitance network. Formulas to obtain the values of the lumped circuit elements, from the heat conduction and capacitance values of the materials, are derived.

The discussion is mostly concerned with the lumping of the thermal capacitance of the elements. The conductivities are also important but are less problematic. The thermal response of the building can be regarded as approximately linear, so that the mean and swing thermo-flow components can be handled separately. We assume that the swing component is sinusoidal without loss of generality since any periodic swing can be obtained from a superpositioning of sinusoidal components, according to Fourier's theorem. The total response is given by the superposition of the mean component and the sinusoidal swing. During consideration of the mean heat flow, the capacitive effects play no role and the conductances are the total heat conductance of the wall. For the sinusoidal swing, heat storage effects and capacitances are most important and the conductances should ideally be so defined, that they, together with the capacitance, yield a good approximation of the distributed response. Mathews and Richards retain the values of the conductances which are valid for the mean components also for the

## THEORETICAL FOUNDATION OF A NOVEL METHOD

swing components. This is very convenient but theoretically it might be possible to obtain better lumped representations by choosing both the R's and the C's for the most accurate representation of the distributed elements [34].

One approach to lumping is to choose parameters which will accurately reflect the total available heat storage capacity of the structure. This approach is justified when the Biot number (see next section) of the structure is small. Another approach is to preserve the actual amount of heat stored in the structure. However, it is not important that the value of the lumped C reflects the total available heat capacity of the structure, or the actual amount of stored heat. It is far more important that the correct amount of active heat<sup>12</sup> for a specific change in temperature distribution, be reflected by the value assigned to C. This leads to the concept of *active thermal capacitance*. We shall see that this capacitance is only indirectly related to the physical capacitance of the structure.

### a) Lumping for walls with small Biot numbers

A well known condition for lumping [29] is that the ratio of external resistance (surface resistance) to internal conduction resistance of the wall, must be much less than 1. This condition ensures that the temperature drop across the wall is small relative to the temperature drop across the surface coefficients. The condition is conveniently expressed in terms of the Biot number defined by:

$$Bi = h_c \cdot \Delta x / k \quad (2.17)$$

with  $h_c$  the convective heat transfer coefficient [W/m<sup>2</sup>·K],  $\Delta x$  the thickness of the layer [m], and  $k$  the thermal conductance of the material [W/m·K]. Biot numbers are small for good thermal conductors

---

<sup>12</sup>See the last paragraph of the previous section for a discussion of the concept of active stored heat.

THEORETICAL FOUNDATION OF A NOVEL METHOD

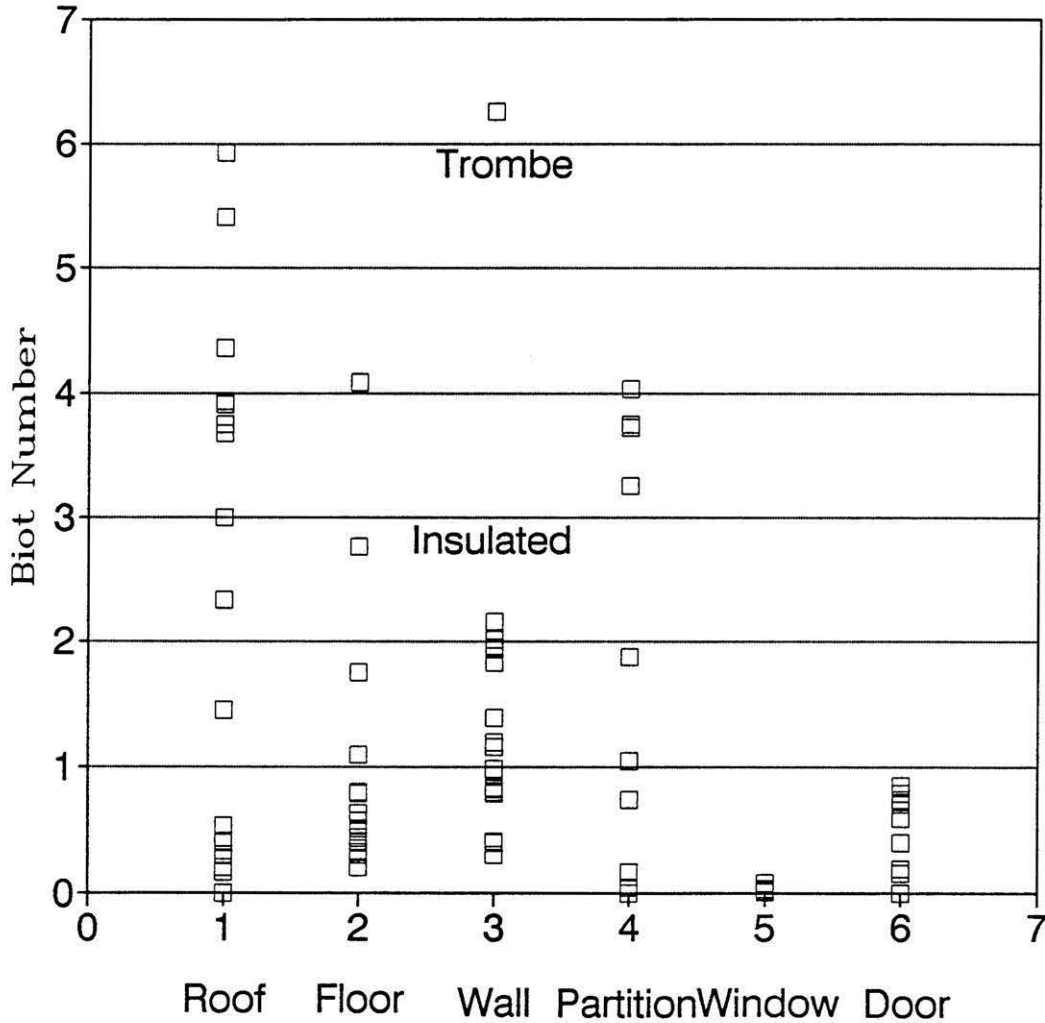


**FIGURE 2.11** Biot numbers for building surfaces with respect to a film coefficient of  $3 \text{ W/m}^2 \cdot \text{K}$ . The walls with  $Bi > 1$  are insulated and cavity walls.

i.e. metallic elements. Most building materials are heat insulators rather than conductors. However, in buildings the surface coefficients also are often quite small and it is not at all obvious that the Biot number for

## THEORETICAL FOUNDATION OF A NOVEL METHOD

walls should be large. If the Biot number of a wall (calculated from the total conduction resistance of all the layers) is small, further assumptions about the temperature distribution across the wall, for the purpose of defining the active capacitance is unnecessary. A small Biot number actually indicates that the interior temperature distribution is approximately uniform. Therefore, the distinction between active stored heat and stored heat can be dropped and all the physical available capacitance can be regarded as active. Calculation of the Biot numbers for many actual structures indicates that this assumption is often justified for uninsulated walls.

In figure 2.11 we show the Biot numbers obtained for 106 different wall structures from 20 existing buildings. These Biot numbers were calculated with reference to a film coefficient of  $3 \text{ W/m}^2\cdot\text{K}$  and from the combined resistance of all the layers of the wall. From the figure we see that for most elements the Biot number is in the numerical range 0 to 2.

Strictly speaking the lumped model is only accurate for Biot numbers below 0.1. Obviously, this condition is not satisfied by most of the elements in the figure, but nevertheless, many important wall constructions have quite small Biot numbers as set out in table 2.2. Notably, we find for brick and concrete walls of thickness up to 110 mm, Biot numbers below 0.5. For a double brick wall of 220 mm the Biot number is close to 1. Examination of these results reveal that it is mostly insulated walls or cavity walls which have Biot numbers above 0.5. In appendix 2A these results are listed. Details of the construction of the walls are available in the file 'results.txt' on the floppy diskette in the back-cover. It is seen that it is mostly the insulated walls and constructions with cavities which have large Biot numbers. These results indicate that for many uninsulated, uniform structures, one could probably take the total heat capacitance of the structure as active capacitance. However, based on the results in

## THEORETICAL FOUNDATION OF A NOVEL METHOD

figure 2.11, one can come to no firm conclusion about the accuracy of lumping, except to say that the Biot numbers are not so large that the possibility of a lumped model must be totally discarded.

Wall Description	Biot number
110 mm brick	0.4
220 mm brick	0.8
330 mm brick	1.2
150 mm concrete	0.3
200 mm concrete	0.4
cavity wall	0.8
9 mm asbestos	0.04

**TABLE 2.2** Biot numbers for some typical buildings walls. The total conduction resistance of the wall is compared to a surface coefficient of  $3 \text{ W/m}^2 \cdot \text{K}$ .

For sinusoidal heat flow, another condition which will also lead to a lumped representation, is that the wavelength of the thermal wave, as it propagates through the walls, is much longer than the thickness of the wall. While this condition is clearly also connected with the conductivity of the wall, it differs from the condition represented by a small Biot number, in that the propagation wavelength is completely determined by the material from which the wall is constructed, and the frequency of the swing. It is independent of the film coefficients. Note that a small Biot number will always ensure accurate lumping, independent of the forcing temperatures, while this condition is only applicable to sinusoidal temperature variations, i.e. to the swing component. To investigate the accuracy of this method the exact solution of the diffusion equation, for sinusoidal temperature variations, is obtained in the next section.

## THEORETICAL FOUNDATION OF A NOVEL METHOD

If the wall is very thick, a single lumped capacitor representation is not possible unless some assumption is made of the variation of the temperature distribution across the wall and the concept of active capacitance is invoked. Another approach is to use a multiple RC representation as discussed in [21 and 36]. In general, the procedure is as follows:

- i) decide on the number of nodes (capacitors) which will be used to represent the distribution,
- ii) choose the values of the lumped elements to minimize the difference of the RC response with the distributed response.

According to Davies [21] three capacitors are quite adequate to represent common building structures. For very thick structures 5 nodes are sometimes required. We wish to avoid using more than one capacitor to represent the walls since the simplicity of the model is largely centered in the single pole treatment of the variable flow.

### b) Exact Solution of the Heat Conduction Equation with Matrices

It is assumed the heat flow through the wall is one dimensional (see discussion §2.4.1). The one dimensional heat conduction equation is:

$$\frac{\partial q_0}{\partial t} = \alpha \cdot \frac{\partial^2 q_0}{\partial x^2} \quad (2.18)$$

where:

$$\alpha = \frac{k}{\rho \cdot c_p}$$

is the thermal diffusivity of the material. Assume a sinusoidally varying heat flow with time (more complicated forcing functions can be built up from sinusoidal functions according to Fourier's theorem) i.e.

$$q_0(t) = q(x) \cdot e^{j\omega t} \quad (2.19)$$

The solution of (2.18) for this input (with time dependency suppressed for notational reasons) is:

$$q(x) = q_1 \cdot e^{-\zeta x} + q_2 \cdot e^{\zeta x} \quad (2.20)$$

where:

$$\zeta = \sqrt{\frac{\omega}{2 \cdot \alpha}} \cdot (1+i) \quad (2.21)$$

## THEORETICAL FOUNDATION OF A NOVEL METHOD

This solution can be rewritten in the equivalent format:

$$q(x) = A \cdot \cosh(\zeta \cdot x) + B \cdot \sinh(\zeta \cdot x) \quad (2.22)$$

For a wall of thickness  $\ell$  the flow into the wall at  $x = 0$  and at  $x = \ell$  is:

$$q(0) = A = q_1 \quad (2.23)$$

$$q(\ell) = q_1 \cdot \cosh(\zeta \cdot \ell) + B \cdot \sinh(\zeta \cdot \ell) = q_2 \quad (2.24)$$

In a similar way one also obtains for the temperature in the wall, which is subject to the same diffusion equation:

$$T(0) = T_1 \quad (2.25)$$

$$T(\ell) = T_1 \cdot \cosh(\zeta \cdot \ell) + D \cdot \sinh(\zeta \cdot \ell) \quad (2.26)$$

At the surfaces of the wall we define the following matrix description of the flows and temperatures:

$$\begin{bmatrix} T(\ell) \\ q(\ell) \end{bmatrix} = \begin{bmatrix} \mathcal{A} & \mathcal{B} \\ \mathcal{C} & \mathcal{D} \end{bmatrix} \cdot \begin{bmatrix} T(0) \\ q(0) \end{bmatrix} \quad (2.27)$$

Or in vector/matrix notation:

$$W(\ell) = T \cdot W(0) \quad (2.28)$$

where:  $W(x) = \begin{bmatrix} T(x) \\ q(x) \end{bmatrix}$  and  $T = \begin{bmatrix} \mathcal{A} & \mathcal{B} \\ \mathcal{C} & \mathcal{D} \end{bmatrix}$

The  $[\mathcal{A} \ \mathcal{B} / \ \mathcal{C} \ \mathcal{D}]$  or  $T$  matrix is known as the transmission or cascade matrix which gives the values of the heat flow and temperature at  $x = \ell$  from the specified values at  $x = 0$ . The cascade matrix is symmetrical for symmetric structures. It is a very convenient two port representation of the solution of the diffusion equation. Note, we define the flow at surface  $x = \ell$  into the wall and at surface  $x = 0$  out of the wall as in figure 2.12, this convention is often used but may differ from others in the literature. The cascade matrix is one of a family of two-port descriptions of the sinusoidal heat flow through the wall. A general theory for complicated systems of coupled two ports exists. For a thorough discussion of these methods see [8 and 35].

THEORETICAL FOUNDATION OF A NOVEL METHOD

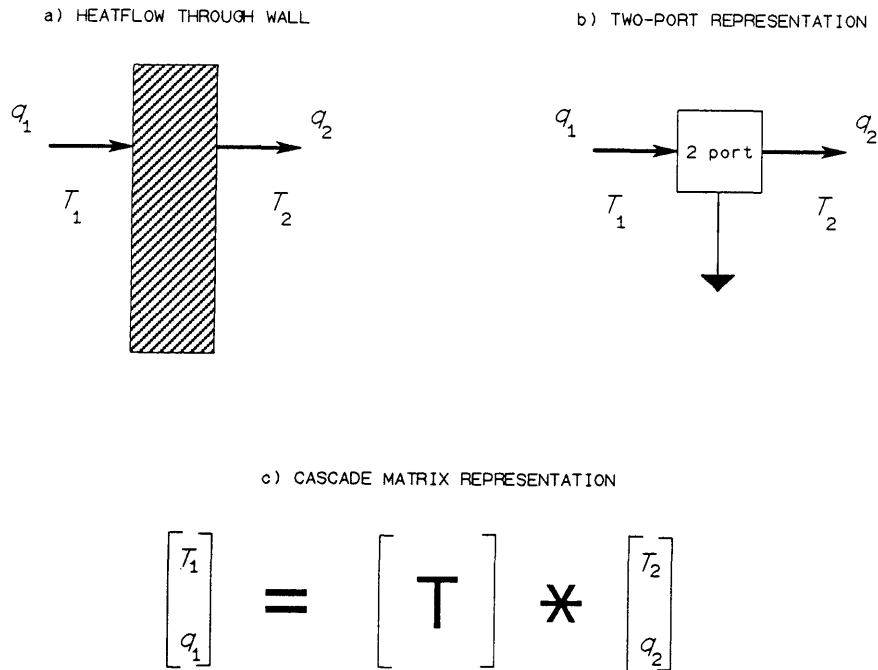


**FIGURE 2.12** The cascade matrix or transmission matrix. A two port representation of the solution of the heat conduction equation.

The values of the matrix elements are calculated from (2.22) to (2.26) together with the heat flux equation (Fourier's law of conduction):

$$q(x) = k \cdot \frac{\partial T(x)}{\partial x} \tag{2.29}$$

Differentiating (2.26) with respect to  $\ell$ :

$$\begin{aligned} k \cdot \frac{\partial T(\ell)}{\partial \ell} &= q(\ell) \\ &= k \cdot \zeta \cdot [T_1 \cdot \sinh(\zeta \cdot \ell) + D \cdot \cosh(\zeta \cdot \ell)] \end{aligned} \tag{2.30}$$

Comparison of this equation with (2.16) gives:

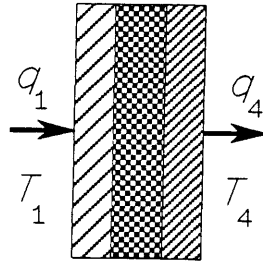
$$B = k \cdot \zeta \cdot T_1 \quad \text{and} \quad D = q_1 / (k \cdot \zeta) \tag{2.31}$$

Therefore the values of the matrix elements are:

$$\begin{aligned} \mathcal{A} &= \cosh(\zeta \cdot \ell) & \mathcal{B} &= Z_0 \cdot \sinh(\zeta \cdot \ell) \\ \mathcal{C} &= 1/Z_0 \cdot \sinh(\zeta \cdot \ell) & \mathcal{D} &= \cosh(\zeta \cdot \ell) \end{aligned} \tag{2.32}$$

## THEORETICAL FOUNDATION OF A NOVEL METHOD

a) A LAMINATED STRUCTURE



b) TWO-PORT REPRESENTATION

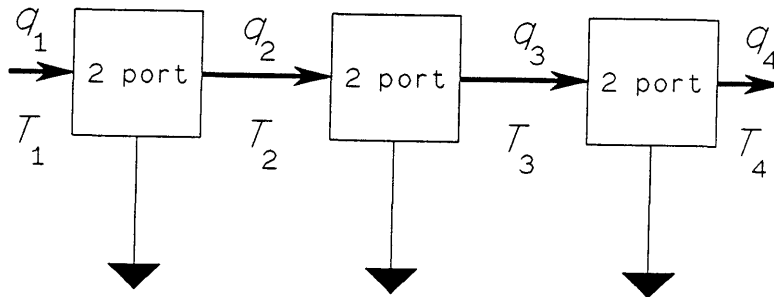


**FIGURE 2.13** Cascade matrix for layered structure. The heat-flow is continuous through the structure and the temperatures at the interfaces are equal. Therefore the cascade matrix for the combined structure is the product of the matrices of the layers.

with  $Z_0$  the *characteristic thermal impedance* of the structure defined by:

$$Z_0 = \frac{1}{k \cdot \zeta} = \frac{1}{\sqrt{i \cdot \omega \cdot k \cdot c_p \cdot \rho}} = \frac{1}{\sqrt{2 \cdot \omega \cdot k \cdot c_p \cdot \rho}} \cdot (1 - i) \quad (2.33)$$

$Z_0$  is an important property of the material and gives the ratio of

## THEORETICAL FOUNDATION OF A NOVEL METHOD

temperature over heat flow anywhere on a semi-infinite slab.

The above equations give the exact solution for the 1 dimensional sinusoidal heat flow problem. The advantage of the cascade matrix representation is now evident:- when the wall consists of various layers laminated together, the heat flow into layer  $j$  equals the heat flow out of layer  $i$  and the temperatures at the interfaces must be the same, consequently

$$q_i = q_j \quad \text{and} \quad T_i = T_j. \quad (2.34)$$

The solution for the layered structure of figure 2.13 must then be:

$$W_1 = T_1 \cdot (T_2 \cdot (T_3 \cdot W_4)) = T_1 \cdot T_2 \cdot T_3 \cdot W_4. \quad (2.35)$$

Therefore the  $T$  matrix of the composite structure is:

$$T_c = T_1 \cdot T_2 \cdot T_3 \quad (2.36)$$

and for a general composite consisting of  $n$  layers:

$$T_c = \prod_{i=1}^n T_i. \quad (2.37)$$

### c) Theoretical Values for the Lumped Elements

As indicated before various lumped circuit representations of the wall are possible. Davies [21] discusses the optimum values for lumped models using a minimum mean square error criterion for the elements of the transmission matrix. We derive simpler approximations which turn out to be valid for thin structures.

For the T section of figure 2.14 with resistances  $R$  in the branches and capacitance  $C$  in the trunk the cascade matrix is:

$$T_{rc} = \begin{bmatrix} 1+i \cdot \omega \cdot R \cdot C & 2 \cdot R + i \cdot R^2 \cdot \omega \cdot C \\ i \cdot \omega \cdot C & 1+i \cdot \omega \cdot R \cdot C \end{bmatrix} \quad (2.38)$$

## THEORETICAL FOUNDATION OF A NOVEL METHOD

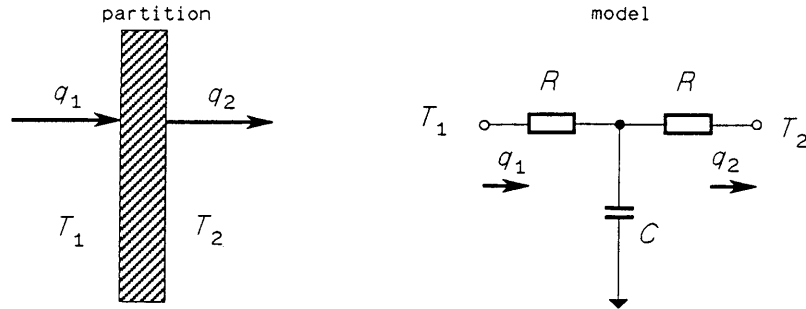


FIGURE 2.14 Lumped RCR T section.

We shall shortly show that this network will adequately represent the distributed parameter system, when the frequency of oscillation  $\omega$  is small, or equivalently, when the wavelength of the thermal wave is very long. In practice this condition reduces to the statement that the thickness of the wall must be small compared to the wavelength of the temperature wave propagating through the wall. Intuitively, the condition is easily understood by reasoning that if the frequency is small, the wavelength is very long and consequently the temperature across the wall will be approximately uniform if the wall is thin. It is a very satisfactory method of lumping since the two elements  $R$  and  $C$  of the lumped model are uniquely identified with the two intrinsic properties of the material,  $k$  and  $c_p$ , exactly as in the case above for small Biot number.

The values of the circuit elements  $R$  and  $C$  are found from the polynomial expansions of the hyperbolic functions. For the  $\mathcal{A}$  and  $\mathcal{D}$  elements of the matrix we need to have for a valid approximation

$$\begin{aligned}
 \cosh(\zeta \cdot \ell) &\approx 1 + i \cdot \omega \cdot R \cdot C. & (2.39) \\
 &= 1 + \frac{(\zeta \cdot \ell)^2}{2!} + \frac{(\zeta \cdot \ell)^4}{4!} + \dots
 \end{aligned}$$

## THEORETICAL FOUNDATION OF A NOVEL METHOD

For small values of  $\zeta \cdot \ell$  the first term in the series expansion of the hyperbolic function suffice. That is when

$$\frac{(\zeta \cdot \ell)^4}{4!} \ll \frac{(\zeta \cdot \ell)^2}{2!} \text{ or } |\zeta \cdot \ell| \ll 12 \quad (2.40)$$

we can put

$$\frac{(\zeta \cdot \ell)^2}{2!} = \frac{i \cdot \omega \cdot \sigma \cdot \rho \cdot \ell^2}{2 \cdot K} = i \cdot \omega \cdot R \cdot C. \quad (2.41)$$

For the  $\mathcal{B}$  element we want

$$\begin{aligned} Z_0 \cdot \sinh(\zeta \cdot \ell) &\approx 2 \cdot R + i \cdot R^2 \cdot \omega \cdot C \\ &= Z_0 \cdot \left[ \zeta \cdot \ell + \frac{(\zeta \cdot \ell)^3}{3!} + \dots \right]. \end{aligned} \quad (2.42)$$

For

$$\frac{(\zeta \cdot \ell)^3}{3!} \ll \zeta \cdot \ell \text{ or } |\zeta \cdot \ell| \ll 6 \quad (2.43)$$

we find

$$Z_0 \cdot \zeta \cdot \ell = \ell/k = 2 \cdot R + i \cdot R^2 \cdot \omega \cdot C. \quad (2.44)$$

Setting

$$\ell/k = 2 \cdot R \quad (2.45)$$

and with the further condition that

$$R \cdot C \cdot \omega \ll 2 \quad (2.46)$$

so that the imaginary part of (2.44) is negligible, we have the approximate value of the  $\mathcal{B}$  element. For the  $\mathcal{C}$  element it is required that

$$\begin{aligned} \frac{\sinh(\zeta \cdot \ell)}{Z_0} &\approx i \cdot \omega \cdot C \\ &= \frac{1}{Z_0} \cdot \left[ \zeta \cdot \ell + \frac{(\zeta \cdot \ell)^3}{3!} + \dots \right]. \end{aligned} \quad (2.47)$$

Again, for  $|\zeta \cdot \ell| \ll 6$  we have

$$\frac{\zeta \cdot \ell}{Z_0} = k \cdot \zeta^2 \cdot \ell = i \cdot \omega \cdot \sigma \cdot \rho \cdot \ell = i \cdot \omega \cdot C. \quad (2.48)$$

These results and the conditions are summarized in table 2.3.

THEORETICAL FOUNDATION OF A NOVEL METHOD

Element	Distributed	Lumped RCR	Equivalent	Conditions
$\mathcal{A}, \mathcal{D}$	$\cosh(\zeta l)$	$1+i\omega RC$	$1+\frac{i\omega c_p \rho l^2}{2K}$	$ \zeta l  \ll 12$
$\mathcal{B}$	$Z_0 \sinh(\zeta l)$	$R(2+i\omega RC)$	$l/K$	$\begin{cases} \zeta l \omega \ll 6 \\ RC \omega \ll 2 \end{cases}$
$\mathcal{C}$	$\frac{\sinh(\zeta l)}{Z_0}$	$i\omega C$	$i\omega c_p l$	$ \zeta \cdot l  \ll 6$

TABLE 2.3 Conditions and lumped RCR representation.

Note that the equations are consistent if we set:

$$C = c_p \cdot \rho \cdot l \quad (2.49)$$

and

$$R = l/(2 \cdot k). \quad (2.50)$$

The most stringent condition for the above relations to be valid is:

$$R \cdot C \cdot \omega = \frac{c_p \cdot \rho \cdot l^2}{2 \cdot k} \cdot \omega \ll 2 \quad (2.51)$$

In practice, the frequency is fixed at  $1/24 \cdot h$  (diurnal frequency) so that this is a condition on the thickness of the structure. In figure 2.15 we show a graph of this condition for various values of the thermal time constant of the structure defined by:

$$\tau = R \cdot C = \frac{c_p \cdot \rho \cdot l^2}{2 \cdot k} \quad (2.52)$$

with  $\omega = 2 \cdot \pi/24$  [1/h].

## THEORETICAL FOUNDATION OF A NOVELMETHOD

Figure 2.15 shows the relation (2.51) in the equivalent format:

$$l \ll \sqrt{48/\pi \cdot \alpha}.$$

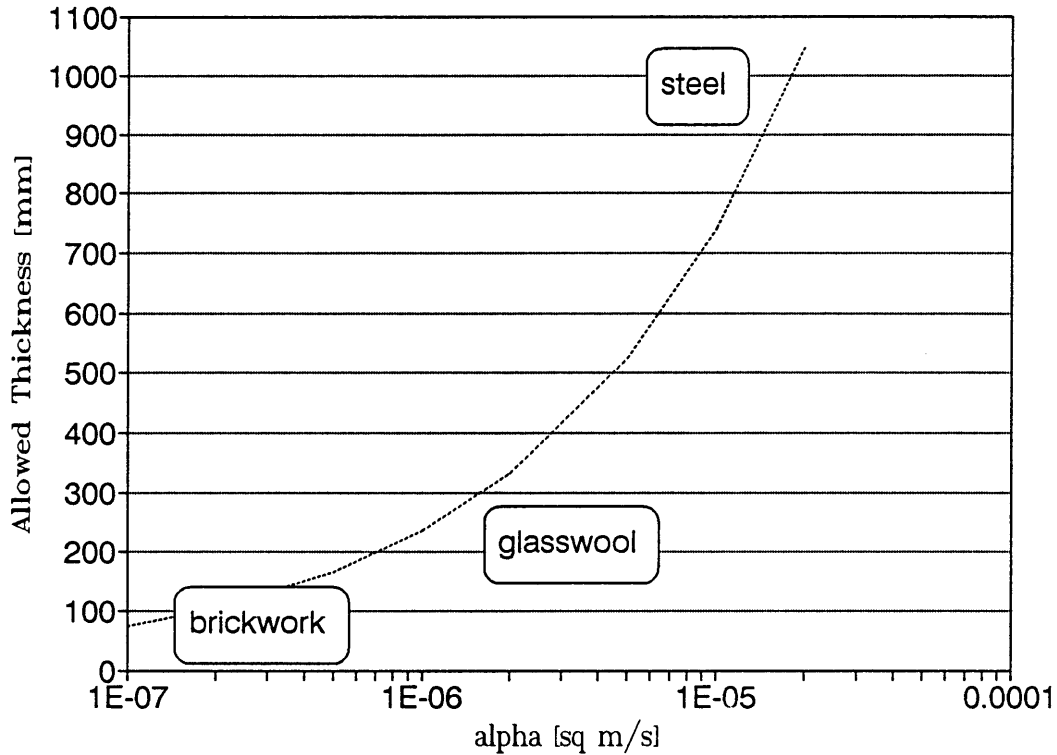


**FIGURE 2.15** The lumping condition  $\tau \cdot \omega = 2$  for various values of  $\alpha$  and  $\omega = 2 \cdot \pi/24$  h.

The condition can also be expressed in terms of the wavelength  $\lambda$  of the sinusoidal temperature wave propagating through the structure:

$$l/\lambda < 1/\pi \quad (2.53)$$

or in terms of the Fourier modulus with respect to the period  $T$ , defined by [27]  $Fo = \alpha \cdot T/\ell^2$ :

$$Fo > \pi/2 \quad (2.54).$$

THEORETICAL FOUNDATION OF A NOVEL METHOD

The Fourier modulus is a characteristic of a specific material at a specific thickness and a specific frequency. For a laminated structure there is no unique definition and one must treat the layers separately. In order to evaluate the above condition for real buildings, the Fourier moduli for over 200 laminae of existing buildings were calculated. The results are given in figure 2.16, with numerical details in appendix 2B.

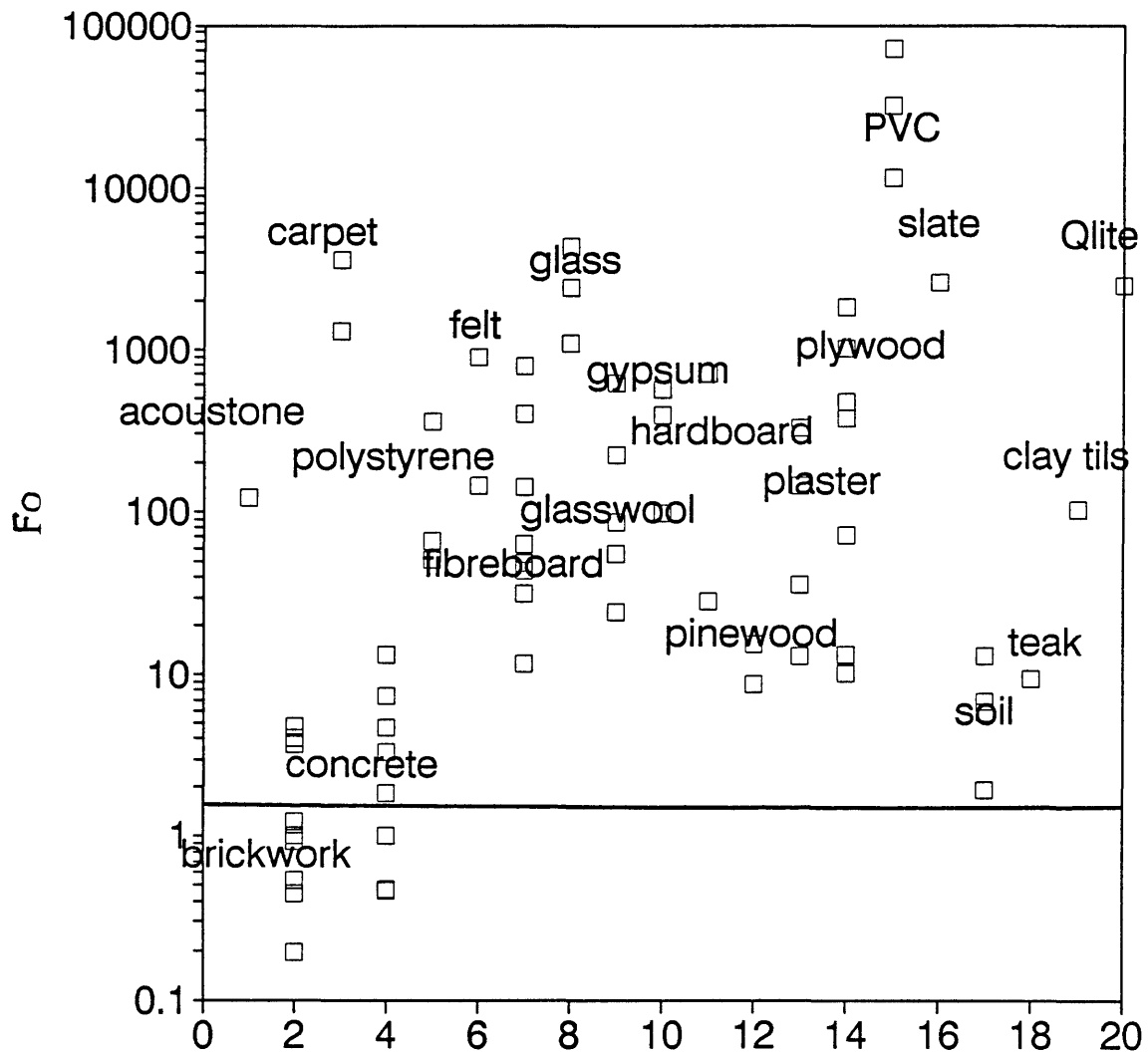
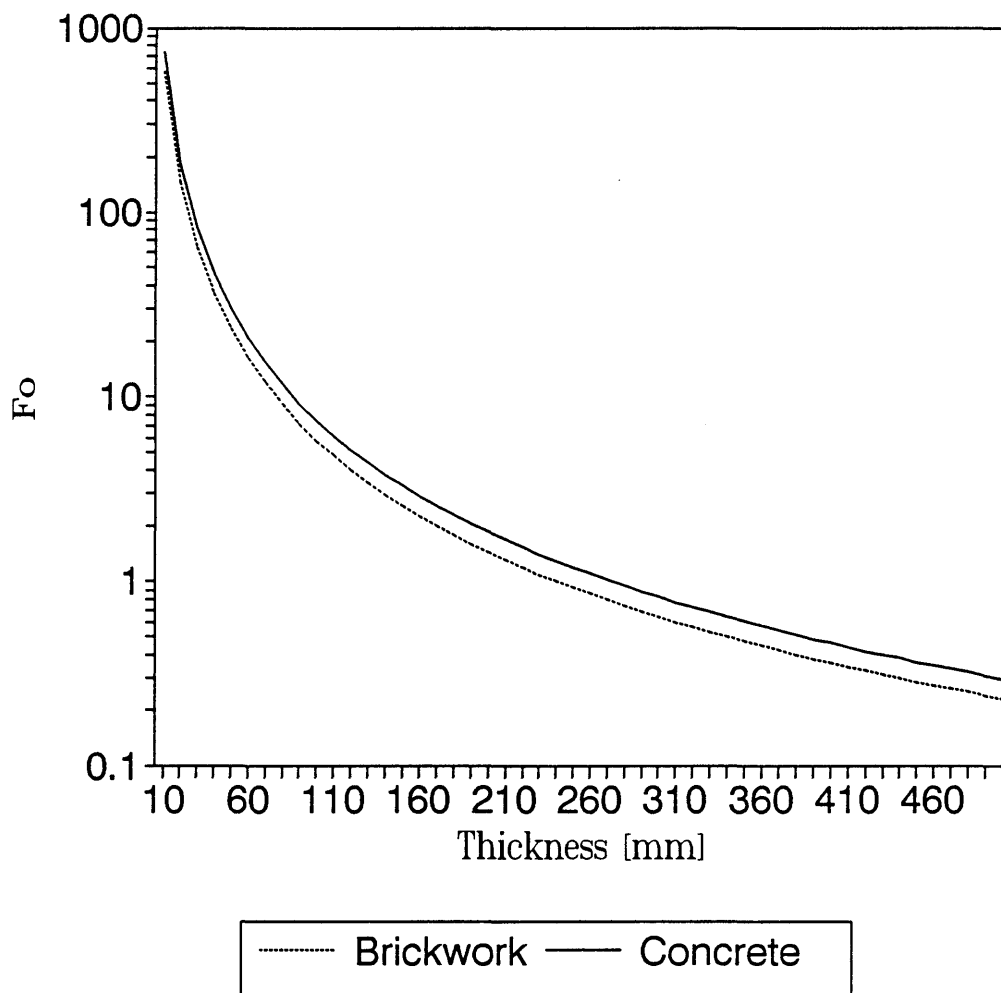


FIGURE 2.16 Fourier moduli for materials of the laminae of real buildings.

THEORETICAL FOUNDATION OF A NOVEL METHOD

Figure 2.16 shows that for most building elements (note that the  $F_0$  number is strongly dependent on the thickness of the layer) the Fourier modulus exceeds 10. The only exceptions are brick-work and concrete layers. It appears that condition (2.54) is well satisfied by most layers. In figure 2.17 we give the Fourier modulus of concrete and brick layers as a function of wall thickness. The condition (2.54) is satisfied for layers of brick and concrete up to a thickness of 110 mm.



**FIGURE 2.17** Fourier modulus of brick-work and concrete layers as a function of layer thickness.

## THEORETICAL FOUNDATION OF A NOVEL METHOD

It seems that for most *thin walled* building structures the approximation is reasonably accurate. The definitions of  $R$  and  $C$  (2.49) and (2.50) are intuitively satisfactory. They indicate that the total heat storage capacitance of the structure is represented by  $C$  and the total heat conductance by the two resistances in the branches of the T network. This must indeed be the case if the wall is thin and the temperature difference across the wall is small. Using a similar approach Davies [21] shows that a thick wall is well approximated by taking two, three or more of the T networks in cascade. Thick walls could thus be specified as consisting of two or more layers of the same material. In the exact solution, that is, in the cascade matrix with hyperbolic–trigonometric functions, it makes no difference if a layer is specified as a single layer of thickness  $\ell$  or  $n$  sublayers of thickness  $\ell/n$ . However, in the approximate RCR representation it does make a difference, and the accuracy of the RCR approximation increases with the number of sublayers. Of course the number of capacitors and hence the order of the circuit increases with each layer. Since we desire a single C representation, the high order network this procedure yields, consisting of an RCR T section for each layer, must be simplified to a single RCR T section, which represents the complete wall. It will be indicated later that this procedure, for reducing the high order network to a single capacitor network, has the effect that it makes no difference if the thick uniform layer is represented by one or more layers. This single C representation will necessarily represent the active capacitance for non–uniform walls and not the physical capacitance. The procedure for reducing the multiple T section network to a single T section is described next.

### d) Laminated Structures

According to (2.37) the transmission matrix of a composite is given by the product of the transmission matrices of the laminae. If each laminate is approximated by a T section as in figure 2.18, *viz.*  $T_1$ ,  $T_2$ ,

## THEORETICAL FOUNDATION OF A NOVEL METHOD

the resultant transmission matrix for a wall consisting of two layers is:

$$T_1 \cdot T_2 = \begin{bmatrix} \mathcal{A}_r & \mathcal{B}_r \\ \mathcal{C}_r & \mathcal{D}_r \end{bmatrix} \quad (2.56)$$

where:

$$\mathcal{A}_r = 1 + i\omega \cdot (R_1 C_1 + [R_2 + 2R_1] \cdot C_2) - \omega^2 \cdot (R_1 R_2 + R_1^2) \cdot C_1 C_2 \quad (2.57)$$

$$\begin{aligned} \mathcal{B}_r = & 2 \cdot (R_1 + R_2) + i\omega \cdot (2R_1 R_2 \cdot [C_1 + C_2] + C_2 R_2^2 + C_1 R_1^2) \\ & - \omega^2 \cdot R_1 R_2 C_1 C_2 \cdot (R_1 + R_2) \end{aligned} \quad (2.58)$$

$$\mathcal{C}_r = i\omega \cdot (C_1 + C_2) - \omega^2 C_1 C_2 \cdot (R_1 + R_2) \quad (2.59)$$

$$\mathcal{D}_r = 1 + i\omega \cdot (R_1 C_1 + [R_2 + 2R_1] \cdot C_2) - \omega^2 \cdot (R_1 R_2 + R_2^2) \cdot C_1 C_2 \quad (2.60)$$

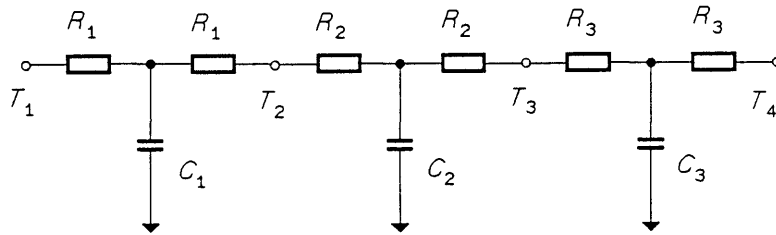


FIGURE 2.18 T sections in cascade.

We wish to approximate the composite structure with a single T network. Therefore, the matrix elements must be reduced to the form of (2.38). Clearly, this is not generally possible. The  $\mathcal{C}$  element, for instance, is purely imaginary in (2.38) but contains a non-vanishing real part in (2.59). But, if we neglect all terms in  $\omega^2$  we see that the  $\mathcal{A}$  and  $\mathcal{D}$  elements do reduce to the required  $1 + i \cdot \omega \cdot \tau$  form. The effective time constant of the composite is then given by:

$$\tau = R_1 \cdot C_1 + [2 \cdot R_1 + R_2] \cdot C_2. \quad (2.61)$$

Comparison of this equation with figure 2.18 shows a trend:— the time constant is given by the sum of the products of the capacitances with the total resistance to the left of the capacitor. For a rough approximation we may use for the composite structure the single T

## THEORETICAL FOUNDATION OF A NOVEL METHOD

structure with branch resistances given by half the total resistance, so that the exact steady state response is obtained:

$$R_c = \sum_{i=1}^n R_i = \sum_{i=1}^n \frac{\ell_i}{2 \cdot k_i} \quad (2.62)$$

The trunk capacitance is given by a generalized (2.61) divided by this definition of  $R_c$  so that the time-constant is preserved and given by  $\tau = R_c \cdot C_c$ :

$$C_c = \left[ R_1 \cdot C_1 + \sum_{j=2}^n [R_j + 2 \cdot \sum_{i=1}^{j-1} R_i] \cdot C_j \right] / R_c \quad (2.63)$$

We note from (2.61) that the T matrix for a uniform thick layer, as obtained from a cascade of two layers of half the thickness, would give  $\tau = 4 \cdot R \cdot C$  identical to what would result from a single thick layer.

That the formula for the capacitance (2.63) provides an active capacitance and not the physical capacitance can be seen by taking two layers with the same thickness and capacitance, but with the resistance of the first layer very large i.e.  $R_1 > R_2$ . From (2.62) we obtain  $R_c = (R_1 + R_2) \approx R_1$  for the resistance, and similarly for the capacitance  $C_c = [R_1 \cdot C + (R_2 + 2R_1) \cdot C] / R_1 \approx 3 \cdot C$  from (2.63). The physical capacitance is only  $2 \cdot C$  so that the active capacitance exceeds the physical capacitance. This somewhat baffling result is easily explained by noting that the definition of the active capacitance (2.63) attempts to preserve the effective time-constant  $\tau$  in (2.61). The capacitance  $C_c$  is therefore fictitious and the result indicates that since  $R_1$  isolates the mass from the external surface, the stored heat will have a larger influence on the interior surface temperature. The converse happens if  $R_1 < R_2$ . In this case we find  $C_c \approx C$  which is only half the physical capacitance; indicating that it is only the capacitance of the second layer which is active since the first layer is isolated from the inner surface. These physical interpretations of the active capacitance should not be taken too seriously. The definitions in (2.61) and (2.62)

## THEORETICAL FOUNDATION OF A NOVEL METHOD

are fairly arbitrary and designed to obtain a satisfactory approximation to the distributed two-port. The only reason why some sort of physical interpretation is possible at all, is because the resistance  $R_c$  were chosen to correspond with the steady state physical resistance.

It was indicated that two related conditions for accurate lumping are:

- A Small Biot number for the wall, or
- B Large Fourier modulus for each lamination.

The first condition will ensure that both the mean and the swing components of the temperatures and heat flows are accurately represented by the lumped model. The second condition applies only to the swing component. However, the heat capacitance plays no part in calculating the mean component and the definition of the resistances are such that the steady state response is obtained exactly. Therefore, the second condition which applies to non-steady swings is the more important. Fortunately, condition B is also more readily satisfied in buildings than condition A, as can be deduced from figures 2.11 and 2.16.

Equations (2.62) and (2.63) will be accurate when  $h_o$  is small and  $h_i$  is large. In these circumstances the matrix element  $\mathcal{A}$  is the most important and the elements  $\mathcal{A}$  and  $\mathcal{D}$  are more accurately approximated by the above equations, than elements  $\mathcal{C}$  and  $\mathcal{B}$ <sup>13</sup>. In buildings, it is rather the converse which is true and the element  $\mathcal{D}$  is the most important. To evaluate the accuracy of (2.62) and (2.63) we have computed the exact matrix description and the single RCR description for the walls of more than 20 existing buildings.

To evaluate the accuracy of the cascade matrices, where 4 complex components must be compared, which differ in significance according to

---

<sup>13</sup>The influence of the various elements of the cascade matrix can be inferred from the transfer function  $G$  defined by equation (2.64). E.g. if  $h_i$  is very large only  $\mathcal{A}$  and  $\mathcal{D}$  are important.

## THEORETICAL FOUNDATION OF A NOVEL METHOD

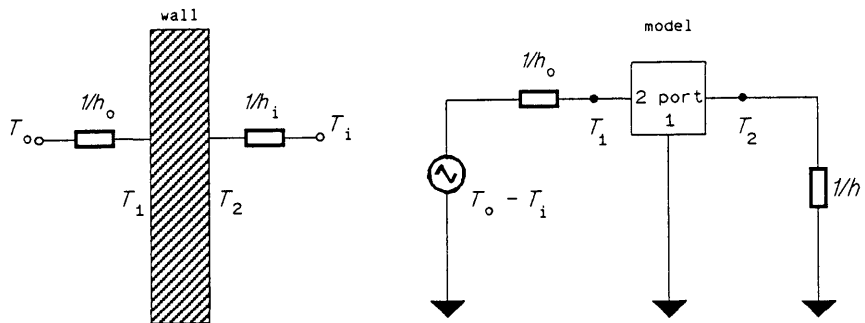


**FIGURE 2.19** The transfer factor of a wall,  $G$ , is the ratio of the interior surface temperature to the external surface temperature.

the boundary conditions. Davies [21] "minimizes the sums of the squares of the differences between the corresponding elements in the real and model wall matrices". This criterion is not acceptable since it is unclear what its physical interpretation may be. It is better to calculate the effect of the matrices on the surface temperatures, rather than to compare the components themselves. This entails terminating the matrices in the correct boundary conditions and comparing the resultant temperatures on the boundaries. The calculation assumes the boundary conditions at the surfaces are:  $h_o = 20 \text{ W/m}^2 \cdot \text{K}$  and  $h_i = 3.5 \text{ W/m}^2 \cdot \text{K}$ . In this case, if the two port is driven via  $h_o$  and terminated in  $h_i$  as in figure 2.19, the ratios  $T_i/T_f = G$  for the exact solution and the RCR approximation can be used to compare the accuracy of the lumping. This ratio, which we call the transfer factor, is a complex number which gives the attenuation and phase shift of the sinusoidal temperature wave through the wall. The circuit of figure 2.19 is approximately realized in buildings if  $T_f$  is identified with the external sol-air forcing function and  $T_i$  with the interior air temperature, provided the contribution of the particular wall to the total heat flow to the interior of the zone is not dominant;  $T_i$  must be

## THEORETICAL FOUNDATION OF A NOVEL METHOD

largely independent of the particular wall under consideration. In this case, we find from figure 2.19:

$$G = \left[ \mathcal{A} + h_0 \cdot \mathcal{B} + \mathcal{C}/h_i + \mathcal{D} \cdot h_0/h_i \right]^{-1}. \quad (2.64)$$

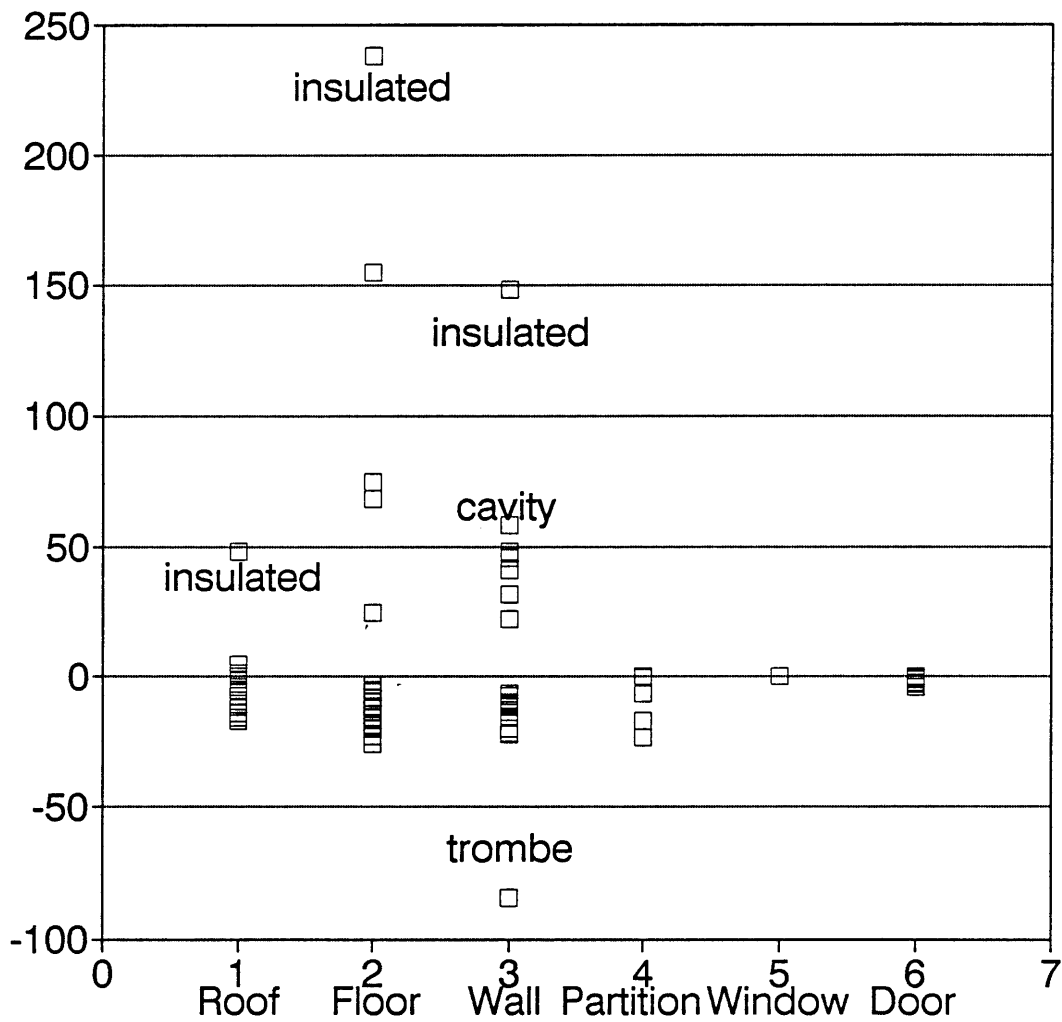


FIGURE 2.20 a Percentage error of the magnitude of the lumped transfer factor.

## THEORETICAL FOUNDATION OF A NOVEL METHOD

In figures 2.20 a and b we show the magnitude and phase errors of the lumped transfer factor for 106 existing walls. These results are also tabulated in appendix 2A. Results for the some walls are tabulated in table 2.4. The magnitude error is below 10% for all lightweight constructions and below 20% for a large number of massive constructions. Scrutiny of table 2.4 reveals that the magnitude error for brick and concrete walls are below 15% for thicknesses up to 330 mm. For cavity constructions the error is in the region of 22% and for very thick walls and insulated walls the error is in the order of 50%. The same tendency is visible for the phase error. For 110 mm solid brick walls the phase error is 0.3 h, increasing rapidly to 3 h for 220 mm thicknesses. Cavity and insulated walls have phase errors from 2 to 15 h. These results indicate that the attenuation of the thermal wave as obtained from the lumped model is fairly accurate for most solid and uninsulated walls. The phase error unfortunately grows rapidly if the thickness exceeds 110 mm. For cavity walls the magnitude error of 20% is already significant and the phase error of 3 h is not acceptable.

These results may be interpreted in the following way:

- Since the lumping is accurate for the thin elements such as windows, doors, 110 mm brick and concrete walls etc. the lumped representation will be adequate if these elements determine the heat flow to the interior of the zone.
- If however, the solid, thick elements contribute significantly to the heat flow, a phase error can be expected.
- If insulated and cavity walls also contribute to the heat flow, the magnitude as well as phase will be significantly in error.

If we assume that the thermo-flow in actual buildings is largely determined by the weakest part of the shell, i.e. by the windows and doors and not by the thick insulated elements, we come to the conclusion that the lumped representation is adequate with a magnitude error below 15 % and a phase error below 3 h. However, if the

### THEORETICAL FOUNDATION OF A NOVEL METHOD

building is entirely constructed from thick, well insulated walls, with insulated windows and doors, large errors can be expected.

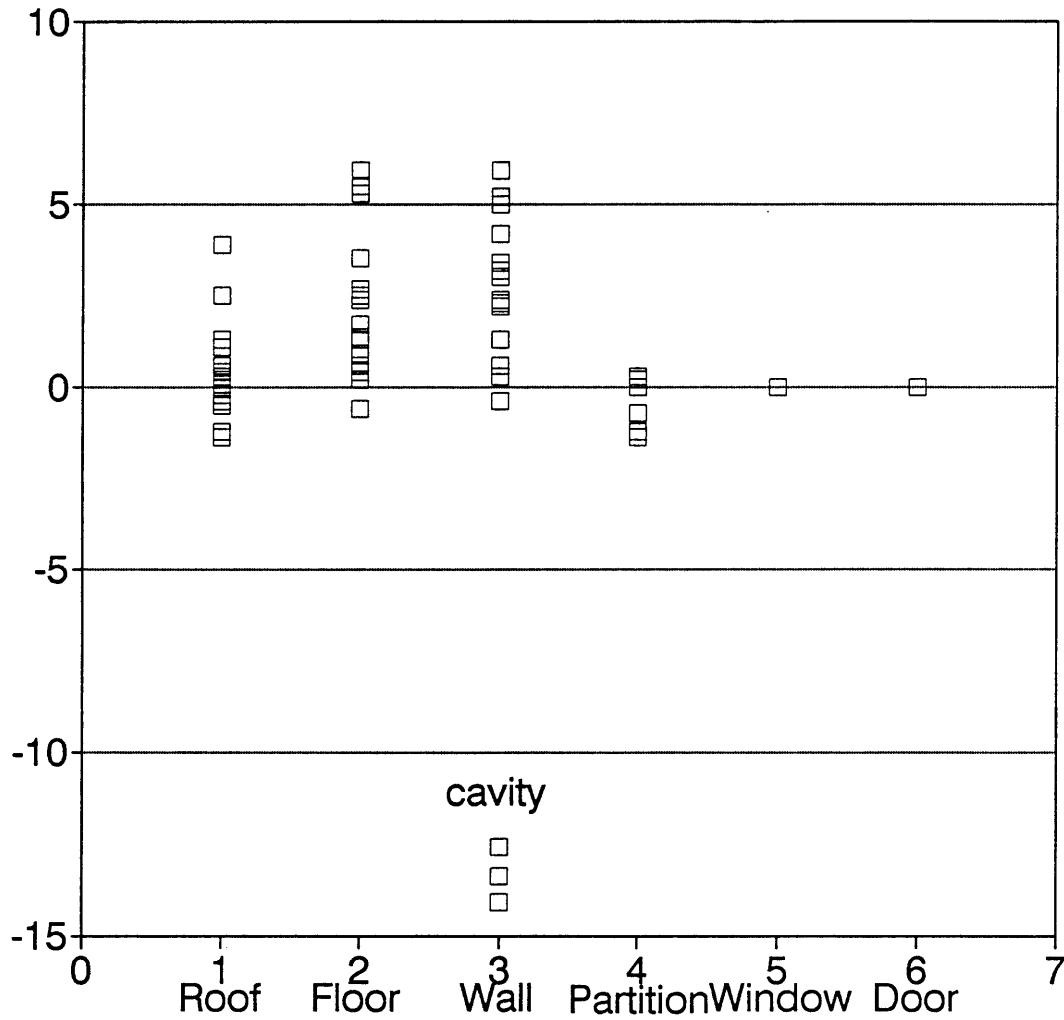


**FIGURE 2.20 b** Phase error, in hours, of the lumped transfer factor.

## THEORETICAL FOUNDATION OF A NOVEL METHOD

Wall Description	Gain (%)	Lag (h)	Gain Error (%)	Lag Error (h)
110 mm brick	7.4	-3.4	-10.5	0.3
220 mm brick	2.1	-8.1	-9.8	3.2
330 mm brick	1.2	-10.4	-14.9	5
150 mm concrete	6.5	-4.4	-11.9	0.6
200 mm concrete	4.6	-5.7	-15.8	1.3
cavity wall	0.3	7.7	45.7	-13.4
9 mm asbestos	12.5	-0.2	~0	~0

TABLE 2.4 Transfer factor accuracy for some typical walls.

In conclusion of this section we note that the value of the total time constant given by (2.61) agrees with the definition of the *Thermal Time-Constant (TTC)* of Bruckmayer in [5] if the external surface resistance is also included in the summation of (2.63).

 e) Combining the Surfaces

Besides laminated walls, a zone will consist of typically six or more surfaces forming the shell of the enclosure. These walls will also consist of different sections such as brick-work, windows, doors etc.

## THEORETICAL FOUNDATION OF A NOVEL METHOD

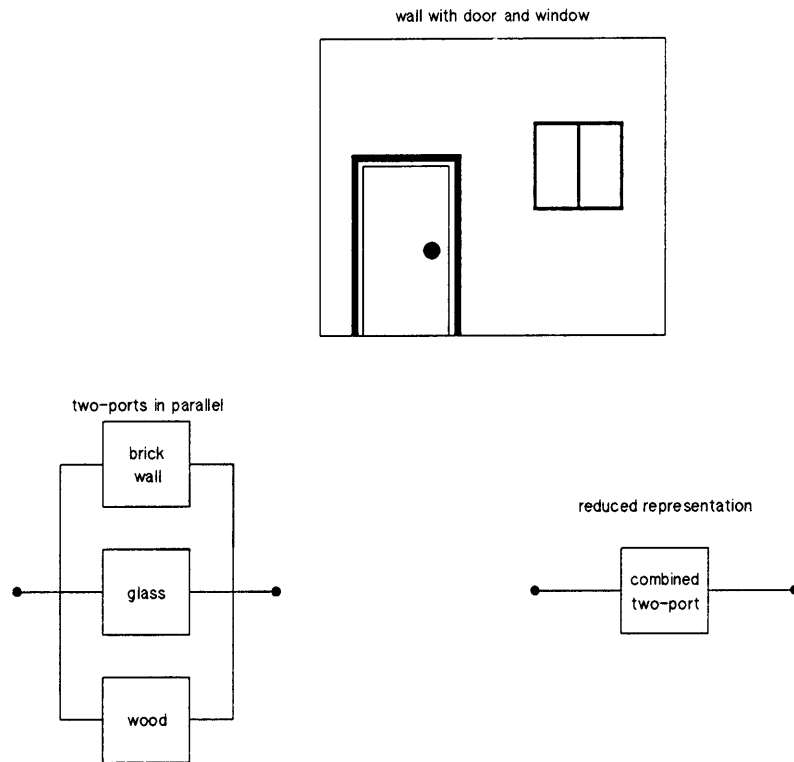


**FIGURE 2.21** A typical shell consist of areas of different physical construction, e.g. brick, wood, glass.

E.g. in figure 2.21 the partition consists of several sections differing in area, construction and thermal properties. These sections are effectively connected in parallel if it is assumed that the temperatures on the surfaces are equal. In general, as discussed in §2.5.2, the temperatures on the external surfaces will differ; some surfaces will be in the shade and others will receive direct sun-light. The reduction of the various elements and walls to a single two-port was also discussed in §2.5.2 and it was pointed out, that, depending on the assumptions, various possibilities exist. (See figures 2.8 and 2.9.) The simplest procedure is obtained when the assumption of isothermal surfaces on both sides are

## THEORETICAL FOUNDATION OF A NOVEL METHOD

used. If this is the case, we see that the above condition for parallel walls are assumed to exist, and that simple two port theory can be used to combine the walls. In this section we discuss only this simple method. A more accurate method is discussed in the next section, in connection with the technique for reducing the external forcing functions to one effective forcing function. In the most general case, the procedures outlined in §2.5.2 must be followed. The objective is still to derive a single RCR T section description, but this time for the total shell.

A rule for combining the various surfaces is given in [5], where Hoffman describes the *Total Thermal Time-Constant (TTTCB)* method and gives for the total time constant of an enclosure:

$$TTTCB = \frac{\sum_k \cdot A_k \cdot TTC_k}{\sum_k \cdot A_k} + \text{Interior mass terms}$$

where the summation is carried out over all surfaces,  $k$ , with areas  $A_k$ , of the enclosure and  $TTC_k$  is Bruckmayer's thermal time constant for the wall (see discussion above). This method simply takes the area weighted averages of the time constants of the walls. We shall soon see that this method cannot be justified on theoretical grounds.

In previous paragraphs of this section we have derived a solution for the one dimensional heat flow problem in the form of a cascade matrix  $T$ , which gives the output temperature and heat flow for a specified input temperature and flow

$$\begin{bmatrix} T_o \\ q_o \end{bmatrix} = \begin{bmatrix} \mathcal{A} & \mathcal{B} \\ \mathcal{C} & \mathcal{D} \end{bmatrix} \cdot \begin{bmatrix} T_i \\ q_i \end{bmatrix}. \quad (2.65)$$

To combine circuits in parallel it is expedient to use a different set of equations for the heat flow through the wall, namely those giving the

## THEORETICAL FOUNDATION OF A NOVEL METHOD

flows  $q$  in terms of the temperatures  $T$ .

$$\begin{bmatrix} q_i \\ q_o \end{bmatrix} = \begin{bmatrix} y_{11} & y_{12} \\ y_{21} & y_{22} \end{bmatrix} \cdot \begin{bmatrix} T_i \\ T_o \end{bmatrix} \quad (2.66)$$

The matrix  $Y = [y_{11} \ y_{12} / y_{21} \ y_{22}]$  is also a two port descriptor and is known as the admittance matrix. When elements are connected in parallel, as in figure 2.21, the temperatures at the ports are equal and the flows add. The admittance matrix of the parallel circuits is therefore the sum of the admittance matrices of the individual elements

$$Y_p = Y_1 + Y_2. \quad (2.67)$$

The admittance matrix and transmission matrix representation is transformed from one to the other by the following rules:

$$\begin{aligned} y_{11} &= \mathcal{D}/\mathcal{B}, & y_{12} &= \mathcal{C} - \mathcal{D} \cdot \mathcal{A}/\mathcal{B} \\ y_{21} &= 1/\mathcal{B}, & y_{22} &= -\mathcal{A}/\mathcal{B} \end{aligned} \quad (2.68)$$

$$\begin{aligned} \mathcal{A} &= -y_{22}/y_{21}, & \mathcal{B} &= 1/y_{21} \\ \mathcal{C} &= y_{21} - y_{11} \cdot y_{22}/y_{21}, & \mathcal{D} &= y_{11}/y_{21} \end{aligned} \quad (2.69)$$

With these rules it is straight-forward to convert between the admittance and the cascade matrices. The procedure for finding the cascade representation of parallel elements is now:

- convert T matrices to Y matrices with (2.68).
- add the components of the Y matrices to find the total Y matrix.
- convert the Y matrix back to a T matrix with (2.69).

This procedure is very general and applicable to any type of T matrix; lumped or distributed elements.

In our application, we are interested in walls which typically consists of two or more areas or sections of different construction. To calculate the parameters of the T section of the combined wall directly from the

## THEORETICAL FOUNDATION OF A NOVEL METHOD

physical parameters of the sections, we may use the approximations [11]:

$$R_t = \frac{1}{2} \left[ \frac{A_1 \cdot k_1}{\ell_1} + \frac{A_2 \cdot k_2}{\ell_2} + \dots \right]^{-1} \cdot A_t \quad (2.70)$$

$$C_t = [A_1 \cdot \ell_1 \cdot \rho_1 \cdot \sigma_1 + A_2 \cdot \ell_2 \cdot \rho_2 \cdot \sigma_2 + \dots] / A_t \quad (2.71)$$

where  $A_t$  is the total area of the shell.

In (2.70) and (2.71) the numerical subscripts refer to the different sections and areas. If the sections are laminated structures the laminae must first be combined with the aid of (2.62) and (2.63).

These equations are rather rough approximations. They are derived on the assumption that the capacitances and conductances of the two areas can be thrown together. For more accurate calculation, it is essential to carry out the matrix procedure outlined before. The nature of this approximation can be demonstrated for the  $y_{11}$  parameter of the wall consisting of 2 sections in parallel. For the T section<sup>14</sup> the first of (2.68) gives:

$$y_{11} = \frac{1 + i \cdot \omega \cdot R \cdot C}{R \cdot (2 + i \cdot \omega \cdot R \cdot C)} \quad (2.72)$$

For 2 similar partitions in parallel; respectively identified by subscripts 1 and 2:

$$y_{11} = \frac{1 + i \cdot \omega \cdot R_1 \cdot C_1}{R_1(2 + i \cdot \omega \cdot R_1 \cdot C_1)} + \frac{1 + i \cdot \omega \cdot R_2 \cdot C_2}{R_2(2 + i \cdot \omega \cdot R_2 \cdot C_2)} \quad (2.73)$$

This equation must be compared with one obtained directly from the

---

<sup>14</sup>For full accuracy the distributed two port description of the sections must be used.

## THEORETICAL FOUNDATION OF A NOVEL METHOD

physical properties via (2.70) and (2.71):

$$y_{11}' = \frac{1 + i \cdot \omega \left[ \frac{R_1 \cdot R_2}{R_1 + R_2} \cdot (C_1 + C_2) \right]}{\frac{R_1 \cdot R_2}{R_1 + R_2} \cdot \left[ 2 + i \cdot \omega \cdot \left[ \frac{R_1 \cdot R_2}{R_1 + R_2} \right] \cdot (C_1 + C_2) \right]} \quad (2.74)$$

Equations (2.73) and (2.74) are obviously not compatible; (2.73) is an equation with terms in  $\omega^2$  (if placed over a common denominator) and in (2.74)  $\omega$  appears only to the first power. It can be shown though, that these equations are similar in many respects if the swing frequency is small, so that the  $\omega^2$  terms vanish. Despite the incompatibility, (2.74) is may be used for convenience.

If (2.74) is compared with the procedure of Hoffman above, it is seen that the average time constant is only obtained if the resistance  $R_1$  equals  $R_2$  in (2.74). It follows that Hoffman's procedure is subject to this condition of equal wall resistances and is therefore a very rough approximation of (2.74), which is again only an approximation of (2.73).

Equations (2.74) and (2.73) can be more easily compared if further simplifications are assumed. If, for instance, we assume  $R_1 = R_2 = R$  and  $C_1 = C_2 = C$  i.e. similar sections, both (2.73) and (2.74) furnish the correct value:

$$y_{11} = \frac{2 \cdot (1 + i \cdot \omega \cdot R \cdot C)}{R \cdot (1 + i \cdot \omega \cdot R \cdot C)} = y_{11}' \quad (2.75)$$

In the general case, where the areas and properties are dissimilar, both the magnitude and the phase of the approximate equation (2.74) is somewhat in error because of the  $\omega^2$  terms.

Similar equations can be derived for the other elements of the Y matrix. The same observation apply; terms in  $\omega^2$  are neglected. In practice, we expect that equations (2.70) and (2.71) will be sufficiently accurate for calculating diurnal swings, where  $\omega = 2\pi/24$  h which is quite small.

## THEORETICAL FOUNDATION OF A NOVEL METHOD

The main cause of error, in this procedure for combining the elements, is then the assumption that the external and internal surfaces of all the sections are respectively isothermal. Since Mathews and Richards [10] employ (2.70) and (2.71) to combine the various elements of the shell, the assumption of isothermal mass is inherent in their model. Mathews and Richards in fact state that they assume isothermal interior surfaces, and further, obtain a mean sol-air temperature, which affect all external surfaces. Obviously, the simple model of figure 2.1 represents the temperature of the massive parts of the shell with a single node, and therefore requires one representative temperature for all the massive structures. The definition of this mean sol-air temperature is further discussed in the §2.5.4.

Numerical evaluation of the accuracy of equations (2.70) and (2.71) requires a complete implementation of the exact solution. The areas of the various sections are important and the only acceptable calculation should use the actual areas as they occur in practice. Since a full implementation of the exact matrix method is outside the scope of this thesis, we have to content with the admittedly somewhat vague, qualitative discussion above.

We conclude, that from the results obtained here, a simple one capacitor circuit representation of the two port, such as in figure 2.14, can be justified if the frequency of the temperature and load swing is small. This condition is satisfied by the diurnal variations of temperature in buildings.

### f) Lumping of Interior Mass

In the network of figure 2.6 we have included a one port model of interior mass, by which we mean all massive objects which are in contact with the interior air, and which have significant heat capacitance, so that heat will be absorbed and released from the mass

## THEORETICAL FOUNDATION OF A NOVEL METHOD

in sympathy with temperature changes of the internal air. This includes furnishings, partitions etc. and also the capacitance of the internal air itself, although the latter is often negligible compared to the others.

The one-port description of the interior massive elements is obtained from the solution of the conduction equation with all the boundary conditions set to the interior air temperature<sup>15</sup>. The internal objects are only of interest in the modelling of the interior temperature swing so that we may seek solutions for sinusoidally varying temperatures only. The one-port description of the object,  $D_p$ , at a specified frequency, models the heat flow across the surfaces of the object  $q_m$  in terms of the temperature of the surfaces  $T_m$ :

$$q_m = D_p \cdot T_m. \quad (2.76)$$

$D_p$  is also known as a driving point function in electrical terminology and must have the units of an admittance. It is a function of the specific characteristics of the object as well as the geometry. From (2.76) can be seen that the determination of  $D_p$  requires the full solution of the three dimensional heat conduction equation with sinusoidal temperature variations, which is often an arduous task. However, when the Biot number of the object is small it is again possible to use a simple lumped model consisting of a resistance  $R_m = 1/h \cdot A$  which models the surface resistance, and a single capacitor  $C_m = \rho \cdot c_p \cdot V$  which models the heat storage. If the Biot number is small the interior conduction resistance of the object is not important.

A similar, simple solution is obtained for small structures, where the size of the object is small compared to the wavelength of the temperature wave in the structure. In this case we can again find a single  $R$ , single  $C$  description of the object when the Fourier modulus of

---

<sup>15</sup>We are assuming all surfaces of the object are in contact with the internal air, and radiation heat exchange between internal surfaces and the object can be ignored.

## THEORETICAL FOUNDATION OF A NOVEL METHOD

the object is large. The Fourier modulus is now defined with respect to one period of the variation of the surface temperature and a characteristic body dimension. The method is completely analogous to that described above for determining a lumped representation of the walls. It follows that lumping is possible under the same conditions as before, and that the lumped model for the internal object is a single capacitor, driven through a single resistor connected to the interior air temperature.

We shall therefore assume that it is possible to model the effect of interior mass with a single capacitor  $C_m$ , connected to the interior air node via resistance  $R_m$ , where,  $C_m$  includes only the active storage of the object for diurnal sinusoidal variations, and  $R_m$  includes the convective surface resistance. The completely reduced model for thermo-flow in buildings is thus as given in figure 2.22. The model of figure 2.22 contains two capacitances, one for the massive elements forming part of the shell, and another for the internal masses. It is not permitted to combine these two capacitances in a single capacitance, unless it is assumed that the bulk temperature of the internal mass is always equal to that of the walls. This assumption can not be justified; the interior mass is driven by the interior air temperature, and the massive parts of the shell are driven by the difference between internal and external temperatures. In figure 2.22, combination of the two capacitors in a single capacitor is clearly tantamount to the assumption  $R_2 + R_m > R_1$ . However, this can not be true unless the shell contains a layer of insulation on the external surface. For most buildings we will have  $R_1 \approx R_2 \approx R_m$  and the condition is violated. We have not attempted to calculate the error which will result from the breakdown of this assumption; for the same reasons given at the end of the previous section. The errors are probably not too severe since most zones contain only relatively light internal structures.

## THEORETICAL FOUNDATION OF A NOVEL METHOD

The circuit of figure 2.22, although very close to, still differs significantly from the model of Mathews and Richards of figure 2.1. These differences are discussed in §2.6 and §2.7.

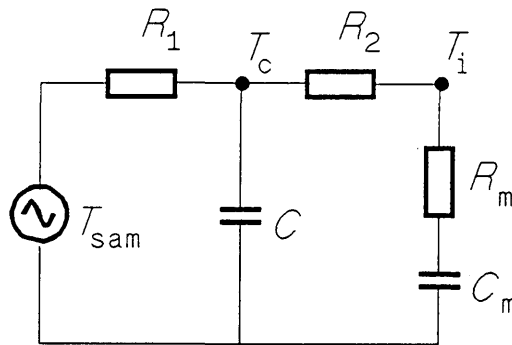


**FIGURE 2.22** The completely reduced model. Lumped circuits model the massive elements. The interior heat exchange is modelled with a combined surface coefficient  $h_i$ , and the exterior forcing functions are combined in a single effective forcing function  $T_{sa}$ .

### 2.5.4 The Definition of the Mean Sol–Air Temperature

The mean sol–air temperature of Mathews and Richards is based on the assumption that the interior surfaces are isothermal, but takes into account only the conductances of the walls and the external surface coefficients [11]. The capacitance of the walls are ignored. The exact procedure, as discussed in §2.5.2, yields a two port description of the combined shell elements as well as a more complicated definition of the mean sol air temperature, in which all the elements of the circuit, including the capacitance and the interior surface coefficients play a part.

In fact, if the simple T section lumped model for the walls are retained, it is possible to obtain a simple exact definition of the mean sol–air temperature in the way indicated in §2.5.2. In figure 2.23 we have

## THEORETICAL FOUNDATION OF A NOVEL METHOD

combined the surface coefficients of figure 2.9b in the T section description of the wall. If the Thevenin equivalent representation of all the wall elements and forcing functions are found, the exceedingly simple circuit of figure 2.24 results. This figure is very similar to the model of Mathews and Richards.

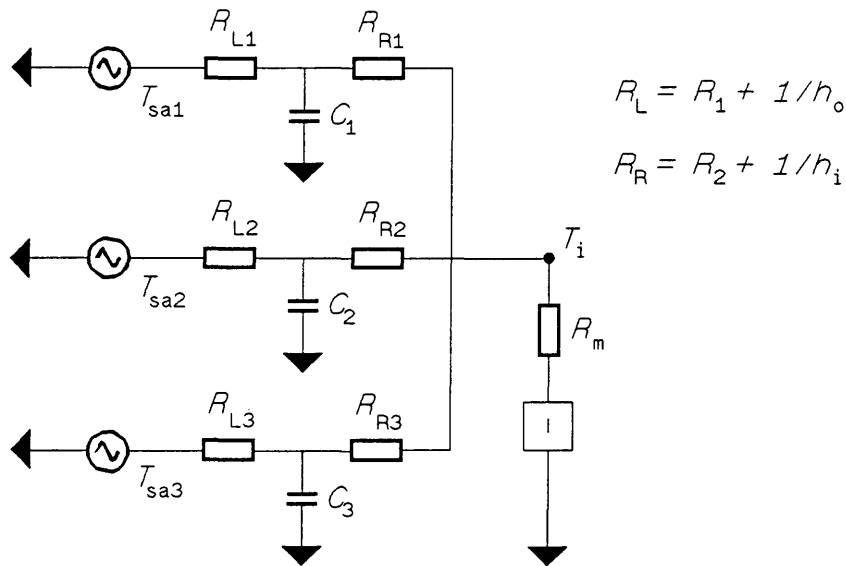


FIGURE 2.23 The lumped representation with surface coefficients absorbed in the branch resistances of the T section.

The mean sol-air temperature,  $T_{sa_m}$ , in figure 2.24 is given exactly by:

$$T_{sa_m} = \sum_i T_{sa_i} / (1 + i \cdot \omega \cdot \tau_i). \quad (2.77)$$

Where  $T_{sa_i}$  is the forcing function for section  $i$  and  $\tau_i$  the time constant for surface element  $i$  given by:

$$\tau_i = (R_{t_i} + A_i/h_{o_i}) \cdot C_{t_i} \quad (2.78)$$

with  $R_{t_i}$  and  $C_{t_i}$  the parameters of the T section, and  $h_{o_i}$  is the surface coefficient for the external area,  $A_i$ , of element  $i$ .

## THEORETICAL FOUNDATION OF A NOVEL METHOD

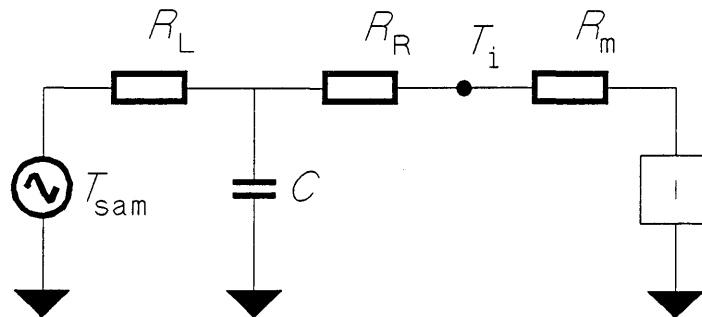
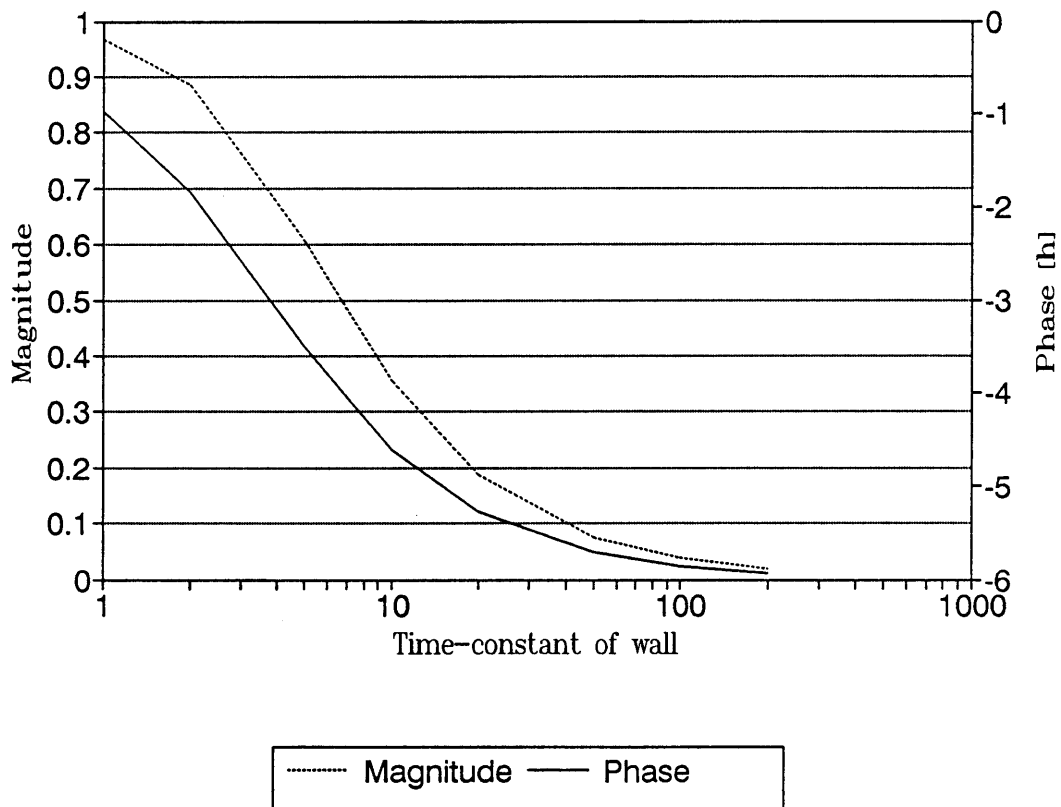


FIGURE 2.24 The Thevenin equivalent circuit of the forcing functions of figure 2.23 represents the mean sol-air temperature.

In figure 2.25 the magnitude and delay of the sol-air contribution is shown as a function of the total time constant of the wall. For single layer brick walls of thickness 110 mm ( $\tau = 6$  h) the attenuation is 0.54 and the delay is 3.8 h. For a double layer brick wall of thickness 220 mm ( $\tau = 24$  h) the corresponding values are 0.16 and 5.4 h. It is clear that these delays are of the same order as the delay correction which Mathews and Richards have to apply as an *ad hoc* correction [10]. The attenuation and delay of the contribution to the mean sol-air is related to the transfer factor discussed before. It is different though, since in the definition of the mean sol-air, the two-port of the wall is terminated in  $h_i = 0$  (see figure 2.19), i.e. it is assumed no heat flows across the inner surface. The mean sol-air is just a convenient mathematical artifact for calculating the solution. It allows the sol-air forcing temperatures to be combined in a single forcing function so that the combined response can be calculated at once. In principle, it is completely equivalent to obtaining the responses to the various sol-air temperatures one by one, and then afterwards combine them to find the total response.

THEORETICAL FOUNDATION OF A NOVEL METHOD



**FIGURE 2.25** Attenuation and delay of the sol-air contributions of walls as a function of the thermal time constant of the wall, with resistance from sol-air node to interior air node.

## THEORETICAL FOUNDATION OF A NOVEL METHOD

The values of  $R_1$ ,  $R_2$  and  $C$  in figure 2.21 are not so easily obtainable. Each element in figure 2.22 will contribute a capacitor so that the exact representation is a high order network. Methods for obtaining approximate values for the circuit parameters were discussed in §2.5.3. It was shown that reasonable approximations are possible when the frequency of variation is small. Alternatively, if it is assumed that the massive elements are at approximately equal temperatures,  $C$  represents the total capacitance of the structure and  $R_1 + R_2$  the total thermal resistance of the shell.

The definition of the mean sol air temperature as given in (2.77) is exact for the T section description of the walls. Mathews and Richards [11] ignores the capacitance of the walls when computing the mean sol-air temperature. Equation (2.77) indicates that the individual forcing functions of each external suffers a phase shift according to the time constant of the wall. This effect in all probability explains the empirical phase shift Mathews and Richards [10] requires. Their empirical correction, which is based on the total time constant of the zone, is thus justified if all the walls are of similar construction but will fail when the time constants of the walls differ manifestly.

### 2.5.5 Interior Heat Transfer

Since the assumption of Mathews and Richards – and others notably [24] – that the interior surfaces are at the same temperature, is not substantiated by measurements [8], it deserves some further attention. According to [8] the surfaces of windows are approximately 10 K below the average wall surface temperature in winter. Nevertheless, Mathews and Richards [10] have found that adequate temperature predictions are possible with this assumption. Similarly Mitalas [30] concludes: "... for (the) emissivities  $\epsilon = 0.9$  and  $\epsilon = 0.0$  (results) indicate that the heat interchange by radiation between the inside room envelope surfaces is not a major factor affecting the cooling load." We have in previous paragraphs indicated that it is possible to obtain a simple structure

## THEORETICAL FOUNDATION OF A NOVEL METHOD

without the assumption of isothermal surfaces, by way of network synthesis, although it is not clear at all that in this case the simple one capacitor network will be adequate. However, it was indicated that the assumption of isothermal interior surfaces directly leads to a simple thermo-flow network.

To investigate quantitatively the magnitude of the temperature differences between internal surfaces, the difference in the internal temperatures of two opposing walls can be evaluated. A computer program was written which calculates the temperature difference between the internal surfaces of two walls, when the external surfaces are subjected to a temperature difference<sup>16</sup>. The calculation is done both for a steady (mean) temperature difference and for a sinusoidal temperature swing with period 24 h. The program is based on the thermo-flow network of figure 2.6. The mean temperature difference between the walls are easily found since the heat storage in the massive elements plays no part. If the temperature difference across the external surfaces of the walls is  $T_0$  one finds that the steady temperature difference,  $\Delta T$ , between the interior surfaces are given by (assuming the convective coefficient,  $h_c$ , is the same for both surfaces):

$$\Delta T/T_0 = \frac{1}{\frac{(Bi_1 + Bi_2)}{2} \cdot \left(\frac{2 \cdot h_r}{h_c} + 1\right) + 1} \quad (2.79)$$

where  $Bi_i$  is the Biot number of wall  $i$  with respect to the internal convection coefficient  $h_c$ .

It is seen that the temperature difference is determined solely by the mean Biot number of the walls in relation to the convective and radiative coefficients. In figure 2.26 the fractional mean temperature

---

<sup>16</sup>It is available on the floppy disk in the back-cover.

THEORETICAL FOUNDATION OF A NOVEL METHOD

difference,  $\Delta T/T_0$ , is shown as a function of the mean Biot number, with  $h_r/h_c$  as a parameter. In table 2.5 the fractional mean temperature difference is given for the walls of a typical office, details are given in appendix 2c. Similar results for 20 other buildings are available on the floppy disk in the back-cover in the file named 'results.txt'.

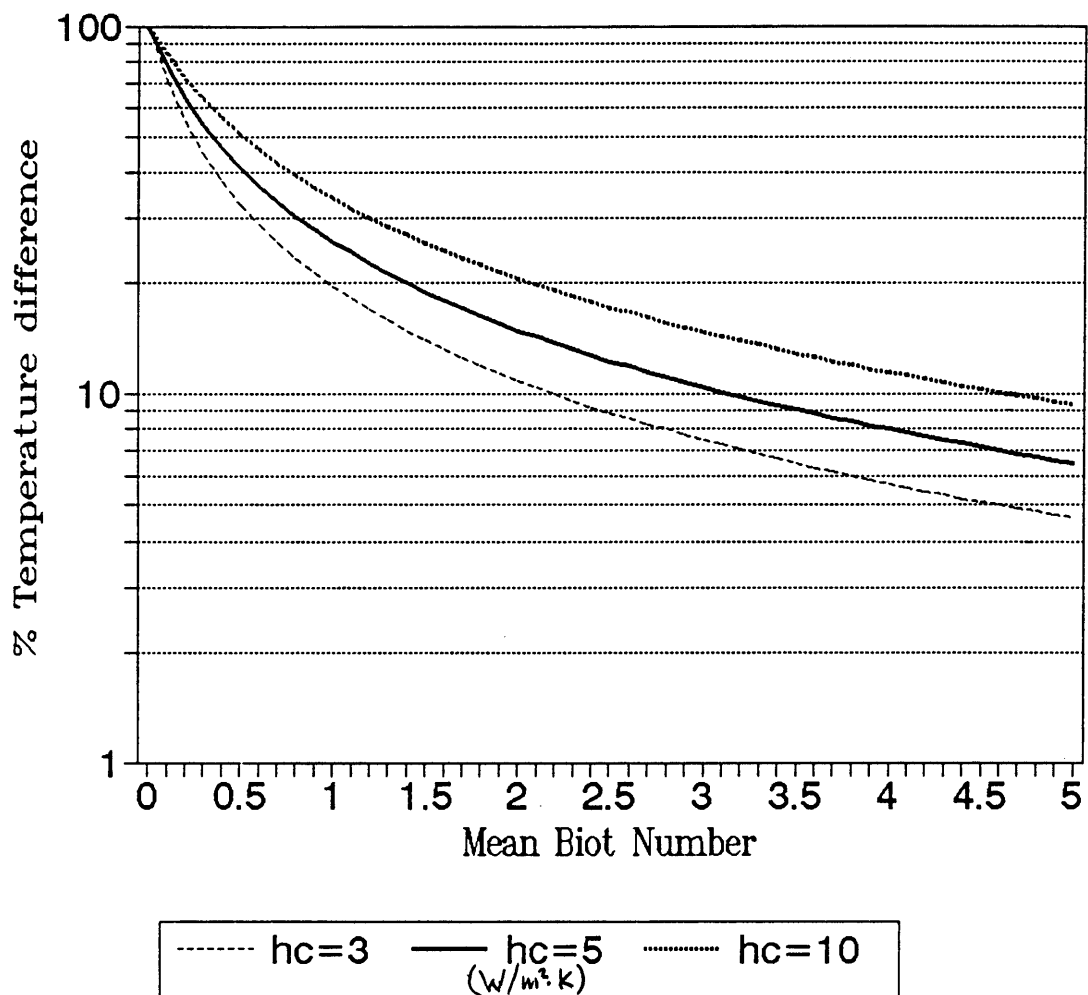


**FIGURE 2.26** Fractional mean interior surface temperature difference, as a function of the mean of the Biot numbers of the walls.

## THEORETICAL FOUNDATION OF A NOVEL METHOD

	Roof	Floor	Brick (C)	Window	Brick	Door
Roof	26.064					
Floor	25.551	25.057				
Brick (cavity)	22.465	22.083	19.74			
Window	36.346	35.355	29.709	60.023		
Brick (114 mm)	27.901	27.314	23.817	40.021	30.018	
Door	25.252	24.77	21.86	34.786	26.973	24.489

**TABLE 2.5** Mean temperature difference between interior wall surfaces as a percentage of the external temperature difference. These results were calculated from data describing an actually existing office. For more details see appendix 2C. The rows and columns indicate the temperature differences for opposing walls taken in pairs.

Figure 2.11 shows Biot numbers for more than 100 elements of existing buildings. These elements have been sorted into 6 groups namely, roof, floor, wall (massive), partition (light), window and door. The Biot numbers were computed from the total resistance of the various laminae which form the elements. It is evident from the figure that the Biot numbers for buildings surfaces fall mostly in the range 0 to 2. Consequently, from figure 2.23 it follows that we must expect quite high mean temperature differences between the surfaces. The results in table 2.5 show that the mean temperature difference between the internal surfaces of two opposing windows may be above 60% of the temperature difference between external surfaces. Examination of the complete set of results indicate that, if one surface is a window and the other a brick wall, the mean interior temperature difference is typically about 20 to

THEORETICAL FOUNDATION OF A NOVEL METHOD

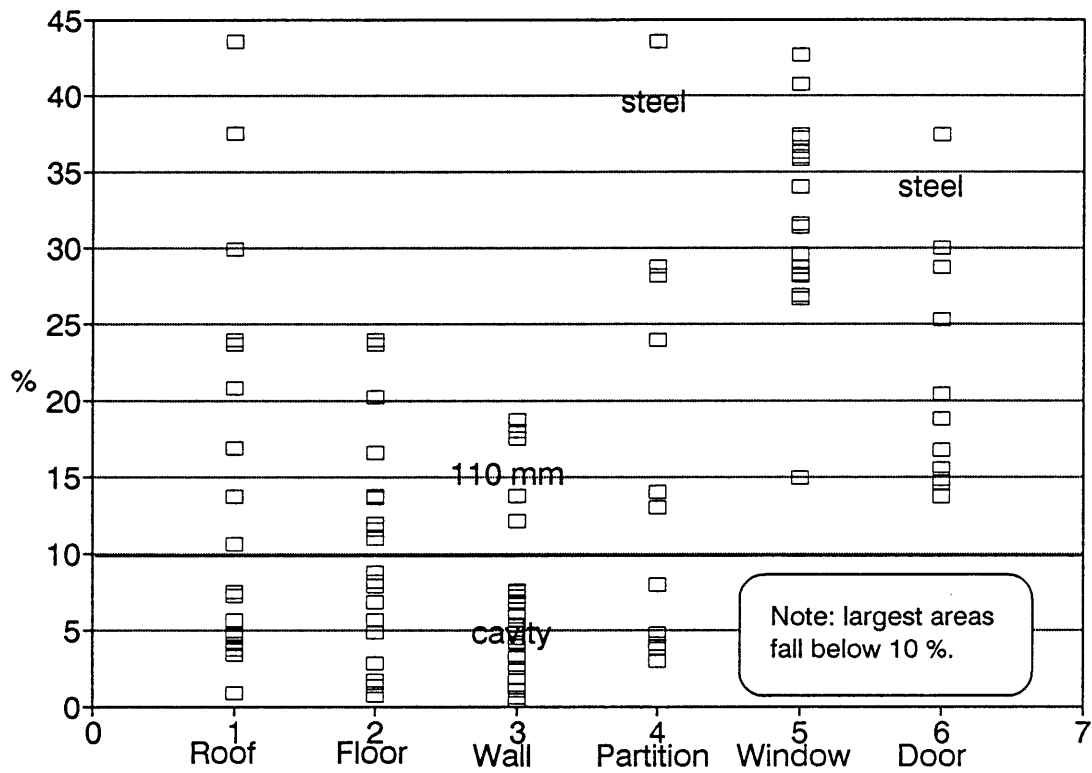


FIGURE 2.27 Averaged temperature swing differences between interior surfaces as a percentage of external temperature swing.

## THEORETICAL FOUNDATION OF A NOVEL METHOD

30 % of the external difference. These results indicate that steady state heat transfer between interior surfaces can not be negligible.

To determine the temperature difference between the walls when the external temperature difference is sinusoidal, the heat storage capacity of the walls must be taken into account. We use the two port representation (see §2.5.3) and two port theory to obtain the solution. The detailed results for a typical office are given in appendix 2c. Figure 2.27 shows the average temperature swing difference between interior surfaces when one surface (the one on the side of the forcing temperature) is of the indicated type. The 'average' indicating that the results for opposing surfaces of all other types existing in the building, have been averaged. The results indicate that also for the swing component, a large fraction of the exterior temperature difference appears across the interior surfaces for roofs, windows and doors. For walls the difference is below 20% with most walls actually in the range 0 to 10%.

In figure 2.28 the averaged swing temperature difference is also shown against the time-constant of the wall. There is a definite dependency for the swing temperature difference to decrease for massive, insulated walls.

These results were obtained by calculating the temperature difference which would exist on the interior surfaces of two infinitely large walls of the given construction, when a temperature difference exists between the exterior surfaces. Both convection and radiative heat transfer were taken into account. In actual buildings, surfaces are also at right angles to each other, in which case the convective heat transfer will probably be the same but radiative transfer will be reduced.

THEORETICAL FOUNDATION OF A NOVEL METHOD

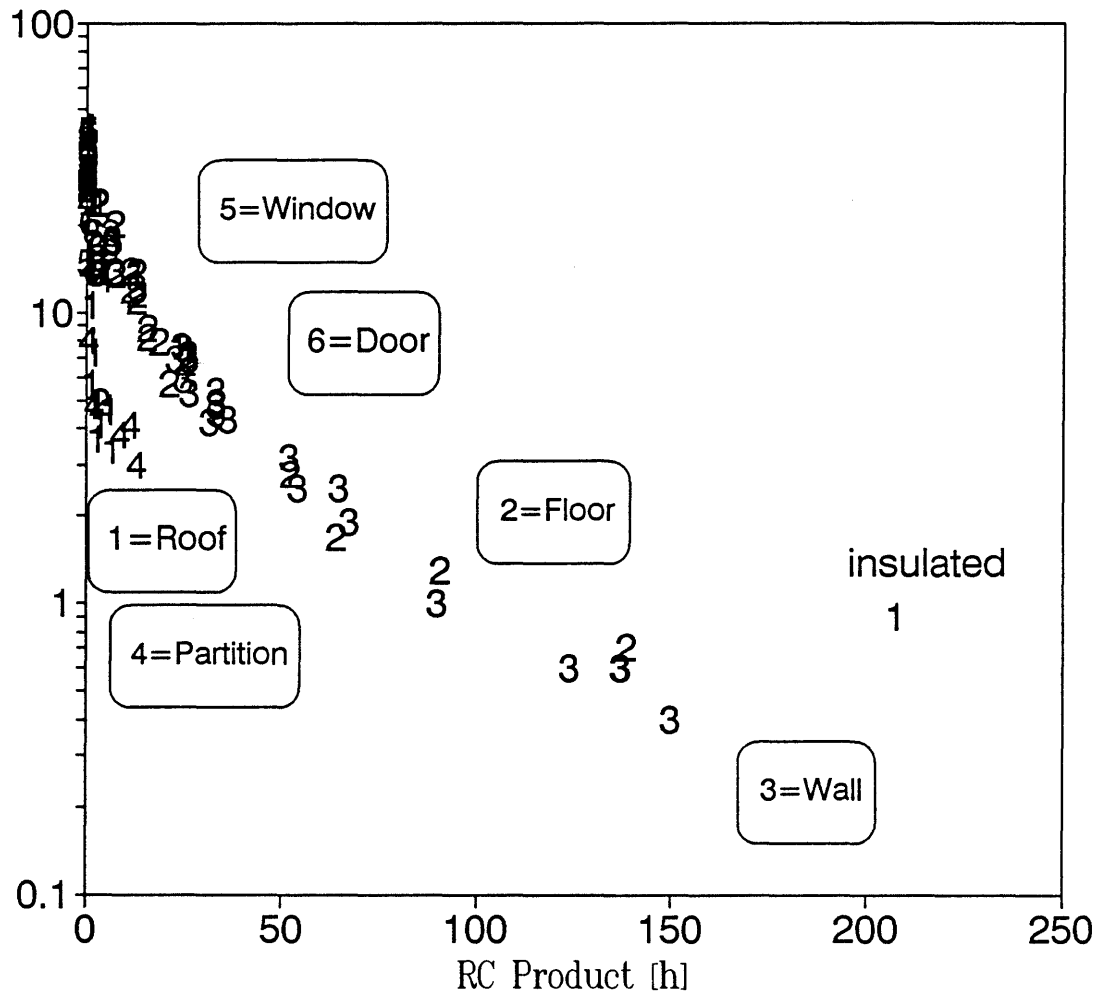


FIGURE 2.28 Averaged temperature swing differences against thermal time constant of the wall.

## THEORETICAL FOUNDATION OF A NOVEL METHOD

We can summarize these results by noting that:

- The temperature difference between interior surfaces are above 20% of the exterior temperature difference if one of the surfaces is a door or a window.
- The temperature differences are larger for the steady state component than for the diurnal swing component.
- Massive insulated walls exhibit very small temperature differences across their interior surfaces.

In deriving these results, we have not taken into account the areas and relative prevalence of the various surfaces since these differ much from one design to another.

The correct interpretation of these results is that they indicate that it cannot be assumed *a priori* that heat transfer between interior surfaces are negligible. This basic assumption of Mathews and Richards is therefore not tenable and, theoretically, better accuracy could be obtained with a network which treats the interior surfaces individually. However, with the difficulties experienced in practice in specifying many thermo-flow details, this theoretical improvement will be very difficult to realize. Essentially all the advantages of the simple thermo-flow network will be sacrificed, for marginal improvement, if the assumption is dropped.

It is important to realize that, in actual buildings, temperature differences between interior surfaces are not only due to the temperature differences between the external surfaces but is also the result of solar energy penetrating through the windows and selectively heating some surfaces. This latter factor, although very important, is difficult to calculate in practice because of the hourly variation of the sun angle during the day, the presence of blinds and curtains, shading devices, trees etc. Mitalas [32] investigated the effect of penetrating radiation on the cooling load. He modelled a floor slab, as a single slab at uniform

## THEORETICAL FOUNDATION OF A NOVEL METHOD

temperature and as two slabs, one adjacent to the window, which received all the solar energy, and another part which received no solar energy. The difference on the calculated cooling load with these two models was very small, less than half of one percent. From this result it appears that energy is quickly distributed to other surfaces from a surface of higher temperature. This would be the case if the inter-surface heat exchange coefficients are much larger than the conductances to the external surfaces. The Biot numbers of figure 2.11, defined as the ratio between the combined coefficient  $h_i$  and the conductance of the wall, indicates that this assumption is in general not true since the Biot numbers are of the order of 1 for many building elements.

We are forced to conclude that the internal heat transfer between wall surfaces can not be neglected. It would thus be more appropriate to attempt to derive the simplified network from the second alternative discussed in §2.5.2, i.e assumption iii), which do not require the assumption of equal interior surface temperatures. This task was not attempted since it can not lead to a simplified network with a well defined physical interpretation of the parameters.

### 2.6 A Refined Simple Model

In the previous sections of this chapter we have simplified the comprehensive thermo-flow network of figure 2.2 to the simple network of figure 2.22. This network can not be further simplified to the network of Mathews and Richards in figure 2.1 without a rather arbitrary assumption that the two resistors in figure 2.1, which represent the shell resistance, can be combined in the single resistor  $R_o$  of figure 2.1. This would have no influence on the calculation of the steady state response but it will definitely affect the swing component of the response. It is also not possible to combine the interior massive structures in a single capacitor with the massive parts of the shell since these masses are subjected to different boundary conditions..

## THEORETICAL FOUNDATION OF A NOVEL METHOD

Although the circuit of figure 2.22 is a second order network (two capacitors) and thus more complicated than the first order network of Mathews and Richards it displays some significant advantages.

- The representation of the distributed elements with an RCR T section instead of an RC section is more satisfactory since the capacitance is not directly available through the interior surface coefficient. The capacitance but will be isolated from the surface if an insulating material covers the interior surface. In the model of Mathews and Richards the active capacitance would be reduced if the interior surface is insulated but it is still directly available to the interior air.
- The more balanced representation of the shell and the separate model of internal masses leads to a clearer physical interpretation of the model.
- The circuit contains a node,  $T_2$ , which clearly represent the interior surface of the shell. The temperature of the interior surface is required for a better definition of comfort temperature which must take into account radiation from the walls.
- The modelling of internal mass in a separate capacitor,  $C_m$ , will increase the accuracy of the prediction if significant interior mass is present.
- It is also a more satisfactory model to extend to multi-zones because the mass of interior partitions are treated separately. It is shown in chapter 4 that a very natural extension to multi-zone thermal response is possible.
- It is easier to extend the model of figure 2.22 because it is a better approximation of reality.

The only drawback is that it is more complicated with 9 elements (including the ventilation resistance) instead of only 4 as in figure 2.1. Because it is a second order network, it is governed by a second order differential equation and it's solution will be only half as efficient. Nevertheless, we are convinced that the benefits of the model of

## THEORETICAL FOUNDATION OF A NOVEL METHOD

figure 2.22 outweigh its disadvantages and that it would be prudent to investigate this network further.

### 2.7 Conclusion, Chapter 2

We set out in this chapter to determine the theoretical foundation of the thermo-flow model of Mathews and Richards as in figure 2.1. We have been able to derive the model of figure 2.22 – which is very similar to the network of figure 2.1 – from a more comprehensive model with the following assumptions:

- I The building can be regarded as a single zone for purposes of thermal-analysis. This is justified if the building is air conditioned, the zones are similar and subject to similar conditions, or the zones are isolated from each other.
- II The walls are thin so that the heat flow is effectively one-dimensional. This is a very good approximation for most building structures, except for floors with ground contact.
- III The massive parts of the structure are thin enough so that the single RCR T section, lumped model can be used instead of the thermal wave solutions of the conduction equation. An alternative statement of this condition is that the frequency of the variation of the forcing functions must be small. This assumption is justified for diurnal variations, and walls not thicker than 220 mm.
- IV The interior surfaces can be regarded as approximately isothermal so that the network of interior heat transfer between the surfaces can be simplified. We have shown that this assumption is not tenable but it is required in order to arrive at a simplified model with a clear physical interpretation.
- V The bulk temperatures of the massive structures, which form part of the shell, are sufficiently similar that a simplified combination rule can be used. In effect this assumption

## THEORETICAL FOUNDATION OF A NOVEL METHOD

implies the external surfaces must be isothermal. It is not tenable on empirical grounds.

The practical effect of the breakdown of the last two assumptions is that they set a theoretical limit to the accuracy of the simplified model. This theoretical limit is probably within the practical limit set by unknown details of the physical construction, the weather, internal loads etc.<sup>17</sup> If we compare the model of figure 2.22 with the model of Mathews and Richards in figure 2.1, we see that they differ in the following aspects:

- A Mathews and Richards use a single capacitor to describe heat storage in both the internal masses as well as walls forming part of the shell. This representation is only possible if it is assumed the bulk temperature of all the massive parts – the shell as well as internal masses – of the building are equal. According to [11] only a part of the internal mass is active in storing heat and is included in the capacitance of figure 2.1. This procedure ignores the fact that the internal mass is forced by the interior air and not by the external surface temperatures. It can be shown that this simplification will cause a magnitude and a phase error in the solution of the temperature swing.
- B In figure 2.22 the conductance of the shell is split in two parts on either side of the capacitance. This ensures that the surface temperatures of the walls are well defined and also the bulk structure temperature. In the model of figure 2.1 it is difficult to ascribe a specific temperature to the interior wall surfaces.
- C The definition of the mean sol-air forcing function as given in §2.5.3 includes the delaying effect of the massive walls.

We may conclude this section by noting that the method of Mathews and Richards is, to a large extent, theoretically justified. The accuracy of this method is not determined, in the first place, by the lumping of the distributed elements, but rather, by the assumptions which are made

---

<sup>17</sup>This is a personal opinion of the author.

## THEORETICAL FOUNDATION OF A NOVEL METHOD

to obtain simple definitions of the parameters of the network in terms of the physical properties of the materials, or, which are required for simple combination rules of the various elements. We have further obtained a better founded simplified network for the description of thermo-flow in buildings, which appears to be a refinement of the model of Mathews and Richards, and which may well be worthy of further investigations, implementation and verification.

THEORETICAL FOUNDATION OF A NOVEL METHOD

REFERENCES Chapter 2

- [1] ASHRAE HANDBOOK, FUNDAMENTALS, *American Society of Heating, Refrigerating and Air-Conditioning Engineers, Inc.*, 1989.
- [2] CIBS, A5, Thermal Response of Buildings, *Chartered Institution of Building Services*, 1979.
- [3] R. W. R. Muncey, Heat Transfer Calculations in Buildings, *Applied Science Publishers*, 1979.
- [4] P. J. Walsh, A. E. Delsante, Calculation of the Thermal Behaviour of Multi-Zone Buildings, *Energy and Buildings*, 5(1983) 231 - 242.
- [5] B. Givoni, Man, Climate and Architecture, 2nd edition, *Applied Science Publishers*, 1976.
- [6] J. D. Wentzel, R. J. Page-Shipp, J. A. Venter, The Prediction of the Thermal Performance of Buildings by the CR-Method, *NBRI Research Report BRR 396*, CSIR, Pretoria, 1981.
- [7] D. Tuddenham, *Computers in Air-Conditioning Load Estimation, Air-Conditioning System Design for Buildings*, Editor A.F.C. Sherrat, McGraw-Hill, pp. 96 -111.
- [8] A. K. Athienitis, Application of Network Methods to Thermal Analysis of Passive Solar Buildings in the Frequency Domain, *PhD Thesis, Department of Mechanical Engineering, Waterloo, Ontario*, 1985.
- [9] A. K. Athienitis, H.F. Sullivan, K.G.T. Hollands, Discrete Fourier Series Models for Building Auxiliary Energy Loads Based on Network Formulation Techniques, *Solar Energy*, Vol. 39, No. 3, pp. 203 - 210, 1987.
- [10] E. H. Mathews, P. G. Richards, A Tool for Predicting Hourly Air Temperatures and Sensible Energy Loads in Buildings at Sketch Design Stage, *Energy and Buildings*, 14(1989) 61 - 80.
- [11] E. H. Mathews, P. G. Rousseau, P. G. Richards, C. Lombard, A Procedure to Estimate the Effective Heat Storage Capability of a Building, *Energy and Buildings*, accepted for publication, 1990.

THEORETICAL FOUNDATION OF A NOVEL METHOD

- [12] QUICK, User's and reference Manual, Release 3.0 of 1990, *Centre for Experimental and Numerical ThermoFlow*, Department of Mechanical Engineering, University of Pretoria.
- [13] N. O. Milbank, J. Harrington Lynn, Thermal response and the admittance procedure, *B.S.E, May 1974*, VOLUME 42.
- [14] G. P. Mitalas, D. G. Stephenson, Room Thermal Response Factors, *ASHRAE Semiannual Meeting, Detroit, Mich., January 30 – February 2, 1967*, No. 2019, III.2.1 – III.2.10.
- [15] K.-I. Kimura, Scientific Basis of Air Conditioning, *Applied Science Publishers*, 1977.
- [16] R. K. Otnes, L. Enochs, *Applied Time Series Analysis*, Volume 1, Basic Techniques, *John Wiley and Sons*.
- [17] D. G. Stephenson, G. P. Mitalas, Cooling Load Calculations by Thermal Response Factors, *ASHRAE Semiannual meeting, Detroit, Mich., January 30 – February 2, 1967*, No. 2018, III.1.1 – III.1.7.
- [18] L. A. Pipes, L. R. Harvill, *Applied Mathematics for Engineers and Physicists*, Third Edition, *McGraw-Hill Book Company*, 1970.
- [19] L. O. Chua, P.-M. Lin, *Computer Computer-Aided Analysis of Electronic Circuits*, *Prentice-Hall, INC*.
- [20] L. A. Pipes, Matrix analysis of heat transfer problems, *J. Franklin Institute*, Marc., 1957.
- [21] M. G. Davies, Optimum Design of Resistance and Capacitance Elements in Modelling a Sinusoidally Excited Building Wall, *Building and Environment*, Vol. 18, No. 1 2, pp. 19 – 37, 1983.
- [22] B. C. Raychaudhuri, Transient Thermal Response of Enclosures: the Integrates Thermal Time-Constant, *Int. J. Heat Mass Transfer*, Vol. 8, pp. 1439 – 1449.
- [23] M. H. De Wit, H. H. Driessen, ELAN-A Computer Model for Building Energy Design, *Building and Environment*, Vol. 23, No.4, pp. 285 – 289, 1988.
- [24] G. N. Walton, Thermal Analysis Research Program Reference Manual, *National Bureau of Standards, U.S. Department of Commerce*, March 1983, NBSIR 83-2655.

THEORETICAL FOUNDATION OF A NOVEL METHOD

- [25] L. Laret, Use of General Models with a Small Number of Parameters, *CLIMA 2000: 7th Int. Cong. of Heating and Air Conditioning*, Budapest, 1980.
- [26] J. A. Crabb, N. Murdoch, J. M. Penman, A simplified thermal response model, *Building Serv. Eng. Res. Technol.* 8 (1987) 13–19.
- [27] M. E. Hoffman, [5] *Chapter 19, §19.8*, pp. 434 – 450.
- [28] ASHRAE, Procedures for Determining Heating and Cooling Loads for Computerizing Energy Calculations, *American Society of Heating, Refrigerating and Air-Conditioning Engineers, Inc*, 1975.
- [29] J. P. Holman, Heat Transfer, SI Metric Edition, *McGraw-Hill Book Company*, 1989.
- [30] A. E. Delsante, Steady-State Heat Losses from the Core and Perimeter Regions of a Slab-on-Ground Floor, *Building and Environment*, Vol. 24, No. 3, pp. 253 – 257, 1989.
- [31] J. F. van Straaten, Thermal Performance of Buildings, *Elsevier Publishing Company*, 1967.
- [32] G. P. Mitalas, An Assessment of Common Assumptions in Estimating Cooling Loads and Space Temperatures, *ASHRAE 72nd Annual Meeting, July 5–7, 1965, Portland, Ore., No. 1949*, pp. 72 – 80.
- [33] C. O. Mackey and L. T. Wright, The sol-air thermometer—a new instrument, *Heat. Pip. Air Condit.*, May 1940.
- [34] E. A. Guillemin, The Mathematics of Circuit Analysis, *John Wiley & Sons, Inc.*, 1959.
- [35] J. M. Penman, Second Order System Identification in the Thermal Response of a Working School, *Building and Environment*, Vol. 25, No. 2, pp. 105–110, 1990.
- [36] M. G. Davies, Transmission and Storage Characteristics of Walls Experiencing Sinusoidal Excitation, *Applied Energy* 12(1982) 269–316.

## THEORETICAL FOUNDATION OF A NOVEL METHOD

## SYMBOLS Chapter 2

$A$	Area [m <sup>2</sup> ].
$\mathcal{A}$	Upper left element of transmission matrix.
$ach$	Air changes per hour [/h].
$\mathcal{B}$	Upper right element of transmission matrix.
$Bi$	Biot number.
$C$	Heat storage capacitance per unit shell area [kJ/m <sup>2</sup> ·K].
$C_c$	Capacitance of composite structure [kJ/m <sup>2</sup> ·K].
$C_t$	Trunk capacitance of T section [kJ/K].
$\mathcal{C}$	Lower left element of transmission matrix.
$c_p$	Specific heat capacity at constant pressure [kJ/kg·K].
$D_p$	Driving-point function, 1 port description of interior mass [kW/K].
$\mathcal{D}$	Lower right element of transmission matrix.
$F_0$	Fourier modulus.
$F_{12}$	Radiation shape factor between surfaces 1 and 2.
$G$	Complex ratio between interior- and exterior surface temperatures.
$h_c$	Wall surface convection coefficient [W/m <sup>2</sup> ·K].
$h_{ce}$	Exterior wall surface convection coefficient [W/m <sup>2</sup> ·K].
$h_i$	Wall interior surface effective film coefficient [W/m <sup>2</sup> ·K], convection combined with radiation. Different version are identified with superscripts.
$h_m$	Fictitious coefficient arising from simplification of interior heat transfer [W/m <sup>2</sup> ·K].
$h_o$	External wall surface effective film coefficient [W/m <sup>2</sup> ·K].
$h_r$	Surface radiation coefficient [W/m <sup>2</sup> ·K].
$I_s$	Irradiance [W/m <sup>2</sup> ].
$i$	Imaginary number.
$k$	Thermal conductivity [W/m·K].
$\ell$	Wall thickness [m].

THEORETICAL FOUNDATION OF A NOVEL METHOD

$Q_c$	Convective interior load per unit shell area [kW/m <sup>2</sup> ].
$Q_r$	Radiative interior load per unit shell area [kW/m <sup>2</sup> ].
$q$	Usually heat-flow [W], sometimes heat-flux [W/m <sup>2</sup> ].
$q_1$	Heat flow at node 1 [W/m <sup>2</sup> ].
$q_c$	Convective heat loss to outside air [W/m <sup>2</sup> ].
$q_l$	Longwave radiation [W/m <sup>2</sup> ].
$q_m$	Heat flow through surfaces of interior mass [W].
$q_s$	Shortwave radiation from the sun [W/m <sup>2</sup> ].
$R_a$	Film heat resistance from interior surface of shell to interior air [K·m <sup>2</sup> /kW].
$R_c$	Surface convection resistance [K·m <sup>2</sup> /kW], Resistance of composite structure [K·m <sup>2</sup> /kW].
$R_o$	Shell partial heat resistance [K·m <sup>2</sup> /kW], sometimes divided by shell area [K/kW].
$R_r$	Radiative resistance [K·m <sup>2</sup> /kW].
$R_t$	Branch resistance of RCR T section [K/kW].
$R_v$	Ventilation equivalent resistance [K·m <sup>2</sup> /kW].
$S$	Conduction shape factor, subscripts w,e, and c denote wall, edge and corner.
$T$	Transmission matrix (bold).
$T_{rc}$	Transmission matrix of RCR T – section.
$T$	Usually denotes temperature if not bold [°C].
$T_1$	Temperature at node 1 [°C].
$T_c$	Mean bulk temperature of the massive parts of the structure [°C].
$T_f$	Forcing temperature
$T_i$	Bulk interior air temperature [°C].
$T_m$	Mean radiant\environment temperature [°C], surface temperature of interior mass [°C].
$T_o$	Outdoor air temperature [°C].
$T_{sa}$	Effective Sol–Air temperature [°C], combined contribution from all external surfaces.
$TTC$	Bruckmayer's thermal time–constant [h].

THEORETICAL FOUNDATION OF A NOVEL METHOD

$TTCB$	Total thermal time-constant of Hoffman [h].
$T_w$	Wall surface temperature [ $^{\circ}C$ ].
$T_{\infty}$	Free stream fluid temperature [ $^{\circ}C$ ].
$t$	Independent variable – time [s].
$V$	Volume of element [ $m^3$ ].
$Vol$	Zone volume [ $m^3$ ].
$W$	2 Dimensional vector of temperature and heat flow.
$x$	Independent variable – space [m].
$Y$	Admittance matrix or Y matrix (2-port description).
$y_{11..}$	Elements of admittance (Y) matrix [W/K].
$Z_0$	Characteristic thermal impedance $1/k \cdot \zeta$ [K/kW].
$\alpha$	Surface absorptivity (radiation), thermal diffusivity [ $m^2/h$ ].
$\epsilon$	Surface emissivity.
$\lambda$	Wavelength of thermal wave [m].
$\omega$	Independent variable – radian frequency [rad/h].
$\rho$	Specific density [ $kg/m^3$ ].
$\sigma$	Boltzman's constant = $5.669 \cdot 10^{-8}$ W/ $m^2 \cdot K$ .
$\tau$	Time-constant of network [h].
$\zeta$	Thermal wave phase factor $\sqrt{\omega/i \cdot \alpha}$ .

## APPENDIX 2A

### ACCURACY OF LUMPING

#### Wall Types

- 1 - Roof
- 2 - Floor
- 3 - Wall
- 4 - Partition
- 5 - Window
- 6 - Door

This table list for various walls from existing buildings the following:

- a) Magnitude and phase of attenuation of sinusoidal temperature wave propagating through the wall.
- b) Magnitude and phase error of the lumped representation.
- c) The Biot number of the wall.

Wall description	Type	Attenuation			Error	
		Biot	Magnitude	Phase[h]	Mag. [%]	Phase [h]
ROOF 270 concrete	1	0.54	0.029	-7.5	-16.9	2.5
ROOF 200 concrete	1	0.4	0.046	-5.7	-15.8	1.3
ROOF insulated steel	1	5.924	0.021	-0.7	-13.8	-1.4
ROOF 150 concrete	1	0.3	0.065	-4.4	-11.9	0.6
ROOF fibreglass	1	3.914	0.03	-0.2	-7.4	-1.2
ROOF 100 concrete	1	0.2	0.089	-2.9	-5.9	0.2
ROOF 100 concrete	1	0.2	0.089	-2.9	-5.9	0.2
ROOF insulated slate	1	3.942	0.029	-1.1	-3.8	-0.2
ROOF insulated steel	1	4.361	0.027	-0.6	-2.9	-0.4
ROOF insulated steel	1	2.332	0.043	-0.4	-2.8	-0.5
ROOF insulated steel	1	1.455	0.057	-0.3	-0.9	-0.2
ROOF steel	1	0	0.13	0	0	0
ROOF steel	1	0	0.13	0	0	0
ROOF insulated steel	1	0.407	0.096	-0.2	0	0.1
ROOF insulated steel	1	3	0.036	-0.4	0.3	0.3
ROOF insulated steel	1	3.75	0.03	-0.4	0.3	0.3

## APPENDIX 2A

## 2A.2

ROOF clay insulated	1	0.162	0.112	-0.8	1.3	0.4
ROOF 9 asbestos insulated	1	3.68	0.03	-1.3	4.7	1.1
ROOF insulated 200 concrete	1	5.4	0.003	-9.3	48.1	3.9
FLOOR 125 concrete on soil	2	0.515	0.037	-6.5	-26	1.7
FLOOR concrete on soil	2	0.415	0.052	-5.2	-22.9	0.9
FLOOR concrete on soil	2	0.415	0.052	-5.2	-22.9	0.9
FLOOR 100 concrete on soil	2	0.487	0.042	-6	-20	1.4
FLOOR concrete on soil	2	0.326	0.067	-4.2	-18.5	0.4
FLOOR 200 concrete	2	0.4	0.046	-5.7	-15.8	1.3
FLOOR 200 concrete	2	0.4	0.046	-5.7	-15.8	1.3
FLOOR 200 concrete	2	0.4	0.046	-5.7	-15.8	1.3
FLOOR 150 concrete on soil	2	0.3	0.065	-4.4	-11.9	0.6
FLOOR 270 concrete	2	0.578	0.026	-7.6	-7.9	2.7
FLOOR 100 concrete	2	0.2	0.089	-2.9	-5.9	0.2
FLOOR 100 concrete	2	0.2	0.089	-2.9	-5.9	0.2
FLOOR 100 concrete	2	0.2	0.089	-2.9	-5.9	0.2
FLOOR fibreglass	2	2.763	0.038	-0.8	-5.4	-0.6
FLOOR 398 concrete	2	0.811	0.012	-10.7	-3.2	5.3
FLOOR concrete on soil	2	1.106	0.008	-11.3	24.7	5.9
FLOOR 75 concrete on soil	2	0.794	0.026	-6.2	68	2.5
FLOOR 150 concrete	2	0.633	0.033	-5.5	75	2.4
FLOOR 150 concrete on soil	2	1.759	0.005	-10.6	154.3	5.5
FLOOR 9 asbestos insulated	2	4.08	0.004	-7.8	238.2	3.5
TROMBE insulated 100 brick	3	6.255	0.011	-5.3	-84.6	-0.4
WALL 110 brick cavity	3	0.829	0.029	-7.1	-21.9	2.3
WALL 110 brick cavity	3	0.834	0.029	-7.1	-21.9	2.3
WALL 114 brick cavity	3	0.837	0.028	-7.3	-21.6	2.4
WALL 114 brick cavity	3	0.839	0.028	-7.3	-21.6	2.4
WALL 220 brick	3	0.805	0.03	-7	-21.5	2.2
WALL 230 brick	3	0.841	0.028	-7.3	-21.5	2.4
WALL 220 brick	3	0.992	0.022	-8	-20	3
WALL 220 brick	3	0.992	0.022	-8	-20	3
WALL 220 brick	3	0.992	0.022	-8	-20	3
WALL 200 concrete	3	0.4	0.046	-5.7	-15.8	1.3
WALL 115 brick cavity	3	0.946	0.023	-7.9	-15.3	3
WALL 330 brick	3	1.207	0.012	-10.4	-14.9	5
WALL 150 concrete	3	0.3	0.065	-4.4	-11.9	0.6

## APPENDIX 2A

## 2A.3

WALL 114 brick	3	0.417	0.072	-3.5	-11.2	0.3
WALL 114 brick	3	0.417	0.072	-3.5	-11.2	0.3
WALL 110 brick	3	0.402	0.074	-3.4	-10.5	0.3
WALL 220 brick	3	0.992	0.021	-8.1	-9.8	3.2
WALL 330 brick	3	1.395	0.009	-11.4	-7.8	5.9
WALL 400 concrete	3	0.8	0.012	-10.7	-6.5	5.2
WALL 220 brick insulated	3	1.162	0.017	-8.1	22.5	3.4
WALL 500 brick	3	1.829	0.003	8.4	32.1	-14.1
WALL 500 brick	3	1.94	0.003	7.7	41	-13.4
WALL 200 brick cavity	3	1.959	0.003	7.7	45.7	-13.4
WALL 110 brick cavity	3	1.163	0.025	-6.1	48.2	2.4
WALL 550 brick	3	2.012	0.002	6.9	58	-12.6
WALL 220 brick insulated	3	2.169	0.007	-8.6	148	4.2
WALL 9 asbestos insulated	4	3.723	0.029	-1.5	-23.4	-1.4
WALL asbestos	4	4.035	0.026	-2.3	-23.2	-0.7
WALL asbestos	4	3.259	0.033	-1.3	-16.9	-1.2
WALL hardboard	4	0.745	0.074	-1.9	-6.3	0
WALL fibreboard	4	1.049	0.068	-0.3	-0.2	0
WALL steel	4	0	0.13	0	0	0
WALL steel	4	0	0.13	0	0	0
WALL 9 asbestos	4	0.044	0.125	-0.2	0	0
WALL hardboard	4	0.168	0.114	-0.2	0	0
WALL insulated steel	4	1.875	0.049	-0.3	0.2	0.2
WALL insulated steel	4	3.75	0.03	-0.4	0.3	0.3
WINDOW 3	5	0.012	0.129	0	0	0
WINDOW 3	5	0.012	0.129	0	0	0
WINDOW 3	5	0.012	0.129	0	0	0
WINDOW 3	5	0.012	0.129	0	0	0
WINDOW 3	5	0.012	0.129	0	0	0
WINDOW 4	5	0.016	0.129	0	0	0
WINDOW 6	5	0.024	0.128	-0.1	0	0
WINDOW 6	5	0.024	0.128	-0.1	0	0
WINDOW 6	5	0.024	0.128	-0.1	0	0
WINDOW 6	5	0.024	0.128	-0.1	0	0
WINDOW 6	5	0.024	0.128	-0.1	0	0
WINDOW 6	5	0.024	0.128	-0.1	0	0
WINDOW 6	5	0.024	0.128	-0.1	0	0

APPENDIX 2A

2A.4

WINDOW 6	5	0.024	0.128	-0.1	0	0
WINDOW qlite	5	0.027	0.127	0	0	0
WINDOW 4 double	5	0.032	0.127	-0.2	0	0
WINDOW 4 double	5	0.076	0.122	-0.2	0	0
DOOR	6	0.794	0.074	-1.5	-3.8	0
DOOR	6	0.8	0.075	-1.2	-2.8	0
DOOR	6	0.706	0.078	-1.2	-2.6	0
DOOR	6	0.706	0.078	-1.2	-2.6	0
DOOR	6	0.857	0.073	-1	-2.1	0
DOOR	6	0.75	0.078	-0.8	-1.3	0
DOOR	6	0.6	0.085	-0.8	-1.1	0
DOOR	6	0.4	0.096	-0.4	-0.3	0
DOOR steel	6	0	0.13	0	0	0
DOOR steel	6	0	0.13	0	0	0
DOOR	6	0.148	0.116	0	0	0
DOOR	6	0.187	0.112	-0.1	0	0

## APPENDIX 2B

### FOURIER MODULI

Non-Air, Non-Metallic layers.

Description	[mm]	Biot	Fo
ACOUSTONE	15	0.563	121.9
BRICKWORK	100	0.366	4.85
BRICKWORK	110	0.402	4.008
BRICKWORK	114	0.417	3.732
BRICKWORK	115	0.421	3.667
BRICKWORK	200	0.732	1.212
BRICKWORK	220	0.805	1.002
BRICKWORK	230	0.841	0.917
BRICKWORK	300	1.098	0.539
BRICKWORK	330	1.207	0.445
BRICKWORK	500	1.829	0.194
CARPET	3	0.2	3600
CARPET	5	0.333	1296
CONCRETE POURED	75	0.15	13.18
CONCRETE POURED	100	0.2	7.416
CONCRETE POURED	125	0.25	4.746
CONCRETE POURED	150	0.3	3.296
CONCRETE POURED	200	0.4	1.854
CONCRETE POURED	270	0.54	1.017
CONCRETE POURED	398	0.796	0.468
CONCRETE POURED	400	0.8	0.463
EXPANDED POLYSTYRENE	15	1.364	362.1
EXPANDED POLYSTYRENE	35	3.182	66.5
EXPANDED POLYSTYRENE	40	3.636	50.91
FELT UNDERCARPET	6	0.4	900
FELT UNDERCARPET	15	1	144
FIBREBOARD	6	0.31	397.3
FIBREBOARD	10	0.517	143
FIBREBOARD	15	0.776	63.56
FIBREBOARD	18	0.931	44.14
FIBREBOARD	35	1.81	11.67
FIBREGLASS	10	0.937	789.9
FIBREGLASS	40	3.75	49.37
FIBREGLASS	50	4.687	31.6
GLASS	3	0.012	4328
GLASS	4	0.016	2434

## APPENDIX 2B

2B.2

GLASS	6	0.024	1082
GLASS WOOL	15	1.125	614.4
GLASS WOOL	25	1.875	221.2
GLASS WOOL	40	3	86.4
GLASS WOOL	50	3.75	55.3
GLASS WOOL	75	5.625	24.58
GYPSUM PLASTER BOARD	5	0.088	563.5
GYPSUM PLASTER BOARD	6	0.106	391.3
GYPSUM PLASTER BOARD	12	0.212	97.83
HARDBOARD	4	0.06	708.4
HARDBOARD	20	0.3	28.34
PINE WOOD	30	0.6	15.58
PINE WOOD	40	0.8	8.766
PLASTER	10	0.063	326.8
PLASTER	15	0.094	145.3
PLASTER	30	0.188	36.31
PLASTER	50	0.313	13.07
PLYWOOD	3	0.064	1811
PLYWOOD	4	0.086	1019
PLYWOOD	15	0.321	72.45
PLYWOOD	35	0.75	13.31
PLYWOOD	40	0.857	10.19
PRESSED ASBESTOS CEME	8	0.039	480.2
PRESSED ASBESTOS CEME	9	0.044	379.4
PVC FLOOR COVERING	2	0.015	72000
PVC FLOOR COVERING	3	0.022	32000
PVC FLOOR COVERING	5	0.037	11520
SLATE	5	0.011	2580
SOIL	50	0.176	13.06
SOIL	69	0.244	6.856
SOIL	75	0.265	5.803
SOIL	130	0.459	1.931
TEAK WOOD	40	0.706	9.367
TILES BURNT CLAY	20	0.071	102.6
TRANSLUCENT Q LITE	2	0.027	2475

## APPENDIX 2C

Detailed results for OFFICE building.

\*\*\*\*\*OFFICE\*\*\*\*\*

Number of Walls: 6

**WALL NUMBER 1 - ROOF 270 concrete Type = 1**

Material	Thickness [mm]	Bi
CONCRETE POURED	270.0	0.540
R = 180.000 m <sup>2</sup> •K/kW	C = 471.874 kJ/m <sup>2</sup> •K	RC = 84937.256 s
Wall Bi (re hi) = 0.540		
T matrix		
(-0.554, 2.764)	(0.123, 0.177)	
(-33.730, 23.543)	(-0.554, 2.764)	

**WALL NUMBER 2 - FLOOR 270 concrete Type = 2**

Material	Thickness [mm]	Bi
PVC FLOOR COVERING	5.0	0.037
CONCRETE POURED	270.0	0.540
R = 192.500 m <sup>2</sup> •K/kW	C = 472.474 kJ/m <sup>2</sup> •K	RC = 90951.172 s
Wall Bi (re hi) = 0.578		
T matrix		
(-0.976, 3.058)	(0.117, 0.212)	
(-33.857, 23.509)	(-0.562, 2.769)	

**WALL NUMBER 3 - WALL 114 brick cavity Type = 3**

Material	Thickness [mm]	Bi
BRICKWORK	114.0	0.417
AIRSPACE	10.0	0.005
BRICKWORK	114.0	0.417
R = 279.662 m <sup>2</sup> •K/kW	C = 333.062 kJ/m <sup>2</sup> •K	RC = 93144.791 s
Wall Bi (re hi) = 0.839		
T matrix		
(-0.860, 2.959)	(0.175, 0.298)	
(-25.934, 15.074)	(-0.860, 2.959)	

**WALL NUMBER 4 - WINDOW 3 Type = 5**

Material Thickness [mm] Bi  
 GLASS 3.0 0.012  
 $R = 4.000 \text{ m}^2\cdot\text{K}/\text{kW}$   $C = 4.991 \text{ kJ}/\text{m}^2\cdot\text{K}$   $RC = 19.963 \text{ s}$   
 Wall Bi (re hi) = 0.012  
 T matrix  
 (1.000, 0.000) (0.004, 0.000)  
 (-0.000, 0.363) (1.000, 0.000)

**WALL NUMBER 5 - WALL 114 brick Type = 3**

Material Thickness [mm] Bi  
 BRICKWORK 114.0 0.417  
 $R = 139.024 \text{ m}^2\cdot\text{K}/\text{kW}$   $C = 166.531 \text{ kJ}/\text{m}^2\cdot\text{K}$   $RC = 23151.899 \text{ s}$   
 Wall Bi (re hi) = 0.417  
 T matrix  
 (0.882, 0.835) (0.136, 0.039)  
 (-3.387, 11.825) (0.882, 0.835)

**WALL NUMBER 6 - DOOR Type = 6**

Material Thickness [mm] Bi  
 PINE WOOD 30.0 0.600  
 $R = 200.000 \text{ m}^2\cdot\text{K}/\text{kW}$   $C = 27.720 \text{ kJ}/\text{m}^2\cdot\text{K}$   $RC = 5544.000 \text{ s}$   
 Wall Bi (re hi) = 0.600  
 T matrix  
 (0.993, 0.201) (0.200, 0.013)  
 (-0.135, 2.013) (0.993, 0.201)

**Film coefficients in  $\text{W}/\text{m}^2\cdot\text{K}$** 

$h_r = 4.667$   $h_i = 3.000$   
 $h_r/h_i = 1.556$   $h_e = 12.334$   
 $h_o = 20.000$

**MEAN BIOT NUMBERS**

WALL:	1	2	3	4	5	6
1	0.540					
2	0.559	0.578				
3	0.689	0.708	0.839			
4	0.276	0.295	0.425	0.012		
5	0.479	0.497	0.628	0.215	0.417	
6	0.570	0.589	0.719	0.306	0.509	0.600

**FRACTIONAL MEAN DIFFERENCE \*100**

WALL:	1	2	3	4	5	6
1	26.064					
2	25.551	25.057				
3	22.465	22.083	19.740			
4	36.346	35.355	29.709	60.023		
5	27.901	27.314	23.817	40.021	30.018	
6	25.252	24.770	21.860	34.786	26.973	24.489

**INTERIOR/FORCING TEMPERATURE \* 100**

WALL:	1	2	3	4	5	6
1	11.030	11.006	12.597	10.822	13.235	16.294
2	10.014	9.991	11.433	9.823	12.009	14.774
3	10.006	9.981	11.645	9.826	12.356	15.921
4	54.361	54.226	62.135	49.991	64.383	75.113
5	25.090	25.023	29.489	24.300	31.356	40.873
6	26.538	26.446	32.643	24.355	35.113	48.464

**FRACTIONAL TEMPERATURE SWING DIFFERENCE \* 100**

WALL:	1	2	3	4	5	6
1	8.537	8.556	7.335	9.283	6.831	4.675
2	7.750	7.767	6.658	8.425	6.199	4.238
3	7.744	7.759	6.781	8.428	6.377	4.567
4	42.071	42.155	36.183	42.880	33.230	21.548
5	19.418	19.453	17.172	20.843	16.184	11.726
6	20.538	20.559	19.008	20.890	18.123	13.903

WALL	Type	Bi	R	C	RC	dT	
ROOF	270 concrete	1	0.540	180.0	471.9	23.6	7.5
FLOOR	270 concrete	2	0.578	192.5	472.5	25.3	6.8
WALL	114 brick cavity	3	0.839	279.7	333.1	25.9	6.9
WINDOW	3	5	0.012	4.0	5.0	0.0	36.3
WALL	114 brick	3	0.417	139.0	166.5	6.4	17.5
DOOR		6	0.600	200.0	27.7	1.5	18.8

## STRUCTURAL STORAGE

### CHAPTER 3

---

#### 3 EXTENSION OF THE MODEL TO INCLUDE A FORCING FUNCTION FOR STRUCTURAL STORAGE

Structural storage is by definition an indoor climate control system where the heat storage capability of the massive structures of the building are actively utilized. For instance, if the outdoor air temperature is lower than the bulk structure temperature during the night, this cool night air may be used to cool the structure. During the hot hours the structure is then allowed to absorb some of the excess heat of the interior air. The functioning and application of this type of system is further discussed in §3.1. It is the objective of this chapter to examine the modelling of this type of system and to extend the model of Mathews and Richards to cater for such systems.

##### 3.1 Introduction

It is by now fairly well known (see references [1] and [2]) that the highveld climate, with large diurnal temperature swings, admits the possibility of conditioning of buildings without mechanical refrigeration. In addition, since a mechanical refrigeration system is complex, expensive to install and in constant need of maintenance, a considerably economic advantage can be realized even if just the cooling capacity of an active indoor climate control system can be reduced. One method for achieving these objectives is to use cool night time air to remove heat from the massive structure of the building when the building is unoccupied. During the hot, occupied hours the temperature of the interior air is then reduced by the absorption of excess heat into the pre-cooled structure. This concept is known as structural storage since it actively utilizes the heat storage capability of the building. It is obviously only applicable to buildings which are relatively massive and which are unoccupied during the night i.e. office blocks. To be successful, structural storage systems require careful thermal design of the passive thermal response of the building and close co-operation between architect and engineer. According to an analysis by

## STRUCTURAL STORAGE

van Aarle and Herman [1], structural storage systems are successful if the thermal design of the building takes into account the following criteria:

"(a) Fenestration

Minimum possible, and shaded on the outside from solar penetration, not only direct, but also sky- and reflected radiation.

double glazing is not necessary for summer (maybe should be considered for winter.) Higher heat loss during the night is beneficial and just about offsets higher heat gain during the day.

(b) Walls

Heavy structure to provide storage mass. Insulation not a necessity for summer.

(c) Roof

Heavy structure. Should always be insulated. Insulation to be on outside.

(d) Lighting

Efficient lighting can now be provided at not more than 10–15 W/m<sup>2</sup>.

(e) People density

The number of people in a room can obviously not be controlled.

(f) Equipment load

Normal office equipment can easily be handled. Typing pool type loads in the order of 40 W/m<sup>2</sup> require an increased air quantity."

Van Aarle and Herman also point out that the highveld climate, with its relatively large diurnal temperature variations, are ideally suited for these systems. But if structural cooling is to find general acceptance in South Africa, an appropriate design tool is required for predicting the performance of buildings containing these systems. From the considerations given above it is clear that such a tool must be dual purpose. It must be

## STRUCTURAL STORAGE

able to guide the architect in the initial design stages of the building; so that a building design with optimum thermal properties results. In addition, it must be an aid to the consulting engineer for designing the conditioning system. The simple model and accompanying computer program of Mathews and Richards, as discussed in previous sections of this thesis, will be extremely suitable as an aid for designing buildings with structural storage, if it is extended to include the possibility of heat extraction from the structure.

In this thesis the fundamental principles behind structural storage is briefly dealt with. A simple model, applicable to most types of structural storage systems, is derived. The implementation of this model is accomplished in a manner that the data input requirements are modest and reasonable. The operator must specify which surfaces are subject to structural storage and what the heat exchange coefficients of these surfaces are. In addition, the operator can either specify the use of external air for storage purposes, or alternatively, pre-cooled air such as would be obtained from an evaporative cooling system. The inclusion of these extra capabilities is done without jeopardizing the speed and ease of use of the simulation of the thermal response.

In this thesis we are not so much concerned with the merits of structural storage. The aim is simple; to be able to simulate the effect of structural cooling on the thermal performance of buildings, in a sufficiently general way, that various cooling systems may be evaluated. With regard to the use of the model and computer program, it is recognized that the building designer will only be able to make use of the program if the data input and user interface is sufficiently simple and logical. If a very detailed specification of the structure is required, at a stage when the structure is still largely undefined, the program will have no use for architects. It seems appropriate to simplify to the extreme and to sacrifice some accuracy of prediction in order to have a useful architectural tool. It must be

## STRUCTURAL STORAGE

remembered that the architect will mainly utilize the program to compare the relative merits of different designs.

On the other hand, if the program is to be useful for engineers designing the conditioning systems which control the indoor climate, the method must be sufficiently accurate and contain enough detail for valid design optimization. By balancing these two – somewhat contradictory – requirements of architect and engineer, we believe a very useful and generally applicable program results which can be used with confidence by all. Furthermore, the combination of passive building response and conditioning design in one program, will hopefully facilitate a design methodology, where these two aspects are treated in an integrated manner and the optimum design is realized. (At least in so far as the passive thermal response is concerned). Our final aim is to be able to evaluate various conditioning systems and building designs, and to optimize these, in a program which assimilates building and conditioning unit in one total thermal system.

### 3.2 The Principles of Structural Storage

In its widest sense the term structural storage can be applied to any conditioning system which, instead of directly attempting to affect the interior air-temperature, does so indirectly by attempting to influence the amount of heat stored in the massive structure. Strictly speaking, such systems include extraction or addition of heat from and to the structure by any means, e.g. by means of a fluid being forced through channels inside the structure. In practice the method employed is normally to force cool air to flow across the surfaces of the structure, a method which requires very little extra complications in the structural design of the building. In all these systems the rate of heat transfer between fluid and structure is the primary design characteristic. It is, as usual, expressed in terms of a

## STRUCTURAL STORAGE

heat transfer coefficient. In this section we briefly investigate the models for convective heat transfer from the literature<sup>1</sup>. We restrict ourselves to forced convection between a surface and a fluid flowing across the surface.

If the surface is flat and isothermal, and, a constant heat flux exists between the surface and the fluid, and furthermore, the air flow is laminar, Holman [3] indicates that the heat transfer between surface and fluid is given by:

$$\overline{T_w - T_\infty} = \frac{q_w \cdot L/k \cdot A}{0.6795 \cdot Re^{1/2} \cdot Pr^{1/3}} \quad (3.1)$$

In this equation  $\overline{T_w - T_\infty}$  is the mean temperature difference between the surface and the free-flowing fluid,  $L$  is a typical contact length [m],  $k$  is the conductivity of the fluid [kW/m·K],  $A$  is the area across which heat transfer takes place [m<sup>2</sup>],  $Re$  is the Reynolds number, defined in terms of the contact length:

$$Re = \rho \cdot u_\infty \cdot L/\mu \quad (3.2)$$

with  $\rho$  specific density [kg/m<sup>3</sup>],  $u_\infty$  free stream velocity [m/s] and  $\mu$  the dynamic viscosity [kg/s·m].  $Pr$  is the Prandtl number given by:

$$Pr = c_p \cdot \mu/k \quad (3.3)$$

with  $c_p$  the specific heat capacity of the fluid [kJ/kg·K]. This equation can obviously be written in the form of a generalized Newton's law of cooling:

$$q = \bar{h}_w \cdot A \cdot \overline{(T_w - T_\infty)} \quad (3.4)$$

with the appropriate definition of the mean convective heat transfer coefficient  $\bar{h}_w$ . Although equations (3.1) to (3.4) can often be used to obtain a preliminary estimate of the order of magnitude of the heat transfer coefficient it (and other similar equations) is not sufficiently accurate for design purposes. For a more accurate value it is essential to build a mock-up and to investigate the matter experimentally.

---

<sup>1</sup>These results are well known and are included here for the sake of completeness and to aid newcomers to the topic.

## STRUCTURAL STORAGE

In general, Newton's law of cooling can only be applied locally to the interface in the form:

$$q(x) = h_w(x) \cdot [T_w(x) - T_\infty]. \quad (3.5)$$

with  $x$  the distance measured in the direction of the flow from the first point of contact between surface and fluid. (Actually this is a definition of the local heat transfer coefficient per unit area.) The heat transfer coefficient depends upon the details of the thermal boundary layer and hence on the details of the flow and construction. In the theories of boundary layer heat transfer, it is convenient to work with non-dimensional groups and the local heat transfer coefficient is usually given in terms of the non-dimensional Nusselt number given by:

$$Nu_x = \frac{h_w x}{k} \quad (3.6)$$

with  $x$  a spatial dimension in the direction of the flow. The Nusselt number is a strong function of the flow details (laminar, turbulent, surface friction etc.), and also of distance along the direction of the flow. To determine the Nusselt number it is thus necessary to know the exact geometry and also the velocity profile of the flow. However, many simplified relations are available in the literature which correlates total heat transfer in terms of the average Nusselt number  $\bar{Nu}$ . Holman [3] gives the following empirical formula:

$$\bar{Nu} = C \cdot Re^m \cdot Pr^n \quad (3.7)$$

with  $C$ ,  $n$  and  $m$  empirical constants to be determined from the experimental data for each type of structure. In (3.7) the Nusselt number is defined with reference to the total length of the surface in contact with the fluid, in the direction of the flow.

## STRUCTURAL STORAGE

Doyle and Johannsen [2] thoroughly investigated the thermal heat transfer coefficient for a structure consisting of a 100 mm thick concrete slab in a plenum. Different air velocities were used with continuous monitoring of the slab and air temperatures. They found that the actual heat transfer coefficients at the surface of the slab ranged from 9 to 18 W/m<sup>2</sup>·K, for air velocities between 0,46 and 2 m/s. The theoretical values were 2,3 to 5,9 W/m<sup>2</sup>·K. They ascribed this discrepancy to the turbulent nature of the air and to radiative heat exchange. Nonetheless, they found good agreement with the heat transfer coefficient derived by exact numerical modelling of the heat exchange mechanism. From these results it appears unlikely that the simple theoretical or empirical relationships above will be of much practical value, unless values for the coefficients in (3.7) is determined experimentally. Alternatively, one can also use extensive computer modelling and simulation of the exact structural geometry and air flow to obtain better estimates of the heat transfer coefficients.

A standard reference, ASHRAE Handbook [4], presents the following simplified equations for forced convection between a vertical plane surface and air:

For wind speeds  $V$  in the range  $5 < V < 30$  m/s:

$$h = 7.2 \cdot V^{0.78} \quad (3.8)$$

For wind speeds  $V < 5$  m/s:

$$h = 5.6 + 18.6 \cdot V \quad (3.9)$$

These equations do not correspond with equations from other authors, e.g. (3.1), where the wind speed normally enters with a half power law. They also disagree with the measured coefficients from [2] given in the previous paragraph<sup>2</sup>.

---

<sup>2</sup>Actually (3.9) yields highly unrealistic values, e.g. with  $V = 4$  m/s,  $h$  is 80 W/m<sup>2</sup>·K, a very dubious value. The equation is probably in error and the original reference must be consulted.

## STRUCTURAL STORAGE

One is forced to conclude that the literature is of little benefit with regard to the provision of accurate values for the heat transfer coefficients, and that good engineering judgment will be required. There is no valid, sufficiently general relation for determining the value of the heat transfer coefficient. Each particular case will require individual attention. It is hopeless to try to include in a model all the various geometrical structures and flow conditions which may be encountered in practice. Such an approach will furthermore seriously inhibit the creativeness of the designer and reduce the scope available to the engineer. It will be sufficient to assume that Newton's law of cooling is applicable in a general sense and to leave the problem of deciding what heat transfer coefficient to use, to the judgment of the designer. It will be necessary to give some guidance in this respect to the architect, probably in the form of a suggestion of what coefficient to use for certain types of structures, based on actual measurements. The air-conditioning engineer will obviously need to investigate the dependence of the heat transfer coefficient on the volume flow and other parameters, to optimize the design. This facility can be included in the program by programming equation (3.7) so that the engineer can specify experimental values for  $C$ ,  $n$  and  $m$  and then investigate the consequences when e.g. the flow velocity or other parameters are varied. The architect need not even be aware of this facility in the program since he simply picks a heat transfer coefficient (possibly guided by a help screen) as a design goal for the engineer or from past experience. Obviously architect and engineer should closely co-operate.

To summarize this section we observe that it will be convenient and sufficient to assume Newton's law of cooling valid for the mean temperature difference between wall and fluid, and to include all the structural and flow details in the value assigned to the heat transfer coefficient.

## STRUCTURAL STORAGE

### 3.3 The Equivalent Electrical Circuit with Structural Storage

In this section a simple model for structural storage, based on Newton's law of cooling, is presented and it is shown that this model can be easily incorporated in the thermo-flow network of Mathews and Richards; discussed in chapter 2.

#### 3.3.1 The Definition of the Heat Transfer Coefficient

It was indicated in §3.2 that Newton's law of cooling, will be assumed generally valid for structural storage heat transfer. In (3.4)  $T_w$  is the surface temperature of the wall, a quantity which is not represented in the simplified network of figure 2.1. In the thermal model of Mathews and Richards only one temperature,  $T_c$ , is used which represents the bulk storage temperature. The temperature at the wall surface will normally differ considerably from this bulk temperature, since a thermal gradient exists across the wall. The problem of correct identification of the wall surface temperature in the model of Mathews and Richards is one of the main reasons which led to the proposal of a somewhat more refined model in §2.6. Nevertheless, to keep the network simple, and to stick to the model of Mathews and Richards, the convective surface temperature  $T_w$  will be identified with  $T_c$  in figure 2.1. In effect this implies that the heat transfer coefficient must be defined in the following manner:

$$h_{sc} = \frac{\overline{T_{sc} - T_c}}{q \cdot A} \quad (3.10)$$

where  $T_{sc}$  is the free-stream temperature of the fluid and  $q$  is the heat flux, and the bar designates the average difference between bulk structure temperature and free-stream fluid temperature. This definition of the heat transfer coefficient differs significantly from the normal definition as used in (3.4), so that it will not be possible, strictly speaking, to use the transfer coefficients from the literature in our model. This disadvantage can be overcome by using the more refined model of figure 2.21, but for the present discussion, we limit ourselves to the model of Mathews and Richards.

## STRUCTURAL STORAGE

Note that the above definition of  $h_w$  will correspond with those in the literature when the temperature of the structure is uniform. In practice, uncertainties in the flow rates, fluid temperature, surface finish etc. probably overshadow this uncertainty caused by the actual differences in definition. The main point is that in future, empirical research aimed at determining structural storage heat transfer coefficients, to be used with this thermal model, should preferably use the definition (3.10). Also, when transfer coefficients are taken from the literature, the differences in definitions must be recognized and taken account of.

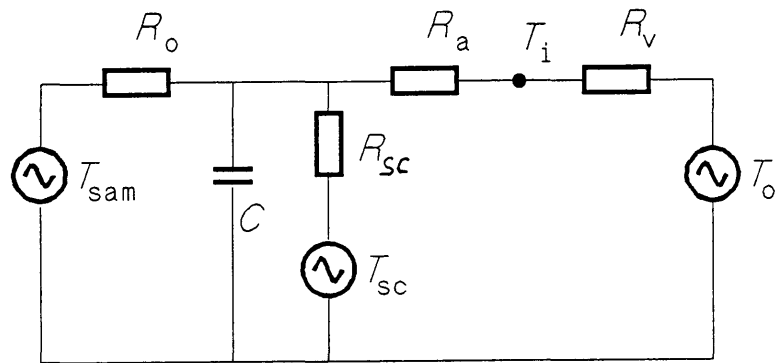


**FIGURE 3.1** The model of figure 2.1 extended to include structural storage.  $T_{sc}$  is the additional forcing function which operates on the structure, through the time dependent resistor  $R_{sc}$ .

The definition according to equation (3.10) is easy to incorporate in the network of figure 2.1. The heat transfer coefficient can be modelled as a conductance connecting the  $T_c$  node with a new independent source, the structural storage source  $T_{sc}$ , which represents the free-stream temperature of the fluid. In many practical systems the outside air will be used as cooling fluid so that  $T_{sc}$  will be equal to the outside air-temperature. If pre-cooled air is used as fluid,  $T_{sc}$  must equal the temperature of the

## STRUCTURAL STORAGE

pre-cooled air. The new network appears in figure 3.1 where we have defined

$$q = \frac{T_{sc} - T_c}{R_{sc}} \quad (3.11)$$

$R_{sc}$  represents the inverse of the combined heat transfer coefficients of all the surfaces. It's value will approach infinity when the heat transfer coefficients of all the surfaces are zero. If the heat transfer coefficients are very large  $R_{sc}$  will vanish, indicating that the temperature of the structure must equal that of the outside air.

### 3.3.2 The Combined Heat Transfer Coefficient

In figure 3.1 we have blandly used one resistance and one source to model the combined effect of the various surfaces subject to structural storage. This requires some further explanation. The thermal network contains a single heat store, the capacitance in figure 3.1, which represents the combined effect of all the massive elements of the structure. The assumption underlying this network is that all the massive elements of the building, which contribute to the storage of heat, are at the same instantaneous temperature<sup>3</sup>. The assumption is founded on the premise that the interior surfaces of the walls are all approximately at the same temperature, due to radiative and convective exchange of heat in the interior. Furthermore, it is assumed that the bulk temperature of all the massive structures is fairly uniform. An obvious objection which might be raised, is that those surfaces which are subjected to cooling will have lower temperatures than the other uncooled structures. This objection is well justified, but is to some extent countered by the assumption that the interior surfaces will, via radiation, tend to equalize the temperatures. The advantage of the network of figure 3.1 is it's clear physical interpretation, and from measurements it appears that the essential features of the thermo-flow problem, that is, the mean rate of heat energy inflow minus outflow to the building structure, is adequately modelled.

---

<sup>3</sup>For a discussion of the assumptions on which the network of figure 3.1 is based refer to chapter 2 of this thesis.

## STRUCTURAL STORAGE

Assuming then that all the surfaces are being cooled with air at the same bulk temperature  $T_{sc}$ , the combined effect is given by adding the contribution of each surface to the total heat flow, so that the active heat stored in the structure is correctly represented. This is fully in accordance with the philosophy of the simplified network as discussed in chapter 2. That is, the capacitor in the network is not the physical capacitance but represents the active heat stored in the massive structure. The total effect of all the surfaces subject to structural cooling is conveniently obtained by adding the individual heat transfer coefficients together. Normally the coefficients would be given in terms of a unit of area so that the total heat transfer coefficient of all  $n$  surfaces is:

$$h_{sc} = 1/R_{sc} = A_1 \cdot h_{s1} + A_2 \cdot h_{s2} + \dots + A_n \cdot h_{sn} \quad (3.12)$$

where  $A_i$  is the area and  $h_{si}$  the structural storage heat transfer coefficient of surface number  $i$ .

### 3.4 Implementation

The solution of the network of figure 3.1 is very straightforward and can be obtained in exactly the same form as the solution of the network of figure 2.1. The solution of the network of Mathews and Richards is discussed in chapter 5, where it is shown that all the forcing function can be combined in two effective forcing functions,  $T_x$  and  $T_y$  of (5.24). The solution of the circuit of figure 3.1 is given by redefining  $T_y$  in (5.24) to include the new independent temperature  $T_{sc}$ :

$$T_y = \frac{Q_r \cdot R_o \cdot R_{sc} + T_{sa} \cdot R_{sc} + T_{sc} \cdot R_o}{R_o + R_{sc}} \quad (3.13)$$

and to define a new resistance  $R_y$ , taking the place of  $R_o$  in the solution:

$$R_y = \frac{R_o \cdot R_{sc}}{R_o + R_{sc}} \quad (3.14)$$

## STRUCTURAL STORAGE

With this new definition of  $T_y$ , and by substituting  $R_y$  for  $R_o$ , the solution proceeds as before via equations (5.23) to (5.34).

Very little programming changes are required to include the extra calculations. Of more importance is the additional input data required to specify the heat transfer coefficient of each surface which are subjected to structural cooling, the temperature of the cooling air and the daily cycle of structural storage. By daily cycle we mean more than just switching the system on and off. Some practical systems use the structural storage system to provide ventilation during the day [2]. In this case, the air is diffused into the zones after it's contact with the structure. This setup provides for both ventilation and structural cooling with a single system. In these systems the daytime flow-rate is usually much lower than during the night. In the next section we examine the modelling of such systems.

### 3.4.1 The Daily Cycle

Specification of the daily cycle presents something of a problem. In §3.1 it was pointed out that the dependency of the convective heat transfer on the velocity of the cooling air depends on specific details, such as the level of turbulence and the geometry of the flow. A generally valid equation, which gives the heat transfer coefficient in terms of the fluid velocity, does not exist. Consequently, it appears impracticable to incorporate a rule which determines the heat transfer from specified hourly volume flows or speeds, although this seems the most natural method. This problem may be circumvented by adjusting the value of the heat transfer coefficient hourly to yield the correct heat flux. A straightforward way of accomplishing this is to specify percentage cooling on an hourly basis. This will plainly indicate the percentage heat flow on a linear scale, with 100 % cooling equal to the maximum heat flux. To demonstrate: if a total area of 10 m<sup>2</sup>, with heat transfer coefficient 20 W/m<sup>2</sup>·K is subject to 50% cooling, with a 10 °C temperature difference between structure and cooling air, the total heat flux will be 20 [W/m<sup>2</sup>·K]·10 [m<sup>2</sup>]·50%·10 [°C] = 1 [kW]. This method is not fully satisfactory, but until a proper, acceptable law is available for the

## STRUCTURAL STORAGE

heat transfer coefficient under diverse circumstances, it will have to suffice. If the flow rate is reduced during the day, the designer must determine the heat transfer rate with the lower flow speed as a percentage of the heat transfer rate at maximum speed. These percentages are then specified hourly. It is assumed that all the surfaces are similarly affected and the percentage value will have the effect of reducing the total heat flux to the prescribed percentage of the maximum.

The enhanced model of figure 3.1, which incorporates structural storage, was implemented in the program. A listing of the relevant sections of the program is provided on the floppy diskette included in the back-cover of this thesis.

### 3.4.2 Verification of the Model

The verification of the model is straightforward. Since an empirical variable – the heat transfer coefficient – is used, the accuracy of the prediction will be determined solely by the accuracy of the specified heat transfer coefficient. In fact, the best way for determining the heat transfer coefficient is to work backwards, and to select a heat transfer coefficient which gives the best prediction in relation to measurements, in each particular case. This procedure is demonstrated in the next section. The implementation of the thermal model, with structural storage included, can be further verified by examining the behavior of the program in limiting cases. When no structural cooling takes place, i.e. when the heat transfer coefficients for all the surfaces are 0, the program should yield the same results as previous versions which did not incorporate structural cooling. Furthermore, when the heat transfer rate is very large, the interior temperature should be close to the temperature of the outside air<sup>4</sup>. Figure 3.2 presents demonstrative results where all the surfaces of a building are subjected to cooling at a large rate. It can be seen that the interior

---

<sup>4</sup>If it is assumed that outside air is used as cooling fluid. A more accurate statement is: the temperature should approach the free-stream temperature of the cooling fluid.

## STRUCTURAL STORAGE

temperature closely approximates the temperature of the exterior air, which was used to cool the structure.

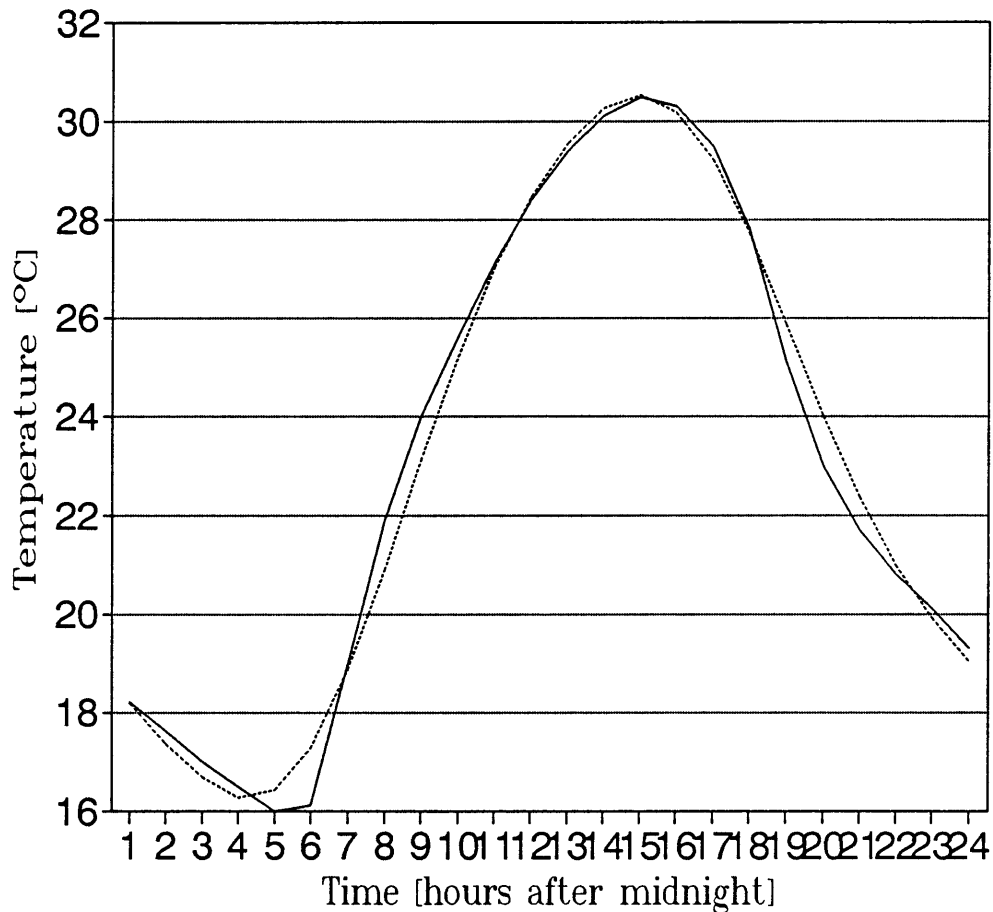


**FIGURE 3.2** Interior temperatures in a building with all walls cooled at a large rate. The interior temperature should approach the exterior air-temperature.

The program seems to be behaving quite well when the hourly rate of cooling is varied. Problems do arise though when the heat transfer rate is excessively high (non physical rates exceeding  $50 \text{ W/m}^2\cdot\text{K}$ ) and large

## STRUCTURAL STORAGE

hourly variations are specified. In this case the sudden, extreme changes in heat transfer rate causes serious numerical errors in the answer. This problem can be eliminated by limiting the heat transfer coefficients to the range 0 to 50 W/m<sup>2</sup>·K.

### 3.4.3 Measured Heat Transfer Coefficients in a Test Hut<sup>5</sup>

The model can also be verified by comparison of measured results with predicted results, provided the exact heat transfer coefficient is known. Unfortunately, as discussed before, the definition of the heat transfer coefficient in (3.10) differs from the usual definition in the literature, so that theoretical or empirical predictions can not be used. In any case, there is some doubt about the validity of the usual equations in the literature [2], as indicated in §3.2. To investigate this issue an experiment was set up in a test hut, which was equipped with air ducts in the concrete floor. For a complete description of the experiment see [5]. Pre-cooled air was blown through the ducts during the hours 18h00 to 06h00. The heat transfer rate from the slab to the air in the ducts was determined iteratively by guessing values until the predicted interior temperature of the thermal model closely resembled the measured interior temperature. The value so obtained was  $\underline{h}_w \approx 7$  W/m<sup>2</sup>·K. This 'measured' coefficient was compared with the value obtained from the empirical correlation of Ditties and Boelter [3], which was applicable to the flow. The values agreed very well. This result must be viewed in contrast with the results reported in [2], where it was found that the usual equations for convection coefficients are insufficient. We come to the conclusion that each case will merit individual attention, and that the correct heat transfer coefficient for a specific design must be experimentally determined.

### 3.5 Some Typical Results

The main aim of structural storage is to reduce the daytime temperature

---

<sup>5</sup>Acknowledgment is due to JH Grobler who carried out the experiments in the test hut, described in §3.4.3.

## STRUCTURAL STORAGE

by cooling the structure with cool night air. It should be possible, from analysis of the network of figure 3.2, to study the economics and applicability of structural storage in various climates and seasons. Since the brief of this study is the inclusion of structural storage in the thermal model, it is not the intention to discuss the relative merit of such a system here. These issues are, to some extent, treated in references [1,2 and 6] which all come to the conclusion, that, provided care is taken in the design of the building and the conditioning system, real energy savings are possible on the highveld.

In this section we present some illustrations of the influence of night time cooling of the structure on the interior temperature of buildings, with the aim to demonstrate the utility and application of the new modified program.

### 3.5.1 A massive structure

Figure 3.3 presents the influence of structural storage on a massive structure, an office block with 300 mm poured concrete floors. A typical centre floor north office in this block is simulated. The office possesses a north wall consisting of 150 mm poured concrete. The other walls are of light construction. In figure 3.3 graphs of the outside air and the inside air with various heat transfer coefficients are shown. It was assumed that the cool night air is used between 21h00 and 06h00 to cool the intermediate floors. Heat transfer coefficients of 0, 5, 10, 20 and 30 W/m<sup>2</sup>°C were used. (Note that these values refer to the office being simulated. Since there are two offices bordering each intermediate floor, the one above and the one below, the actual heat transfer rate from the slab must be twice these values.)

STRUCTURAL STORAGE

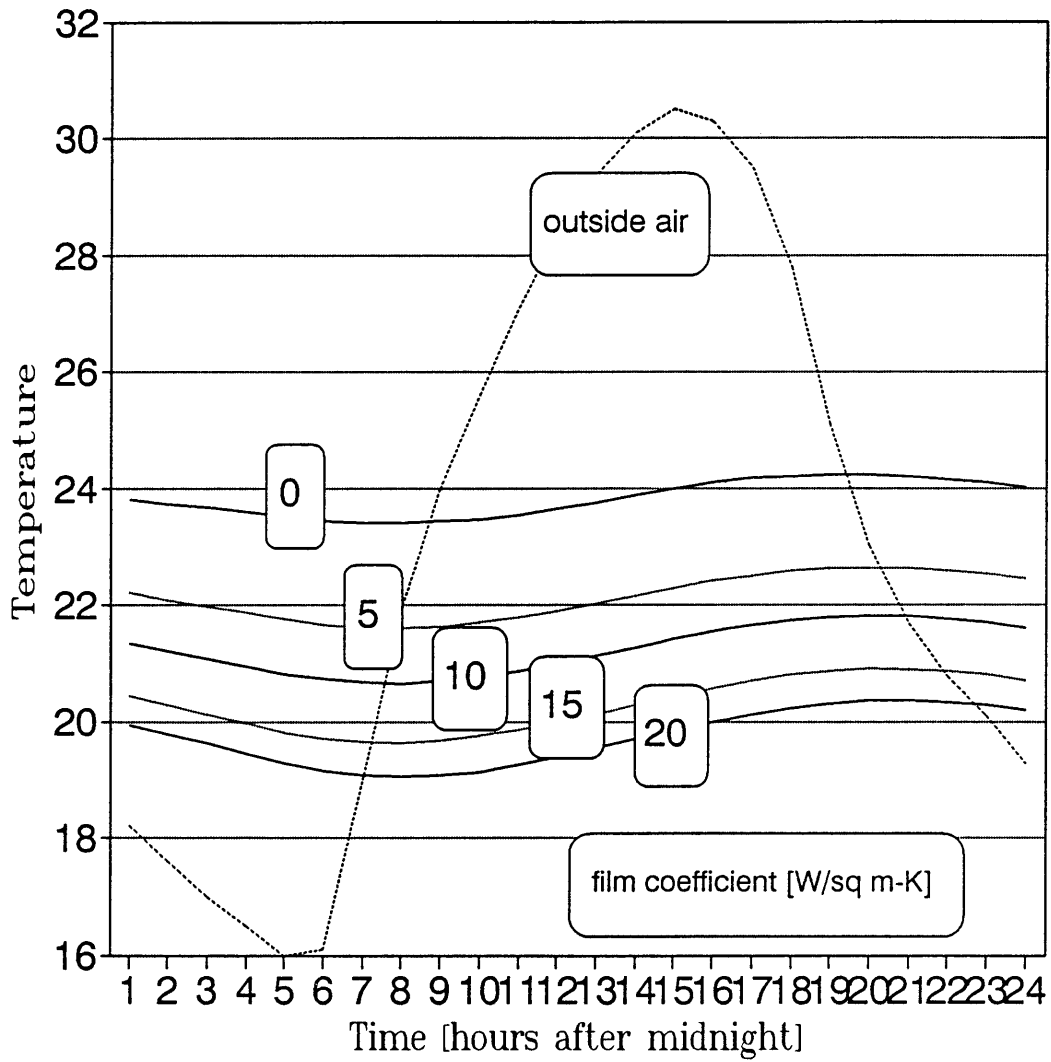


FIGURE 3.3 Night cooling of a massive structure (office).

The structural storage clearly has a pronounced effect on the interior temperature. With a heat transfer coefficient of only 5 W/m<sup>2</sup>°C the interior temperature is lowered by nearly 2 °C. The graphs indicate that increases in the value of the heat transfer coefficient yields diminishing

STRUCTURAL STORAGE

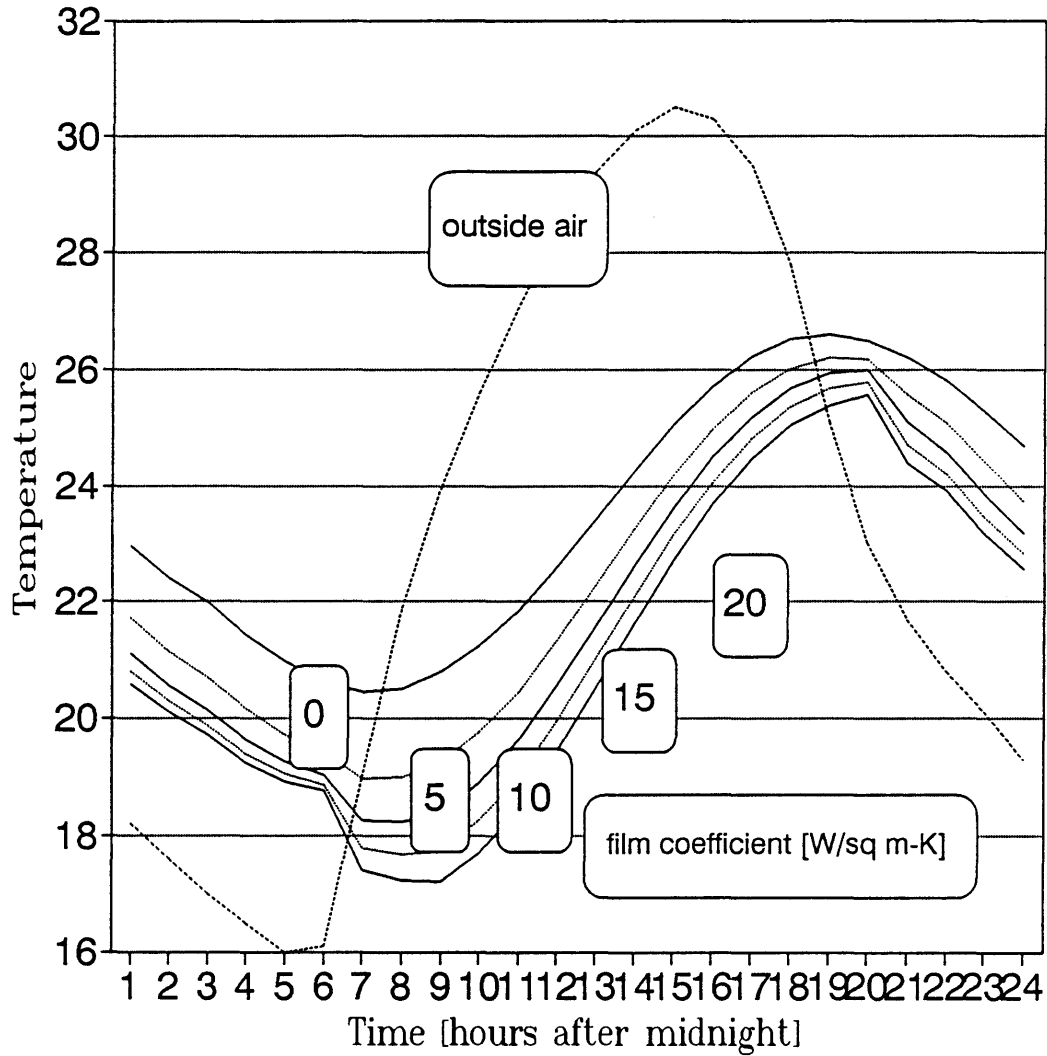


FIGURE 3.4 Night cooling of a lightweight structure.

returns. This is easily explained by noting that the slab temperature can not be lowered below the air temperature. A large heat transfer coefficient would bring the slab temperature to the outside air temperature and further increases in the coefficient will not yield any returns. It follows that

## STRUCTURAL STORAGE

an optimum (in the economic sense) heat transfer coefficient must exist where the maximum effect is obtained for the lowest expense.

### 3.5.2 A lightweight structure

Figure 3.4 shows similar results for a relatively lightweight structure; a test hut in Israel with a pressed asbestos cement roof with well insulated ceiling, walls of pressed asbestos cement insulated with polystyrene and gypsum board, and a plywood floor insulated from the ground. The simulation was done for cooling of the floor with various heat transfer coefficients. The structure contains no massive parts and is obviously not suited for structural storage. The simulation results indicate that the cooling only succeeds in increasing the diurnal swing of the interior temperature, with little effect on the peak temperature. These results conform with intuitive expectations.

### 3.6 Conclusions, Chapter 3

The following conclusions can be stated on the basis of the implementation of – and various simulations with – structural storage.

- The extension of the thermal model to incorporate structural storage appears successful and the results agree with intuitive expectations. In particular these results confirm the contention of Van Aarle and Herman [1] that structural storage is only applicable to massive buildings with well designed shells.
- Incorporation of structural storage in the thermal prediction computer program causes no discernible decrease in the speed of calculation. The extra input data requirements are not excessive but specification of the heat transfer coefficients is somewhat problematic since no general law is available.
- Regarding the verification of the new calculations and procedures; correct results are obtained in limiting cases, but

## STRUCTURAL STORAGE

experimental verification is difficult since the exact value of the convective heat transfer coefficients is not known.

Further verification experiments are required. These experiments must be so designed that the heat transfer coefficient can be directly measured.

It further seems feasible at this stage to instigate a further study, employing the simple model for structural storage presented here, with the objective to investigate the relative merit of structural storage versus other systems e.g. night ventilation. Such a study should consider both capital and running costs, the influence on the design of the building and the relative interior comfort.

## STRUCTURAL STORAGE

### REFERENCES Chapter 3

- [1] T. Van Aarle, A. F. E. Herman, Potential for the air-conditioning of office buildings without mechanical refrigeration, *The South African Mechanical Engineer*, Vol 36 June 1986, pp. 192 – 197.
- [2] C. C. Doyle, A. Johannsen, Computer-modelling of a structural storage air-conditioning system, *CSIR Division of Production Technology Report*, C/DTP 75.
- [3] J. P. Holman, Heat Transfer, *Mcgraw-Hill*, 1986 6th Edition ISBN 0-07-Y66459-5.
- [4] ASHRAE, Handbook Fundamentals, *American Society of Heating Refrigeration and Air-Conditioning Engineers*, 1985.
- [5] J. H. Grobler, Final Year Thesis, *Department of Mechanical Engineering, University of Pretoria*, Pretoria, 1990.
- [6] R. Zmeureanu, P. Fazio, Thermal Performance of a Hollow Core Concrete Floor System for Passive Cooling, *Building and Environment*, Vol 23, No 3, pp. 243 – 252, 1988.

## STRUCTURAL STORAGE

### SYMBOLS Chapter 3

$A$	Heat transfer area [m <sup>2</sup> ].
$C$	Empirical coefficient.
$c_p$	Specific heat capacity at constant pressure [kJ/kg·K].
$h$	Air convection coefficient [kW/m <sup>2</sup> ·K].
$h_{sc}$	Structural cooling convection coefficient [kW/m <sup>2</sup> ·K].
$h_w$	Convection coefficient [kW/m <sup>2</sup> ·K].
$k$	Conductivity of fluid [kW/m·K].
$L$	Length of heat transfer surface in direction of flow [m].
$m$	Empirical exponent.
$Nu$	Nusselt number of fluid–surface interface.
$n$	Empirical exponent.
$Pr$	Prandtl number of fluid.
$q_w$	Surface heat flux [kW/m <sup>2</sup> ].
$Re$	Reynolds number of flow.
$R_{sc}$	Film resistance for structural cooling heat transfer [kW/K].
$T_c$	Bulk structure temperature [°C].
$T_{sc}$	Temperature of air cooling the structure [°C].
$T_w$	Surface temperature [°C].
$T_\infty$	Free–stream fluid temperature [°C].
$u_\infty$	Free–stream velocity of fluid [m/s].
$V$	Windspeed [m/s].
$\rho$	Specific density [kg/m <sup>3</sup> ].
$\mu$	Dynamic viscosity of fluid [kg/s·m].

## CHAPTER 4

---

### 4 INTER-ZONE HEAT FLOW

One of the more important limitations of the method of Mathews and Richards is the single zone treatment of building thermo-flow. In essence this assumption ignores the possibility of heat flow between adjacent rooms, but instead, assumes all the internal volumes have identical temperatures. While verification experiments indicate that adequate predictions are possible with this assumption [1], the limitations of the single zone assumption can only be accurately determined if a more refined model is available for comparison. It is also the objective of this thesis to refine the program if feasible. For these reasons, a study was instigated to determine theoretically the most convenient method for implementing a multi-zone thermal analysis method. This chapter presents the results of this study.

#### 4.1 Background and Objective of this Chapter

A convenient method for extending the single-zone thermo-flow model to a multi-zone model is provided by the method of the admittance matrix as described by Athienitis [2]. This method, with modifications as suggested here, uses a Thevenin equivalent temperature source which is derived from the single zone model to represent each individual zone (see figure 4.1). These sources are coupled with an admittance matrix which describes the heat flow between the zones. The method requires that each zone be analyzed as a single isolated zone, prior to determining the heat flow between the zones and the final temperatures in each zone. To obtain the inter-zone heat flows and final temperatures the inversion of a matrix of complex numbers is required. The size of this matrix is determined by the number of zones being analyzed.

In this chapter the analysis of the multi-zone system is performed under the assumption of a steady, time invariant thermal network.

## INTER-ZONE HEAT FLOW

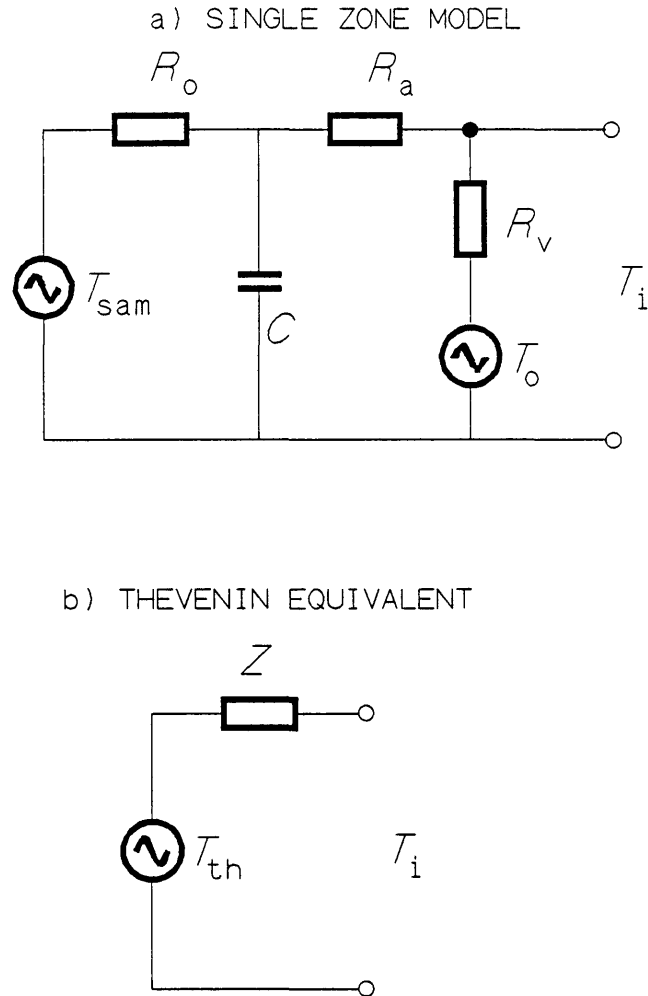


**FIGURE 4.1** The Thevenin equivalent temperature of each zone is the interior air temperature which would result when no heat is lost to adjacent zones. The internal impedance is the interior temperature drop per unit of heat lost to adjacent zones.

Nevertheless, the equations and also the considerable complications which arise when the network becomes time dependent, are indicated. In particular, it is shown that while the problem can easily be solved with

## INTER-ZONE HEAT FLOW

transform techniques and matrix algebra in the time invariant case, the more general time variant case requires the solution of a system of differential equations with time dependent coefficients.

It is the objective of this chapter to extend the single zone model and to establish a multi-zone thermal model and analysis technique. The present single zone model serves as the point of departure:- it is assumed valid for every zone in the multi-zone structure. This study then investigates how these individual zones are to be tied together in the multi-zone model. It also investigates methods for rapidly obtaining true or approximate solutions for the resulting complicated network. The solutions are verified by comparison with results obtained from measurements in a model.

### 4.2 Multi-zone Extension

In the multi-zone building we have a number of inter-reacting zones each of which we assume is basically described by the network of figure 2.1. The interaction between the zones are calculated by coupling the zones with a multi-port network which models the heat exchange between the zones as shown in figures 4.2 to 4.4b. This approach is essentially the same as that described by Athienitis [2]. The multi-port network is easily derived from the physical structures which partition the zones. The solution for the multi-zone network is obtained from the matrix representation of the multi-port network coupled to the Thevenin source of the zone at each port. The Thevenin source representation of a zone is defined as the interior temperature of the zone under adiabatic conditions, i.e. with no heat flow to adjacent zones. With the Thevenin source is associated an internal impedance for each zone which gives the drop in interior temperature of the zone, for each unit of heat which is lost to adjacent zones, as in figure 4.1. The contributions from the partitioning structures are not to be included again in the calculation of

## INTER-ZONE HEAT FLOW

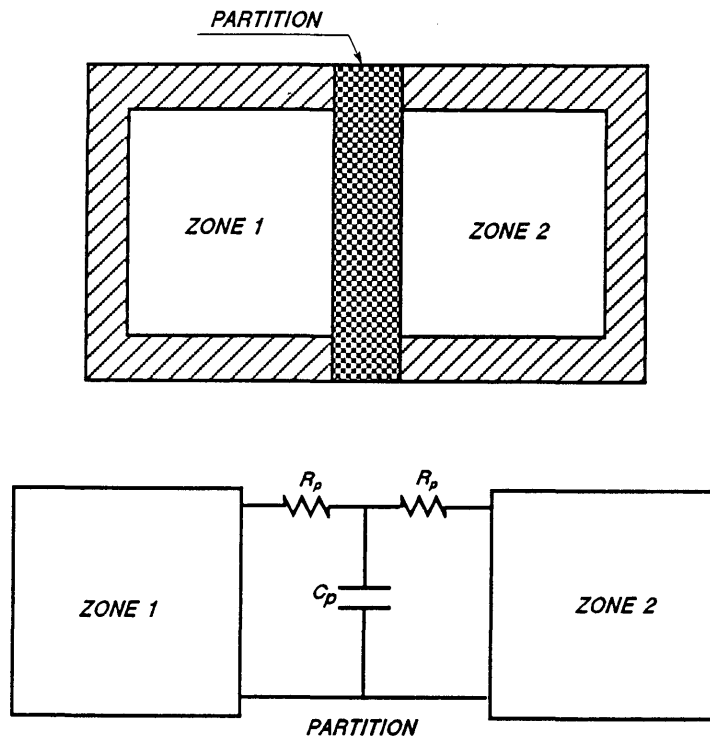


**FIGURE 4.2** The lumped representation of the partition between zones is the RCR T section described in chapter 2. The surface coefficients must be included with the branch resistances.

the capacitance or resistance of any zone but internal capacitance in each zone is included in that zones' model as before<sup>1</sup>. In essence, we simply assume the single zone model for each zone and couple the zones with the RCR T section of figure 4.2b, which, according to the

---

<sup>1</sup>Another alternative is to imagine the partition as split in two and to include the half sections in each zone. The adiabatic line will then run through the middle of the partition. The coupling network between the partitions is then a straight connection without resistances or capacitances. This procedure will be very convenient if the refined model of chapter 2 is used, where internal mass is treated separately. Half the mass of the partition is then included as part of the internal mass of each zone. For the thermal model of Mathews and Richards the procedure in the text is appropriate.

INTER-ZONE HEAT FLOW

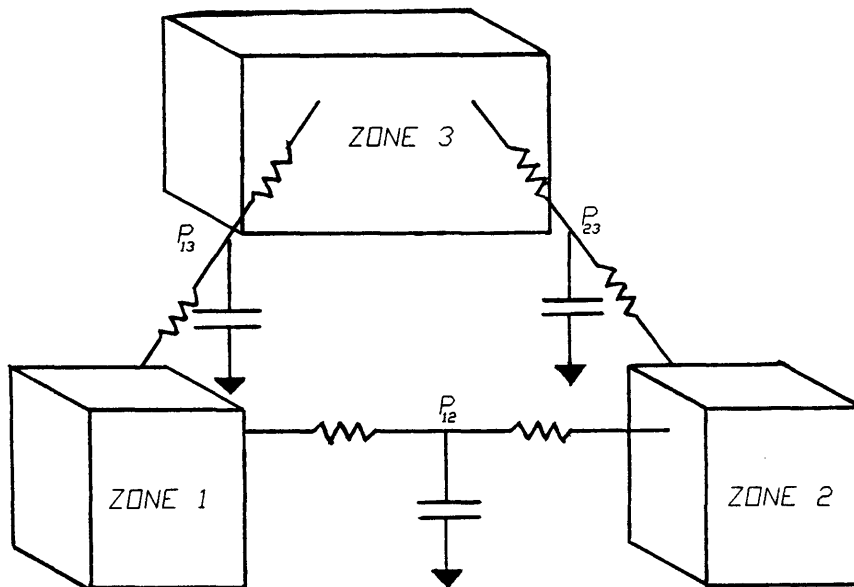
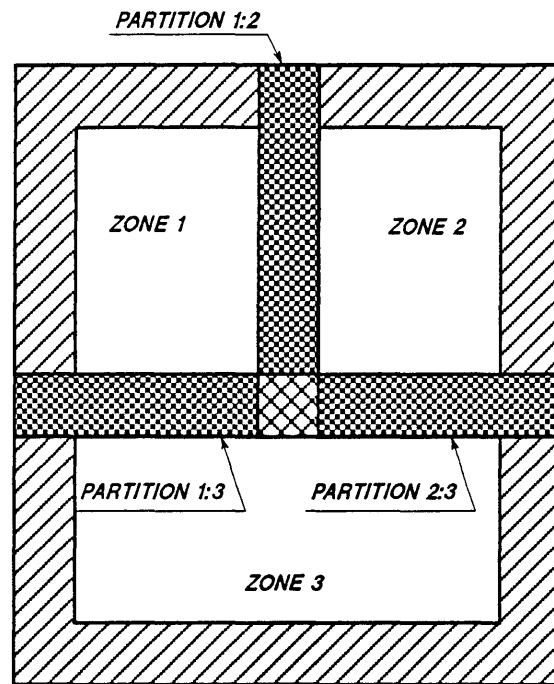


FIGURE 4.3 Representation of a three zone thermal system.

INTER-ZONE HEAT FLOW

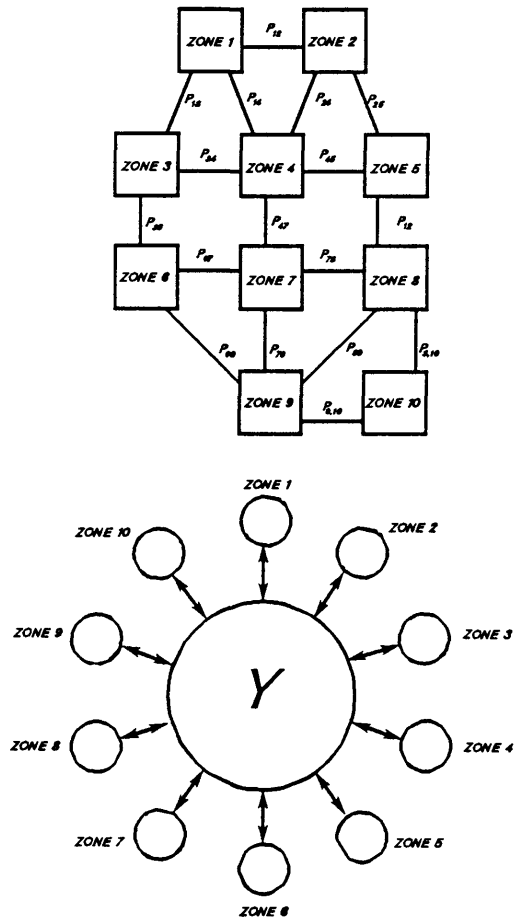


FIGURE 4.4 Representation of a general  $n$ -zone thermal system.

## INTER-ZONE HEAT FLOW

discussions on lumping in chapter 2, adequately models the partitions between the zones. To demonstrate: the three zone structure of figure 4.3a is modelled as in figure 4.3b. The general  $n$ -zone structure of figure 4.4a is modelled with the network of figure 4.4b where the effect of all the partitions coupling the various zones have been combined in the single admittance matrix  $Y$ , and the arrows indicate the internal impedances of the zones.

### 4.3 Solution of the Multi-Zone Network

The solutions of networks such as in figures 4.2, 4.3 and 4.4 can be obtained by various standard techniques. Particularly well known are mesh (loop) analysis and nodal (cut-set) techniques [3]. These powerful techniques are systematic and guarantee a solution, consequently they are amenable to computer implementation for automatic solution. Many programs exist which can find the solution for an almost arbitrary complex network. The objective here is different, we wish to find a solution for the particular network of interest which can be very quickly evaluated, and which requires no knowledgeable input from the operator as far as the solution of the thermal network is concerned (e.g. identification of network nodes for nodal analysis). In the network of figure 4.4 the operator will be required to identify the zones and the partitions between the zones only. Note that the forcing functions will in general be different for each zone (e.g. west facing zones receive sun energy in the afternoons and east facing zones in the morning).

To increase the speed of computation we use the known solutions, equations 5.23 to 5.34, for the single zone network. The forcing functions of each zone are combined in a Thevenin equivalent source  $T_e$  and the effect of the circuit is taken into account by the network operator  $\mathfrak{Z}$  as in figure 4.5. The operator representing the partition between the two zones is indicated by  $\mathfrak{P}$ . The multi-zone thermal circuit is now completely and generally represented by the operators  $\mathfrak{Z}$  and  $\mathfrak{P}$ . This is the 'Y-diakoptic' method as described by Athienitis [2]

## INTER-ZONE HEAT FLOW

with the difference that we prefer to use the Thevenin representation of the sources to the Norton equivalents, because it facilitates appreciation of the effect of the adjacent zones on the indoor temperatures.

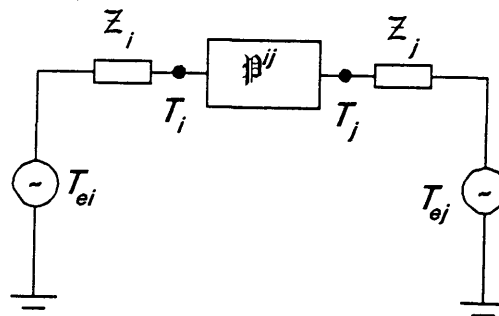


**FIGURE 4.5** The Thevenin representation of two coupled zones. The subscript  $i$  refers to zone number  $i$ , and  $j$  to zone number  $j$ . The superscript  $ij$  refers to the partition between these two zones.

For ease of computation, the operators  $\mathfrak{Z}_i$ , of all the zones, are combined in a diagonal matrix  $Z$  and the partitions operators  $\mathfrak{P}^{ij}$  in an admittance matrix  $Y$ . The nature of these operators depends on the nature of the circuit parameters and the thermal model. In the most general case,  $Z$  and  $Y$  are matrices of partial differential operators, coupling the temperatures and heat flows. If the thermal elements are lumped together a lumped circuit description is obtained, and the partial differential equations reduce to ordinary differential equations, with time the only independent variable. If the parameters are linear and time invariant, the Laplace Transform can be applied to the problem and the operators reduce to matrices of rational polynomials in the Laplace

## INTER-ZONE HEAT FLOW

domain variable  $s$ , with real coefficients, determined by the constant circuit elements.

The operators can be determined with standard 2-port theory by calculating open circuited voltages and short circuited currents, or, from inspection of the heat flow path. Details are given by Athienitis [2]. We next discuss the nature of these operators in more detail for the linear time invariant case and also for the linear time variant case.

### 4.3.1 The Zone Circuit Operators and Thevenin Sources

#### Case 1: time invariant elements, interior temperature calculation

The zone circuit operators and Thevenin sources are determined by reducing the network of heat flows from exterior sources and interior storage to a single effective forcing function  $T_e$  operating through an internal impedance  $\mathfrak{Z}$ . Both the forcing function and impedance will be highly frequency dependent but linear (for linear circuit elements), so that superposition can be used to obtain the total effect of the various forcing functions for all the frequency components they possess. If we assume the thermal model of figure 4.1, the Thevenin sources are just the indoor temperatures calculated from the model, with the assumption that no heat exchange takes place between the different zones. (The open circuit temperature or temperature with adiabatic partition.) In the Laplace domain the Thevenin source for zone number  $i$  is from equation 5.1:<sup>2</sup>

$$T_{ei}(s) = \frac{1}{s\tau_{pi} + 1} \left[ (s\tau_{zi} + 1) \cdot (R_{ai} + R_{oi}) \cdot (T_{oi} + R_{vi} \cdot Q_{ci}) + R_{vi} \cdot (T_{sai} + R_{oi} \cdot Q_{ri}) \right] \frac{1}{R_{ai} + R_{vi} + R_{oi}} \quad (4.1)$$

---

<sup>2</sup>For full definitions of the symbols see chapter 5. The extra subscript  $i$  in (4.1) indicates that the parameters all refer to zone  $i$ , the zone currently under consideration.

## INTER-ZONE HEAT FLOW

where: 
$$\tau_{pi} = \frac{R_{oi}(R_{ai} + R_{vi})}{R_{oi} + R_{ai} + R_{vi}} \cdot C_i \quad (4.2)$$

$$\tau_{zi} = \frac{R_{oi} \cdot R_{ai}}{R_{oi} + R_{ai}} \cdot C_i \quad (4.3)$$

The impedances through which the Thevenin sources operate are the driving point functions at the indoor temperature node, obtained by suppressing all the external sources and calculating the impedance seen from this node into the zone, with all other inter-zone connections removed. From figure 4.6 this impedance is found in the Laplace domain as:

$$Z_i = \frac{[R_{oi} + R_{ai} \cdot (R_{oi}sC_i + 1)] \cdot R_{vi}}{R_{oi} + (R_{vi} + R_{ai}) \cdot (R_{oi}sC_i + 1)} \quad (4.4)$$

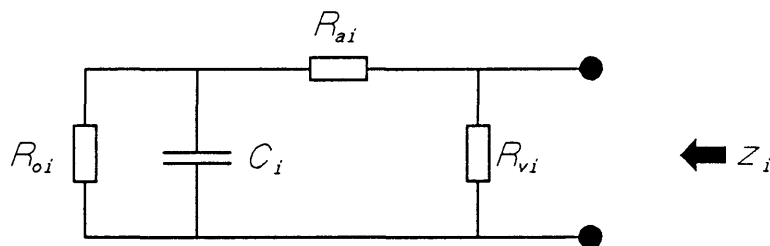


**FIGURE 4.6** Method for finding the internal impedance of a zone.

Case 2: time variant elements, interior temperature calculation

When the parameters are variable, considerable complications arise because the circuit differential themselves equations must be used and

## INTER-ZONE HEAT FLOW

the equation for the Thevenin source becomes:

$$\begin{aligned}
 T_{ei} + \left[ \frac{R_{oi} \cdot R_{vi}}{R_{oi} + R_{ai} + R_{vi}} \right] \cdot \frac{d}{dt} \left[ \frac{C_i \cdot (R_{ai} + R_{vi})}{R_{vi}} \cdot T_{ei} \right] \\
 = \left\{ R_{vi} \cdot \left[ T_{sai} + R_{oi} \cdot Q_{ri} \right] + (R_{oi} + R_{ai}) \cdot \left[ T_{oi} + R_{vi} \cdot Q_{ci} \right] + \right. \\
 \left. R_{oi} \cdot R_{vi} \cdot \frac{d}{dt} \left[ \frac{C_i \cdot R_{ai}}{R_{vi}} \cdot \left[ T_{oi} + R_{vi} \cdot Q_{ci} \right] \right] \right\} / [R_{ai} + R_{vi} + R_{oi}] \quad (4.5)
 \end{aligned}$$

The operator  $\mathfrak{Z}_i$  is now defined as that operator, which, when applied to a test load at the terminals of the circuit, will yield the temperature which will arise at the terminals due to the influence of the circuit on the test load (see appendix 4A).

$$T_{\text{test}} = \mathfrak{Z}_i \{ I_{\text{test}} \}$$

$$\mathfrak{Z}_i \{ \square \} = \mathfrak{Y}_f^{-1} \{ \mathfrak{X}_i \{ \square \} \} \quad (4.6)$$

where:  $\mathfrak{Y}_f \{ \square \} = \mathfrak{D}_t \{ \square \} + \mathfrak{X}_i \{ \square \}$  (4.7)

$$\mathfrak{D}_t \{ \square \} = \frac{1}{R_{vi}} \cdot \square + \frac{d}{dt} \{ C_i \cdot R_{ai} \cdot \square \} \quad (4.8)$$

$$\mathfrak{X}_i \{ \square \} = \frac{R_{oi} + R_{ai}}{R_{oi}} \cdot \square + \frac{d}{dt} \{ C_i \cdot R_{ai} \cdot \square \} \quad (4.9)$$

Case 3: time invariant elements, load calculation

For the sensible heat load we find from equation 5.10 when the Laplace

## INTER-ZONE HEAT FLOW

transform is applicable:

$$Q_{ci}(s) = \frac{T_{rei}(s\tau_{pi} + 1) \cdot (R_{ai} + R_{vi} + R_{oi}) - R_{vi} \cdot (T_{sai} + R_{oi} \cdot Q_{ri})}{R_{vi}(s\tau_{zi} + 1) \cdot (R_{ai} + R_{vi})} - \frac{T_{oi}}{R_{vi}} \quad (4.10)$$

Where  $Q_{ci}$  gives the required convective load to maintain the zone air at temperature  $T_{rei}$ .

### Case 4: time variant elements, load calculation

For the more general case where the parameters are time dependent the equation is:

$$\begin{aligned} & \left[ \frac{R_{oi} + R_{ai}}{R_{oi} \cdot R_{vi}} \right] \cdot (T_{oi} + R_{vi} \cdot Q_{ci}) + \frac{d}{dt} \left\{ \frac{R_{ai} \cdot C_i}{R_{vi}} \cdot (T_{oi} + R_{vi} \cdot Q_{ci}) \right\} \\ & = \left[ \frac{R_{ai} + R_{vi} + R_{oi}}{R_{vi} \cdot R_{oi}} \right] \cdot T_{ri} + \frac{d}{dt} \left\{ \frac{(R_{vi} + R_{ai}) \cdot C_i}{R_{vi}} \cdot T_{ri} \right\} \\ & \quad - \frac{T_{sai} + R_{oi} \cdot Q_{ri}}{R_{oi}} \end{aligned} \quad (4.11)$$

In principle the time-variant system can be solved in the same way as the invariant system, but obviously these equations are considerably more complicated than the equations for an invariant system, and solution is extremely difficult. In this study we limit ourselves to demonstrating the solution of the problem in the Laplace domain for time invariant elements.

### 4.3.2 The Partition Circuit Operators

The interactions between the zones are modelled by assuming the lumped parameter RCR T section of figure 4.2 for the partitions

## INTER-ZONE HEAT FLOW

separating the zones. The lumped parameters are obtained from the distributed characteristics of the structure as explained in chapter 2. More generally, the partition circuit is described by a two port admittance matrix for two zones and a general n-port admittance matrix for n-zones where the admittance matrix includes distributed elements.

In figure 4.2, the heat reservoir of the partition is modelled by  $C_p$ . The parameter  $R_p$  models the surface plus internal heat flow resistance. The admittance matrix for this 2-port with time invariant parameters is obtained from (2.68):

$$\begin{aligned} \mathfrak{P}^{ij} &= \begin{bmatrix} \mathfrak{P}_{11} & \mathfrak{P}_{12} \\ \mathfrak{P}_{21} & \mathfrak{P}_{22} \end{bmatrix} \\ &= \frac{1}{R_p \cdot (2 + i \cdot \omega \cdot R_p \cdot C_p)} \cdot \begin{bmatrix} 1 + i \cdot \omega \cdot R_p \cdot C_p & -1 \\ -1 & 1 + i \cdot \omega \cdot R_p \cdot C_p \end{bmatrix} \end{aligned} \quad (4.12)$$

When the circuit parameters of the T section are time variant the partition operator must be determined by the application of test sources to the ports, in a manner similar to the method used in appendix 4A to determine the zone impedance operator. The elements of  $\mathfrak{P}^{ij}$  will then be differential operators, which, when applied to the temperatures at the ports will yield the differential equations of the heat flow.

When the partition is a compound structure the total effect from all the elements of the partition must be included in the numerical values assigned to the parameters of the T section. For instance, if the partition consists of two distinct surfaces of different construction, the contribution from each surface is easily included by adding the corresponding elements of the two admittance matrices for the two distinct areas (see §2.5.3). For laminated partitions, the equivalent T section for the laminae must first be obtained via (2.62) and (2.63). If heat is also exchanged between the rooms via convection, this

## INTER-ZONE HEAT FLOW

contribution must also be included. In chapter 2 many of these issues are discussed in more detail. Some of the results obtained there are repeated below for convenience.

If the partition is a laminate of  $n$  layers of material the contributions of each layer to  $R_p$  and  $C_p$  are calculated from the following formulae:

$$R_{pc} = \sum_{i=1}^n R_{pi} + \frac{1}{h} = \left[ \frac{1}{2} \cdot \sum_{i=1}^n \frac{\ell_i}{k_i} + \frac{1}{h} \right] \quad (4.13)$$

$$C_{pc} = \left[ R_{p1} \cdot C_{p1} + \sum_{j=2}^n [R_{pj} + 2 \cdot \sum_{i=1}^{j-1} R_{pi}] \cdot C_{pi} \right] / R_{pc} \quad (4.14)$$

with:  $C_{pi} = c_{pi} \cdot \rho_i \cdot \ell_i$

The symbols in (3.13) and (3.14) are:

$\ell_i$  the thickness of layer  $i$

$k_i$  the thermal conductivity of layer  $i$

$c_{pi}$  the specific heat capacity of layer  $i$

$\rho_i$  the specific density of layer  $i$

$h$  film coefficient

and  $A$  the area of the partition.

If the partition consists of  $m$  different areas (e.g. a wall with a door) the contributions of each area are found from:

$$1/R_{pt} = A_t \cdot \sum_{k=1}^m A_k / R_{pk} \quad (4.15)$$

$$C_{pt} = \frac{1}{A_t} \cdot \sum_{k=1}^m A_k / R_{pk} \quad (4.16)$$

where the subscript  $t$  refers to the total taken over all areas of the partition and  $k$  refers to the area of each component.

## INTER-ZONE HEAT FLOW

The contribution due to heat exchange between zones by ventilation can be incorporated by regarding the open areas between the zones, through which ventilation takes place, as areas with no capacity

$$C_{pv} = 0 \quad (4.17)$$

and resistance given by:

$$R_{pv} = R_v/2 \quad (4.18)$$

where the subscript  $v$  refers to the T section modelling the effect of the ventilation.  $R_v$  is the ventilation resistance which depends on the volume of flow between the zones (See [4,5]).

### 4.3.3 Solution

The solution consists of first finding the correct admittance matrix and then inverting a matrix equation to find the interior temperatures and loads.

#### a) Admittance matrix

The solution for time invariant linear parameters is obtained by combining the partition operators  $\mathfrak{P}_{ij}$  between each pair of zones in a general admittance matrix, which by definition gives the vector of heat flows from the vector of temperatures, i.e.

$$\mathbf{q} = \mathbf{Y} \cdot \mathbf{T} \quad (4.19)$$

with:

$$\mathbf{q} = [q_1 \ q_2 \ q_3 \ \dots \ q_n]^t$$

the vector of heat flows into each partition and:

$$\mathbf{T} = [T_1 \ T_2 \ T_3 \ \dots \ T_n]^t$$

the vector of temperatures at the surface of each partition. In the above definitions  $[\ ]^t$  indicates the vector transpose operator.

## INTER-ZONE HEAT FLOW

For two zones, the admittance matrix will correspond with the partition operator

$$Y = \mathfrak{P}^{ij} \quad (4.20)$$

but for three or more zones the elements of  $Y$  is combined from the elements of the  $\mathfrak{P}^{ij}$  for each pair of interconnected zones. The elements of  $Y$  can normally be found by inspection of the interconnections between the zones, since at each zone's port, the flows through all the partitions connecting this zone to other zones, add together. As an illustration of the method, the admittance matrix for the three zone structure of figure 4.3 is:

$$Y = \begin{bmatrix} (\mathfrak{P}_{11}^{12} + \mathfrak{P}_{11}^{13}) & \mathfrak{P}_{12}^{12} & \mathfrak{P}_{12}^{13} \\ \mathfrak{P}_{21}^{12} & (\mathfrak{P}_{22}^{12} + \mathfrak{P}_{11}^{23}) & \mathfrak{P}_{12}^{23} \\ \mathfrak{P}_{21}^{13} & \mathfrak{P}_{21}^{23} & (\mathfrak{P}_{22}^{13} + \mathfrak{P}_{22}^{23}) \end{bmatrix} \quad (4.21)$$

In (3.21) the superscripts refer to the zones and the subscripts to the matrix element, i.e.  $\mathfrak{P}_{11}^{12}$  refers to the element in row 1, column 1 of the partition between zones 1 and 2. To demonstrate:- the first element is obtained from figure 4.3 by noting that zone 1 is coupled to both zones 2 and 3. The total flow from this zone is therefore the sum of the flows to the two zones, and consequently, the first element is given by the sum of the first elements of the partitions from zone 1 to zone 2 and from zone 1 to zone 3.

### b) Interior Temperature

With the Thevenin sources for each zone and the admittance matrix giving the coupling between the zones known, the final solution for the interior temperature in each zone is obtained by matrix inversion. Define

$$T_e = [T_{e1} \ T_{e2} \ T_{e3} \ \dots \ T_{en}]^t \quad (4.22)$$

a vector of Thevenin interior temperatures for the zones,

## INTER-ZONE HEAT FLOW

and

$$Z = \begin{bmatrix} z_i & 0 \\ 0 & z_j \end{bmatrix} \quad (4.23)$$

a diagonal matrix with the internal impedances of the zones. From the definition of the admittance matrix  $Y$  (4.19) we have:

$$q = Y \cdot T \quad (4.24)$$

But from the circuit in figure 4.5:

$$T = T_e - Z \cdot q = T_e - Z \cdot (Y \cdot T) \quad (4.25)$$

Finally solving for  $T$  from this equation gives the interior temperature of the couples zones:

$$T = [I + Z \cdot Y]^{-1} \cdot T_e \quad (4.26)$$

Equation (4.26) gives the final answer for the interior temperature  $T$ , in terms of the interior temperature  $T_e$  when the zones were isolated from each other. In this equation, the contribution from the partitions is represented by  $Y$  and the influence of the shells of the zones (internal impedance) is given by  $Z$ .

c) Sensible Heat Load

To calculate the sensible load to maintain a given temperature  $T_{re}$  in the zones, the required Thevenin sources for the zones  $T_e$  is solved from (4.26) with  $T = T_{re}$  the specified indoor temperatures. From the required Thevenin sources, the required convective load is obtained exactly as in the case of the single zone model, except that the required interior temperature is taken as the required Thevenin temperature, and the partitions are ignored. Thus setting  $T = T_{ir}$  in (4.26) and solving

## INTER-ZONE HEAT FLOW

for  $T_e = T_{er}$ , the required Thevenin temperature, gives:

$$T_{er} = [I + Z*Y] * T_{ir} \quad (4.27)$$

With  $T_{er}$  known the heat load is calculated for each zone from (4.10).

### 4.4 Computer Implementation

The obvious method to calculate the final indoor temperature for the multi-zone network is via (4.26) with the matrix inversion calculated via the Gauss-Jordan algorithm or a similar procedure. This will involve finding the inverse of a  $n \times n$  complex matrix where  $n$  is the number of zones present. The method is illustrated in appendix 4B. Note that when the mean temperatures on each side of the partition are equal no mean flow of heat across the partition takes place. Nevertheless, the partition still influences the swing as the capacitance of the partition contributes to the dampening of the swing. The multi-zone matrix calculation must still be carried out to obtain the correct indoor temperature.

The sensible load calculation via equation (4.27) is quite straight forward.

#### 4.4.1 Time Invariant System

For a time invariant system the multi-zone implementation is rather straightforward and is designed to be a natural natural extension to the program of Mathews and Richards, in the following manner:

To find INTERIOR TEMPERATURE in the zones

- Specify each zone exactly as with the single zone model, but do not include contributions from the partitions, i.e. treat each zone as though the partition is a perfect insulator.

## INTER-ZONE HEAT FLOW

- Calculate the interior temperature in each zone with the partitions regarded as insulators.<sup>3</sup> Combine the temperatures in a vector; definition (4.22).
- Find the impedance matrix  $Z$  for the various zones; definition (4.23).
- Find the admittance matrix  $\mathfrak{P}^{ij}$  for each partition and combine them in the admittance matrix  $Y$ ; (4.21).
- Find the indoor temperatures via matrix inversion; (4.26).

To find SENSIBLE LOADS (assuming interior temperatures have been found first).

- Specify the required indoor temperature for each zone.
- Solve for the values of the Thevenin sources; (4.27).
- Find the convective load that will give the specified indoor temperature in each zone, with the partition regarded as an insulator; (4.10)

### 4.4.2 Time Variant System

Implementation of the general case with variable parameters are similar except that the differential equations with variable coefficients must be solved instead of polynomials in  $s$ . Because  $\mathfrak{Z}_i$  is determined by (4.6) to (4.9), equations (4.26) and (4.27) must be solved with  $Z$  and  $Y$  re-interpreted as impedance operators, yielding differential equations coupling  $T$  to  $T_e$  and  $T_{er}$  to  $T_r$ . Instead of obtaining the solution by matrix inversion and multiplication, these differential equations will have to be solved, possibly by numerical means.

An alternative approximate procedure is to use a time dependent definition of  $Z = Z(t)$  and then to carry out the matrix inversion at

---

<sup>3</sup>Up to here the procedure is exactly as with the single zone model.

## INTER-ZONE HEAT FLOW

each time instant. The procedure is:

- Calculate the insulated interior temperatures (Thevenin temperatures) with the present variable parameter network solutions.
- Assume that the parameters of the partition are invariant i.e. doors are not opened and closed between the zones etc.<sup>4</sup>
- Define  $\mathfrak{Z}_i(t)$  as the complex time dependent ratio between test voltage and test current as opposed to equation 3.6. Define  $Z = Z(t)$ ; Definition (4.23).
- Carry out the matrix inversion for every time instant to find the interior temperature; (4.26).
- Find the load by matrix multiplication for every time instant, as before.

This procedure will be approximate only as the derivatives of the time dependent circuit elements also contribute terms to the differential equations. These terms are ignored in the above procedure. In the actual solution of the time variant equations (4.5 and 4.11) it is expedient to solve the equivalent equations for the energy stored in the massive structure, rather than the equations for temperatures and heat flows. The stored heat is a reasonably smooth function of time with small derivatives, (see chapter 5). For this reason this approximate technique can provide reasonable answers. But a considerable amount of computation is still required since an  $n \times n$  matrix inversion is required at each time instant. Another, more accurate alternative, would be to write the differential equations as difference equations and to use standard numerical techniques for solution. The investigation of these techniques are, however, outside the scope of this study.

---

<sup>4</sup>This assumption is not essential but it will reduce the complexity of the solution. When the parameters of the partition are also functions of time, the admittance matrix  $Y$  also becomes a function of time  $Y(t)$ .

## INTER-ZONE HEAT FLOW

### 4.5 Verification

Obviously the best method for establishing the validity of the model is to obtain measurements in actual buildings. Such an experiment will require detailed logging of temperatures, loads and all human activity in the various zones and, consequently, will be very difficult and expensive to execute. A second best, more practical method is to use a model of a building. Such an experiment is described here.

#### 4.5.1 Experimental results

To verify the procedure for combining the zones an experiment was conducted in a model consisting of two similar zones which could be interconnected or isolated with various partitions. The model was placed in a laboratory beneath ground level where the indoor temperature was found to be almost constant. To test the multi-zone solution method, the zones were first insulated from each other and a heat source was placed in one zone. To ensure a uniform interior temperature a small fan was placed in each zone stirring the air continuously. The power dissipation of the fan was considered negligible. The temperature changes due to the heat source being switched on and off were recorded in both zones with a thermograph. The heat storage capacity of the thermographs were taken into account. The results from this measurement is given in figures 4.7a&b. In figure 4.7a we have the temperature in the active zone and in figure 4.7b in the passive zone. Clearly, almost no heat transfer between the two zones took place. The measured temperature swing in zone 1 must therefore correspond to the Thevenin temperature  $T_{e1}$  of (4.10) while for zone 2 we have  $T_{e2} = 0$ . (We disregard the constant mean component.) To determine the interaction between the zones, a semi-conducting partition was next placed between the zones and the temperature in each zone was again recorded. The results from this second experiment is shown in figures 4.8a and 4.8b, and clearly some of the heat is transferred to zone 2, which now also exhibits temperature swings, while the swing in zone 1 is reduced. If the multi-zone analysis technique is capable of correctly

## INTER-ZONE HEAT FLOW

predicting the change in temperature swings between figures 4.7 and 4.8, in each zone, it will be verified for the two zone model. By measuring the Thevenin temperature in this way, we are able to circumvent any calibration inaccuracies in the thermographs and can obtain accurate numerical values for the zone parameters, as explained in the next section.

### 4.5.2 Application of multi-zone procedure to model

To apply the analysis technique to the model we need an accurate thermal model of the type of figure 4.1. The values of the resistors and capacitances in the model can be found from the physical construction, but since we only wish to verify the multi-zone procedure, and not the thermal modelling, it is easier and more accurate to obtain the zone model directly from the measured response when the zones are isolated. Note in figure 4.7 the temperature swing corresponds to the step-response of a single time constant RC network. By definition the time constant  $\tau$  is the time until 63% of the final value is attained and from the figure this is estimated to be 2.7 hours. The internal impedance can be found from figure 4.6 by calculating the driving point impedance as seen at the interior air node, with all sources suppressed and no ventilation:

$$\mathfrak{Z}_1 = \mathfrak{Z}_2 = R_a + \frac{R_o}{\tau \cdot s + 1} \quad (4.28)$$

Besides the value of the time constant, the values of  $R_a$  and  $R_o$  are required to find the impedance  $\mathfrak{Z}$ . To obtain the value of  $R_o$ , the measured temperature swing is compared with the theoretical temperature swing when the zones are isolated. The step response to a 50 W radiative source of the circuit of figure 4.1, in the absence of ventilation is:

$$T(t) = 50 \cdot R_o \cdot (1 - e^{-t/\tau}). \quad (4.29)$$

## INTER-ZONE HEAT FLOW

The measured amplitude of the step response is 9°C from which it follows that  $R_o = 180$  K/kW. The value of  $R_a$  is determined by the inside film coefficient. This is the only parameter of the zone model which is undetermined by the measurements. In general it is extremely difficult to determine surface heat transfer coefficients. In the model, one side of the partition is subject to intense radiation from the heat source and convective transfer plays a minor role. On the other side, in the passive zone, the heat transfer takes place both through radiation and convection. Determination of the heat transfer coefficients requires detailed knowledge of the air movement in each zone and also of the difference in temperature between the various surfaces. In the verification calculation it was assumed the film coefficient in zone 1 is very large, due to the radiation directly heating the surface. The film coefficient in zone 2 was taken as  $12$  W/m<sup>2</sup>·K, a value based on a (probably debatable) calculation in appendix 4C.

The RC elements of the T section representing the semi-conducting partition is obtained from the thermal parameters of the construction material and the area of the partition (under the assumption that the film coefficient in zone 1 is very large):

$$R_p = \frac{1}{2} \cdot \left[ \frac{1}{k} + \frac{1}{h_2} \right] \cdot \frac{1}{A} = 116.9 \text{ K/kW}$$

$$C_p = c_p \cdot \rho \cdot \ell \cdot A = 6.6 \text{ kJ/K}$$

where:  $k = 0.62$  W/m·K thermal conductivity  
 $h_2 = 12$  W/m<sup>2</sup>·K partition film coefficient in zone 2<sup>5</sup>  
 $A = 0.419$  m<sup>2</sup> area of the partition  
 $c_p = 0.83$  kJ/Kg·K specific heat capacity  
 $\rho = 2100$  kg/m<sup>3</sup> specific density of asbestos  
and  $\ell = 9$  mm thickness of the partition.

---

<sup>5</sup>Determined from radiative and convective heat transfer in appendix 4.C.

INTER-ZONE HEAT FLOW

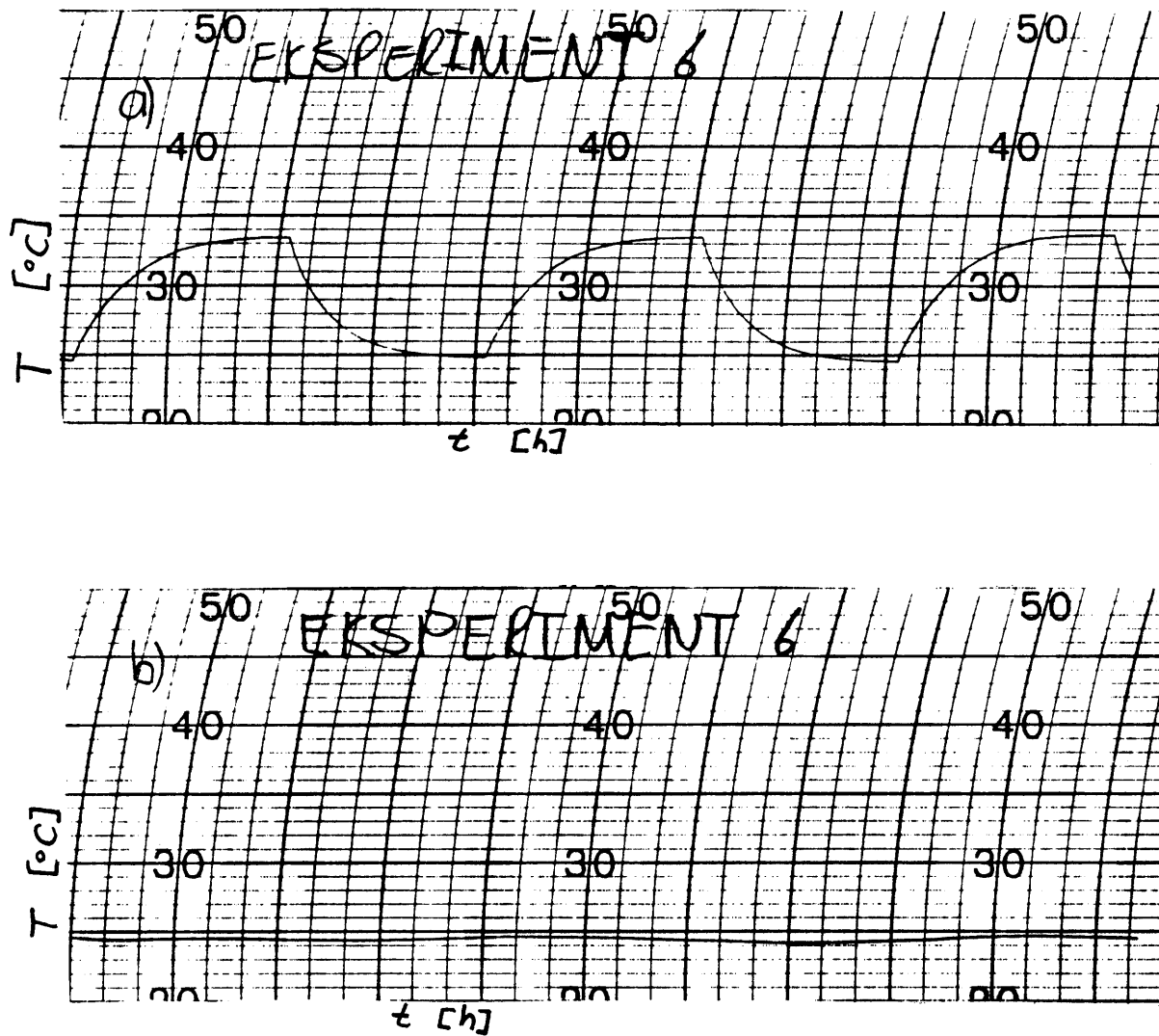
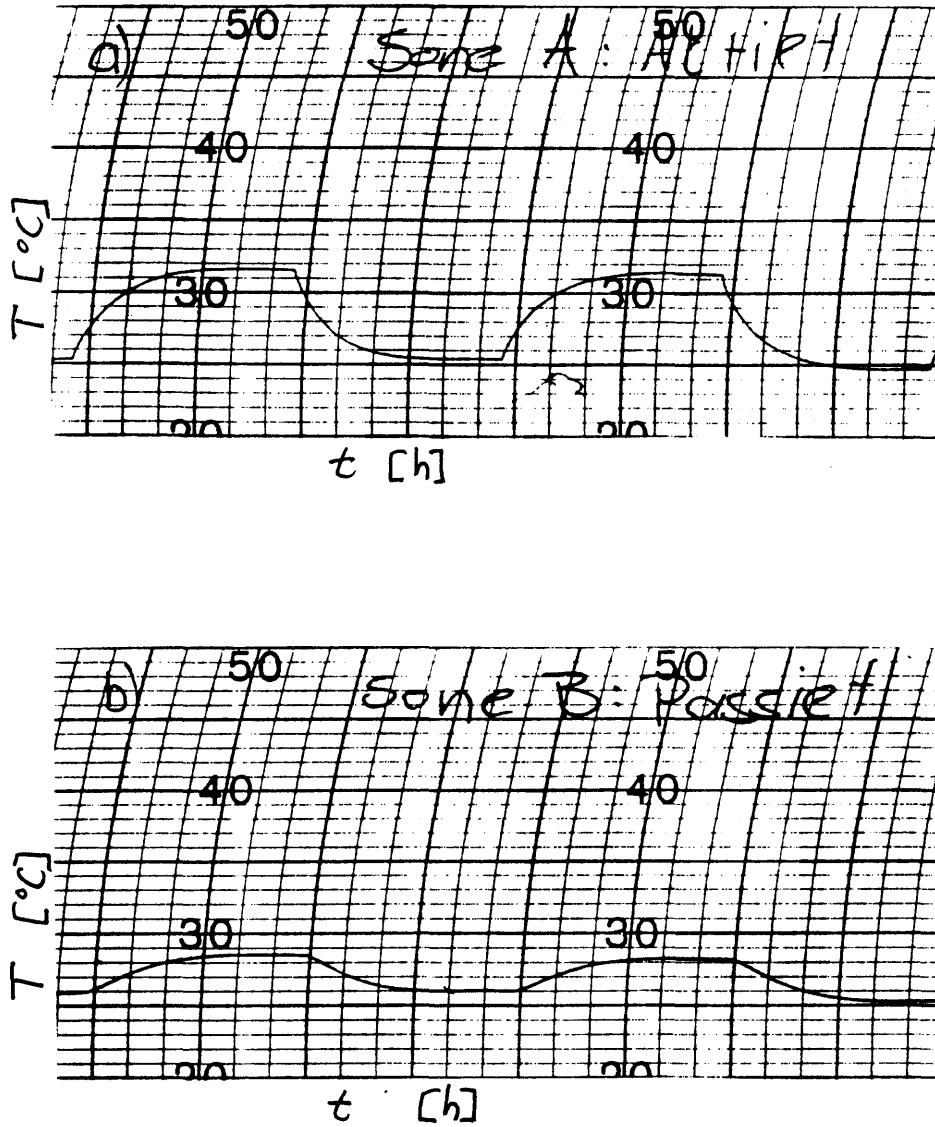


FIGURE 4.7 Measured temperatures in the zones with insulation between the zones, a) is the temperature in the zone with the heat source, b) is the temperature in the passive zone. The horizontal axis is marked every 2 hours.

INTER-ZONE HEAT FLOW



**FIGURE 4.8** Measured temperatures in the zones with a partially conducting partition, a) is the temperature in the zone with the heat source, c) is the temperature in the passive zone. The horizontal axis is marked every 2 hours.

## INTER-ZONE HEAT FLOW

With these numerical values of the circuit elements the multi-zone analysis can proceed for each frequency component of the square wave forcing function. The calculation is carried out in appendix 4D and the predicted temperature swings in the zones are 6 °C in zone 1 and 2.5 °C in zone 2. These values are essentially the same as the measured swings given in figures 4.8a & b so that the predictions compare very favorably with the actual temperatures.

To investigate the sensitivity of the procedure with respect to the unknown surface coefficients, the calculation was repeated for a heat transfer coefficient  $h_2 = 20 \text{ W/m}^2 \cdot \text{K}$ . The predicted temperature in zone 1 was 6 °C and in zone 2, 3 °C. Bearing in mind the difficulty of determining the correct heat transfer coefficient the procedure appears to be well verified by the measurements in the model.

### 5.6 Conclusions, Chapter 4

This part of the study has been successful in as much as it proved possible to find a reasonably effective and accurate method to obtain the solution to the multi-zone thermal model when the parameters of the circuit are time invariant. The method is also applicable to the more general time variant case but in this case considerable implementational difficulties arise which will result in cumbersome and time consuming computations. It has not been determined whether a more practical approach to the time dependent problem exists.

Before the techniques suggested in this program can be implemented a careful analysis of the data input, output and required operator interface must be made in order to design a logical and user friendly multi-zone program. Note however that the method facilitates separate calculation of each zone's influence followed by combining the zones via the partition admittance matrix and calculation of the final temperatures. This procedure is exactly the same as the current method of combining the energy requirements of the various zones in the program.

## INTER-ZONE HEAT FLOW

Nevertheless, an extensive rethink of especially the output procedures is required since currently the temperature results for each zone are found before the zones are combined whereas the multi-zone procedure will only supply the final temperature results after the zones have been combined. Furthermore, before the zones can be combined the partitions and heat flow paths between the zones must be identified and described.

Final verification of the method and its implementation will be required. This will entail extensive measurements in various types of existing buildings and models. Note however, that the procedure for combining the zones is a mathematically exact procedure; if any discrepancies surface, they must be attributed to the models describing the zones or the partitions, or to inadequacies in the numerical implementation.

The detailed implementation and effectiveness of the method for time varying circuit parameters have not been investigated in this study. It is also possible that in this instance a more effective calculation procedure than that suggested here exists. These questions will take considerable effort and time to investigate properly, since few convenient mathematical techniques for treating systems of differential equations with variable coefficients exist. A numerical and/or iterative approach might possibly be more rewarding.

## INTER-ZONE HEAT FLOW

### REFERENCES Chapter 4

- [1] E. H. Mathews, P. G. Richards, A Tool for Predicting Hourly Air Temperature and Sensible Energy Loads in Buildings at Sketch Design Stage, *Energy and Buildings*, Vol 14 No 1 pp 61–80.
- [2] A. K. Athienitis, Application of Network Methods to Thermal Analysis of Passive Solar Buildings in the Frequency Domain, *PhD Thesis, University of Waterloo, Ontario* 1985.
- [3] L. O. Chua, P.-M. Lin, Computer-Aided Analysis of Electronic Circuits, *Prentice-Hall, Inc.*
- [4] D. Hill, A. Kirkpatrick, P. Burns, Analysis and Measurements of Interzonal Natural Convection Heat Transfer in Buildings, *Journal of Solar Energy Engineering*, Vol 108 No 3 August 1986, pp. 178 – 184.
- [5] S. A. Barakat, Inter-Zone Convective Heat Transfer in Buildings: A Review, *Journal of Solar Energy Engineering*, Vol 109 No 71 May 1987, pp. 71 – 76.

## INTER-ZONE HEAT FLOW

### SYMBOLS Chapter 4

$A$	Load contribution factor of interior air temperature.
$\mathcal{A}$	Element of transmission matrix.
$a$	Temperature contribution factor of out door air temperature.
$B$	Load contribution factor of sol-air temperature.
$\mathcal{B}$	Element of transmission matrix.
$b$	Temperature contribution factor of convective source.
$C$	Heat storage capacitance per unit area of shell [kJ/m <sup>2</sup> ·K], load contribution factor of radiative source.
$C_p$	Heat storage capacitance of partition.[kJ/m <sup>2</sup> ·K]
$\mathcal{C}$	Element of transmission matrix.
$c$	Temperature contribution factor of sol-air temperature.
$c_p$	Specific heat capacity [kJ/kg·K].
$D$	Load contribution factor of out door air temperature.
$\mathcal{D}$	Element of transmission matrix.
$d$	Temperature contribution factor of radiative source.
$h_i$	Internal wall film coefficient [W/m <sup>2</sup> ·K].
$h_o$	External wall film coefficient [W/m <sup>2</sup> ·K].
$i$	Imaginary number, index – natural number.
$I_t$	Test current.
$k$	Thermal conductivity [W/m·K].
$\ell$	Wall thickness [m].
$Q_c$	Convective load [kW/m <sup>2</sup> ].
$Q_r$	Radiative load [kW/m <sup>2</sup> ].
$R_a$	Film heat resistance from interior surface of shell to interior air [K·m <sup>2</sup> /kW].
$R_o$	Shell partial heat resistance [K·m <sup>2</sup> /kW], sometimes divided by shell area [K/kW].
$R_p$	Partial heat resistance of partition [K/kW].
$R_v$	Ventilation equivalent resistance [K·m <sup>2</sup> /kW].

## INTER-ZONE HEAT FLOW

$R_v$	Ventilation equivalent resistance between zones [K/kW].
$s$	Laplace domain independent variable [1/h].
$T$	Transmission matrix, vector of temperatures.
$T$	Temperature [°C].
$T_c$	Mean structure temperature [°C].
$T_e$	Effective forcing temperature [°C].
$T_{ei}$	Thevenin equivalent temperature in zone $i$ [°C].
$T_i$	Interior air temperature [°C].
$T_{ir}$	Required (thermostat) interior air temperature [°C].
$T_o$	Outdoor air temperature [°C].
$T_{sa}$	Effective Sol–Air temperature [°C], combined contribution from all external surfaces.
$T_t$	Test temperature [°C].
$t$	Time [h].
$q$	Heat flux density [kW/m <sup>2</sup> ].
$U$	Vector of temperature and heat flow.
$Y$	Admittance matrix.
$x$	Spatial dimension [m].
$\omega$	Radian frequency [rad/h].
$\rho$	Specific density [kg/m <sup>3</sup> ].
$\tau_z$	Time constant of network zero [h].
$\tau_p$	Time constant of network pole [h].
$\mathfrak{D}_t$	A linear operator.
$\mathfrak{P}^{ij}$	Partition between zones $i$ and $j$ (operator).
$\mathfrak{R}_i$	A linear operator.
$\mathfrak{V}_f$	A linear operator.
$\mathfrak{Z}_i$	Internal impedance of zone $i$ (operator) [K·m <sup>2</sup> /kW].

## APPENDIX 4A

## APPENDIX 4A

Derivation of the  $\mathfrak{Z}$  impedance operator.

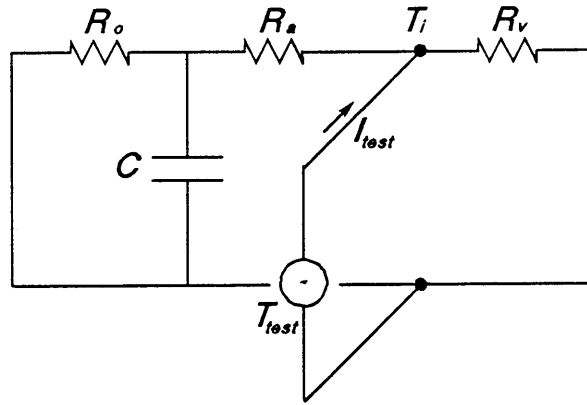


Figure 4A

In figure 4A we apply the test source  $T_t$  to the terminals of the interior air node. The current into the circuit from this test source is  $I_t$  and is given by:

$$I_t = T_t/R_v + I_a \quad (\text{A.1})$$

$$I_a = I_c + I_o \quad (\text{A.2})$$

$$I_c = \frac{d(C \cdot T_c)}{dt}, \quad I_o = \frac{T_c}{R_o} \quad (\text{A.3})$$

But

$$T_c = T_t - I_a \cdot R_a \quad (\text{A.4})$$

so 
$$I_a = \frac{d}{dt} \left\{ C \cdot (T_t - I_a \cdot R_a) \right\} + \frac{T_t - I_a \cdot R_a}{R_o}$$

This equation can be written in the form:

$$I_a \cdot \left[ 1 + \frac{R_a}{R_o} \right] + \frac{d}{dt} \left\{ C \cdot R_a \cdot I_a \right\} = \frac{d}{dt} \left\{ C \cdot T_t \right\} + \frac{T_t}{R_o} \quad (\text{A.5})$$

APPENDIX 4A

If we now define:  $\mathfrak{D}_i\{i\} = \left[ \frac{R_o + R_a}{R_o} \cdot i + \frac{d}{dt} \{ C \cdot R_a \cdot i \} \right]$

$$\mathfrak{D}_t\{i\} = \left[ \frac{i}{R_o} + \frac{d}{dt} \{ C \cdot i \} \right]$$

equation (A.5) becomes:

$$\mathfrak{D}_i\{I_a\} = \mathfrak{D}_t\{T_t\} \quad (\text{A.6})$$

and with equation B.1 this is written as:

$$\mathfrak{D}_i\left\{ I_t - \frac{T_t}{R_a} \right\} = \mathfrak{D}_t\{T_t\} \quad (\text{A.7})$$

Note however that  $\mathfrak{D}_i$  is a linear operator so from this equation can be solved for  $I_t$  in the following way:

$$\mathfrak{D}_i\{I_t\} = \mathfrak{D}_t\{T_t\} + \mathfrak{D}_i\left\{ \frac{T_t}{R_a} \right\} \quad (\text{A.8})$$

Finally with:

$$\mathfrak{D}_f\{\square\} = \mathfrak{D}_t\{\square\} + \mathfrak{D}_i\left\{ \frac{\square}{R_a} \right\} \quad (\text{A.9})$$

we obtain:

$$T_t = \mathfrak{D}_f^{-1}\{\mathfrak{D}_i\{I_t\}\} = \mathfrak{Z}\{I_t\} \quad (\text{A.10})$$

In the above derivation we have used the inverse of an operator as though it always exists and can be found. In practice finding the inverse of a differential operator is not a trivial task and may well be impossible. In general the differential equation obtained by the application of the operator must be solved and the inverse of the resultant solution must be obtained. It is not at all certain that this is possible in practice. The investigation of these questions fall outside the scope of this study and we shall not attempt to obtain the solution for the general time variant case.

## APPENDIX 4B

Demonstration of multi-zone solution via matrix inversion.

A) Calculation of temperature and heat flow swings.

Define units:    length    mass    time    temperature  
                   m ≡ 1L    kg ≡ 1M    s ≡ 1T    C ≡ 1Q

$$J \equiv \text{kg} \cdot \text{m}^2 \cdot \text{s}^{-2} \quad W \equiv \text{J} \cdot \text{s}^{-1}$$

$$\text{kJ} \equiv \text{J} \cdot 10^3 \quad \text{kW} \equiv \text{W} \cdot 10^3$$

$$\text{h} \equiv 60 \cdot 60 \cdot \text{s} \quad \text{rad} \equiv 1$$

$$\text{deg} \equiv \frac{\pi}{180} \cdot \text{rad}$$

Resistance units:                     $\Omega \equiv \text{m}^2 \cdot \text{C} \cdot \text{kW}^{-1}$

Capacitance units:                     $F \equiv \text{kJ} \cdot \text{m}^{-2} \cdot \text{C}^{-1}$

Define frequency 1/24h:

$$f \equiv 1 \cdot 24^{-1} \cdot \text{h}^{-1}$$

$$\omega \equiv 2 \cdot \pi \cdot f \quad \text{s} \equiv \text{i} \cdot \omega$$

Two zone demonstration. The upper value of the vectors below applies to zone 1 and the bottom value to zone 2. The zones are physically equivalent except that zone 2 has 10 times the shell capacitance of zone 1.

Outside temperature swings:                     $T_o := \begin{bmatrix} 15 \\ 15 \end{bmatrix} \cdot \text{C}$

$$T_{sa} := \begin{bmatrix} 25 \\ 25 \end{bmatrix} \cdot \text{C}$$

Shell resistances:                     $R_o := \begin{bmatrix} 100 \\ 100 \end{bmatrix} \cdot \Omega$

Internal surface coefficients:                     $R_a := \begin{bmatrix} 10 \\ 10 \end{bmatrix} \cdot \Omega$

Ventilation resistances:                     $R_v := \begin{bmatrix} 200 \\ 200 \end{bmatrix} \cdot \Omega$

Heat storage capacitance:                     $C_a := \begin{bmatrix} 200 \\ 2000 \end{bmatrix} \cdot F$

Thermal time constants:

$$\tau_p := \frac{[Ro \cdot (Ra + Rv) \cdot Ca]}{[Ro + Ra + Rv]}$$

$$\tau_p = \left[ \begin{array}{c} 3.8 \\ 37.6 \end{array} \right] \cdot h$$

$$\tau_z := \frac{[Ro \cdot Ra \cdot Ca]}{[Ro + Ra]}$$

$$\tau_z = \left[ \begin{array}{c} 0.5 \\ 5.1 \end{array} \right] \cdot h$$

Calculated interior Thevenin temperatures:

$$Ti(s) := \frac{[Rv \cdot Tsa + (s \cdot \tau_z + 1) \cdot (Ra + Ro) \cdot To]}{[s \cdot \tau_p + 1] \cdot (Ra + Rv + Ro)}$$

$$Ti(s) = \left[ \begin{array}{c} 11.237 - 10.368i \\ 0.926 - 2.083i \end{array} \right] \cdot C$$

Source internal impedances:

$$Zi(s) := \frac{[Rv \cdot (Ro + Ra \cdot (Ro \cdot s \cdot Ca + 1))]}{[(Rv + Ra) \cdot (Ro \cdot s \cdot Ca + 1) + Ro]}$$

$$Zi(s) = \left[ \begin{array}{c} 40.702 - 30.719i \\ 10.15 - 6.173i \end{array} \right] \cdot \Omega$$

$$Z(s) := \begin{bmatrix} Zi(s) & & \\ & 0 & 0 \cdot \Omega \\ & & Zi(s) \\ 0 \cdot \Omega & & & 1 \end{bmatrix}$$

Partition admittance matrix:

The partition consists  
 of a T network with arms  
 of resistance  $R_p$  and trunk  
 of capacitance  $C_p$ .

$$R_p := 50 \cdot \Omega$$

$$C_p := 50 \cdot F$$

$$Y(s) := \frac{1}{R_p \cdot (R_p \cdot s \cdot C_p + 2)} \cdot \begin{bmatrix} R_p \cdot s \cdot C_p + 1 & -1 \\ -1 & R_p \cdot s \cdot C_p + 1 \end{bmatrix}$$

$$Y(s) = \begin{bmatrix} & -4 & & -4 \\ 0.01 + 9.02 \cdot 10^{-4} i & & -0.01 + 9.02 \cdot 10^{-4} i & \\ & -4 & & -4 \\ -0.01 + 9.02 \cdot 10^{-4} i & & 0.01 + 9.02 \cdot 10^{-4} i & \end{bmatrix} \cdot \Omega^{-1}$$

Multizone solution via matrix inversion:

$$I := \begin{bmatrix} 1 & 0 \\ 0 & 1 \end{bmatrix} \quad T(s) := (I + Z(s) \cdot Y(s))^{-1} \cdot Ti(s)$$

Interior temperature swing:  $Ts := T(s)$   $Ts = \begin{bmatrix} 8.716 - 6.633i \\ 1.303 - 2.941i \end{bmatrix} \cdot C$

$$\left| \begin{matrix} Ts \\ 0 \end{matrix} \right| = 10.953 \cdot C \quad \arg \begin{bmatrix} Ts \\ 0 \end{bmatrix} = -37.272 \cdot \text{deg}$$

$$\left| \begin{matrix} Ts \\ 1 \end{matrix} \right| = 3.217 \cdot C \quad \arg \begin{bmatrix} Ts \\ 1 \end{bmatrix} = -66.098 \cdot \text{deg}$$

Heatflow between zones:  $Q(s) := Y(s) \cdot T(s)$

$$Q(s) = \begin{bmatrix} 0.084 - 0.029i \\ -0.065 + 0.045i \end{bmatrix} \cdot \text{kW} \cdot \text{m}^{-2}$$

$$\left| \begin{matrix} Q(s) \\ 0 \end{matrix} \right| = 0.088 \cdot \text{kW} \cdot \text{m}^{-2} \quad \arg \begin{bmatrix} Q(s) \\ 0 \end{bmatrix} = -18.935 \cdot \text{deg}$$

$$\left| \begin{matrix} Q(s) \\ 1 \end{matrix} \right| = 0.079 \cdot \text{kW} \cdot \text{m}^{-2} \quad \arg \begin{bmatrix} Q(s) \\ 1 \end{bmatrix} = 145.068 \cdot \text{deg}$$

B) Solution for required heat load.

Required interior temperatures:  $Tr := \begin{bmatrix} 24 \\ 24 \end{bmatrix} \cdot C$

Required Thevenin sources:  $Tth(s) := (I + Z(s) \cdot Y(s)) \cdot Tr$

$$Tth(s) = \begin{bmatrix} 25.489 + 1.641i \\ 24.307 + 0.415i \end{bmatrix} \cdot C$$

$$\left| Tth(s)_0 \right| = 25.542 \cdot C \quad \arg \left[ Tth(s)_0 \right] = 3.683 \cdot \text{deg}$$

$$\left| Tth(s)_1 \right| = 24.311 \cdot C \quad \arg \left[ Tth(s)_1 \right] = 0.978 \cdot \text{deg}$$

Heat flow into partition:  $Qr(s) := Y(s) \cdot Tth(s)$

$$Qr(s) = \begin{bmatrix} 0.014 + 0.057i \\ -0.01 + 0.033i \end{bmatrix} \cdot kW \cdot m^{-2}$$

$$\left| Qr(s)_0 \right| = 0.059 \cdot kW \cdot m^{-2} \quad \arg \left[ Qr(s)_0 \right] = 76.225 \cdot \text{deg}$$

$$\left| Qr(s)_1 \right| = 0.034 \cdot kW \cdot m^{-2} \quad \arg \left[ Qr(s)_1 \right] = 106.304 \cdot \text{deg}$$

C) Calculation of mean temperature and heat flow.

Outside mean temperatures:

$$T_{om} := \begin{bmatrix} 15 \\ 15 \end{bmatrix} \cdot C$$

$$T_{sam} := \begin{bmatrix} 25 \\ 25 \end{bmatrix} \cdot C$$

Calculated interior Thevenin temperatures:

$$T_{im} := \overline{\left[ \frac{R_v \cdot T_{sam} + (R_a + R_o) \cdot T_{om}}{R_a + R_v + R_o} \right]}$$

$$T_{im} = \begin{bmatrix} 21.452 \\ 21.452 \end{bmatrix} \cdot C$$

Source internal impedances:

$$Z_{im} := \overline{\left[ \frac{(R_o + R_a) \cdot R_v}{R_v + R_a + R_o} \right]}$$

$$Z_{im} = \begin{bmatrix} 70.968 \\ 70.968 \end{bmatrix} \cdot \Omega$$

$$Z_m := \begin{bmatrix} Z_{im} & 0 \\ 0 & Z_{im} \\ 0 \cdot \Omega & 1 \\ 0 \cdot \Omega & 1 \end{bmatrix}$$

Partition admittance matrix:

$$Y_m := \frac{1}{R_p \cdot 2} \cdot \begin{bmatrix} 1 & -1 \\ -1 & 1 \end{bmatrix}$$

$$Y_m = \begin{bmatrix} 0.01 & -0.01 \\ -0.01 & 0.01 \end{bmatrix} \cdot \Omega^{-1}$$

Multizone solution via matrix inversion:

$$I := \begin{bmatrix} 1 & 0 \\ 0 & 1 \end{bmatrix} \quad T_m := (I + Z_m \cdot Y_m)^{-1} \cdot T_{im}$$

Mean Interior temperature:

$$T_m = \begin{bmatrix} 21.452 \\ 21.452 \end{bmatrix} \cdot C$$

Heatflow between zones:

$$Q_m := Y_m \cdot T_m$$

$$Q_m = \begin{bmatrix} 0 \\ 0 \end{bmatrix} \cdot kW \cdot m^{-2}$$

D) Solution for required mean heat load.

Required interior temperatures:  $T_r := \begin{bmatrix} 24 \\ 24 \end{bmatrix} \cdot C$

Required Thevenin sources:  $T_{thm} := (I + Z_m \cdot Y_m) \cdot T_r$

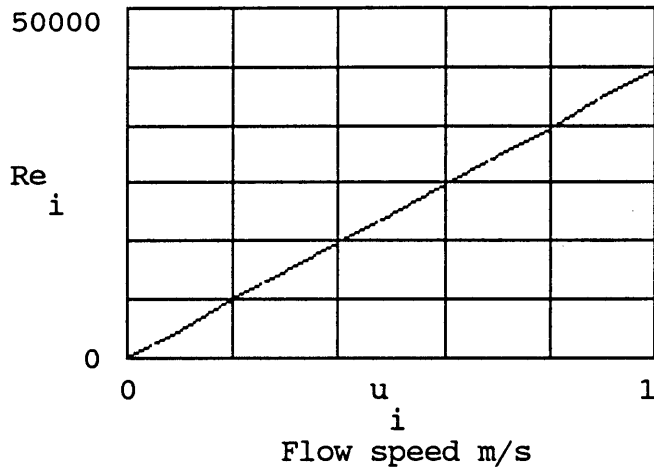
$$T_{thm} = \begin{bmatrix} 24 \\ 24 \end{bmatrix} \cdot C$$

Heatflow into partition:  $Q_h := Y_m \cdot T_{thm}$

$$Q_h = \begin{bmatrix} 0 \\ 0 \end{bmatrix} \cdot kW \cdot m^{-2}$$



Reynolds number

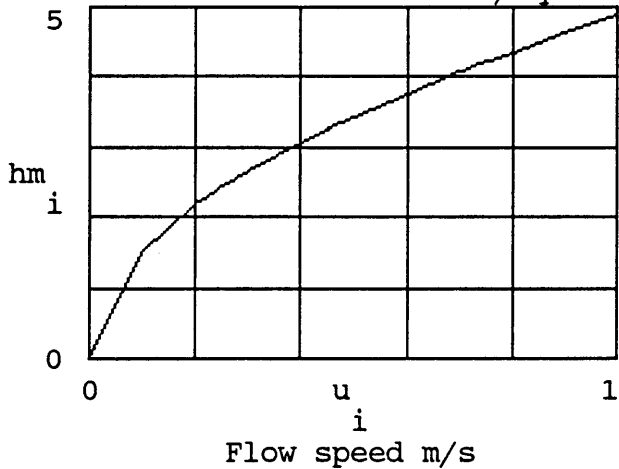


The Reynolds number is less than 500000 so it can be assumed the flow is reasonably laminar. Holman gives an equation for the mean Nusselt number across the surface for these conditions.

$$\text{Nusselt number: } Nu_i := 0.664 \cdot Re_i^{0.5} \cdot Pr^{0.333}$$

$$\text{Mean heat transfer coefficient: } h_{m,i} := Nu_i \cdot \frac{k}{x}$$

Heat transfer coefficient W/sq m K



Flow speed	Reynolds	Coefficient
$u = \begin{bmatrix} 0 \\ 0.1 \\ 0.2 \\ 0.3 \\ 0.4 \\ 0.5 \\ 0.6 \\ 0.7 \\ 0.8 \\ 0.9 \\ 1 \end{bmatrix}$ m/s	$Re = \begin{bmatrix} 0 \\ 4123.109 \\ 8246.217 \\ 12369.326 \\ 16492.435 \\ 20615.544 \\ 24738.652 \\ 28861.761 \\ 32984.87 \\ 37107.979 \\ 41231.087 \end{bmatrix}$	$hm = \begin{bmatrix} 0 \\ 1.542 \\ 2.18 \\ 2.67 \\ 3.083 \\ 3.447 \\ 3.776 \\ 4.079 \\ 4.36 \\ 4.625 \\ 4.875 \end{bmatrix}$ W·m <sup>-2</sup> ·K <sup>-1</sup>

According to this (probably naive) calculation the forced convection film coefficient is approximately 3.5 W/sq m K.

Convection film coefficient:  $hc := 3.5 \cdot W \cdot m^{-2} \cdot K^{-1}$

In the theoretical model the film heat transfer coefficient includes all contributions of heat flow from the surface of the partition to the air node. It is therefore necessary to include flow contributions via radiation to the other walls and convection from these walls. This contribution is calculated by assuming the radiation causes no appreciable warming of the air. In this case the heat transfer coefficient for the other walls is found by adding the radiation resistance to the convection resistance, since no conduction takes place through the walls.

#### Estimate of Radiation Resistance

Stefan-Boltzman constant:	$\sigma := 5.669 \cdot 10^{-8} \cdot W \cdot m^{-2} \cdot K^{-4}$
Shape factor: (For closed box)	$F := 1$
Emmissivity for asbestos:	$\epsilon := 0.96$ (Holman table A-10)
Mean Temperature:	$T := 300 \cdot K$

Linearized radiative heat transfer coefficient:

$$h_r := 4 \cdot F \cdot \sigma \cdot \epsilon \cdot T^3$$

$$h_r = 5.878 \cdot W \cdot m^{-2} \cdot K^{-1}$$

Surface area of box walls excluding partition:

$$A_r := 3 \cdot 0.93 \cdot m \cdot 0.45 \cdot m + 2 \cdot 0.45 \cdot m \cdot 0.45 \cdot m$$

$$A_r = 1.661 \cdot m^2$$

Radiation resistance:  $R_r := \frac{1}{A_r \cdot h_r}$   $R_r = 0.102 \cdot K \cdot W^{-1}$

Convection resistance:  $R_c := \frac{1}{A_r \cdot h_c}$   $R_c = 0.172 \cdot K \cdot W^{-1}$

Partition surface area:  $A_p := 0.45 \cdot m \cdot 0.93 \cdot m$

$$A_p = 0.419 \cdot m^2$$

Effective film coefficient referred to partition surface area:

$$h_e := \frac{1}{A_p \cdot (R_r + R_c)}$$

$$h_e = 8.704 \cdot W \cdot m^{-2} \cdot K^{-1}$$

Total partition surface heat transfer coefficient:

$$h_t := h_c + h_e$$

$$h_t = 12.204 \cdot W \cdot m^{-2} \cdot K^{-1}$$

## APPENDIX 4D

Verification of multi-zone solution for two zone model.

Define units:    length    mass    time    temperature  
 $m \equiv 1L$      $kg \equiv 1M$      $s \equiv 1T$      $C \equiv 1Q$

$$J \equiv kg \cdot m^2 \cdot s^{-2} \qquad W \equiv J \cdot s^{-1}$$

$$kJ \equiv J \cdot 10^3 \qquad kW \equiv W \cdot 10^3$$

$$h \equiv 60 \cdot 60 \cdot s \qquad rad \equiv 1$$

$$deg \equiv \frac{\pi}{180} \cdot rad \qquad mm \equiv m \cdot 10^{-3}$$

Resistance units:     $\Omega \equiv C \cdot kW^{-1}$

Capacitance units:     $F \equiv kJ \cdot C^{-1}$

Define frequency 1/24h:

$$f \equiv 1 \cdot 24^{-1} \cdot h^{-1}$$

$$\omega \equiv 2 \cdot \pi \cdot f \qquad s \equiv i \cdot \omega$$

Material parameters

The model is constructed of pressed asbestos cement with the following thermal characteristics.

$$K := 0.62 \cdot W \cdot m^{-1} \cdot C^{-1} \qquad \text{Thermal Conductivity}$$

$$\rho := 2100 \cdot kg \cdot m^{-3} \qquad \text{Density}$$

$$\sigma := 0.83 \cdot kJ \cdot kg^{-1} \cdot C^{-1} \qquad \text{Specific Heat Capacity}$$

$$l := 9 \cdot mm \qquad \text{Thickness}$$

During the experiment the sides and floor of the model were isolated from the environment with 40 mm thick polystyrene tiles. The roof was exposed. The dimensions of the enclosure are 450x450x930 mm. Note that a single asbestos cement layer of 9 mm formed the walls.

$$\text{Area of non-isolated zone walls (roof):} \qquad An := 450 \cdot 930 \cdot mm^2$$

$$An = 0.419 \cdot m^2$$

Total area of zone walls contributing to capacitance:

$$Az := (4 \cdot (450 \cdot 930) + 2 \cdot (450 \cdot 450)) \cdot \text{mm}^2$$

$$Az = 2.079 \cdot \text{m}^2$$

Since the outside of the model is exposed to the almost stationary air in the cellar. The convective heat and radiative heat transfer coefficients are estimated in appendix 4C. If the convective coefficient is taken as approximately 2 W/sq m K and the radiative as 5 W/sq m K the combined outside film coefficient is 5 W/sq m K. Allowing for another 5 W/sq m K for seepage of air through the cracks the total outside film coefficient is approximately 10 W/sq m K.

External film coefficient:  $ho := 10 \cdot \text{W} \cdot \text{m}^{-2} \cdot \text{C}^{-1}$

Shell resistance:  $Ro := \left[ \frac{1}{K} + \frac{1}{ho} \right] \cdot \frac{1}{An}$

$$Ro = 273.635 \cdot \Omega$$

The inside air is stirred with a fan. In appendix 4C the interior film coefficient is crudely estimated at 12 W/sq m K.

Internal film coefficient:  $hi := 12 \cdot \text{W} \cdot \text{m}^{-2} \cdot \text{C}^{-1}$

$$Ra := \frac{1}{Az \cdot hi} \quad Ra = 40.083 \cdot \Omega$$

Heat storage capacitance: Asbestos -  $Ca := \sigma \cdot \rho \cdot l \cdot Az$

Thermograph (3.3 kg Al) -  $Cl := 3.3 \cdot \text{kg} \cdot 0.88 \cdot \text{kJ} \cdot \text{kg}^{-1} \cdot \text{C}^{-1}$

Total capacitance -  $Ct := Ca + Cl \quad Ct = 35.517 \cdot \text{F}$

Thermal time constant:  $\tau_p := Ro \cdot Ct \quad \tau_p = 2.7 \cdot \text{h}$

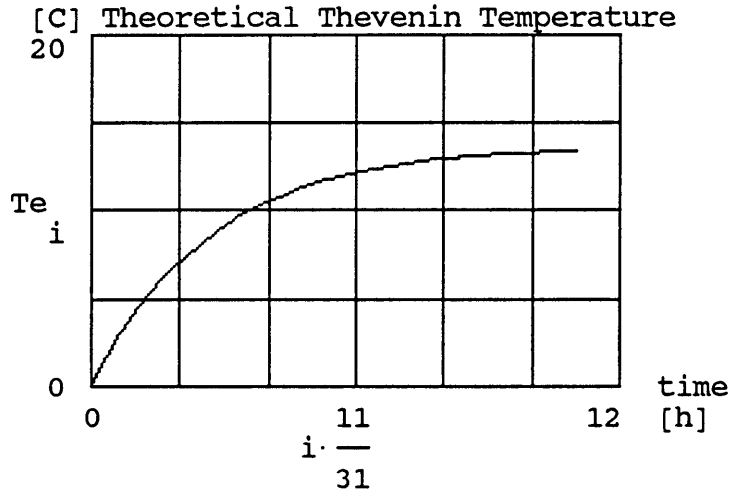
The calculated thermal time constant of 2.7 h agrees very well with the measured time constant of also approximately 2.7 h. It is therefore reasonable to assume that the capacitance and shell resistance values obtained above are not grossly in error.

The measured interior Thevenin temperature appears to be a perfect exponential charge and discharge with an amplitude of 9 degrees C and a time constant of 2.7 h. According to equation 3.1 in the text when  $Rv$  is infinite the theoretical Thevenin temperature for a 50 W step in the radiative source is:

$$Th(t) := 50 \cdot \text{W} \cdot Ro \cdot \left[ 1 - e^{-\left[ \frac{t}{\tau_p} \right]} \right]$$

$i := 0 \dots 31$       Hours index

$$Te_i := Th \left[ i \cdot \frac{11}{31} \cdot h \right]$$



The calculated temperature swing is 14 degrees as opposed to the measured 9 degrees. Note however that we have taken all the heat dissipated by the lamp as radiative heat while, in practice, a fraction would be convective, which enters differently into the solution. Since the calculated time constant seems to agree with the measured time constant, it is suspected that the calculated  $R_o$  is fairly accurate unless the error in  $R_o$  is cancelled by an opposite error in the value of  $C$ . It seems the biggest uncertainties lie in the values of the film coefficients, but, notice that only the outside film coefficient plays a role in establishing the amplitude and time-constant in the absence of ventilation. From the discrepancy it appears probable that more infiltration took place than was accounted for in the outside film coefficient, or heat was lost to the outside through other paths.

Since we are interested in verifying the multi-zone model, and not so much the thermal properties of the construction materials we shall derive the value of the resistance  $R_o$  and capacitance  $C$  from the measured amplitude of the swing and time-constant.

$$R_{om} := \frac{9 \cdot C}{50 \cdot W} \quad R_{om} = 180 \cdot \Omega$$

$$\tau_m := 2.7 \cdot h$$

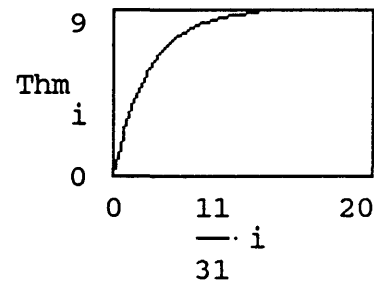
$$C_m := \frac{\tau_m}{R_{om}} \quad C_m = 54 \cdot F$$

Both the resistance and capacitance values differ significantly from the theoretical values. As discussed above the small experimental value of the resistance can be attributed to seepage of air but it is difficult to explain the extra heat capacitance. The density of the asbestos boards were measured and is in agreement with the value used above. The only conclusion we can come to is that either the specific heat capacitance value is underestimated or the isolation of the bottom from the concrete floor was ineffective. The latter effect would explain both the discrepancy in resistance and capacitance.

Fourier Analysis of experimental Thevenin temperature.

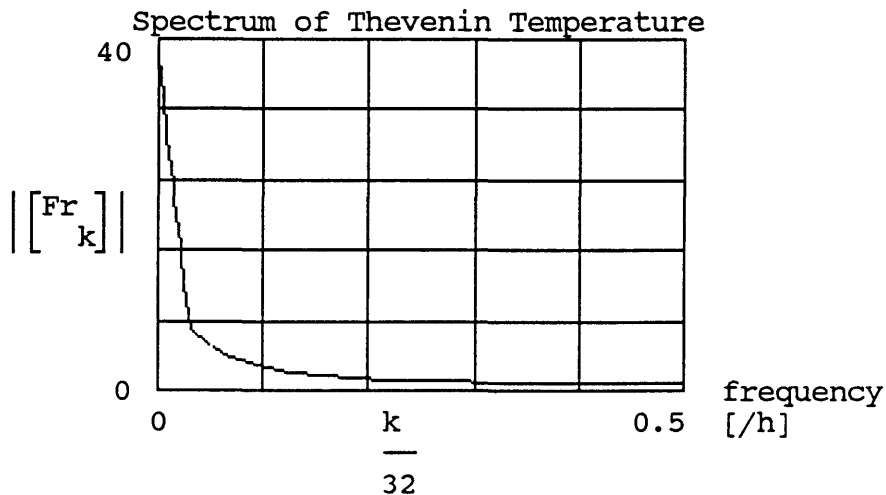
$$T_m(t) := 50 \cdot W \cdot R_{om} \cdot \left[ 1 - e^{-\left[ \frac{t}{\tau_m} \right]} \right]$$

$$Thm_i := T_m \left[ \frac{11}{31} \cdot i \cdot h \right]$$



$$Fr := \text{fft}(Thm)$$

Frequency index"  
 $k := 0 \dots 16$



Source internal impedances:

$$Z_i(s) := \left[ \frac{R_{om} + R_a \cdot (\tau_m \cdot s + 1)}{\tau_m \cdot s + 1} \right]$$

$$Z_i(s) = 160.111 - 84.843i \cdot \Omega$$

Internal impedance matrix:

$$Z(s) := \begin{bmatrix} Z_i(s) & 0 \cdot \Omega \\ 0 \cdot \Omega & Z_i(s) \end{bmatrix}$$

Partition admittance matrix

$$\text{Area of partition: } A_p := 930 \cdot 450 \cdot \text{mm}^2 \quad A_p = 0.419 \cdot \text{m}^2$$

Branch resistances (assuming one side exposed to heat source):

$$R_p := \left[ \frac{1}{K} + \frac{1}{h_i} \right] \cdot \left[ \frac{1}{2 \cdot A_p} \right] \quad R_p = 116.905 \cdot \Omega$$

Trunk capacitance:

$$C_p := \sigma \cdot \rho \cdot l \cdot A_p \quad C_p = 6.565 \cdot \text{F}$$

Partition admittance:

$$Y(s) := \frac{1}{R_p \cdot (R_p \cdot s \cdot C_p + 2)} \cdot \begin{bmatrix} R_p \cdot s \cdot C_p + 1 & -1 \\ -1 & R_p \cdot s \cdot C_p + 1 \end{bmatrix}$$

$$Y(s) = \begin{bmatrix} 0.004 + 1.193 \cdot 10^{-4} i & -0.004 + 1.193 \cdot 10^{-4} i \\ -0.004 + 1.193 \cdot 10^{-4} i & 0.004 + 1.193 \cdot 10^{-4} i \end{bmatrix} \cdot \Omega^{-1}$$

Multizone solution via matrix inversion:

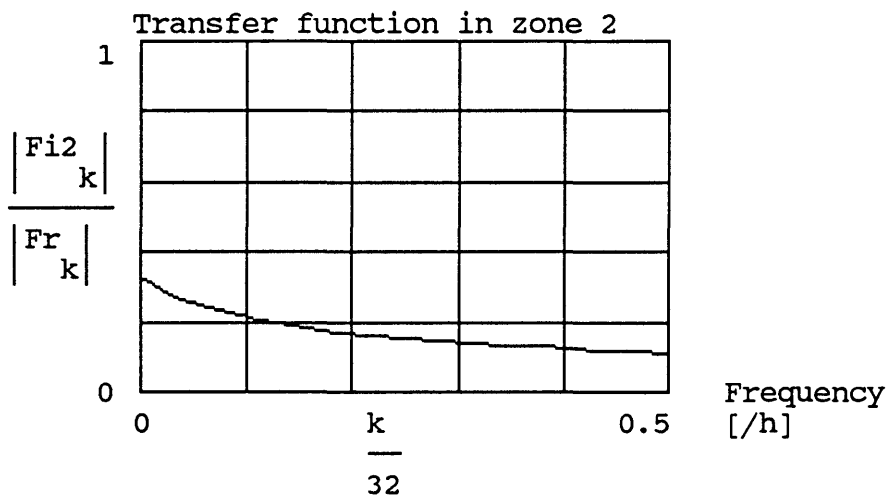
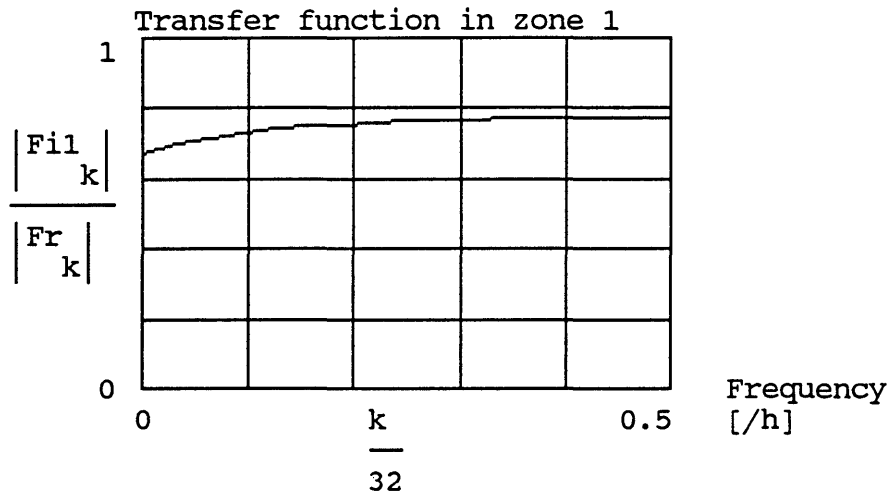
$$I := \begin{bmatrix} 1 & 0 \\ 0 & 1 \end{bmatrix}$$

$$H_i(s) := (I + Z(s) \cdot Y(s))^{-1}$$

Interior temperature swings

$$\text{Zone 1: } \quad F_{i1} := H_i \left[ k \cdot 2 \cdot \frac{\pi}{32 \cdot h} \right] \cdot Fr_k \quad \begin{matrix} 0,0 \\ k \end{matrix}$$

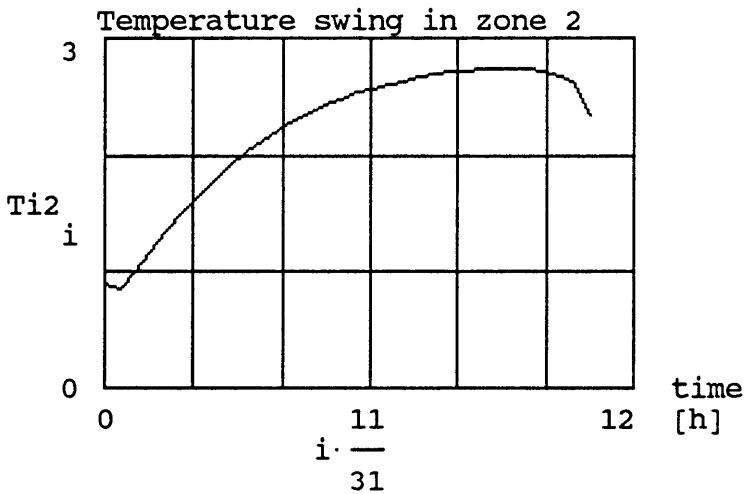
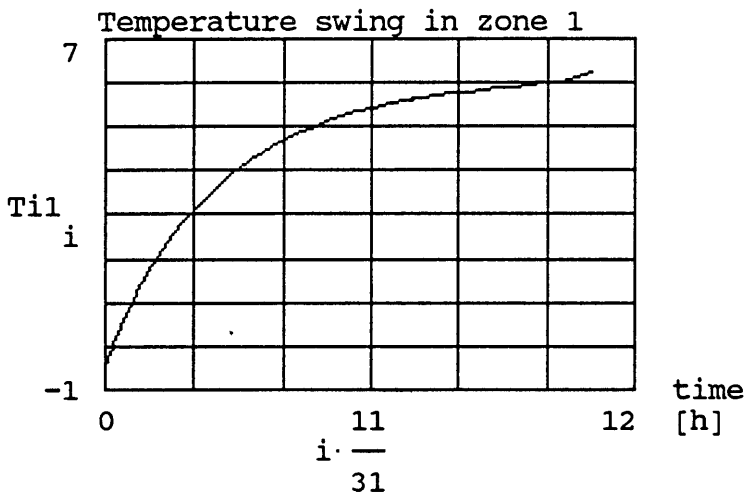
$$\text{Zone 2: } \quad F_{i2} := H_i \left[ k \cdot 2 \cdot \frac{\pi}{32 \cdot h} \right] \cdot Fr_k \quad \begin{matrix} 1,0 \\ k \end{matrix}$$



The graphs indicate the fraction of energy from the active zone which a) remains in the active zone and b) propagates to the inactive zone as a function of frequency. More energy is transferred at the lower frequencies because of the exponential decrease in temperature swing through the partition.

Time signals

Ti1 := ifft(Fi1)                      Ti2 := ifft(Fi2)



The calculated swings are 6 degrees in zone 1 and 2.7 degrees in zone 2. These values are very close to the measured swings in figure 4.8a and 4.8b of 6 and 3 degrees respectively.

Bearing in mind the difficulties experienced to obtain correct values for the surface heat transfer coefficients the measurements verify the theory.

## CHAPTER 5

---

### 5 SOLUTION OF THE THERMAL NETWORK WITH TIME DEPENDENT PARAMETERS

In chapter 2 of this thesis we discussed the theoretical foundation of the simple building thermal analysis method of Mathews and Richards, based on the thermo-flow network of figure 2.1. It was indicated that such a simple model has a number of important advantages which makes it a very useful model on which to base a design tool. Despite its theoretical limitations, the method has proved itself to be accurate, easy to interpret and quick. In this model, as in most other thermal models, it is assumed that the parameters of the thermo-flow network, i.e. the resistances and capacitances in figure 2.1, are time invariant. This assumption is required to enable the application of standard Fourier or Laplace techniques to obtain the solution. However, in actual buildings, some of these parameters are definitely not constant. In passive buildings, people are encouraged to open and close windows to suit themselves. This will have an effect on the ventilation resistance as well as the interior film coefficients. In active buildings, the surface convection coefficients will also vary since the air movement is controlled by the HVAC system. Furthermore, contemporary<sup>1</sup> trends in the design of energy efficient buildings require simulation of such exotic elements as windows with variable transmittance [1], walls with variable thermal conductance [2] and buildings with variable heat storage characteristics. These developments require the investigation of thermal models with variable parameters in order to help assess the viability of these concepts and to aid the designer.

The simple method of Mathews and Richards is ideally suited for extension to time variable systems. Its very simplicity allows the possibility of a practical and efficient implementation of a time variable solution,

---

<sup>1</sup>Actually the control of transmittance of light is not so 'contemporary'. Curtains, shutters and blinds have been used for ages to similar effect.

## SOLUTION WITH TIME DEPENDENT PARAMETERS

something which might be impossible or extremely cumbersome in a more refined model.

In this chapter we investigate the solution of the model of figure 2.1, under the assumption that the parameters are time dependent. The most important application we foresee for such a time dependent simulation, is the proper treatment of time dependent ventilation in naturally ventilated buildings. The prediction of thermal response with time dependent ventilation is sorely lacking in most programs. This serious shortcoming inhibits the practical application of many programs to passive design of buildings.

In this chapter we first examine the solution of the network of figure 2.1 with constant parameters. This is followed by a literature survey to determine possible methods for solving the time dependent system. Since very little formal techniques exist for solving time dependent systems, and those that do exist are not well known, it was felt necessary to discuss the literature in some depth in this chapter. It was discovered that most existing techniques are not applicable, since they assumed that the time dependency of the parameters can be regarded as a small perturbation on the steady value of the parameter. Nevertheless, it was still considered necessary to describe some of the more common methods here, to give some perspective. In this study, it is assumed that the parameters are subject to sudden large variations. This is required if the model is to be useful for predicting the consequences of a sudden opening of a window, or the switching on of forced ventilation. In the end it was decided that a simple numerical procedure, based on a first order difference technique is the most appropriate. But first the solution for the time independent network is discussed.

## SOLUTION WITH TIME DEPENDENT PARAMETERS

### 5.1 Solution of the Model with Constant Parameters: A Systems Approach

In figure 2.1 the electrical network equivalent for the heat flow problem in buildings is shown (from reference [10] of chapter 2). For convenience, the figure is repeated here as figure 5.1. To recap, in this figure  $T_{sa}$  is the combined sol-air temperature,  $T_o$  is the ventilating air temperature,  $T_i$  is the indoor air temperature,  $Q_r$  is a radiative source for penetrating radiation and interior radiative sources and  $Q_c$  is a convective source. The shell resistance and thermal capacity of the building is represented by  $R_o$  and  $C$  respectively,  $R_a$  is the internal surface heat transfer coefficient and  $R_v$  is the ventilation resistance.

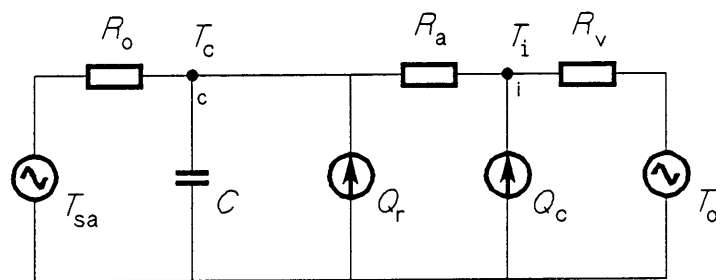


**FIGURE 5.1** The thermo-flow network of Mathews and Richards. From reference [10] chapter 2.

The main purpose of this chapter is to determine the solution of this network when the R's and C become functions of time. As a point of departure we investigate the solution in the time invariant case.

## SOLUTION WITH TIME DEPENDENT PARAMETERS

### 5.1.1 Solution for Calculating Indoor Temperature<sup>2</sup>

The solution of internal temperature,  $T_i$ , for constant parameters in the Laplace domain is:

$$T_i(s) = \frac{1}{s\tau_p + 1} \left[ (s\tau_z + 1) \cdot (R_a + R_o) \cdot (T_o + R_v \cdot Q_c) + R_v \cdot (T_{sa} + R_o \cdot Q_r) \right] \cdot \frac{1}{R_a + R_o + R_v} \quad (5.1)$$

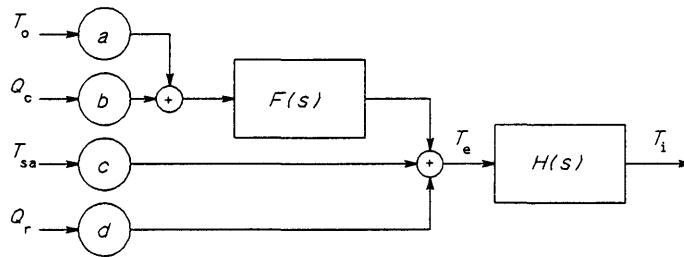


**FIGURE 5.2** Block diagram of the solution of the network of figure 5.1 for interior temperature. The symbols are defined in the text.

The solution is shown schematically in figure 5.2. The definitions of the variables in this figure are:

$$a = \frac{R_a + R_v}{R_a + R_v + R_o} \quad \text{Contribution factor of outside air.} \quad (5.2)$$

$$b = \frac{R_v (R_o + R_a)}{R_a + R_v + R_o} \quad \text{Contribution factor of convective source.} \quad (5.3)$$

---

<sup>2</sup>This solution, as given here, is not different in essence from the one given by Mathews and Richards. It is different though, in that Mathews obtains the response of the system via a Fourier Transform of the response while this solution uses the frequency response of the system directly. This allows a somewhat more efficient implementation. Furthermore, the solution is given in a convenient systems format so that the influence of each individual source becomes very clear. An effective source is defined so that the response can be obtained from a single convolution between effective forcing function and response. Mathews and Richards treat the various sources individually.

## SOLUTION WITH TIME DEPENDENT PARAMETERS

$$c = \frac{R_v}{R_o + R_v + R_a} \quad \text{Contribution factor of sol-air temperature.} \quad (5.4)$$

$$d = \frac{R_v \cdot R_o}{R_o + R_v + R_a} \quad \text{Contribution factor of radiative source.} \quad (5.5)$$

$$T_e = (a \cdot T_o + b \cdot Q_c) \cdot (s\tau_z + 1) + c \cdot T_{sa} + d \cdot Q_r \quad (5.6)$$

$$F(s) = s\tau_z + 1, \quad H(s) = 1/(s\tau_p + 1). \quad (5.7)$$

$$\tau_z = \frac{R_o \cdot R_a}{R_o + R_a} \cdot C \quad \text{Time constant of the zero.} \quad (5.8)$$

$$\tau_p = \frac{R_o (R_a + R_v)}{R_o + R_a + R_v} \cdot C \quad \text{Time constant of the system pole.} \quad (5.9)$$

Note the contribution of the individual sources, through their scaling factors  $a, b, c$  and  $d$  to  $T_e$ . The figure indicates how the various forcing functions contribute to the combined effective forcing function  $T_e$ . The figure indicates that the thermal network can be regarded as a single input single output system with system function given by the single pole designated  $H(s)$  in the figure. The input to this system is the combined forcing function  $T_e$  and the output is  $T_i$ . Consequently, the network displays the characteristics of a single pole system, i.e. the impulse response is an exponential decay. The outside air temperature and convective source enter in the combined forcing function through a single zero network,  $F(s)$ , indicating that the time derivatives of these sources also effect  $T_e$ . A sudden change of the convective load  $Q_c$  will thus impart an impulsive component to  $T_e$ . Physically this implies that if e.g. the convective load suddenly increases, the interior temperature will tend to rise with it and then settle exponentially as the storage effect of the capacitor comes into play. Note also that the contributions from the sol air and radiative sources decrease as  $R_v$  decreases, implying that larger ventilation rates force the temperature to  $T_o$ . Furthermore, the position of

## SOLUTION WITH TIME DEPENDENT PARAMETERS

the pole, thus the time constant, is also influenced by  $R_v$  but the position of the zero is independent of the ventilation.

From figure 5.2 we see that once the effective forcing function,  $T_e$ , has been determined, the response of the building is represented by a single pole network  $H(s)$  with time constant  $\tau_p$ . The usual method for calculating the response of such a circuit, will obtain the indoor temperature via the convolution of the effective forcing function with the circuit's impulse response. Since the discovery of the Fast Fourier Transform this is efficiently done by multiplication in the frequency domain [3] as explained in §5.1.3.

### 5.1.2 Load Calculation

In active systems, the interior air-temperature is not so important, since it is a prescribed quantity. The active system attempts to control the interior temperature so that it will always be close to the set point temperature. Of more importance, in this case, is the load on the HVAC system. This energy load is the convective load,  $Q_c$ , required to keep the interior temperature at a specified level. In actual HVAC systems, the temperature control will be maintained through a closed loop system, where the convective load is adjusted to keep the interior temperature at the prescribed level. Since many different types of controllers exist, there is no unique definition of HVAC load. Normally, the system incorporates some sort of 'dead band' control where the interior temperature is allowed to swing through a specific range. The control action is only activated when the interior temperature strays outside this range.

In addition, various control laws are used. Some controllers will proportionally increase the system load as the interior temperature strays further and further from the set point. Others will switch the system on at full capacity at a certain threshold. Since a specific control law defines a specific HVAC load, a complete system simulation which incorporates the passive response of the building, the response of the plant and the

## SOLUTION WITH TIME DEPENDENT PARAMETERS

controller is required to accurately determine the system load. However, the objective of a simple design tool for thermal response of buildings is not complete system simulation, it is the optimization of the passive design of the building. All that is required is for the program to predict a uniquely defined required capacity of the HVAC system. The building designer can then optimize his design by minimizing this required system capacity. To this purpose, it is convenient to define the system load as the convective load which is required to maintain the interior temperature at a prescribed setting. This definition leads to a simple procedure for determining the load. In §5.1.4 it is shown that the present treatment is easily extended to proportionally controlled systems without a deadband thermostat.

Setting  $T_i$  equal to the set-point temperature  $T_{ir}$  and solving for the system load,  $Q_c = Q_{cr}$ , from (5.1) gives:

$$Q_{cr}(s) = \frac{T_{ir} \cdot (s\tau_P + 1) \cdot (R_a + R_v + R_o) - R_v \cdot (T_{sa} + R_o \cdot Q_r) - \frac{T_o}{R_v}}{R_v \cdot (s\tau_z + 1) \cdot (R_a + R_v)} \quad (5.10)$$

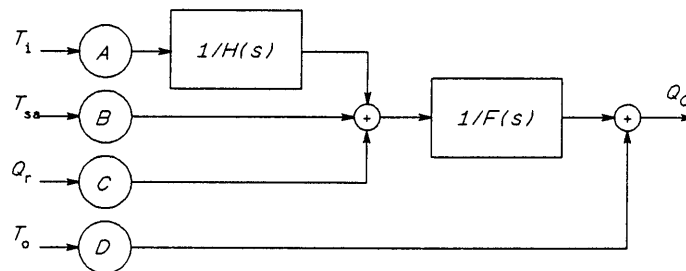


**FIGURE 5.3** Block diagram for load calculation via (5.10). The symbols are defined in the text below.

## SOLUTION WITH TIME DEPENDENT PARAMETERS

Figure 5.3 shows the block diagram for this solution of the system load. The diagram shows how to find the convective load,  $Q_{cr}$ , for a specified interior air-temperature,  $T_{ir}$ . Note that in this case, the system functions,  $H(s)$  and  $F(s)$  are inverted so that the time-constant of the pole is now  $\tau_z$ . Consequently, the system pole is now independent of  $R_v$  and the position of the zero  $\tau_p$  varies with  $R_v$ . Note also that ventilation adds directly to the system load via the contribution factor  $D$  in figure 5.3. The definitions of the new contribution factors in figure 5.3 are:

$$A = \frac{R_a + R_v + R_o}{R_v \cdot (R_a + R_o)} \quad (5.11)$$

$$B = \frac{-1}{(R_a + R_o)} \quad (5.12)$$

$$C = \frac{-R_o}{(R_a + R_o)} \quad (5.13)$$

$$D = \frac{-1}{R_v} \quad (5.14)$$

In both systems, figure 5.2 and figure 5.1, the solution is given by the response of a single pole system to a combined forcing function. In figure 5.2, the time-constant of the system is given by  $\tau_p$  and in figure 5.3 it is given by  $\tau_z$ .

### 5.1.3 The Governing Equation

It may be remarked that, in general, when the position of a system zero is time dependent, no serious complications arise in the calculation of the response. The zero directly effects the input forcing function and not the response. This can be deduced from figure 5.2. The system

$$F = (s\tau_z + 1) = z/x$$

## SOLUTION WITH TIME DEPENDENT PARAMETERS

transforms to the differential equation

$$z(t) = \tau_z \cdot \frac{dx(t)}{dt} + x(t) \quad (5.15)$$

which merely adds  $\tau_z$  times the derivative of the input to the effective forcing function. However, when a system pole becomes time-dependent, the characteristics of the system itself is affected. Any change in a parameter has also another distinct effect; the contributions of the sources to the effective forcing function changes with the parameters. We may therefore conclude that variable parameters will have two separate kinds of effects on the system:

- a The system input function is modulated with the parameter variations, since these variations change the contribution factors of the various sources, *viz.*  $a, b, c, d$  or  $A, B, C, D$  above, and influences the time constant of the system zero. This means that a smooth input function will become discontinuous if the parameters jump, since the contributions of the various sources to the input function will jump with the parameters.
- b Secondly, the response of the system itself is affected since the time-constant of the pole also varies with the parameters. We shall see that this implies a time dependent impulse response.

Since the first type of effect essentially adds no extra complication, (the input function just becomes a stronger function of time), in the rest of this study, we concentrate on calculating the influence of the variable time-constant on the response of the single pole system.

With  $y$  identified as the response, and  $f$  the input forcing function, the differential equation of the single pole system,

$$H = 1/(s\tau_p + 1) = y/f$$

is:

$$\tau_p \cdot \frac{dy}{dt} + y = f(t). \quad (5.16)$$

## SOLUTION WITH TIME DEPENDENT PARAMETERS

If this equation is divided by  $\tau_p$  we obtain the standard first order differential equation with  $\beta = 1/\tau_p$ :

$$\dot{y}(t) + \beta \cdot y(t) = x(t) \quad (5.17)$$

Note that the forcing function,  $f$ , is also divided by  $\tau_p$ . For constant parameters, the impulse response of the system,  $h_o(t)$ , is the response to  $x(t) = \delta(t)$ , where  $\delta(t)$  is Dirac's impulse function, and is given by:

$$h_o(t) = e^{-\beta t} \quad (5.18)$$

The frequency response,  $H_o(\omega)$ , is given by the Fourier transform of (5.18):

$$H_o(\omega) = \frac{1}{\omega + j\beta} \quad (5.19)$$

According to the convolution theorem, the response of the system to any arbitrary forcing function  $x(t)$ , is given by the convolution of  $h_o(t)$  with  $x(t)$ :

$$y(t) = x(t) * h(t) = \int_{-\infty}^t x(u) \cdot h_o(t - u) du. \quad (5.20)$$

The convolution can be efficiently calculated by multiplication in the frequency domain [3,4]:

$$Y(\omega) = X(\omega) / (\omega + j\beta) \quad (5.21)$$

where  $Y(\omega)$  is the Fourier transform of  $y(t)$  and  $X(\omega)$  is the Fourier transform of  $x(t)$ .

In (5.21) we have written the lower integration limit at infinity to indicate

## SOLUTION WITH TIME DEPENDENT PARAMETERS

that we are interested in the steady state solution; after all transients have died out.

In this study, we assume that all the sources are varying periodically and all the results apply only to periodically varying temperatures and loads. Furthermore, we also assume that variations in the parameters of the thermal network occur periodically. It may be argued that conditions in buildings are never perfectly periodic, however, since the earth has presumably been spinning round its axis since time started, it is not possible to assign initial conditions to the climatic forcing functions. They should be regarded as at least quasi-periodic. In many thermal analysis programs arbitrary initial conditions are assumed, the solution is then integrated for a couple of days until all transients are extinct. Our objective is to find an efficient solution which do not require a long initial period of integration. Furthermore, for a design tool, the philosophy of a design day<sup>3</sup>, or a design week is appropriate. In this case the assumption of periodic variation is fully justified.

### 5.1.4 Proportionally Controlled Active Systems

It is very easy to extend the model to include proportionally controlled active systems. By 'proportionally controlled' we mean systems which have no dead band, the system load is set proportional to the difference between the indoor temperature and the set point temperature. It is also assumed that the system has infinite capacity. In practice, this idealized system is realized if the deadband is small and the capacity of the system is always sufficient to maintain the indoor climate.

---

<sup>3</sup>When the designer follows a 'design day' philosophy he chooses a specific day on which he base his designs. The design day is usually statistically significant. E.g. when determining system cooling capacity, a design day is chosen so that only a small percentage of actual days will exceed the maximum temperature of the design day.

## SOLUTION WITH TIME DEPENDENT PARAMETERS

If another convective load, the system load  $Q_s$ , given by:

$$Q_s = \alpha \cdot (T_i - T_t) \quad (5.22)$$

with  $\alpha$  the proportional feedback gain [W/K] and  $T_t$  the thermostat (set-point) temperature, is added to the convective load  $Q_c$  in (5.1), it is found that the behaviour of the system is again governed by (5.17) but with parameter  $\beta(t)$  now given by:

$$\beta_S(t) = \beta_T - \frac{\alpha \cdot R_v^2}{C \cdot (R_a + R_v) \cdot (R_a + R_v - \alpha \cdot R_a R_v)}. \quad (5.23)$$

In the limit  $\alpha \rightarrow \infty$ , we find  $\beta_S \rightarrow \beta_E$  in accordance with the root-locus theorem for closed loop systems. It is seen that by this simple redefinition of  $\beta$ , the method can be extended to proportionally controlled systems. Many thermostats include non-linearities such as dead bands and hysteresis. These effects can also be included in the model, but the solution of the model becomes arduous; the initial value must be found by successive iteration [5].

### 5.2 Variable Network

When the parameters  $R_o$ ,  $R_v$ ,  $R_a$  and  $C$  are functions of time, the system equations are much more complicated. In this discussion we shall concentrate on changes in the value of the ventilation resistance  $R_v$ , since in practice, variable ventilation rates are the most important operation we wish to model. Nevertheless, changes in the other parameters are also important. The ventilation rate also has an influence on the interior surface coefficients, and as explained above, many modern ideas require simulation of time dependent shell conductance etc. Since there is little distinction between changes in  $R_v$  and changes in the other resistances and also the capacitance, we derive general equations valid for all changes which conserve the amount of stored heat in the structure, as discussed in the next paragraph.

## SOLUTION WITH TIME DEPENDENT PARAMETERS

Time depend circuit parameters have a drastic effect on the thermal response. Normally buildings exhibit sluggish behaviour, the time constant of a typical office block might be 30 hours or more. Sudden interior temperature changes are therefore not expected if the parameters are invariant. A change in a circuit parameter, however, might have a very sudden effect on the interior temperature. This effect is often experienced when the door is opened on a cold windy day. The interior air-temperature immediately drops to the outdoor air-temperature but quickly recovers when the door is closed again. Changes in the value of the storage capacitance,  $C$ , may also cause drastic and enduring consequences. This is understandable in view of the fact, that, if the stored energy is assumed to be conserved when the capacitance changes, the temperature of the storage structure must necessarily change with the capacitance. It is also possible to change the capacitance without changing the temperature of the storage structure, e.g. by simultaneous with the change in value of  $C$ , extracting or adding the correct amount of heat to the reservoir. In the first case, a discontinuous change in the value of  $C$  results in a discontinuous temperature. In the second case, the time constant, hence the rate of charge or discharge of the capacitor is affected, and discontinuities in the derivative of the temperature must be expected, while the temperature itself stays continuous. In thermo-flow problems, the capacitance value is changed when a massive structure is added to or removed from the thermal system. Generally, when mass is added to a zone the new mass will be at a different temperature, and both the value of the capacitance and the amount of stored heat will be affected.

In this study we have assumed the amount of stored heat in the structure is not directly affected by the changes in the parameters. The results are therefore applicable only to changes in the value of  $C$  of the first type. Obviously, this type of change in the value of  $C$  will seldom be practicable. The solutions we derive are therefore, in practice, confined to changes in the values of the resistances, since these will have no affect on the stored

## SOLUTION WITH TIME DEPENDENT PARAMETERS

charge. The effect of a change in the value of a resistance is similar to a change in the value of  $C$  of the second kind, i.e. with temperature conserved, since the time constant is affected.

Since we assume the amount of stored heat is not affected by changes in the parameters, it was found a great advantage to write the governing equations in terms of this amount and not in terms of the primary quantities of interest; namely temperature and heat flow. This indirect approach facilitates a great reduction in the formal complexity of the equations and substantially improves the accuracy of the solution.

### 5.2.1 Indoor temperature

The general equations, with all the variables assumed functions of time, which gives the indoor temperature resulting from the various forcing functions, are derived in appendix A: They are:

$$T_i = \frac{T_c \cdot R_v + T_x \cdot R_a}{R_v + R_a} \quad (5.23)$$

where

$$T_x = T_o + R_v \cdot Q_c \quad \text{and} \quad T_y = T_{sa} + R_o \cdot Q_r \quad (5.24)$$

and  $T_c$  is the temperature at the structure node (across the capacitor in figure 5.1).  $T_c$  is given in terms of the stored heat  $q^4$

$$T_c = q/C \quad (5.25)$$

---

<sup>4</sup>For notational consistency with Mathews and Richards ([11] chapter 2) we used  $Q$  for the loads in figure 5.1. We shall therefore use  $q$  for stored charge in this chapter as opposed to its use in chapter 2, where it indicated heat flux.

## SOLUTION WITH TIME DEPENDENT PARAMETERS

which must be obtained from the governing differential equation:

$$\dot{q} + \beta_T \cdot q = f_T \quad (5.26)$$

The forcing function in this equation is:

$$f_T = \frac{T_x}{R_a + R_v} + \frac{T_y}{R_o} \quad (5.27)$$

and the parameter  $\beta_T$  is:

$$\beta_T = \frac{R_a + R_o + R_v}{C \cdot R_o \cdot (R_a + R_v)} = \frac{1}{\tau_p} \quad (5.28)$$

It is possible to substitute (5.24) to (5.28) into (5.23) to obtain an equation which directly gives  $T_i$  in terms of the sources. The equation is:

$$\begin{aligned} \frac{d}{dt} \left[ \frac{(R_v + R_a) \cdot C}{R_v} \cdot T_i \right] + \beta_T \cdot \left[ \frac{(R_v + R_a) \cdot C}{R_v} \cdot T_i \right] = \\ \left[ \frac{R_a + R_o}{R_o \cdot R_v} \right] \cdot T_x + \frac{d}{dt} \left[ \frac{C \cdot R_a}{R_v} \cdot T_x \right] + \frac{T_y}{R_o}. \end{aligned} \quad (5.29)$$

This equation, although of the same form as (5.26), is considerably more difficult to solve accurately. This fact can be demonstrated:— the denominators of the derivative terms contain  $R_v$  as a factor, this implies that the equation is not valid when  $R_v$  vanishes. Therefore, (5.29) is not applicable to the important test case where the ventilation rate is large. In contrast, the correct result immediately follows from (5.23), irrespective of the accuracy of the solution of the differential equation.

### 5.2.2 System Load

The convective load,  $Q_{cr}$ , required to maintain a specified indoor temperature,  $T_{ir}$ , is obtained as before, by setting  $T_i = T_{ir}$  and solving for

## SOLUTION WITH TIME DEPENDENT PARAMETERS

$Q_c = Q_{cr}$  in (5.23) to (5.28). The result is:

$$Q_{cr} = \frac{R_a + R_v}{R_a \cdot R_v} \cdot T_{ir} - \frac{1}{R_a} \cdot T_{cr} - \frac{1}{R_v} \cdot T_o \quad (5.30)$$

where  $T_{cr}$  is the required temperature at the structure node given by

$$T_{cr} = q_r / C. \quad (5.31)$$

In (5.31)  $q_r$  is again the amount of heat stored in the structure, which is obtained from the differential equation:

$$\dot{q}_r + \beta_E \cdot q_r = f_E. \quad (5.32)$$

The forcing function is now:

$$f_E = \frac{T_y}{R_o} + \frac{T_{ir}}{R_a} \quad (5.33)$$

with the same definition of  $T_y$  as before. The parameter  $\beta_E$  is now:

$$\beta_E = \frac{R_a + R_o}{R_a \cdot R_o \cdot C} = \frac{1}{\tau_z}. \quad (5.34)$$

It is once again possible to obtain an equation linking  $Q_{cr}$  directly with  $T_{ir}$ , but the comments of §1.2.1 in this regard, is valid also here.

### 5.2.3 The General First Order Differential Equation

In the previous two sections, we have given the general equations for time varying systems. These equations indicate that the solutions are obtained

## SOLUTION WITH TIME DEPENDENT PARAMETERS

from a linear<sup>5</sup> first order differential equation, with time varying coefficient  $\beta(t)$ .

$$\dot{y}(t) + \beta(t) \cdot y(t) = x(t) \quad (5.35)$$

The forcing function,  $x(t)$ , of (5.35) is a strong function of the circuit parameters via the scaling factors,  $a, b, c, d$  or  $A, B, C, D$  in figures 5.2 & 5.3. In this way, the variable parameters can increase the rate of change of the effective forcing functions. It is important to realize that while the 'natural' forcing functions are probably reasonably smooth and continuous, and can be represented with a small number of Fourier components, sudden changes in the circuit parameters will cause discontinuities in the effective forcing functions, which will now require a large number of Fourier components to represent. However, the single pole circuit always tends to reject all fast changes in the forcing functions, even if the position of the pole is time dependent. It is therefore still possible to obtain fairly accurate answers with a modest number of Fourier components since the influence of the system in the input is to smooth the response.

The solution of the time dependent network is made difficult by the absence of a closed form solution for the impulse response and frequency response of the network, in the form of (5.18) and (5.19). The effect of the changes in the time-constant can be qualitatively understood by recognizing that if, in the frequency response (5.19),  $\beta$  is a function of time  $\beta(t)$ , the amplitude as well as the phase of a sinusoidally varying input signal will be modulated. In consequence, it is to be expected that the response will contain a substantial amount of superimposed signals at frequencies different from the original forcing frequency and the sinusoidal character of the forcing function will be distorted by the variable network.

---

<sup>5</sup>Since the equation is linear, albeit time variant, it is permissible to decompose the input function in a series. The output will be given by the sum of the individual responses to the terms of the series. However, the equation is not linear in  $\beta$  and the parameter  $\beta$  can not be decomposed.

## SOLUTION WITH TIME DEPENDENT PARAMETERS

The objective of the rest of this chapter is to find a solution for the response of the time dependent one pole system of (5.35). The general solution is first examined and, in later sections, we look at specific approximate solutions described in the literature.

The general solution of the differential equation when  $\beta(t)$  is a time dependent parameter is well known [6]:

$$y(t) = \exp[-\Gamma(t)] \cdot \left[ \int_{-\infty}^t \exp[\Gamma(t)] \cdot x(t) dt \right] \quad (5.36)$$

with 
$$\Gamma(t) = \int \beta(t) dt. \quad (5.37)$$

In the equation, the lower limit of the integral was again written as  $-\infty$  to obtain the steady state response to the – now assumed periodic – forcing function  $x(t)$ .

Obviously the general solution can not be evaluated analytically if the function  $\beta(t)$  is only known in tabulated format. Furthermore, it is clear that a numerical integration (e.g. Simpson's rule) will be problematic because of the infinite range and the oscillating nature of the integrand. The indicated range of integration  $(-\infty, t]$ , can be interpreted as indicating that the integration must proceed over a very long initial period, so that the transient response will be well damped. As a rule of thumb the transient response is negligible after about 5 time-constants have elapsed. For buildings with typical time-constants of 30 hours or more, this requires an initial period of integration of more than 150 hours. It follows that direct numerical integration of the general solution will place a heavy burden on the computer. This is nevertheless the approach used by many other existing programs, although they normally integrate the original differential equation with one of the standard procedures (e.g. Runge Kutta). Obviously this method suffers from exactly the same drawback: the

## SOLUTION WITH TIME DEPENDENT PARAMETERS

initial solution contains the transient response superimposed on the steady state response. Numerical methods will be discussed again later. Normally, Fourier series methods are used to find the steady state solution. These are discussed in §5.3.4.

First it should be explained why the existing methods for solution of the constant parameter model, i.e. convolution in frequency domain, can not be extended to the variable parameter case. The answer to this question is in brief: because the impulse response is not time invariant anymore, and the usual method of implementation of the convolution via Laplace or Fourier transform techniques, presupposes time invariance of the impulse response. In fact we see that it is impossible to obtain a closed form solution for the impulse response. This fact can be illustrated by calculating the impulse response of the system via the general solution above (5.35). If the input consists of an impulse  $x(t) = \delta(t-t_0)$ , occurring at time  $t = t_0$  the general solution yields:

$$\begin{aligned} h(t, t_0) &= u(t-t_0) \cdot \exp[-\Gamma(t)] \cdot \left[ \int_{-\infty}^t \exp[\Gamma(t_1)] \cdot \delta(t_1-t_0) dt_1 \right] \\ &= u(t-t_0) \cdot \exp[\Gamma(t_0) - \Gamma(t)]. \end{aligned} \quad (5.38)$$

where  $u(t)$  is the unit step function.

$$u(t) = \begin{cases} 1 & t \geq 0 \\ 0 & t < 0 \end{cases} \quad (5.39)$$

The impulse response  $h(t, t_0)$  is a function of two instances of time:– the time of occurrence of the impulse  $t_0$ , and the time since the occurrence of the impulse  $t$  [7]. This is emphasized by a change of variable from  $t$  to  $\tau = t-t_0$ , the delay since the occurrence of the impulse, so that (5.38) becomes:

$$h(t, \tau) = u(t-t_0) \cdot \exp[\Gamma(t-t_0) - \Gamma(t)]. \quad (5.40)$$

## SOLUTION WITH TIME DEPENDENT PARAMETERS

The frequency response can now be defined as the Fourier transform of the impulse response with respect to the delay [7]:

$$H(\omega, t) = \int_{-\infty}^{\infty} h(t, \tau) \cdot \exp[-j\omega(t-\tau)] d\tau. \quad (5.39)$$

The frequency response is dependent on time as well as frequency so that at every time instance, a different frequency response is valid or, as it is sometimes stated in the literature, the response *evolves* with time. This method will therefore require evaluation of a new impulse and frequency response, thus a Fourier transform, at every time instant. In reference [7], a full frequency domain method which utilizes the bifrequency system function, which is a double Fourier Transform from the  $(t, \tau)$  domain to the  $(\nu, \omega)$  domain, is derived. Frequency domain techniques are discussed further in §5.3.4. We will first examine some other techniques from the literature.

### 5.3 Methods for Solving the Variable Parameter System

Few techniques exist for obtaining solutions of equations with variable coefficients. Time variable networks are discussed in some depth by Zadeh [7,8,9], Pipes & Harvill [10] and by Gibson [11], which refers extensively to Zadeh. The earliest reference in the literature appears to be Carson [12] followed by [13]. More recent work, primarily directed at non-stationary stochastic systems, was reported by Tsao [14]. The contributions of Zadeh seems to be the most important but according to Gibson [11], the theory is still far from satisfactory: "their being as yet no general method applicable to a large class of problems". Attempts in the literature to extend the system impulse response approach to linear variable coefficient systems are not fully satisfactory [11]. The main reason seems to be the modulation effect of the variable parameters, which generate signals at different frequencies than those of the input signal, so that the Fourier components are time dependent or a double Fourier Transform is required. The mixed frequency-time domain techniques can easily lead to confusion because two independent time axes are used,  $t$  and  $\tau$  in (5.40), nevertheless they are

## SOLUTION WITH TIME DEPENDENT PARAMETERS

often preferred by engineers because they seem a natural extension of familiar methods. In this section some methods and results from the literature are briefly surveyed. The objective is to provide background on various problems and techniques for treating equations with variable coefficients.

We start by showing that the Laplace Transformation of the equation with variable coefficients leads to little progress [10]. Indeed, the Laplace transform of the differential equation

$$\frac{dy}{dt} + \beta(t) \cdot y = x(t) \quad (5.40)$$

is:

$$s \cdot Y(s) + y(0) + \mathcal{L}\{\beta(t) \cdot y(t)\} = X(s). \quad (5.41)$$

Using the time multiplication property of the Laplace Transform this expression is written:

$$s \cdot Y(s) + y(0) + \int_{-\infty}^{\infty} \psi(p) \cdot Y(s-p) dp = X(s) \quad (5.42)$$

where

$$\psi(s) = \mathcal{L}\{\beta(t)\}.$$

We see that instead of transforming the differential equation into an algebraic equation, the Laplace transform produces an integral equation. The solution of this integral equation is discussed in §2.4.

### 5.3.1 Solutions for Periodic Coefficients

When the variation in the coefficient  $\beta(t)$  is periodic, with the same period  $T$ , as that of the periodic forcing function (as we have previously assumed), the differential equation (5.35) is invariant under the transform  $t' = t + T$  [10]. Consequently, the solution will also be periodic with period  $T$ , it need only be solved in the interval  $[0, T]$ .

## SOLUTION WITH TIME DEPENDENT PARAMETERS

### a) Constant Segments

When the variation of the coefficient is periodic with period  $T$  and is a constant in every small segment  $\Delta t$  the Laplace Transform can be applied in every segment. Fodor [5] discuss the solution of an RC circuit when the resistance is periodically switched between two values. We take the case where  $\beta(t)$  is constant everywhere, except at two points where the value jumps discontinuously i.e.  $\beta(t)$  given by:

$$\beta(t) = \begin{cases} \beta_0 & 0 \leq t < T_1 \\ \beta_1 & T_1 \leq t < T \end{cases} \quad (5.45)$$

The exact solution for a constant  $\beta$  and a sinusoidal input function given by  $x = X \cdot (1 + m \cdot \cos \omega t)$  is:

$$y(t) = y(t_0) \cdot e^{-\beta t} + A(t) \quad (5.46)$$

with

$$A(t) = \frac{X}{\beta} \cdot \left[ 1 - e^{-\beta t} + \frac{m\beta}{\sqrt{\beta^2 + \omega^2}} \cdot \alpha(t) \right]$$

$$\alpha(t) = \cos(\omega[t+t_0]-\varphi) - \cos(\omega t_0 - \varphi) \cdot e^{-\beta t}.$$

where  $y(t_0)$  is the initial value and  $\tan \varphi = \omega/\beta$ . Next apply this solution to the intervals in (5.45) and set  $y(0) = y(T)$ ,  $y(T_1)$  continuous. The solution for  $y(0) = y_0$  is:

$$y_0 = \frac{A_1 + A_0 \cdot e^{-\beta_1(T-T_1)}}{1 - e^{-\beta_0 T_1 - \beta_1(T-T_1)}} \quad (5.47)$$

with

$$A_0 = A_0(T_1) \quad \text{and} \quad A_1 = A_1(T-T_1).$$

The subscripts 0 and 1 of  $A$  and  $\beta$  in (5.47) refers to the first and second intervals respectively.

## SOLUTION WITH TIME DEPENDENT PARAMETERS

This method can be extended to cater for the situation where the variation of  $\beta$  consists of more than just two constant sub-segments. In this manner, one could obtain a solution for the 24 hour period by assuming that the variation is a constant for every hour and then solving 24 equations similar to (5.46). This process will require for every harmonic component, matching of the initial and final conditions, 24 times. This procedure will be quite accurate but it is fairly intensive computationally. It requires the solution of 24 simultaneous equations for every frequency component.

### b) Sinusoidal Variations of the Coefficient

When the coefficient  $\beta(t)$  varies according to:

$$\beta(t) = \beta_0 \cdot (1 + m \cdot \sin \nu t), \quad (5.48)$$

where  $\beta_0$ ,  $m$  and  $\nu$  are parameters, and  $\nu$  is not necessarily equal to the frequency of the forcing functions  $\omega$ , we have in the general solution (5.36)

$$\Gamma(t) = \beta_0 \cdot (t + m/\nu \cdot \cos \nu t) \quad (5.49)$$

$$y(t) = \exp[-\Gamma(t)] \cdot \int_{-\infty}^t \Gamma(u) \cdot x(u) \, du. \quad (5.50)$$

If we assume, as before, that the input signal also varies sinusoidally and is given by  $x(t) = X \cdot e^{j\omega t}$ , where it is understood that only the real part of the complex phasor is physical (see §5.3.4), we have:

$$\begin{aligned} y(t) &= X \cdot \exp[-\Gamma(t)] \cdot \int_{-\infty}^t \exp[\beta_0(u + m/\nu \cdot \cos \nu u) + j\omega u] \, du \\ &= X \exp[-\Gamma(t)] \cdot \int_{-\infty}^t \exp[(\beta_0 + j\omega)u] \cdot \exp[\beta_0 m/\nu \cdot \cos \nu u] \, du \end{aligned} \quad (5.51)$$

## SOLUTION WITH TIME DEPENDENT PARAMETERS

Now we use the well known Bessel function expansion [10]

$$e^{a \cdot \cos \theta t} = I_0(a) + 2 \sum_{n=1}^{\infty} I_n(a) \cdot \cos n \theta t \quad (5.52)$$

and find

$$y(t) = X \exp[-\Gamma(t)] \cdot \int_{-\infty}^t \exp[(\beta_0 + j\omega)u] \cdot \left[ I_0(\beta_0 m / \nu) + 2 \sum_{n=1}^{\infty} I_n(\beta_0 m / \nu) \cdot \cos n \nu u \right] du$$

but

$$\int e^{bt} \cdot \cos n \theta t dt = K_n e^{bt} \cos(n\theta t - \psi_n)$$

where

$$K_n = \sqrt{b^2 + (n\theta)^2} \quad \text{and} \quad \tan \psi_n = n\theta/b.$$

The integral in the solution (5.51) can therefore be written:

$$\exp[(\beta_0 + j\omega)t] \cdot \left[ I_0(\beta_0 m / \nu) / (\beta_0 + j\omega) + 2 \sum_{n=1}^{\infty} I_n(\beta_0 m / \nu) \cdot K_n \cdot (\cos n \nu t - \cos \psi_n) \right] \quad (5.51)$$

The solution contains the original frequency of the forcing function  $\omega$  in the first factor of (5.53). This frequency is multiplied by a series expansion of overtones of the variation frequency  $\nu$  of the coefficient. For a more general forcing function, consisting of a number of Fourier components, the solution is applicable to every component and they can be superimposed. But it is important to remember that superposition is not valid for the

## SOLUTION WITH TIME DEPENDENT PARAMETERS

components of the variation of  $\beta(t)$ . For more complicated variations in  $\beta$ , consisting of a number of frequency components, the solution is useless. When  $m \ll 1$  the number of components with significant energy rapidly diminishes and (5.53) is more practical.

### 5.3.2 Solution of the Volterra Integral Equation [10]

Carson [12] originally gave the solution for a circuit, in which a part of the resistance is time variant, in the form of a Volterra integral equation. This solution is significant since it shows that a successive approximation technique may be followed to obtain the solution.

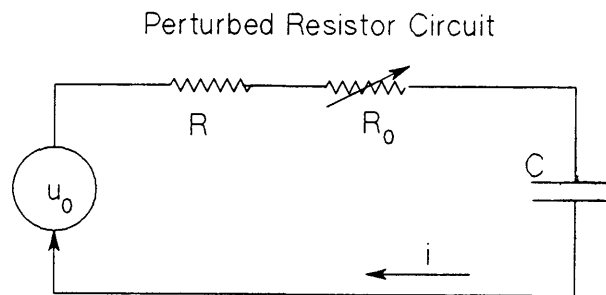


**FIGURE 5.4** Circuit in which a part of the resistance,  $R_0(t)$  is time variant. From [10].

In figure 5.4, the discharge resistance of the capacitor consists of a fixed resistor  $R$ , in series with a variable resistor  $R_0(t)$ . Ignoring the initial conditions and after application of Kirchhoff's voltage law, the circuit is found to be described by the following equation (the variables are as

## SOLUTION WITH TIME DEPENDENT PARAMETERS

indicated in the figure)<sup>6</sup>:

$$R \cdot i + 1/C \cdot \int i(t) dt + R_o(t) i(t) = e(t)$$

After Laplace transformation (indicated by  $\mathcal{L}\{\}$ ) this is equivalent to

$$\left[ R + \frac{1}{sC} \right] I(s) + \mathcal{L}\{R_o(t) \cdot i(t)\} = E(s). \quad (5.54)$$

If we define

$$Z(s) = 1/H(s) = R + \frac{1}{sC} \quad \text{and} \quad G(s) = \mathcal{L}\{R_o(t) \cdot i(t)\}$$

(5.54) becomes:

$$I(s) = H(s) \cdot E(s) - H(s) \cdot G(s). \quad (5.55)$$

the solution obtained via the inverse Laplace Transform is:

$$i(t) = \int_{-\infty}^t h(t-u) \cdot e(u) du - \int_{-\infty}^t h(t-u) \cdot R_o(u) \cdot i(u) du \quad (5.56)$$

with  $h(t)$  the impulse response of the steady circuit, i.e. with  $R_o = 0$ , defined by

$$h(t) = \mathcal{L}^{-1}\{H(s)\}$$

The first integral in (5.56) is the response of the steady system to the applied voltage which we shall call  $i_0(t)$ . The solution is then:

$$i(t) = i_0(t) - \int_{-\infty}^t h(t-u) \cdot R_o(u) \cdot i(u) du. \quad (5.57)$$

---

<sup>6</sup>In this section and elsewhere it is convenient to use electrical terminology. The reader will understand that 'current' relates to heat flux, and 'voltage' to temperature in thermo-flow problems.

## SOLUTION WITH TIME DEPENDENT PARAMETERS

This is a Volterra Integral Equation and the solution can be obtained in the following form [10,12]:

$$i(t) = i_0(t) - i_1(t) + i_2(t) - \dots = \sum_{n=0}^{\infty} (-1)^n \cdot i_n(t)$$

with

$$\begin{aligned}
 i_0(t) &= \int_{-\infty}^t h(t-u) \cdot e(u) \, du \\
 i_1(t) &= \int_{-\infty}^t h(t-u) \cdot R_0(u) \cdot i_0(u) \, du \\
 &\cdot \quad \cdot \quad \quad \quad \cdot \quad \cdot \\
 &\cdot \quad \cdot \quad \quad \quad \cdot \quad \cdot \\
 i_n(t) &= \int_{-\infty}^t h(t-u) \cdot R_0(u) \cdot i_{n-1}(u) \, du \tag{5.58}
 \end{aligned}$$

We are interested in the voltage across the capacitor, given by:

$$v(t) = \frac{1}{C} \cdot \int_{-\infty}^t i(t) \, dt = \frac{1}{C} \cdot \int_{-\infty}^t [i_0(t) - i_1(t) + i_2(t) - \dots] \, dt. \tag{5.59}$$

This solution involves a recursive procedure, where the zeroth approximation is the solution of the steady circuit, and higher order solutions are obtained from this solution by substituting for the forcing function, the previous solution multiplied by the time dependent resistance. The series converges quickly when  $R_0$  is much smaller than  $R$ , in which case the circuit is often called a perturbed circuit. Unfortunately in our application we have to assume that the variation in the ventilation resistance is substantial compared to the mean value so that the Volterra series will require a large number of terms to be accurate. Nevertheless, this solution offers some insight in the physics of the time dependent circuit.

### 5.3.3 The Substitution Theorem [5]

In the previous section it was seen that the Volterra solution is obtained

## SOLUTION WITH TIME DEPENDENT PARAMETERS

by first calculating the steady response, and then adding to this first approximation, the effects of the time variable resistor. The latter effect is obtained by calculating the voltage across the time dependent resistor, with initially the steady current and later, from more refined estimates of the current. This method is indicative of a far more powerful method based on the substitution theorem. The application of the substitution theorem to thermal networks is discussed by Athienitis [16]: "Simply stated (for thermal networks), it says that a network element across which a temperature drop is known, can be replaced by an equivalent heat source, equal to the heat flow through it." Alternatively, if the heat flux through a time dependent resistor is known, the theorem implies a time dependent temperature can be substituted for the resistor. The implementation of the method requires an initial estimate of the heat flux. From this estimate the substitution temperatures are calculated and then the solution. A recursive procedure may be used to refine the result. Since the method is very closely related to the Volterra series solution, we shall not discuss it in more detail.

### 5.3.4 A Recursive Solution<sup>7</sup>

Another recursive solution is obtained directly from the differential equation (5.35) written in the form:

$$\dot{y}(t) + \gamma_0(t) \cdot y = \xi_0(t) \quad (5.60)$$

which is obtained by taking  $\beta(t) = \gamma_0(t)$  and  $x(t) = \xi_0(t)$ . We attempt to find a solution in the form of an initial approximation  $y_0$ , and an error

---

<sup>7</sup>This recursive procedure was devised by the author himself. No serious attempt was made to investigate whether it was previously given in the literature. It probably has a direct connection with the Volterra solution of §5.3.2 and the transfer function approximations of Tsao, discussed later.

SOLUTION WITH TIME DEPENDENT PARAMETERS

term  $y_1$ :

$$y(t) = y_0 + y_1 = \xi_0(t)/\gamma_0(t) + y_1(t). \quad (5.61)$$

Taking the derivative of (5.61)

$$\dot{y}(t) = \frac{\gamma_0 \cdot \dot{\xi}_0 - \dot{\gamma}_0 \cdot \xi_0}{\gamma_0^2} + \dot{y}_1$$

and substituting it in the differential equation (5.60) produces:

$$\dot{y}_1 + \gamma_0 \cdot y_1 = - \frac{\gamma_0 \cdot \dot{\xi}_0 - \dot{\gamma}_0 \cdot \xi_0}{\gamma_0^2} \quad (5.62)$$

which is of exactly the same form as (5.60) if

$$\xi_1 = - \frac{\gamma_0 \cdot \dot{\xi}_0 - \dot{\gamma}_0 \cdot \xi_0}{\gamma_0^2}. \quad (5.63)$$

The whole procedure is now repeated for  $y_1$  to obtain  $y_2$  etc. The final solution is:

$$y(t) = 1/\gamma_0 \cdot [\xi_0 + \xi_1 + \xi_2 + \dots] \quad (5.64)$$

where we have

$$\xi_0(t) = x(t)$$

$$\xi_n(t) = \frac{\xi_{n-1} \dot{\gamma}_0 - \gamma_0 \dot{\xi}_{n-1}}{\gamma_0^2} \quad n = 1, 2, 3, \dots$$

The convergence of this solution has not been determined. The solution is determined in higher orders of derivatives of  $\gamma_0 \cdot \xi_0 / \gamma_0^2$ , and should converge fast if the derivatives of  $\gamma_0$  and  $\xi_0$  vanish, or if  $\gamma_0^2$  is large. For sinusoidal forcing functions, the magnitudes of the derivatives are proportional to the frequency and consequently the series will diverge for

## SOLUTION WITH TIME DEPENDENT PARAMETERS

large frequencies. In general, it appears that it will diverge unless all the functions are reasonably smooth.

### 5.3.5 Fourier Methods and the Modulation Function Equation<sup>8</sup>

The standard approach to obtaining the steady state solution to a time invariant system, is via the phasor (Fourier series) representation as applied in §5.1.4. The application of this method to the differential equation (5.35) leads to a first order differential equation in complex quantities, similar in form to the original equation, which we shall call the modulation function equation (MFE), after Tsao [14]. This equation is well known in the literature where procedures are described to derive it, by inspection, directly from the original equation [7,14]. The advantage of this method is that it is applicable to systems of higher order, and also to non-stationary stochastic systems. We shall derive it by assuming the input and output functions can be represented by a complex Fourier series expansion. [4]

#### a) Phasor Representation of Periodic Forcing Functions

If the forcing function  $x(t)$ , is a periodic function with period  $T$ , it can be expanded in a complex Fourier series:

$$x(t) = \sum_{n=-\infty}^{\infty} C_n \cdot e^{jn\omega_0 t} \quad (5.65)$$

with  $\omega_0 = \frac{2\pi}{T}$  and

$$C_n = \frac{1}{T} \int_{-T/2}^{T/2} x(t) \cdot e^{-jn\omega_0 t} dt. \quad (5.66)$$

Because the system is linear, the contributions from each phasor,  $C_n \cdot e^{jn\omega_0 t}$ , can be calculated independently and the results can be summed

---

<sup>8</sup>This frequency domain method is described in full detail since it is a viable solution method. Although it is the conclusion of this thesis that the numerical procedure of §5.4 is more suitable, future developments may require the use of this alternative method. It is in any case illuminating.

## SOLUTION WITH TIME DEPENDENT PARAMETERS

to find the total solution. At this stage it is important to remember, that in the circuit of figure 5.1, we require the forcing function  $T_e$  to be periodic with period  $T$ , and therefore, since  $T_e$  is dependent on the circuit parameters, they must also be periodic with the same period and hence also  $\beta$ . This condition is satisfied if all signals are specified over a given period (e.g. 24 hours) and it is assumed that all the signals are periodic with this period. This is exactly the assumption we made in §5.1.3.

We propose to use the phasor  $x(t) = X \cdot e^{-j\omega t}$  with  $X$  a constant complex amplitude, as forcing function in equation (5.35) and assume that the response is given by  $y(t) = Y(t, \omega) \cdot e^{-j\omega t}$ .  $Y(t, \omega)$  is the complex function describing the amplitude and phase modulation introduced by the time dependent system. It is explicitly written a function of  $t$ , to emphasize that we expect the amplitude and phase of the response to be functions of time. Substituting these definitions of  $x$  and  $y$  in (5.35) yields:

$$\frac{\partial Y}{\partial t} + [\beta(t) + j\omega] \cdot Y = X. \quad (5.67)$$

This is the MFE. The frequency response of the system is now defined by

$$H(t, \omega) = \frac{Y(t, \omega)}{X}, \quad (5.68)$$

corresponding with the definition for a time invariant system. The frequency response must satisfy:

$$\frac{\partial H(t, \omega)}{\partial t} + [\beta(t) + j\omega] \cdot H(t, \omega) = 1. \quad (5.69)$$

The impulse response is defined as the inverse Fourier Transform of  $H(t, \omega)$  with respect to  $\omega$ . These definitions correspond with the definitions in §5.1.4. In [7,14] a general method for obtaining the MFE is derived and solutions via expansions are given. These solutions will be discussed later.

## SOLUTION WITH TIME DEPENDENT PARAMETERS

Equation (5.69) is of exactly the same form as (5.35) but involves complex quantities. However, the forcing function is a constant. To solve this equation, we need initial conditions for either  $y(0, \omega)$  or  $H(0, \omega)$ . Zadeh [7] indicates that a method for deriving initial conditions is to assume the system was constant and equal to  $H(0, \omega)$  prior to  $t = 0$ . However, we are looking for periodic solutions with  $H(T, \omega) = H(0, \omega)$ . It is therefore not possible to assume that the system was initially invariant, and the initial condition remains unspecified, as with the time domain representation. In the next section, we indicate how the problem of the unknown initial condition can be circumvented by using a suitable approximate transfer function. With the initial condition known, the MFE can be solved by any of the methods discussed so far.

### b) Expansions for the Transfer Function

Zadeh [7] gives a differential equation which must be satisfied by the system function in the following form:

$$\left[ \frac{1}{j\omega + \beta} \right] \cdot \frac{\partial H}{\partial t} + H = \frac{1}{j\omega + \beta} \quad (5.70)$$

This equation obviously corresponds with equation (5.67). But Zadeh gives the following interesting interpretation of (5.70): "The system function of a variable network may be formally regarded as the response of an initially unexcited system, of which [(5.70)] is the fundamental equation, to the frozen system function of the network." And also: "The frozen system function may be regarded as a first approximation to the actual system function of a variable network whenever the coefficients of the fundamental equation do not vary appreciably over the width of the impulse response of the system." Zadeh defines the frozen system function as the function determined by freezing the variable network at the instant of consideration. In the case of the single pole network the frozen system function is,

SOLUTION WITH TIME DEPENDENT PARAMETERS

compare with (5.19):

$$H_f(t, \omega) = \frac{1}{j\omega + \beta(t)} \quad (5.71)$$

We shall encounter (5.71) again later. In reference [7] two approximate methods for solving (5.70) with series expansions are given. These methods are not applicable to our problem where the variations in the parameter  $\beta$  are sudden and large. The problems which arise under these conditions are illustrated in the next paragraph for a similar expansion due to Tsao.

According to Tsao [14] the solution of the MFE equation can be obtained iteratively, where the zeroth order approximation is the frozen system function  $H_f$ . The  $m$ th order approximation is given by<sup>9</sup>:

$${}_m Y(t, \omega) = H_0(t, \omega) \cdot \left\{ X - \frac{\partial \{{}_{m-1} Y\}}{\partial t} \right\}. \quad (5.72)$$

The zeroth order approximation is thus the frozen response as defined above:

$${}_0 H(t, \omega) = H_f = 1/(j\omega + \beta(t))$$

The first order approximation is:

$${}_1 Y(t, \omega) = H_f(t, \omega) \cdot \left\{ X(\omega) - \frac{\partial \{{}_0 Y\}}{\partial t} \right\} \quad (5.73)$$

but 
$$\frac{\partial \{{}_0 Y\}}{\partial t} = H_f(t, \omega)^2 \cdot X(\omega) [-\dot{\beta}(t)]$$

$${}_1 H(t, \omega) = H_f(t, \omega) \cdot [1 + \dot{\beta}(t) \cdot H_f^2]. \quad (5.74)$$

---

<sup>9</sup>A small subscript before a variable is used to indicate the approximation order.

## SOLUTION WITH TIME DEPENDENT PARAMETERS

This expression agrees with that obtained in §5.3.3 when  $\xi_0 = X$  (a complex constant) in (5.60). The error,  $\epsilon$ , in these approximations are given approximately by the next higher order term, which is for the zeroth order approximation:

$${}_0\epsilon(t, \omega) = \dot{\beta}(t) / (\beta + j\omega)^2. \quad (5.75)$$

The error depends on the speed of variation of  $\beta$  and will vanish if  $\dot{\beta}$  vanishes. For the first order approximation one finds:

$$\begin{aligned} {}_1\epsilon(t, \omega) &= -H_f^3 \cdot \ddot{\beta} + 3 \cdot H_f^4 \cdot \dot{\beta}^2 \\ &= 3[{}_0\epsilon(t, \omega)]^2 - H_f^3 \cdot \ddot{\beta}. \end{aligned} \quad (5.76)$$

If the zeroth order error  ${}_0\epsilon$  is small the errors will decrease with higher order approximations. For sudden changes in  $\beta$ , i.e.  $\dot{\beta}$  large one can expect that the expansion (5.72) will diverge, and it appears that greater accuracy is obtained from the frozen system, than from higher order approximations. The zeroth and first order approximations were implemented in a program to test these conclusions and it was indeed found that the expansion diverges.

However, the solution obtained by using just the frozen response,  $H_f$ , appeared to be quite useful. The frozen response is a very convenient approximate solution.  $H_f$  is uniquely specified at each time instant so that the solution is straightforward; the frequency components of the forcing function are simply multiplied with  $H_f$  and added at each time instant, as in (5.77) below. However, at first glance it appears to be a very crude approximation. It amounts to ignoring the derivative term,  $\partial H / \partial t$ , in (5.69). Since we are assuming that  $\beta(t)$  is subject to sudden large changes,  $\partial H / \partial t$  could not possibly be small if it is approximately given by  $H_f$ . However, it was subsequently discovered that the true system function,

## SOLUTION WITH TIME DEPENDENT PARAMETERS

obtained from (5.69), responds very sluggishly to changes in  $\beta$ , since it was governed by the same long time-constant as the original equation (5.35). Therefore the action of the system (5.69) is to dampen the quick changes in  $\beta$ , so that the derivative  $\partial H/\partial t$  may indeed be small. From this point of view, it is seen that the approximation  $H \approx H_f$  will tend to accentuate the variability of the system and the approximate solution will, in a certain sense, overreact to the variation in  $\beta$ . However, investigation showed that if  $\beta$  remained sufficiently small, that is, if the thermal time constant remained sufficiently large, this over-reaction is not visible in the response, and the frozen system gives useful results. The approximate solution of (5.35) using the frozen transfer function is given by:

$$y(t) = \sum_k X_k \cdot \exp(j \cdot k \cdot \omega_0) / (\beta(t) + j \cdot k \cdot \omega_0) \quad (5.77)$$

where  $k$  is an index running over the frequency components,  $\omega = k \cdot \omega_0$ , of the forcing function:

$$x(t) = \sum_k X_k \cdot \exp(j \cdot k \cdot \omega_0). \quad (5.78).$$

The method was implemented in the thermal analysis program. A listing of the relevant routines are supplied on the accompanying floppy diskette.

Intensive investigation of the conduct of this approximate solution was carried out. It indicated some disturbing trends which required further corrective procedures. The thermal forcing functions normally possess a large mean component plus a diurnal swing component. The effective forcing function will therefore exhibit the same characteristic. In the solution of the thermal network it is essential that the mean component be calculated accurately. However, in those cases where the mean component of the input was substantial, the computed mean as well as the swing of the output were inaccurate. The reason seems to be that the too strong modulation effect of the frozen system approximation on the mean

## SOLUTION WITH TIME DEPENDENT PARAMETERS

component of the input. It is crucial to understand that the time variable circuit generates an additional swing component, by modulation of the input, even if the input is held constant.

### c) Separate Treatment of Mean- and Swing Component

It appeared reasonable to expect that better accuracy could be obtained by treating the mean and swing components separately. The original differential equation (5.35) is:

$$\dot{y} + \beta \cdot y = x. \quad (5.79)$$

if  $x, y$  and  $\beta$  consist of a mean part indicated by an over-bar plus a swing component indicated by a tilde, i.e.

$$x = \bar{x} + \tilde{x}, \quad y = \bar{y} + \tilde{y}, \quad \beta = \bar{\beta} + \tilde{\beta} \quad (5.80)$$

(5.79) becomes

$$\dot{\tilde{y}} + \bar{\beta} \cdot \bar{y} + \tilde{\beta} \cdot \bar{y} + \bar{\beta} \cdot \tilde{y} + \tilde{\beta} \cdot \tilde{y} = \bar{x} + \tilde{x}. \quad (5.81)$$

In this equation the terms  $\bar{\beta} \cdot \bar{y}$  and  $\bar{x}$  are constants while the terms  $\dot{\tilde{y}}$ ,  $\tilde{\beta} \cdot \bar{y}$ ,  $\bar{\beta} \cdot \tilde{y}$  and  $\tilde{x}$  have zero mean components. The only remaining term is  $\tilde{\beta} \cdot \tilde{y}$  which contains again a mean and a swing indicated by:

$$\tilde{\beta} \cdot \tilde{y} = \overline{\tilde{\beta} \cdot \tilde{y}} + \tilde{\tilde{\beta}} \cdot \tilde{\tilde{y}} \quad (5.82)$$

Equation (5.81) is now separated into two equations; one for the constant

## SOLUTION WITH TIME DEPENDENT PARAMETERS

terms and another for the swing terms:

$$\bar{\beta} \cdot \bar{y} + \overline{\tilde{\beta} \cdot \tilde{y}} = \bar{x} \quad (5.83)$$

$$\dot{\tilde{y}} + \tilde{\beta} \cdot \bar{y} + \bar{\beta} \cdot \tilde{y} + \overline{\tilde{\beta} \cdot \tilde{y}} = \tilde{x}. \quad (5.84)$$

These equations must be solved simultaneously for  $\bar{y}$  and  $\tilde{y}$ . The following approximate method may be used, in which the solution of the differential equations are obtained from the frozen system function:

- Assume  $\overline{\tilde{\beta} \cdot \tilde{y}} \ll \overline{\tilde{\beta} \cdot \tilde{y}}$  so that  $\tilde{\beta} \cdot \tilde{y} \approx \overline{\tilde{\beta} \cdot \tilde{y}}$ .
- From (5.83) follows that a first approximation for the mean of the output is:

$$\bar{y}_0 = \bar{x} / \bar{\beta} \quad (5.85)$$

- Next apply equation (5.84) in the following form:

$$\dot{\tilde{y}}_0 + \beta \cdot \tilde{y}_0 = \tilde{x} - \tilde{\beta} \cdot \bar{y}_0 = \tilde{x} \cdot (1 - \beta / \bar{\beta}) \quad (5.86)$$

to find  $\tilde{y}_0$ , the first estimate of the swing.

- Next calculate the mean of  $\tilde{y}_0 \cdot \tilde{\beta} = \overline{\tilde{y}_0 \cdot \tilde{\beta}}$  and set the next higher approximation:

$$\bar{y}_1 = \frac{\bar{x} - \overline{\tilde{y}_0 \cdot \tilde{\beta}}}{\bar{\beta}} = \bar{y}_0 - \frac{\overline{\tilde{y}_0 \cdot \tilde{\beta}}}{\bar{\beta}}. \quad (5.87)$$

## SOLUTION WITH TIME DEPENDENT PARAMETERS

- If necessary the iteration can continue by solving again

$$\dot{\tilde{y}}_1 + \beta \cdot \tilde{y}_1 = \tilde{x} - \tilde{\beta} \cdot \tilde{y}_1 = x \cdot (1 - \beta/\tilde{\beta}) \text{ etc.} \quad (5.88)$$

This procedure was programmed (see the listing on the accompanying floppy diskette) and the answers were compared to accurate answers, obtained via the exact solution of the special case, given in §5.3.1a. It was found that a single iteration through (5.85) to (5.87) was sufficiently accurate. Note that the differential equation which is actually approximately solved with the frozen transfer function, is (5.86), which contains no mean output component.

The implementation obtains the frequency components (5.78) of the effective forcing function, via the prime factor FFT algorithm described in [3]. Note that, even though the forcing function contains many harmonics when the parameters change discontinuously – due to the changes of the contribution factors of the various sources in figures 5.2 and 5.3 – not many of these harmonics are required in the solution. The basic response of the differential equation, although time dependent, still remains sluggish, since we have written the governing equation in terms of the stored heat in the structure. From physical considerations it follows that the stored heat must remain a smooth function of time, even when the temperatures are discontinuous. It was found that – for almost all buildings – 5 frequency components are sufficient to obtain an accuracy of 0.5 °C for the predicted interior temperature.

The phasor components  $Y$  are obtained from the components of the forcing function  $X$ , multiplied by the system response  $H$  as given by (5.77). When only a small number of Fourier components is used the method is quick. For  $j$  time points and  $i$  frequency components, the approximation (5.77) requires  $i \cdot j$  complex multiplications. For 24 time points, and 5 frequency components, the total is 120 complex multiplications, which is the same as the number required by frequency domain convolution of time invariant

## SOLUTION WITH TIME DEPENDENT PARAMETERS

systems. In addition, the method requires one 24 point FFT to obtain the spectrum of the forcing function.

This Fourier series method, which uses the frozen system transfer function as an approximation to the actual transfer function, was found to be well behaved and quite accurate. However, in §5.4 a numerical method is described which is far simpler, more efficient and potentially more accurate. Since this latter numerical method subsequently replaced the Fourier series method, the above detailed discussion of the Fourier series method, is strictly speaking, redundant to this thesis. The author nevertheless feels that the method merits the considerable space given to it here. It is a natural extension of the method used for solving the time invariant case, and as such, provides much insight in the behaviour of the time dependent system.

### 5.4 A New Efficient Numerical Algorithm

In §5.3.1a a method was indicated which is based on the assumption that the input functions are constant in small time intervals. It was shown that this method will require the solution of a large number of simultaneous equations. However, since we have written the governing equation (5.35) in terms of the stored heat in the structure, it is reasonable to expect that also the output, will be a fairly smooth function. In this section we obtain an approximate method, based on the assumption that all variables, input output and also  $\beta$ , are constant between sampling points.

The big advantage of writing the governing equation in terms of the amount of stored energy is; it reduces the sensitivity of the solution of  $T_i$  to errors in the solution of the differential equation (5.35). A large part of the variation in  $T_i$  is accurately included in the final calculation of  $T_i$  and  $Q_{cr}$  from  $q$ , in (5.23) and (5.30) respectively. This is easily demonstrated by noting that, in the limit, when the ventilation rate is very large ( $R_v \sim 0$ ), the sole contributor to  $T_i$  in equation (5.23) is  $T_x$ . On the other hand, when  $R_v$  approaches infinity, the sole contributor is  $T_c$ . This is in

## SOLUTION WITH TIME DEPENDENT PARAMETERS

accordance with the network of figure 5.1.

### a) A First Difference Equation

To solve (5.35) we rewrite the equation in the form of an integral equation<sup>10</sup>:

$$\begin{aligned}
 y(t) &= \int_{-\infty}^t x(t_1) - \beta(t_1) \cdot y(t_1) dt_1 \\
 &= \int_{-\infty}^0 x(t_1) - \beta(t_1) \cdot y(t_1) dt_1 + \int_0^t x(t_1) - \beta(t_1) \cdot y(t_1) dt_1 \\
 &= y(0) + \int_0^t x(t_1) - \beta(t_1) \cdot y(t_1) dt_1
 \end{aligned} \tag{5.89}$$

For periodic, steady state solutions with period  $T$ , it is required that the initial value of every period equals the final value of the previous period:

$$y(0) = y(T) = y(0) + \int_0^T x(t_1) - \beta(t_1) \cdot y(t_1) dt_1$$

and therefore

$$\int_0^T x(t_1) - \beta(t_1) \cdot y(t_1) dt_1 = 0. \tag{5.90}$$

The steady, periodic solution of (5.35) is given by (5.89) with initial condition stipulated by (5.90). For discrete data at  $t = t_i = i \cdot \Delta T$ ,  $i = 0, 1, 2, 3, \dots$ ,  $T = N \cdot \Delta T$ , these equations take the form:

$$y_k = y_0 + \sum_{i=0}^{k-1} \Delta T \cdot (x_i - \beta_i \cdot y_i) \tag{5.91}$$

and

$$\sum_{i=0}^{N-1} \Delta T \cdot (x_i - \beta_i \cdot y_i) = 0. \tag{5.92}$$

---

<sup>10</sup>A similar approach using the general solution (5.36) fails, apparently because (5.36) does not contain  $y(0)$  under the integral.

## SOLUTION WITH TIME DEPENDENT PARAMETERS

It is assumed all variables are constant between sampling points and  $x_i = x(t_i)$  as well as  $\beta_i = \beta(t_i)$  are known tabulated functions. Equation (5.91) can be written in the following corresponding, iterative form:

$$y_k = \Delta T \cdot x_{k-1} + (1 - \Delta T \cdot \beta_{k-1}) \cdot y_{k-1} \quad k = 1, 2, 3 \dots N-1 \quad (5.93)$$

Equation (5.93) is a simple first difference equation, and the technique is known in the numerical analysis literature as Euler's method. If one value of  $y_k$  is known, the other values are easily found from (5.93), provided the iteration is stable. The essence of an efficient method is an effective methodology for obtaining one value, so that the others can be obtained from the iteration. In the next section an explicit equation for the initial value is derived.

### b) A Closed Form Solution for the Initial Value<sup>11</sup>

A closed form solution for the initial value  $y_0$  is obtained by starting with

$$y_N = \Delta T \cdot x_{N-1} + (1 - \Delta T \cdot \beta_{N-1}) \cdot y_{N-1} = y_0 \quad (5.94)$$

and substituting previous values of  $y_k$ .

$$\begin{aligned} y_N &= \Delta T \cdot x_{N-1} + (1 - \Delta T \cdot \beta_{N-1}) \cdot (\Delta T \cdot x_{N-2} + \\ & (1 - \Delta T \cdot \beta_{N-2}) \cdot (\Delta T \cdot x_{N-3} + ( \dots \Delta T \cdot x_0 \dots))) + \\ & (1 - \Delta T \cdot \beta_{N-1}) \cdot (1 - \Delta T \cdot \beta_{N-2}) \cdot \dots \cdot (1 - \Delta T \cdot \beta_0) \cdot y_0 = y_0. \end{aligned}$$

---

<sup>11</sup>Although this closed form solution for the initial value is very natural and its derivation straightforward, it appears to be unknown in the literature. However, no exhaustive search in the numerical analysis literature was undertaken and it is probable that this result is common knowledge in some circles.

## SOLUTION WITH TIME DEPENDENT PARAMETERS

Solving for  $y_0$ , this is rewritten compactly:

$$y_0 = \frac{\left[ \sum_{k=0}^{N-2} \Delta T \cdot x_k \cdot \prod_{j=k+1}^{N-1} (1 - \Delta T \cdot \beta_k) \right] + \Delta T \cdot x_{N-1}}{1 - \prod_{k=0}^{N-1} (1 - \Delta T \cdot \beta_k)}. \quad (5.95)$$

When programming equation (5.95), advantage can be taken of the fact that the product expression appears both in the numerator and the denominator, by starting with the highest value of  $k$  and counting down instead of up. By storing at each step  $k$  the partial sum and the partial product, the product expression can be evaluated successively for every term in the sum. The product expression in the denominator is found by multiplying the final product of the numerator with  $(1 - \Delta T \cdot \beta_0)$ .

The complete approximate solution is given by (5.93) with initial value given explicitly by (5.95). We maintain that the method is efficient; no initial period of integration or iterations are required to get rid of the transients and the numerical integration step size is fixed at the sampling period of the data. The accuracy of the solution is discussed later.

### c) Stability

First we need to establish the stability of (5.93). This question is important despite the physical constraints which ensure the absolute stability of the original differential equation. It is well known that the sampling interval has an influence on the stability of a sampled data system [17]. To investigate the stability of (5.93) the  $\mathcal{Z}$  transform method [17] will be used under the assumption that  $\beta$  is independent of time. This assumption is required since it is difficult to establish the stability of the time dependent form. The transfer function of (5.93) in the  $z$  domain is:

$$H(z) = \frac{Y(z)}{X(z)} = \frac{z^{1 \cdot \Delta T} \cdot \beta}{1 - z^{1 \cdot \Delta T} \cdot \beta}. \quad (5.96)$$

## SOLUTION WITH TIME DEPENDENT PARAMETERS

The time invariant system is stable if the pole of the transfer function lies inside the unit circle on the complex  $z$ -plane, i.e.

$$|1 - \Delta T \cdot \beta| \leq 1. \quad (5.97)$$

For the time variable circuit, the position of the pole is time dependent but stability may be assumed if, at all times, the pole never strays outside the unit circle. This is not a stringent condition. Gibson [11] discusses the stability of time variable systems and he gives an example where condition (5.97) is satisfied and yet the system is unstable. However, we have found that (5.97) will indicate stability of (5.93), so that if the sampling interval is chosen so that  $\Delta T \cdot \beta < 2$ , the recursion is stable. For most practical buildings a sampling interval of 1 hour suffices. For some very light constructions, it was found necessary to decrease  $\Delta T$  to 15 minutes.

### d) Accuracy of the Method

The method is essentially Euler's method for the numerical integration of a differential equation. An upper bound for the total propagated error is [18]:

$$|e| \leq \frac{\Delta T \cdot |\ddot{y}|}{2 \cdot \beta} \cdot [\exp(\beta \cdot T) - 1]. \quad (5.98)$$

The error grows rapidly when  $\beta \cdot \Delta T = \Delta T / \tau > 0.1$ . Since we have written the governing equation in terms of the stored heat, which is a slowly varying quantity, one would normally expect  $|\ddot{y}|$  to be quite small. In fact, the derivative of (5.35) gives:

$$\begin{aligned} \ddot{y} &= \dot{x} - \beta \cdot \dot{y} - \dot{\beta} \cdot y \\ &= \dot{x} - \beta \cdot (x - \beta \cdot y) - \dot{\beta} \cdot y \\ &= \dot{x} - \beta \cdot x + (\beta^2 - \dot{\beta}) \cdot y. \end{aligned} \quad (5.99)$$

SOLUTION WITH TIME DEPENDENT PARAMETERS

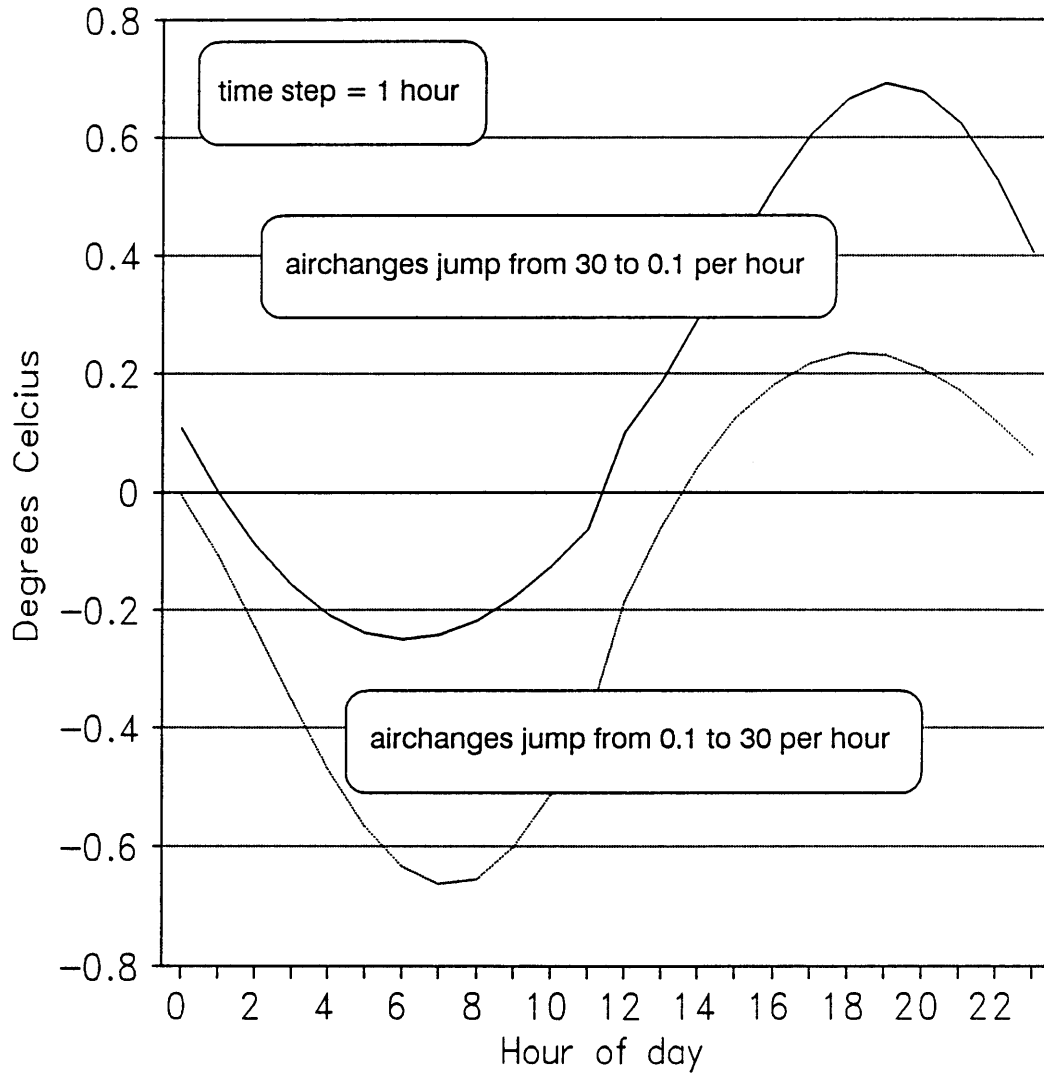


**FIGURE 5.5** Difference between analytically derived exact prediction of interior temperature, for sinusoidal forcing functions, and numerical algorithm. The sampling period is 1 h. Building: low-mass agricultural shed,  $\tau = 5$  h. The upper and lower traces show the error when the air-change-rate jumps from 0.1 to 30 /h, and from 30 to 0.1 /h respectively. The forcing functions are given in the text.

## SOLUTION WITH TIME DEPENDENT PARAMETERS

$|\ddot{y}|$  contains a term proportional to  $\dot{\beta}$  which might be large for large variations of  $\beta(t)$ . Actually, the numerical integration technique is rigorously exact if all variables assume constant values between sampling points, even with discontinuous derivatives at the sampling points. Equation (5.98) must not be taken too seriously, it is not a very tight upper bound and, furthermore, it is derived under the assumption that the functions are all continuous.

To obtain a practical evaluation of the accuracy of the method, the approximate solution can be compared with the exact solution in a special case. In §5.3.1a the analytical solution for a system with constant  $\beta$  in subintervals was given. Figure 5.5 shows the error between analytic solution (5.46), (5.47), and numerical solution (5.93), (5.95), for a low-mass building. The building (an agricultural shed) has a time-constant of about 5 hours (see Table 5.1) with closed windows. This is a very short thermal time-constant for a building, and a practical sampling rate would be 15 min, but to show the robustness of the method, a sampling period of 1 h is used in the calculation. The air change-rate varies between 0.1 and 30 /h resulting in a time-constant jump from 5.7 to 3.8 h, the jump occurring at  $T_1 = 11$  h. The forcing functions used for the calculation are:

$$\begin{aligned} T_{sa} &= 20 + 10 \cdot \cos(2\pi/24 \cdot t) \text{ } ^\circ\text{C}, \\ T_o &= 20 + 5 \cdot \cos(2\pi/24 \cdot t) \text{ } ^\circ\text{C} \text{ and} \\ Q_c &= Q_r = 0 \text{ kW} . \end{aligned}$$

The calculation is given in appendix 4A.

Figure 5.5 shows the error obtained by a sudden increase in the number of air changes as well as a sudden decrease of similar strength. In this worst case,  $\beta \cdot \Delta T = 0.25$ , the temperature error is less than 1°C. The error is decreased to insignificant levels by decreasing the sampling period to 15 min, with linear interpolation between sampling points. Figure 5.6 shows

SOLUTION WITH TIME DEPENDENT PARAMETERS

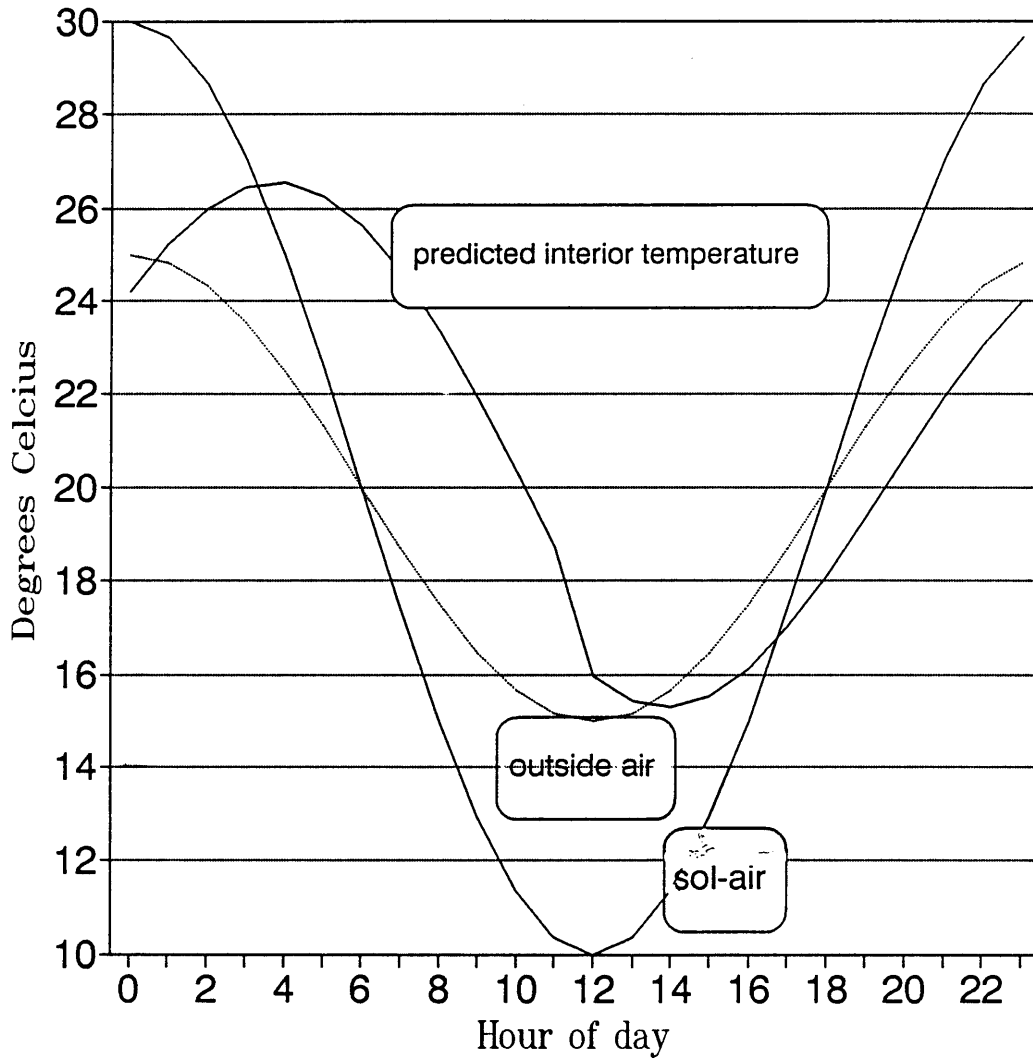


**FIGURE 5.6** Predicted interior temperature for the low-mass building when the air-change rate jumps between 0.1 and 30 /h. The thick-solid line is the assumed sol-air temperature and the thick-broken line the assumed outside air temperature.

the resulting interior temperatures. Note the sharp discontinuity. In practice, the heat capacitance and the finite mixing time of the interior air (both neglected in the model) will tend to smooth the discontinuity so that

## SOLUTION WITH TIME DEPENDENT PARAMETERS

a smooth transition will be measured. (It was also found that, with sudden changes in the ventilation rate, the time constant of the thermograph can often not be neglected.)

The calculations were repeated for a massive building (office block) where the time constant jumped from 144 to 38 h when the ventilation rate was increased from 0.1 to 30 /h. The error between the analytic and approximate solutions in this case,  $T = 1$  h,  $\beta \cdot \Delta T = 0.025$ , were less than 0.1 °C.

When evaluating the numerical error it must be borne in mind that the accuracy of the thermal modelling is definitely limited by the extreme simplicity of the model. It makes no sense to strive for infinite accuracy in the calculation procedure when both the assumptions inherent in the model, and uncertainties in the detail of the construction and ventilation rates limit the practical, attainable accuracy. The objective of creating a simplified and easy to use tool, which will give results quickly, must remain in the forefront.

### e) More Accurate Algorithms

To decrease error propagation for continuous functions one can use a higher order numerical approximation technique. Beginning with the trapezoid rule, for instance, an exactly similar scheme with local error theoretically proportional to the third derivative and square step size results. These and a host of other higher order approximation techniques [5,18] are not as advantageous for discontinuous input functions. Unless the integration is done over continuous subintervals, they tend to smooth the discontinuities and to make the solution appear non-causal, since they pre-empt the sudden change. The effect is easily explained by noting that the higher order techniques in effect interpolate between the sampling points so that values in the immediate future will influence the present result. In practice, we have found the Euler algorithm sufficiently accurate and quick. Further reduction in computation time is possible from implicit and higher order

## SOLUTION WITH TIME DEPENDENT PARAMETERS

methods [e.g. 19], but the simple method is already so fast that the matter is of academic importance only. It is possible to find an expression similar to (5.95) for an implicit discretization of (5.35)<sup>12</sup> The implicit methods have the advantage that they are generally stable, however, they were not investigated in depth.

### f) Extension to Higher Order Systems

The simple numerical method is readily extended to higher order systems. We have, in chapter 2, suggested a refined thermo-flow model, figure 2.22, in which the interior masses are treated separately. By using the state space approach [17], it is possible to represent this system as two first order differential equations, where the 2 state variables must be chosen to respectively correspond with: i) the stored heat in the shell of the building, and ii) the stored heat in the interior masses. By redefining  $y$  to be the state vector, and  $x$  the input vector, the numerical recursion is directly applicable. The initial value takes a somewhat different form because of the matrix operators. In similar manner the method can be extended to systems of any order.

### g) Implementation

A listing of the implementation of the numerical procedure is given on the accompanying floppy diskette. It is quite straightforward. In the implementation provision was made for dynamic selection of the step size by linking the step size to the thermal time-constant of the building through (5.97). In this way, numerical accuracy may be assured while efficiency is maximized. However, it was found that a step size of 1 h is adequate for all buildings, except for some extremely light constructions, where the numerical accuracy is not sufficient. Since the calculation proved to be very efficient, it was decided to use a fixed time step of 15 minutes for all buildings.

---

<sup>12</sup>The implicit method uses a backward difference to discretize the derivative in (5.35) and not the forward difference of (5.95).

## SOLUTION WITH TIME DEPENDENT PARAMETERS

The implementation caters for the prediction of internal temperatures as well as the convective loads, to maintain a specified interior temperature, and, since the two simulations are completely distinct although based on similar equations, an appropriate method for verifying the accuracy of the computer implementation is:

- first determine the load required to maintain a specified interior temperature for an arbitrary building and climate
- add this load to the convective load just specified
- calculate the interior temperature with this load
- verify that the predicted temperature is equal to the initially specified interior temperature.

This method applies the numerical solution twice in a back to back manner. It can also be used to determine the accuracy of the numerical procedure. It was carried out on a number of different buildings with different climatic data. The difference between the specified temperature and the final temperature is insignificant for massive buildings and below 1 °C for very lightweight structures, so that the numerical implementation is well verified.

### h) Verification Measurements<sup>13</sup>

Although this thesis is aimed at the entrenchment and extension of the method of Mathews and Richards, and not so much with the merit and verification of the method, it was deemed necessary to perform at least one set of measurements in order to verify that the predictions of the model with variable parameters are plausible. For this reason two similar experimental test huts at the Division for Building Technology, Council for Scientific and Industrial Research, Pretoria were used. For details of the buildings see reference [5] of chapter 3. In one of the buildings a mechanical ventilation system was installed which delivered 17 air changes per hour. The interior air-temperatures and outdoor air temperature were recorded with Thies Clima thermographs. In addition the temperature of

---

<sup>13</sup>The experiment was suggested by Prof. E.H. Mathews.  
PAGE 214

SOLUTION WITH TIME DEPENDENT PARAMETERS

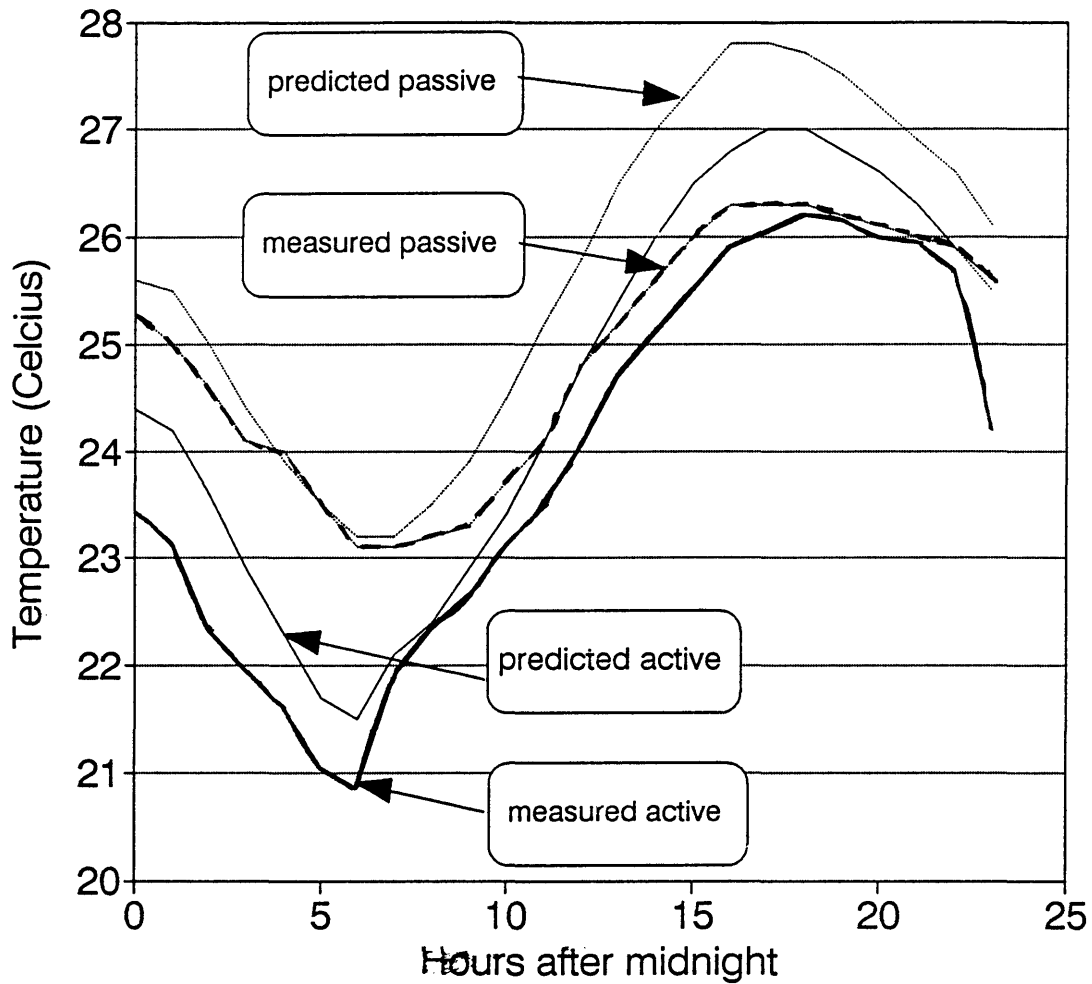


**FIGURE 5.7** Measured and predicted interior air temperatures in two huts. The dotted lines indicate the measured- (thick) and predicted (thin) air temperature in the passive control hut. The solid lines indicate the measured- (thick) and predicted (thin) air temperature in the hut subjected to a forced ventilation of 17 ach from 22h00 – 06h00.

the air delivered to the zone by the ventilation system was recorded with thermocouples. Initially the ventilation system was not switched on and it was verified that the air temperatures in both huts are indeed identical. Afterwards the ventilation system was switched on from 22h00 to 06h00 for a few days. The computer program was also used to predict the interior air temperature. The ventilation rate was estimated at 0.5 air changes per hour in the passive hut and the same value was assumed valid in the

## SOLUTION WITH TIME DEPENDENT PARAMETERS

period 06h00 – 22h00 in the active hut. The measured ventilating air temperature was used in the calculation as well as the measured outdoor air temperature. Results for a typical day are presented in figure 5.7.

Unfortunately, it was not possible to obtain sun radiation data for the period of duration of the measurements so that data of a previous year for the same month and location had to be used. For this reason, the predictions are not as accurate as others which were made at a previous occasion for the same buildings with constant ventilation rates. From the figure it appears that the effect of the night ventilation is somewhat underestimated by the procedure, since the measured drop in temperature between the huts exceeds the predicted value. However, this is probably not significant, given the relative minor effect of the night ventilation. Clearly, these experiments need to be repeated a substantial number of times, with a larger difference between the passive and the active hut (higher ventilation rates and cooler ventilating air<sup>14</sup>), to come to a statistically valid conclusion. However, despite the shortcomings of the experiment it does appear that the influence of the sudden change in the ventilation rate is predicted within reasonable limits.

### 5.5 Conclusion, Chapter 5

Of the many methods in the literature for solving time variant systems two seems practical. They are the Fourier series technique of §5.3.5 which uses the frozen system response as an approximation. Another more efficient method is the numerical method of §5.4. Both these methods were investigated in some detail, implemented in computer programs and evaluated. Of the two methods the numerical procedure seems more fitting because of its efficiency and also because the approximation inherent in using the frozen system response, is difficult to quantify. The numerical method is also more flexible and can be easily adapted to higher order

---

<sup>14</sup>The fan blew air into the room so that the fan load to some extent cancelled the cooling effect of the ventilation. This can be avoided by changing the arrangement so that the fan actually sucks air from the room.

## SOLUTION WITH TIME DEPENDENT PARAMETERS

systems, different discretization methods etc. The Fourier series method has the advantage that it is a straightforward extension of the usual frequency domain methods used for time-invariant systems.

We conclude that it proved possible to find a numerical technique for solving the time invariant system which does not require a long initial period of integration. The method is efficient and sufficiently accurate. The following points and assumptions are of crucial importance for the solution procedure:

- the influence of the changes of the system parameters on the response of the system must be carefully analyzed to determine which types of changes are allowed and what quantities are conserved during the changes,
- the system differential equations must be written in terms of conserved quantities, in this case the stored heat,
- both the forcing functions and the variations must be periodic with the same period.

These assumptions are not overly restrictive and it is possible that the method of §5.4 will find application in diverse fields. It is applicable to any discrete system where periodic solutions are required.

SOLUTION WITH TIME DEPENDENT PARAMETERS

REFERENCES Chapter 5

- [1] E. Boy, S. Meinhardt, TALD – A temperature controlled variable transparent glass, *Building Research and Practice*, The Journal of CIB, Number 4, 1988, pp. 227 – 230.
- [2] E. Boy, Transparente Wärmedämmung im Praxistest, *Bauphysik*, 11(1989), Heft 2, pp. 93 – 99.
- [3] P. H. Joubert, Numerical Simulation of the Thermal Performance of Naturally Ventilated Buildings, M.Eng. Thesis, *Department of Mechanical Engineering, University of Pretoria*, 1987.
- [4] A. Papoulis, The Fourier Integral and its Applications, *McGraw–Hill Book Company, Inc.*, 1962.
- [5] L. O. Chua, P.–M. Lin, Computer–Aided Analysis of Electronic Cicuits, *Prentice–Hall, Inc.*
- [6] E. D. Bedient and P. E. Rainville, Elementary Differential Equations, *The Macmillan Company*, 1969.
- [7] L. A. Zadeh, Frequency Analysis of Variable Networks, *Proc. IRE*, 38 (1950), pp. 291 – 299.
- [8] L. A. Zadeh, Correlation Functions and Power Spectra in Variable Networks, *Porc. IRE*, 38 (1950), pp. 1342 – 1345.
- [9] L. A. Zadeh, C. A. Desoer, Linear System Theory, Chapter 6, *McGraw–Hill Book Company, Inc.*
- [10] L. A. Pipes, L. R. Harvill, Applied Mathematics for Engineers and Physicists, *McGraw–Hill, Inc.*, 1970.
- [11] J. E. Gibson, Nonlinear Automatic Control, *McGraw–Hill Book Company, Inc.*, 1963.
- [12] J. R. Carson, Theory and Calculation of Variable Electrical Systems, *Phys. Rev. 17 Ser 2*, pp. 116 – 134, 1921.
- [13] J. Neufeld, Extension of the Methods of Heaviside's Calculus in Calculating of Circuits containing parameters varying with Time, *Philos. Mag. 15 Ser 17*, pp. 170 – 177, 1933.
- [14] Y. H. Tsao, Time–variant filtering for nonstationary random processes, *J. Acoust. Soc. Am.*, 76 (4), October 1984, pp. 1098 – 1113.

SOLUTION WITH TIME DEPENDENT PARAMETERS

- [15] G. Fodor, Laplace Transforms in Engineering, *Hungarian Academy of Sciences*, 1965.
- [16] A. K. Athienitis, Application of Network Methods to Thermal Analysis of Passive Solar Buildings in the Frequency Domain, PhD Thesis, *University of Waterloo*, Ontario, 1985.
- [17] J. A. Cadzow, H. R. Martens, Discrete-Time and Computer Control Systems, *Prentice-Hall, Inc.*, 1970.
- [18] S. D. Conte, C. de Boor, Elementary Numerical Analysis, *McGraw-Hill Kogakusha, Ltd.*, 1972.
- [19] R. Zmeureanu, P. Fazio, Thermal Performance of a Hollow Core Concrete Floor System for Passive Cooling, *Building and Environment*, Vol. 23, No. 3, pp. 243 – 252, 1988.

SOLUTION WITH TIME DEPENDENT PARAMETERS

SYMBOLS Chapter 5

$A$	Load contribution factor of interior air temperature [kW/K], term of (5.45).
$a$	Interior temperature contribution factor of outside air temperature.
$B$	Load contribution factor of sol-air temperature [kW/K].
$b$	Interior temperature contribution factor of convective source [K/kW].
$C$	Heat storage capacitance of massive structures [kJ/K], load contribution factor of radiative source.
$C_n$	Fouries series expansion coefficient.
$D$	Load contribution factor of outside air [kW/K].
$d$	Interior temperature contribution factor of radiative source [K/kW].
$f$	System forcing function, sometimes with subscripts T for temperature prediction or E for load calculation.
$H$	System transfer function.
$h_o$	System impulse response.
$I_n$	Bessel function.
$j$	Imaginary number.
$K_n$	Bessel function.
$Q_{cr}$	Convective load which will maintain a specified interior temperature [kW].
$Q_c$	Convective load [kW].
$Q_r$	Radiative load [kW].
$Q_s$	Active system load [kW].
$q$	Heat energy stored in the massive structure [kW].
$R_a$	Mean film resistance from interior surface of shell to interior air [K/kW].
$R_o$	Conductive shell resistance [K/kW].
$R_v$	Equivalent ventilation resistance [K/kW].
$s$	Independent variable in Laplace domain [1/h].

SOLUTION WITH TIME DEPENDENT PARAMETERS

$T$	Diurnal period of 24 hours [h], often temperature [ $^{\circ}\text{C}$ ].
$T_c$	Mean structure temperature [ $^{\circ}\text{C}$ ].
$T_{cr}$	Required structure temperature for comfort [ $^{\circ}\text{C}$ ].
$T_{ir}$	Required interior comfort temperature [ $^{\circ}\text{C}$ ].
$T_i$	Zone interior air temperature [ $^{\circ}\text{C}$ ].
$T_{sa}$	Effective sol-air external temperature [ $^{\circ}\text{C}$ ].
$T_o$	Temperature of ventilating air [ $^{\circ}\text{C}$ ].
$T_x, T_y$	Effective forcing temperatures [ $^{\circ}\text{C}$ ].
$T_t$	Thermostat temperature [ $^{\circ}\text{C}$ ].
$\Delta T$	Time interval between sampling points [h].
$t$	Independent variable – time [h].
$t_0$	Initial value of time axis [h].
$u$	Unit step function.
$X$	System input in frequency domain.
$x$	System input.
$Y$	System output in frequency domain.
$y$	System output.
$\alpha$	Proportional feedback constant [W/K], factor in (5.45).
$\beta$	Coefficient of differential equation, equal to inverse of time-constant [1/h]. Subscript T refers to interior temperature, E to energy loads and S to active systems.
$\delta(t)$	Dirac's impulse function.
$\epsilon$	Error term
$\Gamma$	Anti-derivative of $\beta(t)$ .
$\tau$	Thermal time-constant of building [h], elapsed time since stimulation of the system [h].
$\tau_p$	Time-constant of system pole [h].
$\tau_z$	Time-constant of system zero [h].
$\nu$	Frequency [rad/h]
$\omega$	Frequency [rad/h].

## APPENDIX 5A

Evaluation of numerical technique for variable RC against an exact solution for  $\beta$  constant in intervals.

Units:            length    time            mass            temperature  
                   m  $\equiv$  1L    s  $\equiv$  1T            kg  $\equiv$  1M        K  $\equiv$  1Q

$$J \equiv \text{kg} \cdot \text{m}^2 \cdot \text{s}^{-2} \qquad W \equiv \text{J} \cdot \text{s}^{-1}$$

$$\text{kJ} \equiv \text{J} \cdot 10^3 \qquad \text{kW} \equiv \text{W} \cdot 10^3$$

$$\text{h} \equiv 60 \cdot 60 \cdot \text{s} \qquad \text{rad} \equiv 1$$

$$\text{deg} \equiv \frac{\pi}{180} \cdot \text{rad} \qquad \Omega \equiv \text{K} \cdot \text{W}^{-1}$$

$$F \equiv \text{kJ} \cdot \text{K}^{-1} \qquad \text{qh} \equiv \frac{\text{h}}{1}$$

$$f \equiv 1 \cdot 24 \cdot \text{h}^{-1} \qquad \omega \equiv 2 \cdot \pi \cdot f$$

$$T := 24 \cdot \text{h} \qquad T1 := 11 \cdot \text{h}$$

$$\text{Air:} \qquad \rho := 1 \cdot \text{kg} \cdot \text{m}^{-3} \qquad c_p := 1 \cdot \text{kJ} \cdot \text{kg}^{-1} \cdot \text{K}^{-1}$$

$$N := \frac{T}{qh}$$

Variable ventilation. Analytic solution for square wave modulation of  $\beta$ .

Data vir 'STORE.ZNE'.

$$A_o := 1290 \cdot \text{m}^2 \qquad R_a := .000046 \cdot \Omega$$

$$C := 410.61 \cdot A_o \cdot \text{F} \cdot \text{m}^{-2} \qquad R_o := \frac{0.050075}{A_o} \cdot \Omega \cdot \text{m}^2$$

$$\text{ach} := \begin{bmatrix} 30 \\ .1 \end{bmatrix} \cdot \text{h}^{-1} \qquad \text{vol} := 3624 \cdot \text{m}^3$$

$$R_v := \frac{1}{\text{vol} \cdot \rho \cdot \text{ach} \cdot c_p} \qquad R_v = \begin{bmatrix} 0.000033 \\ 0.009934 \end{bmatrix} \cdot \Omega$$

$$\beta := \frac{R_o + R_a + R_v}{R_o \cdot (R_a + R_v) \cdot C} \qquad \beta = \begin{bmatrix} 0.261 \\ 0.176 \end{bmatrix} \cdot \text{h}^{-1}$$

Time constants:

$$\tau := \overline{\begin{bmatrix} -1 \\ \beta \end{bmatrix}} \quad \tau = \begin{bmatrix} 3.832 \\ 5.689 \end{bmatrix} \cdot h$$

$t := 0 \dots N - 1$

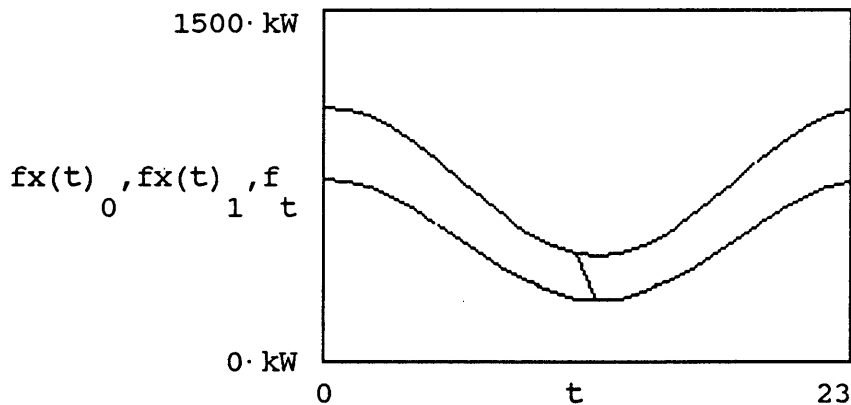
Forcing functions:

$$T_{sa}(t) := (20 + 10 \cdot \cos(\omega \cdot t \cdot qh)) \cdot K$$

$$T_o(t) := (20 + 5 \cdot \cos(\omega \cdot t \cdot qh)) \cdot K$$

$$f_x(t) := \overline{\left[ \frac{T_o(t)}{R_a + R_v} + \frac{T_{sa}(t)}{R_o} \right]}$$

$$f_t := \text{if} \left[ t \cdot qh \leq T1, f_x(t)_0, f_x(t)_1 \right]$$



Solve first order differential equation.

(I) Analytic solution.

$$X := \overline{\left[ \frac{R_o + R_a + R_v}{R_o \cdot (R_a + R_v)} \right]} \quad X = \begin{bmatrix} 768.351 \\ 517.551 \end{bmatrix} \cdot \text{kW}$$

$$m := \overline{\left[ \frac{R_o \cdot 0.25 + (R_a + R_v) \cdot 0.5}{R_o + R_a + R_v} \right]} \quad m = \begin{bmatrix} 0.418 \\ 0.499 \end{bmatrix}$$

$$T_i := \left[ \begin{array}{c} T1 \\ T - T1 \end{array} \right] \quad t_0 := \left[ \begin{array}{c} 0 \cdot h \\ T1 \end{array} \right]$$

$$\phi := \left[ \begin{array}{c} \overline{\left[ \begin{array}{c} \omega \\ - \\ \beta \end{array} \right]} \\ \text{atan} \left[ \begin{array}{c} \omega \\ - \\ \beta \end{array} \right] \end{array} \right] \quad \phi = \begin{bmatrix} 45.094 \\ 56.123 \end{bmatrix} \cdot \text{deg}$$

$$\alpha(t) := \overline{(\cos(\omega \cdot (t + t_0) - \phi) - \cos(\omega \cdot t_0 - \phi) \cdot \exp(-\beta \cdot t))}$$

$$A(t) := \overline{\left[ \begin{array}{c} X \\ - \\ \beta \end{array} \left[ \begin{array}{c} 1 + \frac{m \cdot \beta}{\sqrt{\beta^2 + \omega^2}} \cdot \alpha(t) - e^{-\beta \cdot t} \end{array} \right] \right]}$$

$$\alpha(T1) = \begin{bmatrix} -0.539 \\ 0.114 \end{bmatrix}$$

$$A0 := A(T1)_0 \quad A0 = 2.31 \cdot 10^3 \cdot \text{kW} \cdot \text{h}$$

$$A1 := A(T - T1)_1 \quad A1 = 3.128 \cdot 10^3 \cdot \text{kW} \cdot \text{h}$$

$$y00 := \frac{A0 \cdot \exp\left[-\beta_1 \cdot (T - T1)\right] + A1}{1 - \exp\left[-\beta_0 \cdot T1 - \beta_1 \cdot (T - T1)\right]}$$

$$y00 = 3.383 \cdot 10^3 \cdot \text{kW} \cdot \text{h}$$

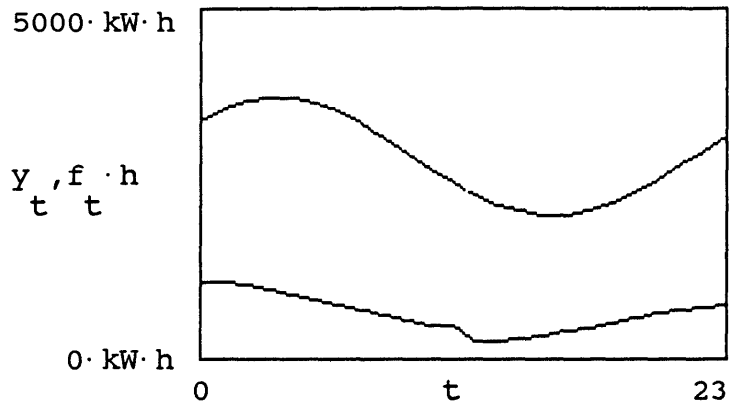
$$y0(t) := y00 \cdot \exp\left[-\beta_0 \cdot t\right] + A(t)_0$$

$$y10 := y0(T1) \quad y10 = 2.502 \cdot 10^3 \cdot \text{kW} \cdot \text{h}$$

$$y1(t) := y10 \cdot \exp\left[-\beta_1 \cdot (t - T1)\right] + A(t - T1)_1$$

$$y1(T) = 3.383 \cdot 10^3 \cdot \text{kW} \cdot \text{h}$$

$$y_t := \text{if}(t \cdot \text{qh} \leq T1, y0(t \cdot \text{qh}), y1(t \cdot \text{qh}))$$

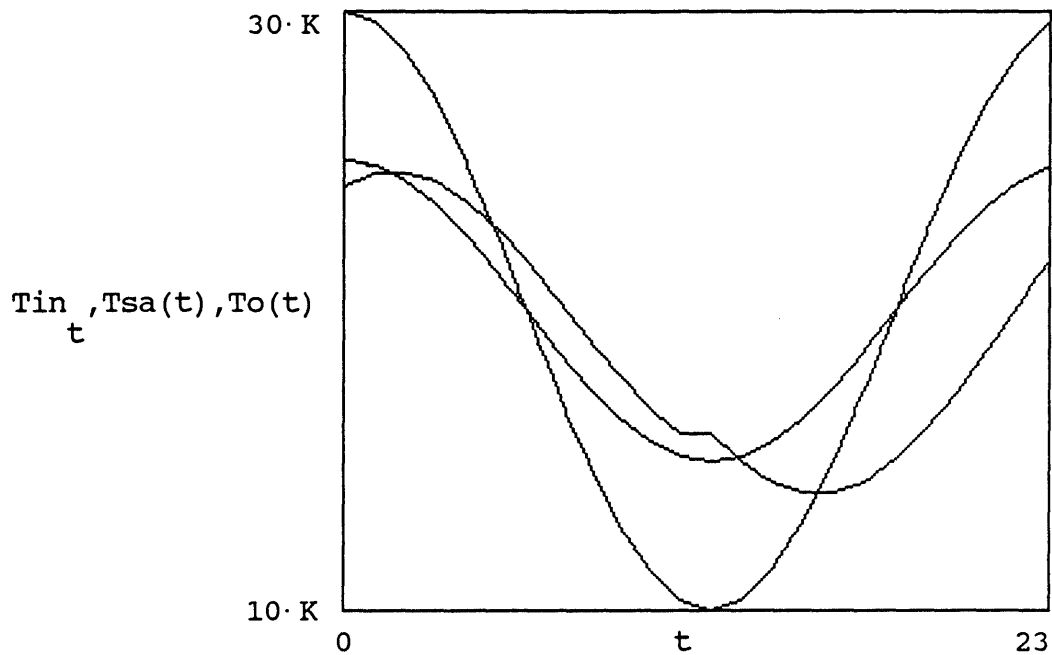


Interior temperature:

$$T_{in}(t) := \left[ \begin{array}{c} y_t \\ \frac{y_t}{C} \cdot R_v + T_o(t) \cdot R_a \end{array} \right] \cdot \frac{C}{R_v + R_a}$$

$$T_{ii}(t) := \text{if} \left[ t \cdot q_h \leq T_1, T_{in}(t)_0, T_{in}(t)_1 \right]$$

$$T_{in_t} := T_{ii}(t)$$



(II) Numerical Approximation

$$k := 1 \dots N - 1$$

$$\text{Beta}_t := \text{if}[t \cdot qh \leq T1, \beta_0, \beta_1]$$

$$\text{prod}_0 := [1 - \text{Beta}_{N-1} \cdot 1 \cdot qh]$$

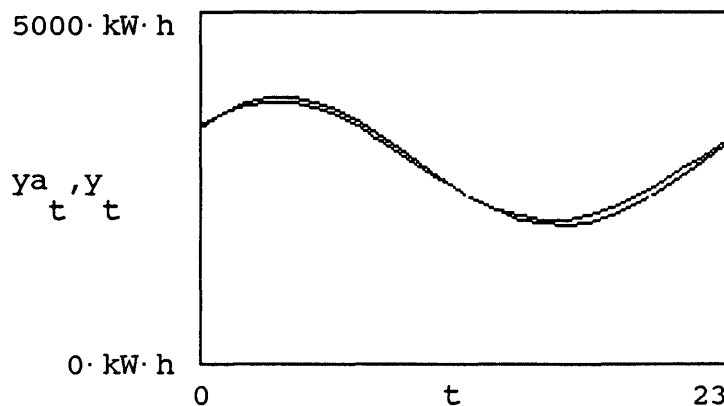
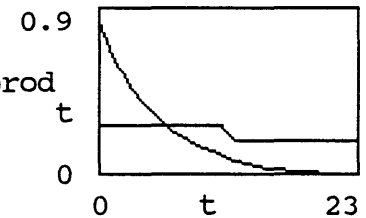
$$\text{prod}_k := \text{prod}_{k-1} \cdot [1 - \text{Beta}_{N-k-1} \cdot 1 \cdot qh]$$

$$l := 0 \dots N - 2$$

$$y_{a0} := \frac{\left[ \sum_1 f_1 \cdot qh \cdot \text{prod}_{N-1-2} \right] + f_{N-1} \cdot qh}{1 - \text{prod}_{N-1}}$$

$$y_{a0} = 3.345 \cdot 10^3 \cdot \text{kW} \cdot \text{h} \quad y_0 = 3.383 \cdot 10^3 \cdot \text{kW} \cdot \text{h}$$

$$y_{ak} := f_{k-1} \cdot qh + [1 - \text{Beta}_{k-1} \cdot qh] \cdot y_{a_{k-1}}$$

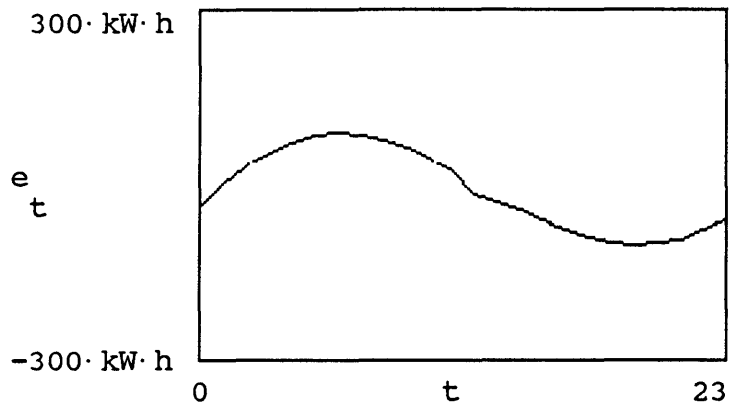


% error:

$$\frac{y_{a0} - y_0}{y_0} \cdot 100 = -1.117$$

Stored Energy Error:

$$e := (y_a - y)$$

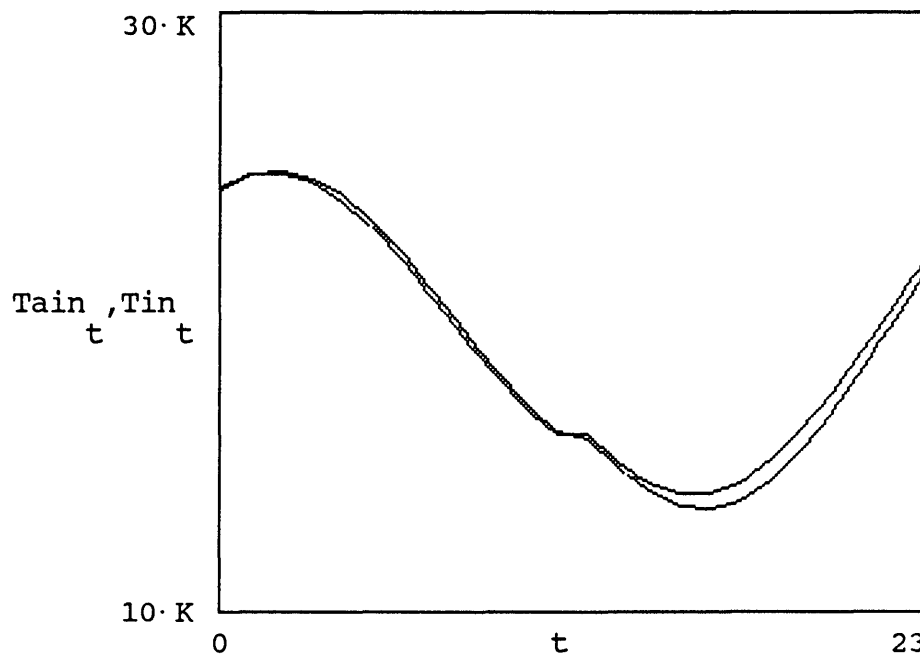


Temperatures:

$$T_{ain}(t) := \frac{\left[ \frac{y_a}{c} \cdot R_v + T_o(t) \cdot R_a \right]}{R_v + R_a}$$

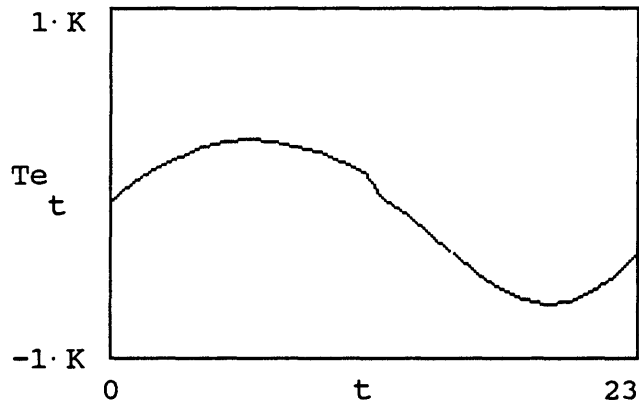
$$T_{ai}(t) := \text{if} \left[ t \cdot q_h \leq T_1, T_{ain}(t)_0, T_{ain}(t)_1 \right]$$

$$T_{ain}_t := T_{ai}(t)$$



$$Te := \overbrace{(T_{ain} - T_{in})}$$

Temperature error



## CHAPTER 6

---

### 6 CLOSURE

In §1.3 the objectives of this study were spelled out. In this final chapter, we examine these objectives again in the light of the results and conclusions of chapters 2 to 5. It is our aim to determine the extend to which we have succeeded in meeting these objectives, and to distill from the conclusions, given at the end of each chapter, some final remarks and suggestions.

#### 6.1 The Theoretical Underpinnings of the Method of Mathews and Richards

We set out in chapter 2 to examine the method of Mathews and Richards from a theoretical point of view, and to determine the extend to which it is possible to derive their novel thermo-flow network, rigorously from a comprehensive model. It must be stressed that this objective was identified consequential to the successful verification programme of the method of Mathews and Richards, in order to elucidate certain aspects of the method, and not in an attempt to be critical. In fact the success of the method, as testified by measurements, coupled with the simplicity and clear physical interpretation, precludes criticism. However, a rigorous derivation of the simplified model from a comprehensive model, shows that it can still be improved in the following aspects:

- a) The definition of the mean sol-air temperature can be improved by including the time constants of the individual structures in the definition. This will to some extent correct the phase shift discrepancy observed in some measurements [4], and relieve the method of the *ad hoc* empirical phase correction.
- b) A more satisfactory lumped model would be obtained by representing the massive elements with an RCR section, as in figure 2.14, instead of an RC section. The advantage of this representation is that a clearer physical interpretation is possible since the interior surface

## CLOSURE

temperatures are uniquely identified and the capacitance is more remote from the interior surface node.

- c) The treatment of interior elements described in [5] are expedient, but may lead to errors in passive zones with massive internal elements. If the internal elements are kept separate from the shell elements, a second order network with two time constants results. This second order network is closer to reality than the single time constant network and may improve the accuracy of the model in the case of zones with massive internal elements.
- d) An analysis of temperature differences between interior surfaces indicates that, in general, heat exchange between interior surfaces can not be ignored and must be included in a model which, in addition to the bulk temperature of the interior air, attempts also to predict the mean interior surface temperature. Since comfort criteria include contributions from both the air- and surface temperatures, the utility of the method will be enhanced by a more refined model of interior heat exchange. This need not complicate the method excessively since various simplifying assumptions are available. One could, for instance, empirically discriminate between northern and southern parts of the shell, and internal walls. These enhancements would obviously require extensive experimentation and verification.

The implementation, solution and ease of use of the method will not be compromised by these enhancement to any significant extend. Note however, one can not realistically expect a large improvement in the accuracy of the method with the incorporation of these enhancements, since the accuracy is already high. However, in the author's opinion these improvements are justifiable on the grounds that the main advantage of these very simplified methods is their clear physical interpretation, and it is precisely the physical interpretation which will most benefit from the improvements.

## CLOSURE

### 6.2 Structural Storage

In chapter 3 we successfully extended the model of Mathews and Richards to cater for buildings with structures which are directly subjected to cooling, by air being forced over their surfaces. To incorporate this addition, it was required to define the convective heat transfer coefficient in terms of the bulk temperature of the wall, since the model of Mathews and Richards does not clearly identify the surface temperatures; which are usually used in the definition. This difficulty will disappear if suggestion b) above is implemented.

### 6.3 Multi-Zone Thermo-Flow

We have shown in chapter 4 that a natural extension of the method to coupled zones is potable. This extended model can be fairly efficiently solved if the parameters are time invariant. However, in the time variant case iterative techniques are required. It was found that the implementation of suggestion c) above will be beneficial for such a multi-zone model.

The implementation of the multi-zone model will increase the accuracy of the temperature predictions in passive buildings with large temperature differences between adjacent zones. It will make possible accurate predictions in buildings which include sun-spaces, solar heated ceiling spaces etc. However, it will be of little benefit to designers of conditioned buildings. Since it will seriously compromise the speed of the solution and also the ease of use of the program, it seems advisable to include it as an appendage to the program, in preference to integrating it completely with the other facilities. In this case, if this extra capability is not required, it can be ignored and will not compromise the rest of the program.

### 6.4 Numerical Solution of a System with Time Dependent Parameters

In chapter 5 we present a new efficient solution of the thermo-flow network of Mathews and Richards. This solution is based on the assumption that both the time dependent parameters of the circuit, as well

## CLOSURE

as the forcing functions, are cyclic with the same period. It proved possible to find a closed form expression for the initial value of the discrete solution, so that the initial value can be found after effectively integrating through just one cycle. This method is very efficient compared to the usual numerical technique, which starts with arbitrary initial conditions, and then integrates until at least 5 time-constants have elapsed, to get rid of transients.

The method is very general and can be applied to any discrete system of cyclic equations to find cyclic solutions. It does not depend on the method, or order, of discretization of the underlying continuous system. The only requirement is a fixed time-step size. It therefore appears to have applications also in celestial mechanics, cyclic combustion etc.

In addition it was shown that a mixed time-frequency domain method can be used which is a logical extension of the Fourier series method to systems with time dependent parameters. It was shown that the method can be used to obtain sufficiently accurate approximate solutions, if the mean part of the solution is treated separately. However, this method requires the solution of an evolution equation for the system and it has no computational benefit compared to the efficient numerical solution of the previous paragraphs.

### 6.5 Suggestions for the Future

This thesis must be seen as part of an ongoing effort, by the Centre for Experimental and Numerical Thermo-flow, to develop and promote a viable tool for building thermal analysis. The results of this study suggests that: (in order of priority)

- a) Methodology of Thermal Modelling. It proved possible to deduce simplified thermal networks from more detailed networks by suitable simplifying assumptions. These assumptions are to a large extent arbitrary and depend on the degree of simplification required. Future simplified models can be constructed logically, by reduction of

## CLOSURE

comprehensive models to the required degree of simplicity. The accuracy of the simplified model can be theoretically deduced from the degree to which actual buildings comply with the simplifying assumptions. However, it must be remembered that the attainable accuracy of a thermal model is often not determined by the assumptions, but rather by the accuracy of the input data. Therefore, even though buildings may violate some of the assumptions of the model, it does not necessarily follow that the model is useless.

- b) Mean Sol–Air. In their definition of the mean sol–air forcing function, Mathews and Richards ignores the heat storage capability of the walls. This contributes to the phase discrepancy they experience. A better definition of the mean sol–air is given in §2.5.4, in terms of the fundamental diurnal frequency of the temperature variation.
- c) Structural Storage. Structural storage systems are easily included in the thermal analysis method. However, a somewhat unusual definition of the heat transfer coefficient is required.
- d) Second Order Network. The second order thermal network of figure 2.22 has some distinct advantages compared to the model of figure 2.1. It provides surface temperatures which are required for comfort criteria, is easier to interpret physically and treats the interior massive elements more correctly. It is also more suitable for extension to multi–zone thermal analysis as well as structural storage since surface temperatures are clearly defined. In the author's opinion it warrants implementation and testing.
- e) Numerical Solution. The numerical solution presented in chapter 5 seems very general and may have applications in diverse fields. Its extension to higher order systems and application to other discretization methods should be investigated. However, it does not seem possible to extend the method to non–linear systems, such as deadband controllers etc., a fact which requires further investigation.
- f) Multi–Zone Thermal Analysis. The multi–zone method can be implemented but it is limited to time invariant systems. For the

## CLOSURE

analysis of some dependent systems, full numerical methods should also be investigated.

### 6.6 The Utility of Highly Simplified Models

In conclusion it is perhaps necessary to repeat our justification for the emphasis we placed, in this study, on highly simplified lumped thermo-flow networks, when, with modern computers, it is feasible to solve the comprehensive models.

It is our objective to create a modern building designer's tool. The comprehensive models may be marginally more accurate than the simplified models, but, they are not suitable for a total systems design approach where the interaction between the passive response of the building, and the system, is of primary importance. Eventually, a design tool must provide more than just a simulation for a given set of conditions, it must aid the designer in his grasp of the problem. The simple network, whether derived from theoretical considerations and simplifying assumptions, or empirical correlations, can have a much clearer physical interpretation since many unessential details are discarded. It is easier to comprehend, to solve, and to extend. In conditioned buildings, the trend is to emphasize the passive response of the building and the system controller. The control engineer needs a simple, sufficiently accurate model of the passive response, to optimize his design.

The success of the original empirical model of Wentzel, Page-Shipp and Venter [1], as well as the later enhancements by Mathews [2], Joubert and Mathews [3], Mathews and Richards [4] and Mathews, Rousseau, Richards and Lombard [5], testifies to the utility of these simplified models. In this study, a firm theoretical foundation is given to these models and their utility is enhanced.

## CLOSURE

### REFERENCES Chapter 6

- [1] J. D. Wentzel, R. J. Page-Shipp, J. A. Venter, The prediction of the thermal performance of buildings by the CR-method, *NBRI research report BRR 396, CSIR, Pretoria* (1981).
- [2] E. H. Mathews, Thermal Analysis of Naturally Ventilated Buildings, *Building and Environment*, Vol. 21, No. 1, pp. 35 – 39, 1986.
- [3] P. H. Joubert, E. H. Mathews, QuickTEMP-A Thermal Analysis Program for Designers of Naturally Ventilated Buildings, *Building and Environment*, Vol. 24, No. 2, pp. 155 – 162, 1989.
- [4] E. H. Mathews, P. G. Richards, A Tool for Predicting Hourly Air Temperatures and Sensible Energy Loads in Buildings at Sketch Design Stage, *Energy and Buildings*, 14(1989) 61 – 80.
- [5] E. H. Mathews, P. G. Rousseau, P. G. Richards, C. Lombard, A Procedure to Estimate the Effective Heat Storage Capability of a Building, *Building and Environment*, accepted for publication 1990.

# APPENDICES

## SYNOPSIS

### SYNOPSIS

#### FURTHER REFINEMENTS AND A NEW EFFICIENT SOLUTION OF A NOVEL MODEL FOR PREDICTING INDOOR CLIMATE

C. Lombard

For the Degree:  
Master of Engineering

Study Leader:  
Prof. E.H. Mathews

In the Faculty of Engineering of the  
UNIVERSITY OF PRETORIA

December 1990

In the nineties and beyond energy conservation will play a dominant role in the design of new buildings. In the past two decades, many energy efficient buildings failed to provide adequate comfort. The main problem seems to have been the lack of a total approach to the design of buildings. Such an approach regards building and air-conditioning unit as a total thermal system, which together, in close co-operation, must ensure acceptable indoor climate. To facilitate a total design approach, a thermal analysis tool is required which is targeted at both the architect, designing the building shell, and the engineer, which installs the air-conditioning system. For such a tool to be successful, it must be simple, easy to use and powerful. This thesis contributes to the enhancement and establishment of such a design tool. In particular, the novel method originally proposed by Mathews and Richards, is enhanced and extended.

As point of departure, the derivation of simplified models from more,  
PAGE A.1

## SYNOPSIS

comprehensive models is discussed. Simplified thermo-flow models for buildings are usually based on apt reasoning about the main thermal storage- and transport- characteristics of buildings. Mathews and Richards base their model on the concept of *active thermal capacitance*, which is an attempt to model the salient features of energy storage in the massive parts of the building. The analysis here indicates that it is possible to derive the simplified model in a logical manner from a more comprehensive model, by suitable assumptions and simplifications. In this manner, the concept of active capacitance is clarified, and the assumptions of Mathews and Richards is illuminated. The theoretical foundation of the concept of active capacitance can be established. The outcome of this study proved fruitful in that a new enhanced simple network, with a better physical interpretation and theoretically more satisfactory treatment of the building shell, as well as internal mass, is suggested. In addition, it is found that the definition of the mean sol-air forcing function, as used by Mathews and Richards, probably causes the phase discrepancy they observe. The study further indicates that the high degree of lumping of the simplified model is acceptable. Theoretically, the accuracy of the model is limited by the assumption that the massive parts of the building are at the same temperature.

The utility of the simplified model is extended by the inclusion of capabilities for structural storage systems, variable parameter thermoflow and proportionally controlled active systems. A further enhancement is the development of a procedure for extending the method to multi-zone thermal analysis. Structural storage can be easily included in the thermal model, but necessitates a somewhat unusual definition of the heat transfer coefficient, since the model of Mathews and Richards does not provide for the prediction of surface temperatures. Inter-zone heat-flow is accomplished in a manner which forms a natural extension of the single-zone method. The proposed method first applies the single zone model to each zone individually and, thereafter, determines the heat-flow between the zones. The procedure requires a single matrix inversion, with the order of the matrix given by the number of zones. Unfortunately, the

## SYNOPSIS

procedure can only be implemented for time invariant systems.

This thesis investigated solutions for a time dependent system in order to make provision for time variable ventilation rates, and variable shell conductance etc. A very simple and highly efficient numerical solution procedure is presented. An explicit solution for the initial value is given so that the usual initial period of integration – to get rid of transients – is not required. An alternative, less efficient Fourier series method is also given. The solution method is quite general and can be extended to higher order systems and implicit discrete systems.

With this thesis, a firm foundation has been laid for the extension of simplified methods, which have been very successfully applied to passive thermal design, to active thermal systems. The novelty of these methods lies in their simplicity, which enables analysis and comprehension of their behaviour. A simple model is a prime requirement for the investigation of the behaviour of systems which incorporate complicated non-linear control. The investigation of these systems is required for the successful design and optimization of comfortable and energy efficient buildings in future.

UITTREKSEL

UITTREKSEL

VERDERE VERFYNINGS VAN 'n METODE VIR DIE  
VOORSPELLING VAN BINNENSHUISE KLIMAAT, INSLUITEND  
'n NUWE EFFEKTIEWE OPLOSSING.

C. Lombard

Vir die graad:  
Magister in Ingenieurswesw

Studie Leier:  
Prof. E.H. Mathews

In die Fakulteit van Ingenieurwese  
UNIVERSITEIT VAN PRETORIA

Desember 1990

In die negentigs, en daarna, sal energie besparing 'n baie belangrike invloed uitoefen op die ontwerp van nuwe geboue. In die vorige twee dekades het heelwat nuwe 'energie effektiewe geboue' gefaal, in die sin dat die binneklimaat nie altyd aanvaarbaar was nie. Die probleem is waarskynlik toe te skryf aan 'n gebrekkige ontwerpsmetodiek, wat die passiewe gebou en aktiewe lugversorgingstelsel apart hanteer. Om 'n geïntegreerde ontwerpsprosedure te bevorder, word 'n rekenaarprogram benodig, wat beide die argitek en die ingenieur kan gebruik, en wat die gebou as 'n termiese stelsel in geheel hanteer. Hierdie tesis is 'n bydrae tot die vestiging en bevordering van so 'n program. In besonder word die unieke, vereenvoudigde metode van Mathews en Richards verder verbeter en uitgebrei.

As vertrekpunt dien die afleiding van vereenvoudigde modelle uit meer omvattende modelle van termiese gedrag. Gewoonlik word vereenvoudigde

## UITTREKSEL

modelle gebaseer op redenasies oor die hoofbeginsels van die berg- en vloei van warmte in 'n gebou. Mathews en Richards baseer hulle model op die konsep van *aktiewe termiese kapasiteit*, wat die heveelheid warmte, geberg in die gebou, en wat 'n rol speel by die bepaling van die binne-temperatuur, weergee. Die studie toon aan dat dit moontlik is om die eenvoudige model te herlei uit 'n omvattende model, d.m.v. logiese beredenering en vereenvoudigende aannames. Op hierdie manier kan die idee van aktiewe kapasitansie, asook die aannames van Mathews en Richards, onder die soeklig geplaas word en 'n teoretiese fondament kan onder die beginsel van aktiewe kapasitansie geplaas word. Hierdie studie het verder daartoe gelei dat 'n teoreties meer gebalanseerde vereenvoudigde model voorgestel kon word, met bepaalde voordele. Hierbenewens word daar gevind dat die definisie van die gemiddelde sol-lug temperatuur, soos gebruik deur Mathews en Richards, waarskynlik verantwoordelik is vir die empiriese korreksie faktor – betreffende die faseverskuiwing van die binne temperatuur – wat hul model benodig. 'n Verdere resultaat van belang is; dat die hoë mate van vereenvoudiging, vanaf 'n akkurate verspreide elementmodel – na 'n lompmoedel, nie die beperkende faktor van die eenvoudige model is nie, maar eerder die aanname dat die massiewe strukture almal altyd dieselfde by temperatuur bly.

Die nuttigheid van die vereenvoudigde model word in hierdie studie verhoog deur die metode uit te brei om voorsiening te maak vir warmte berging in die struktuur, tydafhanklike elemente en proporsioneel beherde stelsels. Nog 'n toevoeging is die ontwikkeling van 'n metode vir die berekening van die termiese gedrag van meervoudige-gebousones. Struktuur berging is redelik maklik om te inkorporeer in die model, maar dit vereis 'n iewat ongewone definisie van die warmte oordrag koëffisiënt, aangesien die model van Mathews en Richards nie oppervlak temperature modelleer nie. Die tegniek vir die hantering van warmte vloei tussen verskillende sones is so ontwerp dat dit 'n natuurlike uitbreiding van die enkelsone-model vorm. Die voorgestelde metode gebruik eers die enkelsonebenadering vir elke sone afsonderlik, waarna die warmtevloed tussen die sones en die finale temperature bereken word. Dit geskied d.m.v. die omkering van 'n

## UITTREKSEL

matriks waarvan die orde bepaal word deur die aantal sones teenwoordig. Ongelukkig kan die metode nie so maklik geïmplementeer word indien die elemente tydafhanklik is nie.

In hierdie tesis word 'n nuwe oplostegniek voorgestel wat voorsiening maak vir tydafhanklike elemente, sodat die model ook gebruik kan word by die termiese ontleding van geboue met variërende ventilasie, dopweerstand ens. 'n Hoogs eenvoudige en uiters effektiewe oplostegniek is ontwikkel met 'n eksplisiete vergelyking vir die beginwaarde. Dit is dus nie meer nodig om 'n lang aanvanklike integrasieperiode te gebruik om van oorgangsverskynsels ontslae te raak nie. Die oplostegniek is algemeen bruikbaar. Dit kan uitgebrei word na hoër orde stelsel asook implisiet versyferde stelsels. 'n Alternatiewe, minder effektiewe metode, gebaseer op Fourier reekse, word ook aangebied.

Met hierdie tesis word 'n stewige fondament gelê vir die toepassing van die vereenvoudigde tegnieke ook op aktiewe stelsels. Die bruikbaarheid van die vereenvoudigde tegnieke is gesetel in die gemak waarmee hulle gemanipuleer kan word en hulle verstaanbaarheid. 'n Eenvoudige model is 'n voorvereiste vir verdere studies oor die gedrag van termiese geboue met nie-liniêre beheerstelsels. Die bestudering van hierdie stelsels is broodnodig vir die ontwerp en optimisering van suksesvolle, energie-effektiewe geboue in die toekoms.

# Efficient, Steady State Solution of a Time Variable RC Network, for Building Thermal Analysis.

Lombard, C and Mathews, E H

Centre for Experimental and Numerical Thermoflow, Department of Mechanical Engineering, University of Pretoria, Republic of South Africa.

## Abstract

*This paper introduces an efficient method for obtaining the steady state, periodic thermal response of a building with arbitrary, time dependant ventilation. The method is applicable to a single time-constant thermal model but can be extended to higher order models. A simple, elementary numerical method for integrating the governing differential equation is proposed which does not need Fourier analysis, convolution or even evaluating an exponential, as required by most other methods. The initial value is also obtained explicitly. Hence, the usual initial period of integration – to get rid of transients – is not required. By direct comparison of the numerical method with an exact analytical solution in a special case, it is proved that the method is sufficiently accurate, provided the sampling interval is not too large, compared to the thermal time-constant of the building. The method is further demonstrated by calculating the interior temperature of a building subjected to forced night cooling.*

## 1 Introduction

The analogy between thermo-flow and electron-flow is often exploited to derive simple models for building thermal analysis [2-4]. In these models it is usual to lump [13] the distributed thermal conductance and capacitance so that instead of the partial differential equation for heat conduction, one is faced with an ordinary differential equation, the order of which is determined by the number of lumped resistances and capacitances (nodes) used to describe the distributed parameters. Other heat transfer phenomena, such as radiative exchange and convection, can be integrated in the electrical analogy by defining the appropriate thermal resistances. In the case of natural ventilation, the ventilation resistances is time dependant since ventilation rates vary appreciably with the hour of the day. To model radiative exchange requires a thermal resistance which is strongly dependant on the temperature, hence strongly non-linear [14]. However, in most methods it is assumed that the parameters (resistances and capacities) are time invariant, to enable the application of Fourier or Laplace techniques to obtain the solution. This limits the solution to cases where the ventilation rate is constant; a serious practical limitation.

In this paper we describe an elementary numerical method for solving the variable coefficient differential equation of the model of Mathews and Richards [1], without sacrificing functional accuracy or computation speed. Furthermore, the method is in

no way restrictive regarding the magnitude or details of the variation of the parameters with time. The solution obtained is also stable and free of transients, even with discontinuous variations of the parameters. The method is generally applicable to the simple RC networks which many investigators use to model heat flow in buildings and other structures [2..4]. It can be extended to more complicated higher order networks by treating the higher order equations as a system of first order equations.

In the next section of this paper, §2, some relevant remarks on computer methods for thermal analysis are presented, In §3, the general governing equation for the network of [1] with time dependent parameters is given. In §4 a few available solutions and standard numerical techniques for solving variable RC networks are discussed. An efficient, approximate method is presented in §5 and the accuracy of this method is discussed in §6. The method can easily be extended to include linear feedback, active indoor climate control systems. In §7, the extension to include an active system, with indoor temperature controlled by a proportionally controlled thermostat is given. Finally, §8 concludes with an example of the application of the method to night cooling of buildings.

## **2 Computer Methods for Building Thermal Analysis**

A large number of computer programs for building thermal

analysis are available. According to Tuddenham [15] there are more than one hundred in the United Kingdom and many hundreds more elsewhere. Most of these methods are based on the 'admittance method' of the CIBS [17] or the 'response factor method' of ASHRAE [17]. The CIBS method was originally developed for manual calculations [18]. It employs pre-calculated tables of decrement- and other factors for building materials. The response factor method was originally developed for computer implementation [19]. It does seem, however, that the method was severely influenced by the very crude computer hardware and software available at the time and the central theme of the method appears to be an attempt to ease the evaluation of the convolution integral, as required to obtain the forced response [14]. In view of the undreamt of growth in computer technology and numerical techniques, both these methods appear outdated. The Fast Fourier Transform has made the evaluation of convolution integrals a very simple and computationally efficient exercise.

Both the CIBS and the ASHRAE method (and others e.g. [21,23]) employ the exact analytical solution of the diffusion equation in the form of matrices. These matrices are then used to obtain the response\decrement factors from which the thermal response is obtained. In the admittance procedure the factors are used to obtain amplitude and phase-shift values for the internal temperature. The response factor method obtains the solution by

superimposing the response to a series of triangular pulses. Both methods only apply to linear time-invariant thermal systems. (In [20] invariability is erroneously stated as a requirement for using the method of superposition. Linearity is sufficient. Invariability is only required for the Laplace transform method to be tractable. See [6].)

Since the exact matrix solution for heat conduction is simple and amendable to computer implementation, and standard two port theory can be used to combine the matrices of various elements, it is inexplicable that computer programs still employ response factors. Certainly, the matrices are limited to time invariant systems, but so are the response factors since they are derived from the matrices. For the time invariant case it seems that an elegant method would compute the matrices for the various elements at a number of frequencies, combine the matrices with two port theory, and compute the exact solution via the superpositioning of the responses to the various frequencies [7]. Computationally this is certainly feasible on modern computers. The method can be used to obtain both transient and steady state solutions by employing either the Laplace or the Fourier domain.

In [19] some emphasis is placed on the response factor method being applicable to non-steady state conditions. To simulate non-steady conditions one would have to specify initial conditions, which can only be guessed or become known by measure-

ments. Therefore, simulation of non-steady conditions seems rather academic. In practice one is confronted with continuous variables which can be described as quasi-periodic. One should therefore rather attempt to find the quasi-periodic solutions which are often sufficiently accurately represented by periodic solutions [27]. Especially if the principle of a design day is adhered to.

In view of the availability of this practical, exact solution for the heat conduction equation with steady excitation, it is also disconcerting to find many programs employing finite difference or finite element techniques. It is often stated that these numerical methods facilitate solution of a time variable, fully non-linear model. In fact the powerful but often tedious and sometimes unpredictable numerical techniques are essentially employed to solve the time invariant, linear, heat conduction equation. The time variability and non-linearities in thermal models of buildings do not arise from heat conduction but from other heat transfer modes. Certainly, one could use the matrix solution for the conduction equation and combine it with time variable non-linear two ports. The complete solution is then obtained from non-linear network methods which were extensively developed in recent years [7].

But the important point we wish to make is that thermal analysis methods can either attempt to be extremely accurate,

with emphasis on exact simulation – and be of academic value only, or sufficiently accurate with a design philosophy (e.g. design day) in mind – and practical.

To create a viable design tool the following points should be borne in mind:

- a) A complete description of the thermo-flow in real buildings requires many details, some of which (e.g. ventilation rates) are wholly unknown or only partly known. This is even more true if the objective is a design tool, since the thermal properties of a building are largely determined in the very early design stages when no details at all are available.
- b) Many studies and empirical models indicate that a few essential parameters of the buildings such as heat storage capacity and shell admittance are crucial and should be emphasized rather than details. It is crucial that the assumptions be clear, easy to explain and to understand.
- c) A successful computer design tool must employ a very simple model with a straightforward physical explanation to allow the designer's good judgment and experience to play its essential part. Highly refined models and exact solutions are better employed in research laboratories for verification purposes and the extension of knowledge and understanding.

- d) For a design tool, extreme numerical accuracy – at the cost of computing time – is detrimental. Certain essential parameters of thermo-flow in buildings, such as ventilation rates, are largely unknown. The emphasis should be on establishing the relative merit of various designs, rather than absolute accuracy.
- e) A design tool should allow innovation and easy extension to cater for creative ideas and new techniques.
- f) A computer procedure should not be based on 'established' techniques which were developed for hand calculations and which are overly simplified or unnecessarily rigid.
- g) A design tool should follow a total approach. Both the passive response of the building and the HVAC system must receive due attention. Many available programs place too much stress on load prediction and the energy audit. This may lead to unnecessary efforts to optimize the HVAC system while much more could be gained by improving the shell.

It was shown by Mathews and Richards [1] that a simple, single time-constant RC network, as given in Figure 1, can be a very useful aid for determining the thermal performance of a building. This extraordinary simple approach has a number of important advantages; the thermal response analysis can be implemented on inexpensive, generally available computers (PC's), and still

provides fairly accurate answers, quite rapidly. In addition, the simple thermal network has a very clear physical interpretation, which is easily explained to designers. The simplicity also enables easy extension to include new ideas and building materials. This facilitates a design process where various options can quickly be evaluated. The data input requirements are modest and no expert knowledge of thermal analysis is required. Furthermore, an extremely user friendly interface can relieve the burden of the specification of construction details. The result is a streamlined and highly efficient program. Complete temperature and load simulations are obtained in a few seconds.

The main limitations of the method are the single zone approach, the assumption of isothermal interior surface temperature and the assumption of well mixed interior air. These assumptions are difficult to establish on theoretical considerations but are vindicated by the excellent results obtained from verification experiments in many buildings [1].

The details of the method appear in [1]. Briefly, in figure 1 the resistances are  $R_o$ : conductive shell resistance including exterior film coefficients,  $R_a$ : film resistance of the interior surfaces and  $R_v$ : ventilation resistance. The ventilation resistance is obtained from:  $R_v = 3.6/Vol \cdot \rho \cdot ach \cdot C_p$  where  $Vol$  [ $m^3$ ] is the interior volume,  $\rho$  [ $kg/m^3$ ] is the density of air,  $C_p$  [ $kJ/kg \cdot K$ ] is the specific heat and  $ach$  [ $/h$ ] is the air change rate. The sources in

figure 1 are  $T_{sa}$ : averaged sol-air temperature of the external surfaces,  $Q_r$ : mean radiation on the interior surfaces,  $Q_v$ : interior air convective sources and  $T_o$ : temperature of the ventilating air. The circuit can easily be extended to also include structural cooling, evaporative cooling etc. by adding more sources. The heat storage of the massive elements of the construction is represented by the capacitor  $C$ . The value of  $C$ , which is critical, includes only the active part of the total heat capacitance of the zone and is determined in a heuristic, experimentally well proven method [22]. Typical values for the network elements are given in table 1. The dependent quantities of interest are firstly; the interior air temperature  $T_i$ , and secondly; the sensible load required to maintain a specified interior temperature. (Latent loads present no problem, but for simplicity's sake this paper will be restricted to dry-bulb temperatures. A new version of the program is commercially available which includes evaporative cooling, latent loads and structural cooling.)

It was extensively validated and has already, in practice, proved a valuable design aid for architects, and for establishing norms for the thermally efficient design of buildings. Presently, the implementation is restricted to periodic, diurnal forcing functions. The philosophy is to calculate the response for a typical hot and cold design day as though every other day is exactly similar. In practice, the method will be grossly erroneous only when the building has a very long time constant (very massive with high

shell isolation) and the thermal energy consumption differs radically on some days from the norm e.g. on weekends, or if the weather pattern is drastically different on a single day. This approach is in line with the philosophy of a design day, where days of typical extreme weather are used. There is no fundamental reason why the method is not applicable to periods of e.g. 7 or 365 days.

The past method of solution of the network was to obtain the convolution between forcing functions and system response in the frequency domain. This method assumes the parameters  $R_o$ ,  $R_a$ ,  $R_v$  and  $C$  are constants in time and the governing equation of the network is a linear, constant coefficient, differential equation. This is rather restrictive; with this assumption the program cannot treat situations where e.g. the ventilation rate varies with the hour of the day. Consequently, the method is only applicable to situations where the windows remain closed or open during all hours and/or a constant rate of forced ventilation and infiltration is maintained throughout the day. Most other thermal analysis programs suffer from the same limitation [18-21]. To relax this restriction, it is necessary to solve the governing equation of the network of figure 1, with circuit elements which are assumed functions of time; a considerably more difficult problem.

### 3 Governing Differential equation

The equation for the interior temperature of the network of figure 1, with resistors and capacitance assumed functions of time, is:

$$T_i = \frac{T_c \cdot R_v + T_x \cdot R_a}{R_v + R_a} \quad (1)$$

where:  $T_x = T_o + R_v \cdot Q_c$  (2)

$T_c$  is the temperature at the structure node (across the capacitor in figure 1) and is given in terms of the stored heat  $q$

$$T_c = q/C \quad (3)$$

which is found from the governing differential equation:

$$\dot{q} + \beta_T \cdot q = f_T \quad (4)$$

In (4) the subscript T refers to the solution for the interior temperature. The forcing function  $f_T$  is:

$$f_T = \frac{T_x}{R_a + R_v} + \frac{T_y}{R_o} \quad (5)$$

with  $T_y = T_{sa} + R_o \cdot Q_r$

and the time dependent coefficient  $\beta_T(t)$  is the inverse of the time-constant  $\tau_T$  of the building:

$$\beta_T = \frac{R_a + R_o + R_v}{C \cdot R_o \cdot (R_a + R_v)} = 1/\tau_T \quad (6)$$

It is possible to substitute (2) to (6) in equation (1) to obtain an equation which directly delivers  $T_i$  in terms of the sources. In practice, it is a great advantage to write the governing equation in terms of the amount of stored heat, and not in terms of the primary quantities of interest. The stored heat is a fairly smooth function of time (provided mass is not added to or removed from the structure), while the temperatures are subject to sharp

discontinuities when the values of the circuit elements suddenly change. Since we are especially interested in sudden, large changes, e.g. when windows are opened and closed or forced cooling is switched on and off, it is important to be able to solve the equation accurately for discontinuous coefficients.

The equations were derived for the general case where any of the elements, and not just  $R_v$ , may be subject to variation, although  $R_v$  is the most important. There is little formal distinction between changes in  $R_v$  and changes in the other elements. Hence the only type of variation the equations do not cater for is, when the storage capacity of the building is varied by introducing or removing mass. This is of more than theoretical importance; the other parameters of the circuit may be subject to various time dependent influences, e.g. the interior film resistance is definitely also affected by the time dependant air circulation rate.

Analogous to equations (1) to (6), the sensible convective load  $Q_{cr}$ , to obtain a prescribed interior temperature  $T_{ir}$ , can be found by substituting  $T_{ir}$  for  $T_i$  in (1) to (6) and solving for the convective load. While this load calculation is highly theoretical – practical thermostats normally include dead bands and/or hysteresis – the calculation is useful for estimating required system

capacities, without troublesome iterative procedures.  $Q_{cr}$  is given by:

$$Q_{cr} = \frac{R_a + R_v}{R_a \cdot R_v} \cdot T_{ir} - \frac{T_{cr}}{R_a} - \frac{T_o}{R_v} \quad (7)$$

with  $T_{cr}$  the required structure temperature.  $T_{cr}$  is determined from the amount of stored heat:

$$T_{cr} = q_r / C \quad (8)$$

which satisfies the differential equation

$$\dot{q}_r + \beta_E \cdot q_r = f_E \quad (9)$$

In this case the forcing function  $f_E$  is

$$f_E = \frac{T_y}{R_o} + \frac{T_{ir}}{R_a} \quad (10)$$

and the coefficient  $\beta_E$  is

$$\beta_E = \frac{R_a + R_o}{R_a \cdot R_o \cdot C} = 1/\tau_E \quad (11)$$

In both instances, (4) and (9), the solution of a linear first order differential equation with time dependent coefficient  $\beta(t)$  must be found. The equation is of the form

$$\dot{y}(t) + \beta(t) \cdot y(t) = x(t). \quad (12)$$

#### 4 Existing Methods of Solutions

The general solution of (12) is well known and can be found in any text book on elementary differential equations. It is

$$y(t) = \exp[-\Gamma(t)] \cdot \int_{-\infty}^t \exp[\Gamma(t)] \cdot x(t) dt \quad (13)$$

with  $\Gamma(t) = \int \beta(t) dt. \quad (14)$

In (13) the lower limit of integration is taken at minus infinity to indicate that the steady state response is required. The

integral can be evaluated by numerical integration (either in the form of (13), or in the form of the original differential equation (12) ) by a standard procedure such as Runge–Kutta. Numerical integration is, unfortunately, relatively inefficient. The initial condition is unspecified, or stated more precisely: is assumed to have occurred far back in history. The integration must continue until the transient response is extinct. Since the time constant of a building can be quite long (30 hours or more is not uncommon), and the transient response can be regarded as sufficiently extinct only after 5 time constants, integration may have to continue for a considerable period to ensure sufficient accuracy of the answer. Since a very high premium is attached to the speed of computation, it is desirable to find a quicker method.

Various methods for treating systems with variable parameters exist in the literature. It was shown by Carson [5] (see also [6]) that the solution can be expressed in the form of a Volterra integral equation. The solution of this integral equation is given in terms of an infinite progression. Alternatively, solutions in terms of a series expansion of Bessel functions can be found when the coefficient varies sinusoidally [6]. These and other similar expansions [8,9], converge rapidly when the variation of the coefficient  $\beta(t)$  is slow, compared to the variation of the forcing function or when  $|\dot{\beta}/\beta| \ll 1$ . For sudden jumps in the value of  $\beta$ , i.e. when  $\dot{\beta}$  is very large, they are of little practical value.

The traditional method for isolating the steady state response is through Fourier series methods. In essence there is little fundamental difference in the application of this method to systems with variable parameters – as opposed to constant parameters – except that it must be assumed that the Fourier coefficients of the output are functions of time [8]. The method leads to a mixed time–frequency domain description. The Fourier technique is so prevalent in the literature that it warrants some further discussion.

Since the differential equation is linear (although time variant) it will be sufficient to determine the solution for the phasor  $x(t) = X \cdot e^{j\omega t}$  ( $X = X(\omega)$  a complex number independent of time). The solution for general periodic inputs can be obtained by superpositioning the phasor components of each constituent frequency component. Assuming the response  $y(t)$  to the phasor input  $x(t)$  is of the form  $y(t) = Y(t, \omega) \cdot e^{j\omega t}$  and substituting these assumed values for  $x$  and  $y$  in (12) furnishes:

$$\frac{\partial Y(t, \omega)}{\partial t} + [j\omega + \beta(t)] \cdot Y(t, \omega) = X(\omega). \quad (15)$$

This is the modulation function equation (MFE) of the system as discussed in [9]. In [8] and [9] methods are presented for directly transforming (12) into (15) for more general systems. See also [24 , 25]. It is customary to define the system transfer function:

$$H(t, \omega) = \frac{Y(t, \omega)}{X} \quad (16)$$

which, from (15), satisfies:

$$\frac{\partial H}{\partial t} + [j\omega + \beta] \cdot H = 1. \quad (17)$$

Equation (17) is of exactly the same form as (12), however, it involves complex functions and the input in (17) is a constant. But obviously, the Fourier series expansion is not beneficial regarding computation time. Instead of the initial value,  $y(0)$  in (12), the initial frequency response  $H(0, \omega)$  is required, and furthermore, (17) must be solved for each frequency component of the forcing function. However, if the time-constant is sufficiently long at all hours, only the first few frequency components will be significant in the solution. Alternatively, an approximate solution for a few components can be obtained by the method of Galerkin [6].

Another approach is to assume the circuit parameters are constant in small intervals and then to solve the equation exactly for each interval [10]. This approach requires matching the final conditions of each interval to the initial conditions of the next interval. For a steady, periodic solution, the initial condition of the first interval must match the final condition of the last interval. It is seen that the process requires the simultaneous solution of a large number of equations. In the next section we obtain an approximate method following this approach with the additional assumption that all forcing functions and output variables are constant between sampling points, in which case an explicit formulation for the initial value is possible.

## 5 Approximate Numerical Solution

The advantage of writing the governing equation in terms of the amount of stored energy is; it reduces the sensitivity of the solution of  $T_i$  to errors in the solution of the differential equation (12). A large part of the variation in  $T_i$  is accurately included in the final calculation of  $T_i$  and  $Q_{ri}$  from  $q$ , in (1) and (7). This is easily demonstrated by noting that in the limit, when the ventilation rate is very large ( $R_v \sim 0$ ), the sole contributor to  $T_i$  in equation (1) is  $T_x$ . On the other hand, when  $R_v$  approaches infinity, the sole contributor is  $T_c$ . This is in accordance with the network of figure 1.

To obtain a numerical solution for (12) we follow the standard procedure of rewriting the equation in the form of an integral equation:

$$\begin{aligned}
 y(t) &= \int_{-\infty}^t x(t_1) - \beta(t_1) \cdot y(t_1) dt_1 \\
 &= \int_{-\infty}^0 x(t_1) - \beta(t_1) \cdot y(t_1) dt_1 + \int_0^t x(t_1) - \beta(t_1) \cdot y(t_1) dt_1 \\
 &= y(0) + \int_0^t x(t_1) - \beta(t_1) \cdot y(t_1) dt_1 \quad (18)
 \end{aligned}$$

For periodic, steady state solutions with period  $T$ , it is required that the initial value of every period equals the final value of the previous period:

$$y(0) = y(T) = y(0) + \int_0^T x(t_1) - \beta(t_1) \cdot y(t_1) dt_1$$

and therefore

$$\int_0^T x(t_1) - \beta(t_1) \cdot y(t_1) dt_1 = 0. \quad (19)$$

The steady, periodic solution of (12) is given by (18) with initial condition stipulated by (19). For discrete data at  $t = t_i = i \cdot \Delta T$ ,  $T = N \cdot \Delta T$ , these equations take the form:

$$y_k = y_0 + \sum_{i=0}^{k-1} \Delta T \cdot (x_i - \beta_i \cdot y_i) \quad (20)$$

and

$$\sum_{i=0}^{N-1} \Delta T \cdot (x_i - \beta_i \cdot y_i) = 0. \quad (21)$$

It is assumed all variables are constant between sampling points and  $x_i = x(t_i)$  and  $\beta_i = \beta(t_i)$  are tabulated functions. Equation (20) can be written in the following corresponding, iterative form:

$$y_k = \Delta T \cdot x_{k-1} + (1 - \Delta T \cdot \beta_{k-1}) \cdot y_{k-1} \quad k = 1, 2, 3 \dots N-1 \quad (22)$$

If one value of  $y$  is known the other values are easily found from (22), provided the iteration is stable. A closed form solution for the initial value  $y_0$  is obtained by starting with

$$y_N = \Delta T \cdot x_{N-1} + (1 - \Delta T \cdot \beta_{N-1}) \cdot y_{N-1} = y_0 \quad (23)$$

and substituting previous values of  $y_k$ .

$$\begin{aligned} y_N &= \Delta T \cdot x_{N-1} + (1 - \Delta T \cdot \beta_{N-1}) \cdot (\Delta T \cdot x_{N-2} + \\ &\quad (1 - \Delta T \cdot \beta_{N-2}) \cdot (\Delta T \cdot x_{N-3} + ( \dots \Delta T \cdot x_0) \dots)) + \\ &\quad (1 - \Delta T \cdot \beta_{N-1}) \cdot (1 - \Delta T \cdot \beta_{N-2}) \cdot \dots \cdot (1 - \Delta T \cdot \beta_0) \cdot y_0 \\ &= y_0. \end{aligned}$$

This can be rewritten compactly:

$$y_0 = \frac{\left[ \sum_{k=0}^{N-2} \Delta T \cdot x_k \cdot \prod_{j=k+1}^{N-1} (1 - \Delta T \cdot \beta_j) \right] + \Delta T \cdot x_{N-1}}{1 - \prod_{k=0}^{N-1} (1 - \Delta T \cdot \beta_k)}. \quad (24)$$

When programming equation (24), advantage can be taken of the fact that the product expression occurs both in the numerator and the denominator, by starting with the highest value of  $k$  and counting down instead of up. By storing at each step  $k$  the partial sum and the partial product, the product expression can be evaluated successively for every term in the sum. The product expression in the denominator is found by multiplying the final product of the numerator with  $(1 - \Delta T \cdot \beta_0)$ .

The complete approximate solution is given by (22) with initial value given explicitly by (24). In effect the iteration is carried out twice through one period. The first iteration is used to determine the initial value, and the second calculates the results at all hours. We maintain that the method is efficient; the initial value is determined after a single iteration, instead of after iterating through five time-constants. It will be shown in the next section that sufficient accuracy can be obtained from a fixed step size.

Firstly we need to establish the stability of (22). The question is important despite the fact that physical constraints ensure the absolute stability of the original differential equation. It is well known that the sampling interval has an influence on the stability of a sampled data system [12]. To investigate the stability of (22) the  $\mathcal{Z}$  transform method [12] will be used under the assumption that  $\beta$  is independent of time. The transfer function of

(22) in the  $z$  domain is then:

$$H(z) = \frac{Y(z)}{X(z)} = \frac{z^{1 \cdot \Delta T \cdot \beta}}{1 - z^{-1} \cdot (1 - \Delta T \cdot \beta)}. \quad (25)$$

The time invariant system is stable if the pole of the transfer function lies inside the unit circle on the complex  $z$ -plane, i.e.

$$|1 - \Delta T \cdot \beta| \leq 1. \quad (26)$$

It must be noted that this condition will not guarantee stability in the time variable case, but it is indicative of stability [24]. In practice we have found the iteration stable under the condition (26) even for sudden large changes in the value of  $\beta$ . According to (26) the sampling interval is chosen so that  $\Delta T \cdot \beta < 2$ . For most practical buildings a sampling period of 1 hour suffices. For extremely light constructions we have found it necessary to decrease the sampling rate to 15 min.

## 6 Accuracy of the method

The method of §5 is essentially Euler's method for the numerical integration of a differential equation. An upper bound for the total propagated error is [11]:

$$|e| \leq \frac{\Delta T \cdot |\ddot{y}|}{2 \cdot \beta} \cdot [\exp(\beta \cdot T) - 1]. \quad (27)$$

The error grows rapidly when  $\beta \cdot \Delta T = \Delta T / \tau > 0.1$ . Since we have written the governing equation in terms of the stored heat, which is a slowly varying quantity, one would normally expect  $|\ddot{y}|$  to be quite small. In fact, the derivative of (12) gives:

$$\ddot{y} = \dot{x} - \beta \cdot x + (\beta^2 - \dot{\beta}) \cdot y. \quad (28)$$

$|\ddot{y}|$  contains a term proportional to  $\dot{\beta}$  which might be large for

large variations of  $\beta(t)$ . Actually, the numerical integration technique is rigorously exact if all variables assume constant values between sampling points, even with discontinuous derivatives at the sampling points. Equation (27) must not be taken too seriously, it is derived under the assumption of continuous functions. To decrease error propagation and accuracy for continuous signals, one can use a higher order numerical approximation technique. Beginning with the trapezoid rule, for instance, an exactly similar scheme with local error theoretically proportional to the third derivative and square step size results. These and a host of other higher order approximation techniques [7] are not as advantageous for discontinuous input functions. Unless the integration is done over continuous subintervals, they tend to smooth the discontinuities and to make the solution appear non-causal, since they pre-empt the sudden change. The effect is easily explained by noting that the higher order techniques in effect interpolate between the sampling points so that values in the immediate future will influence the present result. In practice, we have found the Euler algorithm sufficiently accurate and quick. Further reduction in computation time is possible from implicit and higher order methods [26], but the simple method is already so fast that the matter is of academic importance only. The implicit methods have the advantage that they are generally stable, but they do not readily, explicitly provide the initial condition, in a form similar to (24).

To obtain a practical evaluation of the accuracy of the method, the approximate solution can be compared with the exact solution in a special case. We take the case where  $\beta(t)$  is constant everywhere, except at two points where the value jumps discontinuously i.e.  $\beta(t)$  given by:

$$\beta(t) = \begin{cases} \beta_0 & \text{when } 0 \leq t < T_1 \\ \beta_1 & \text{when } T_1 \leq t < T \end{cases} \quad (28)$$

The exact solution for a constant  $\beta$  and a sinusoidal input function given by  $x = X \cdot (1 + m \cdot \cos\omega[t+t_0])$  is from the Laplace transform:

$$y(t) = y(0) \cdot e^{-\beta t} + A(t) \quad (29)$$

where

$$A(t) = \frac{X}{\beta} \cdot \left[ 1 - e^{-\beta t} + \frac{m\beta}{\sqrt{\beta^2 + \omega^2}} \cdot \alpha(t) \right]$$

$$\alpha(t) = \cos(\omega[t+t_0] - \varphi) - \cos(\omega t_0 - \varphi) \cdot e^{-\beta t}.$$

and  $y(0)$  is the initial value,  $\tan\varphi = \omega/\beta$ . Next, apply this solution to the intervals in (28) and set  $y(0) = y(T)$ , and  $y(T_1)$  continuous. The solution for  $y(0) = y_0$  is:

$$y_0 = \frac{A_1 + A_0 \cdot e^{-\beta_1(T-T_1)}}{1 - e^{-\beta_0 T_1 - \beta_1(T-T_1)}} \quad (30)$$

with

$$A_0 = A_0(T_1) \quad \text{and} \quad A_1 = A_1(T-T_1).$$

The subscripts 0 and 1 of  $A$  and  $\beta$  in (30) refer to the first and second intervals in (28) respectively. Figure 2 shows the error between analytic solution (29), (30), and approximate numerical solution (24), (22), for a low-mass building. The building (an agricultural shed) has a time-constant of about 5 hours (see Table 1) with closed windows. This is a very short thermal

time-constant for a building, and a practical sampling rate would be 15 min but to show the robustness of the method, a sampling period of 1 h is used in the calculation. The air change-rate varies between 0.1 and 30 /h resulting in a time-constant jump from 5.7 to 3.8 h, the jump occurring at  $T_1 = 11$  h. The forcing functions used for the calculation are:

$$T_{sa} = 20 + 10 \cdot \cos(2\pi/24 \cdot t) \text{ } ^\circ\text{C},$$

$$T_o = 20 + 5 \cdot \cos(2\pi/24 \cdot t) \text{ } ^\circ\text{C} \text{ and}$$

$$Q_c = Q_r = 0 \text{ kW} .$$

The figure shows the error obtained by a sudden increase in the number of air changes as well as a sudden decrease of similar strength. In this worst case,  $\beta \cdot \Delta T = 0.25$ , the temperature error is less than 1°C. The error is decreased to insignificant levels by decreasing the sampling period to 15 min, with linear interpolation between sampling points. Figure 3 shows the resulting interior temperatures. Note the sharp discontinuity. In practice, the heat capacitance and the finite mixing time of the interior air (both neglected in the model) will tend to smooth the discontinuity so that a smooth transition will be measured. (We have also found that with sudden changes in the ventilation rate the time constant of the thermograph can often not be neglected.)

The calculations were repeated for a massive building (office block) where the time constant jumped from 144 to 38 h when the ventilation rate was increased from 0.1 to 30 air changes per

hour. The error between the analytic and approximate solutions in this case,  $T = 1$  h,  $\beta \cdot \Delta T = 0.025$ , was less than  $0.1$  °C.

When evaluating the numerical error it must be borne in mind that the accuracy of the modeling is definitely limited. It makes no sense to strive for infinite accuracy in the calculation procedure when both the assumptions inherent in the model, and uncertainties in the detail of the construction and ventilation rates limit the practical, attainable accuracy.

## 7 Proportional Feedback, Active Systems

The method is very easy to extend to active indoor convective systems. If another system convective load,  $Q_s$ , given by:

$$Q_s = \alpha \cdot (T_i - T_t) \quad (31)$$

with  $\alpha$  the proportional feedback gain [W/K] and  $T_t$  the thermostat temperature, is added to the convective load  $Q_c$  in (2), it is found that the behaviour of the system is again governed by (4) but with parameter  $\beta(t)$  now given by:

$$\beta_S(t) = \beta_T - \frac{\alpha \cdot R_v^2}{C \cdot (R_a + R_v) \cdot (R_a + R_v - \alpha \cdot R_a R_v)} \quad (32)$$

In the limit  $\alpha \rightarrow \infty$ ,  $\beta_S \rightarrow \beta_E$  in accordance with the root-locus theorem for closed loop systems. It is seen that by this simple redefinition of  $\beta$  the method can be extended to proportionally controlled systems. Practical thermostats include non-linearities such as dead bands and hysteresis. These effects can also be included in the model, but the solution of the model becomes

arduous; the initial value must be found by successive iteration [7].

## 8 Demonstration of the Method

To conclude the paper, we demonstrate the application of the method to predicting the interior temperature in buildings subjected to night-time forced ventilation. Figure 4 gives the interior temperature obtained for a building of medium (shop) and heavy mass (office); with a ventilation rate of 1/h during the hours 17h00 to 09h00 and a daytime ventilation rate of 2/h, and secondly, with a ventilation rate of 20/h from 20h00 to 07h00 and 2/h during the rest of the day. The outside air temperature is also shown. Both buildings are modeled with an interior load of 2 persons and 0.5 kW during office hours. (More details of the buildings are supplied in Table 1.) Both buildings respond favourably. The peak temperatures drop nearly 4 °C in the office and 2 °C in the shop, bringing them close to the comfort range. The authors will attempt to verify predictions like these in the near future by actual measurement in test huts and real buildings.

## 9 Conclusion

The method of §4 has been implemented in a Pascal routine which calculates the solution of the variable network in a fraction of a second on an ordinary PC. The method is simple, straightforward, efficient and sufficiently accurate. It does not

require Fourier analysis or even the evaluation of exponentials.

The work reported here was supported by the following bodies: Department of Public Works, National Energy Council, Laboratory for Advanced Engineering and University of Pretoria. The authors wish to express their gratitude to Mr. J Basson for his enthusiasm and encouragement and to Mr. P G Richards for many fruitful discussions.

### SYMBOLS

$C$	Heat storage capacitance of massive structures [kJ/K].
$Q_c$	Convective load [kW].
$Q_r$	Radiative load [kW].
$q$	Heat energy stored in the massive structure [kW].
$R_a$	Mean film resistance from interior surface of shell to interior air [K/kW].
$R_o$	Conductive shell resistance [K/kW].
$R_v$	Equivalent ventilation resistance [K/kW].
$T$	Diurnal period of 24 hours [h].
$T_c$	Mean structure temperature [ $^{\circ}$ C].
$T_{cr}$	Required structure temperature for comfort [ $^{\circ}$ C].
$T_{ir}$	Required interior comfort temperature [ $^{\circ}$ C].
$T_i$	Zone interior air temperature [ $^{\circ}$ C].
$T_{sa}$	Effective sol-air external temperature [ $^{\circ}$ C].
$T_o$	Temperature of ventilating air [ $^{\circ}$ C].
$T_x, T_y$	Effective forcing temperatures [ $^{\circ}$ C].

$T_t$	Thermostat temperature [ $^{\circ}\text{C}$ ].
$\Delta T$	Time interval between sampling points [h].
$\beta$	Coefficient of differential equation, equal to inverse of time-constant [/h]. Subscript T refers to interior temperature, E to energy loads and S to active systems.
$\tau$	Thermal time-constant of building [h].

### References

- [1] Mathews, E H and Richards, P G, A Tool for Predicting Hourly Air Temperatures and Sensible Energy Loads in Buildings at Sketch Design Stage. Energy and Buildings, vol 14, No 1, pp 61–80, 1989
- [2] Raychaudhuri, B C, Transient Thermal Response of Enclosures: The Integrated Thermal Time-Constant. Int. J. Heat Mass Transfer, Vol 8, pp 1439–1449, 1965
- [3] De Wit, M H and Driessen, H H, ELAN – A Computer Model for Building Energy Design. Building and Environment, Vol 23, No 4, pp 285–289, 1988
- [4] Penman, J M, Second Order System Identification in the Thermal Response of a Working School. Building and Environment, Vol 25, No 2, pp 105–110, 1990
- [5] Carson, J R, Theory and Calculation of Variable Electrical Systems. Phys. Rev. 17, Ser 2, pp 116–134, 1921
- [6] Pipes, L A and Harvill, L R, Applied Mathematics for Engineers and Physicists. McGraw-Hill, 1970

- [7] **Chua, L O & Lin, P-M**, Computer-Aided Analysis of Electronic Circuits. Prentice-Hall.
- [8] **Zadeh, L A**, Frequency Analysis of Variable Networks. Proc IRE 38, pp 291-299, 1950
- [9] **Tsao, Y H**, Time Variant Filtering for Non-stationary Random Processes. J. Acoust. Soc. Am. 76(4), Oct. 1984
- [10] **Fodor, G**, Laplace Transforms in Engineering. Hungarian Academy of Sciences, 1965
- [11] **Conte, S D and de Boor, C**, Elementary Numerical Analysis. McGraw-Hill Kogakusha, 1972
- [12] **Cadzow, J A and Martens, H R**, Discrete-Time and Computer Control Systems. Prentice Hall, 1970
- [13] **Holman, J P**, Heat Transfer. McGraw-Hill
- [14] **Kimura, K I**, Scientific Basis of Air-Conditioning. Applied Science Publishers, 1977
- [15] **Tuddenham, D**, Computers in Air Conditioning Load Estimation. Air Conditioning System Design for Buildings, Editor Sherratt, A F C, McGraw-Hill
- [16] **CIBS Guide A5**, Thermal Response of Buildings. CIBS 1979
- [17] **ASHRAE Procedure for Determining Heating and Cooling Loads for Computerizing Energy Calculations**, ASHRAE, 1976.
- [18] **Milbank, N O & Harrington Lynn, J**, Thermal Response and the Admittance Procedure. B·S·E, Vol 42, May 1974

- [19] **Mitalas, G P & Stephenson, D G**, Room Thermal Response. ASHRAE Semiannual meeting, Detroit, Mich., January 30 – February 2, 1967.
- [20] **Stephenson, D G & Mitalas, G P**, Cooling Load Calculations by Thermal Response Factor Method. ASHRAE Semiannual meeting, Detroit, Mich., January 30 – February 2, 1967.
- [21] **Muncey, R W R**, Heat Transfer Calculations for Buildings. Applied Science Publishers, 1979.
- [22] **Mathews, E H, Rousseau, P G, Richards, P G & Lombard, C**, A Procedure to Estimate the Effective Heat Storage Capability of a Building. Accepted for publication, Energy and Buildings, 1990.
- [23] **Walsh, P J & Delsante, A E**, Calculation of the Thermal Behavior of Multi-Zone Buildings. Energy and Buildings, 5, 1983.
- [24] **Gibson, J E**, Nonlinear Automatic Control, Chapters 4 & 5, McGraw-Hill, 1963.
- [25] **Zadeh, L A & Desoer, C A**, Linear System Theory, The State Space Approach, chapter 6, McGraw-Hill.
- [26] **Zmeureanu, R & Fazio, P**, Thermal Performance of a Hollow Core Concrete Floor System for Passive Cooling, Building and Environment, Vol.23, No.3, 1988.
- [27] **Athienitis, A K**, Frequency Domain Modelling and Periodic Simulation of Heat Transfer in Passive Solar Buildings. IASTED – Computer Aided Design, Modelling and Simulation, June 1986.

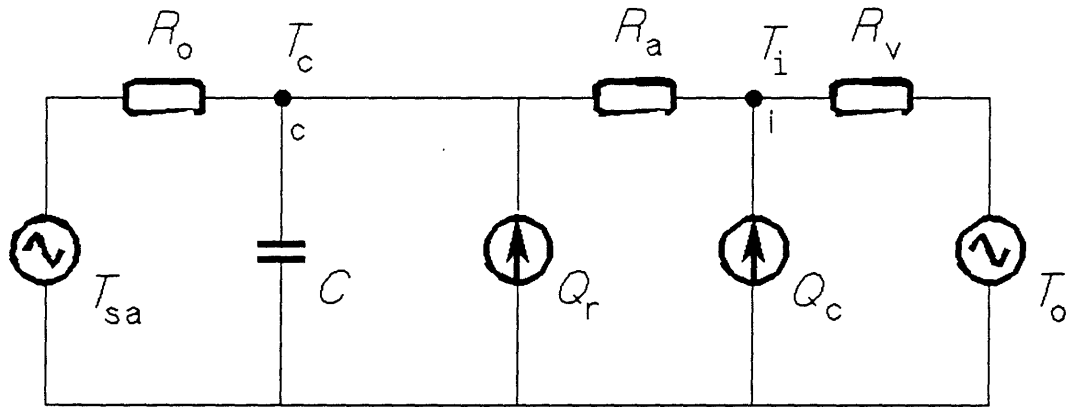
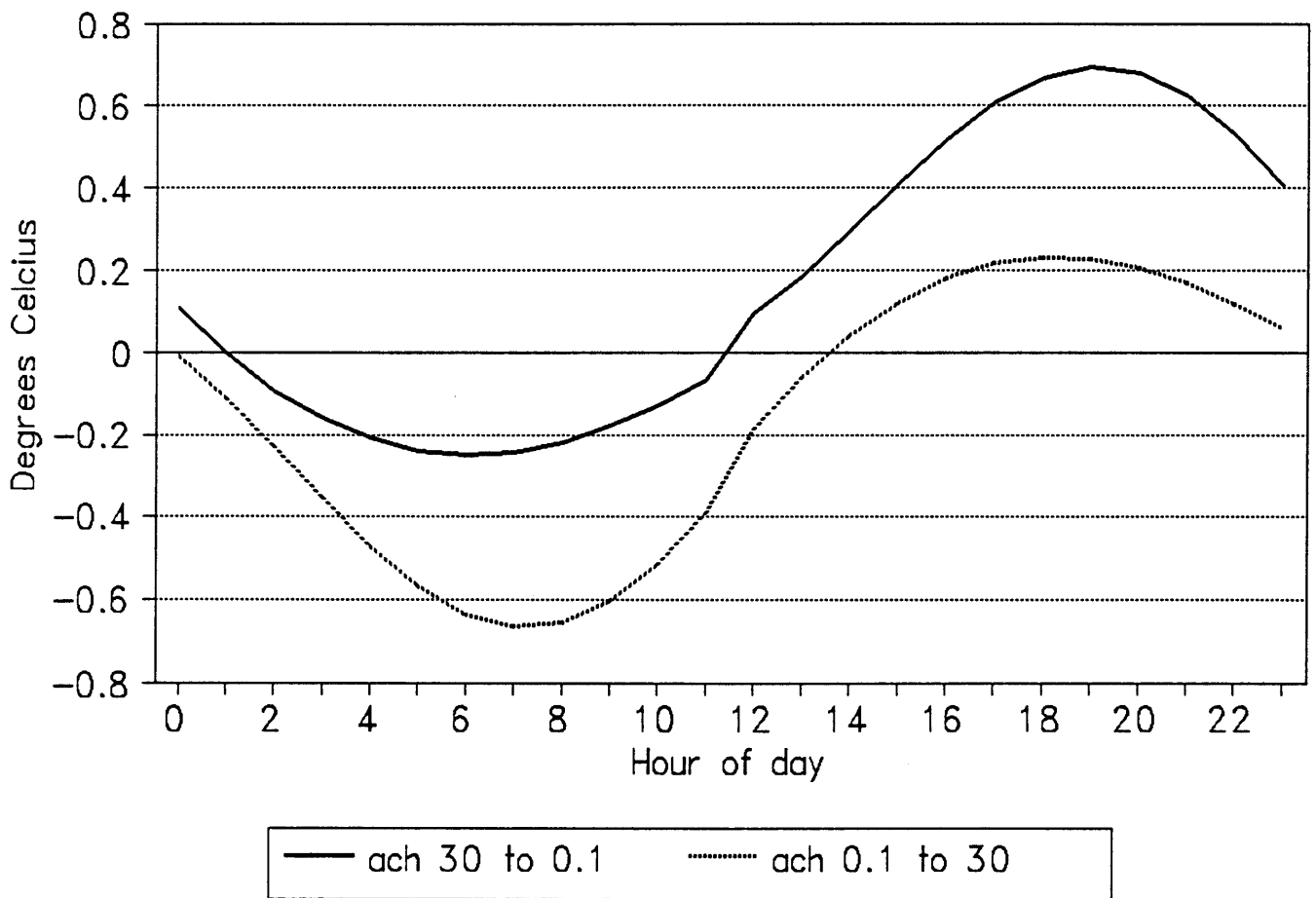


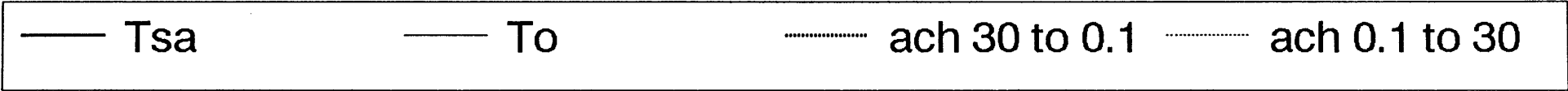
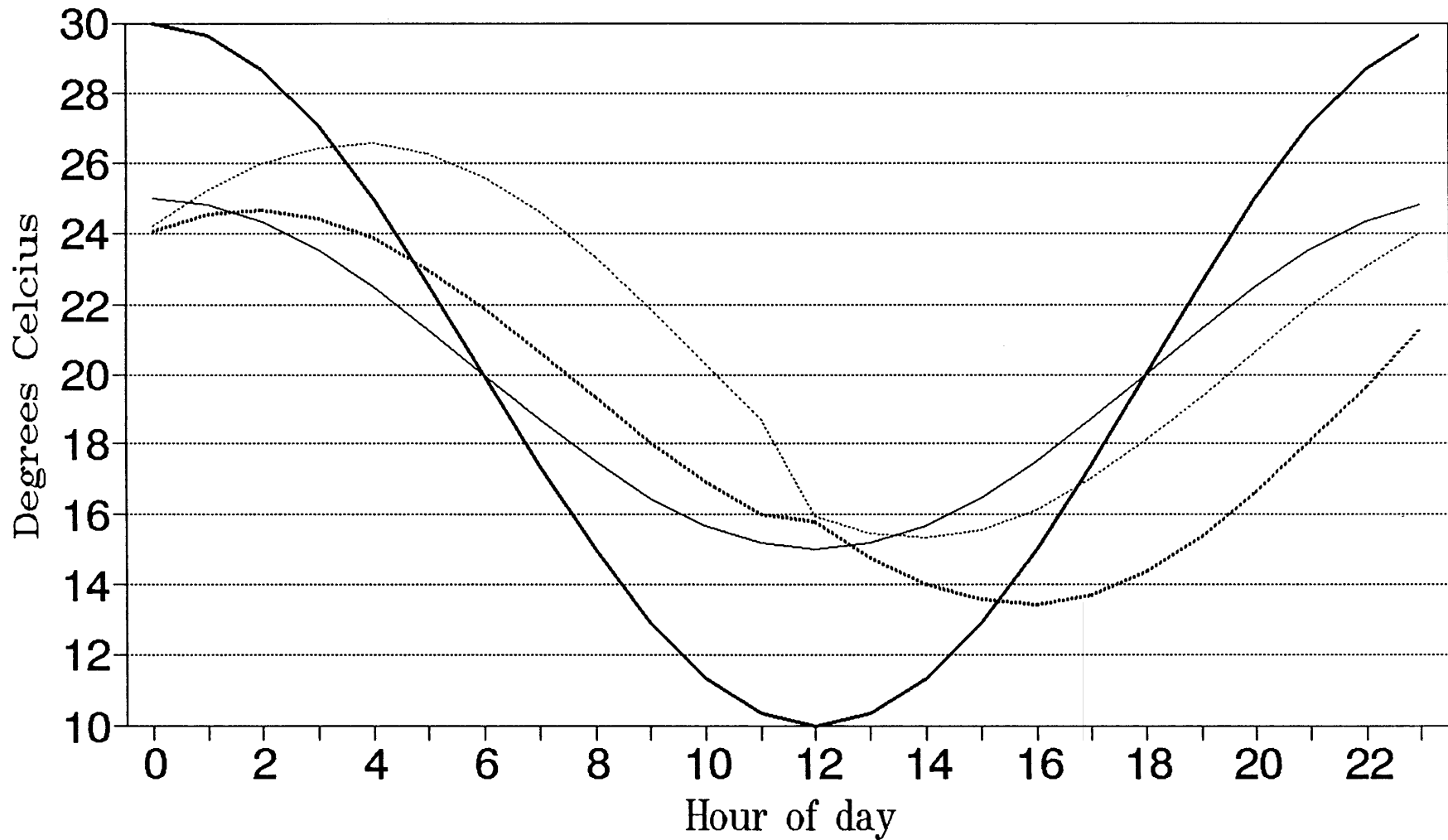
Figure 1

Figure 2  
Numerical Predicted Temperature Error



# Figure 3

## Predicted Temperature (Numerical)



# Figure 4

## Night Cooling

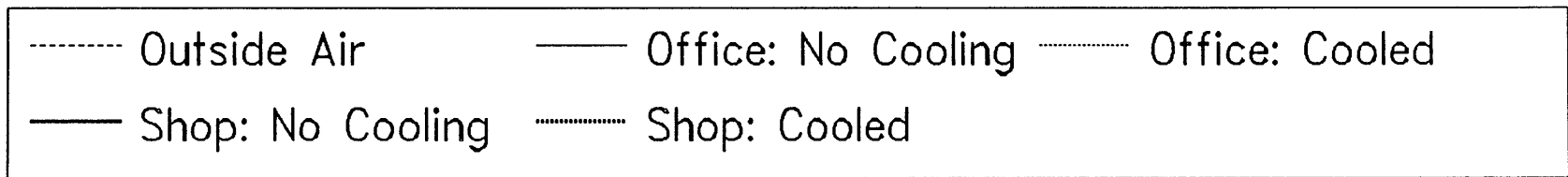
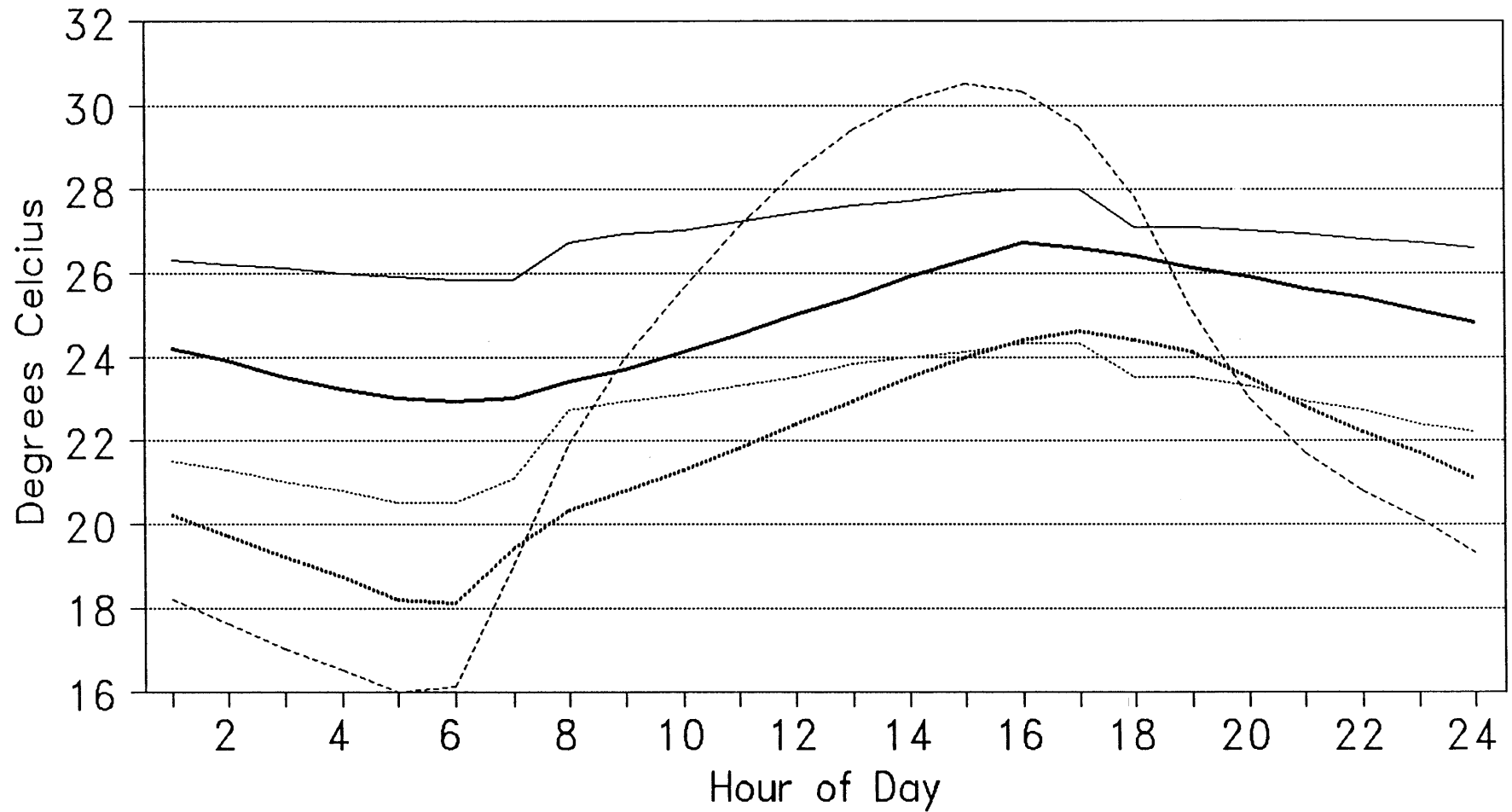


Table 1

Type	C	Ro	Ra	ach	Rv	TauT	TauE
	[kJ/K]	[K/kW]	[K/kW]	[/h]	[K/kW]	[h]	[h]
shop	85114	0.0015	0.0003	0.5	0.0057	32	5
office	44459	0.0118	0.0012	0.6	0.1463	136	14
factory	2.7E+0	2.5E-05	6E-06	1.2	2.8E-05	11	3.7
room	7304.7	0.0164	0.0017	0.57	0.2339	31	3.2
shed	529674	3.9E-05	4.6E-05	5	0.0002	5	3.1

## Captions

Figure 1. Electrical analogue for modelling thermal response of buildings.  $T_{sa}$  mean sol-air temperature,  $T_c$  structure effective temperature,  $T_i$  internal air temperature,  $T_o$  external air temperature.  $R_o$  shell resistance,  $R_a$  mean internal surface film resistance,  $R_v$  ventilation resistance.  $C$  is the effective heat storage capacity of the structure.

Figure 2. Difference between analytically derived exact prediction of interior temperature, for sinusoidal forcing functions, and numerical algorithm. The sampling period is 1 h. Building: low-mass agricultural shed,  $\tau = 5$  h. The upper and lower traces show the error when the air-change-rate jumps from 0.1 to 30 /h, and from 30 to 0.1 /h respectively.

Figure 3. Predicted interior temperature for the low-mass building when the air-change rate jumps between 0.1 and 30 /h. The thick-solid line is the assumed sol-air temperature and the thick-broken line the assumed outside air temperature.

Figure 4. Night cooling of a shop and a massive office. The traces marked 'no cooling' are with an air-change-rate of 1 /h during the night from 17h00 to 09h00 and 2 /h during 09h00 to 17h00. The other traces show the effect of increasing the ventilation during the night to 20 /h.

Table 1. Circuit parameters of some typical buildings. The floor area, air-change-rate ( $ach$ ), time-constant for interior temperature ( $\tau_T$ ) and time-constant for load calculation ( $\tau_E$ ) are also given.

# A Procedure to Estimate the Effective Heat Storage Capability of a Building

E. H. MATHEWS\*  
 P. G. ROUSSEAU\*  
 P. G. RICHARDS\*  
 C. LOMBARD\*

*Building designers usually prefer simplified thermal analysis procedures because these provide short simulation times and are usually easy to use. However, it is difficult to incorporate all the complex heat transfer phenomena for buildings of diverse design into a simplified method. It is especially true for the heat storage of a building. This paper presents a novel method to calculate this aspect. Features of the proposed method, some of which are often omitted in simplified methods, include the following: the modelling of different multi-layered elements in the exterior shell, different multi-layered high mass objects inside the building e.g. high mass suspended floors, floors in ground contact as well as high mass multi-layered partition walls. The method is derived inter alia from physical interpretation and empirical data.*

*The single value for heat storage obtained with the proposed procedure is incorporated in a thermal network which is solved numerically to determine hourly air temperatures and sensible energy loads. The single value of heat storage ensures a very fast and efficient building thermal analysis. Verification for 62 cases showed that for 80% of the time temperature predictions were within 2°C of measurements. This correlation provides an acceptable level of confidence in the use of the new calculation procedure for heat storage.*

## NOMENCLATURE

$A$	area of surface ( $m^2$ )
$\frac{ach}{C}$	flow rate (air change per hour)
$\Sigma C$	total active thermal capacity of building per exposed shell area ( $kJ\ ^\circ C^{-1}\ m^{-2}$ )
$c_p$	specific heat capacity for air at constant pressure ( $kJ\ ^\circ C^{-1}\ kg^{-1}$ )
$h$	combined indoor air convection and radiation heat transfer coefficient ( $W\ ^\circ C^{-1}\ m^{-2}$ )
$R$	thermal resistance ( $^\circ C\ W^{-1}$ )
$R_k$	thermal resistance of layer $k$ (thickness/conductivity) ( $^\circ C\ m^2\ W^{-1}$ )
$R_s$	total thermal resistance of shell calculated from sol-air to indoor surface node ( $^\circ C\ m^2\ W^{-1}$ )
$R_a$	total thermal resistance of shell calculated from sol-air to indoor air node ( $^\circ C\ m^2\ W^{-1}$ )
$T$	temperature ( $^\circ C$ )
$t$	time of day (hours)
$\frac{Vol}{\beta}$	volume of zone ( $m^3$ )
$\beta$	correction factor
$\rho$	density ( $kg\ m^{-3}$ )
$\tau$	thermal time constant (hours)

### Subscripts

a	air
b	building
c	convective
i	indoor air
j	counter for any layer
k	counter for external enclosing element
o	outdoor air
r	radiative

s	shell
sa	sol-air
v	ventilation

### Notation

	resistances in parallel
--	-------------------------

## 1. INTRODUCTION

A GOOD thermal design for a building originates during the sketch design stage. The lack of accessible design tools for this early stage, comprising acceptable analysis methods and user-friendly computer programs based thereon, has contributed to neglect in this field [1]. Part of the problem may be that the scientists have failed to develop efficient tools which designers want to use. Scientists often believe that true science is only where all the basic differential equations are solved without approximations [2]. Such a belief may not help to achieve an efficient tool for designers. A fundamental change is thus needed in this outlook. To develop efficient tools, problem complexity must be reduced without sacrificing too much accuracy. Such a simplified tool must still be able to analyse fairly accurately all types of real buildings [1]. Other criteria for a good design tool [3], which are not discussed in detail in this paper, include the following: user-friendly software; minimum time to become proficient in its use; input of only the necessary data; and quick simulation times.

Adhering to the philosophy for an efficient tool, a new tool to analyse all the important and complex heat transfer phenomena related to buildings was developed,

\*Centre for Experimental and Numerical Thermoflow, Department of Mechanical Engineering, University of Pretoria, R.S.A.

using an interplay between empirical, analytical and numerical techniques. The tool *inter alia* predicts hourly air temperatures and sensible energy loads. In this paper only the treatment of the heat storage will be discussed in detail. It will be shown that with certain well-considered simplifications only one mass mode is needed rather than hundreds as for finite element or finite difference methods. Computer running times are thus drastically reduced. The difficult heat storage problem of buildings with floors not insulated from the indoor air is also efficiently addressed.

Ultimately any simulation method must stand or fall based on its agreement or disagreement with experiments. For this reason the tool, unlike many others, was extensively verified in more than sixty passive, naturally ventilated buildings comprising a wide range of thermal properties. It was found that for 80% of the time temperature predictions were within 2°C of measurements, showing that the heat storage effect was efficiently simulated.

## 2. THERMAL SIMULATION OF A BUILDING ZONE

The thermal simulation was described in detail in a previous article [3]. For the sake of completeness important aspects of the simulation will again be highlighted in this section.

All the important thermal interactions in a building should preferably be simulated by the simulation model. Important building characteristics that should be modelled are *inter alia* the fact that a multi-layered roof or wall can either be exposed to the outdoor environment or to adjacent zones. Furthermore, a multi-layered floor can be suspended as a division between upper and lower zones, or it can be in direct contact with the ground. High interior mass such as multi-layered partition walls should be included. The following should also be simulated: the thermal effects of the outdoor air temperature; solar radiation as well as shading, colour and orientation of different exterior surfaces; solar penetration and window shading devices; internal convective and radiative heat sources as well as varying natural and mechanical ventilation rates. The proposed tool models all the above-mentioned thermal interactions by an extremely simplified thermal network of a single building zone. The network is solved numerically. Detail of the solution technique is given in references [3] and [4].

The network in its original form was developed by Mathews [5, 6] for completely passive buildings, since which time it has been refined by adding convective heat generation or extraction [3, 7, 8]. The latest version of the thermal network for a single building zone is presented in Fig. 1. Various thermal properties can be identified in the network. The time-dependent forcing inputs are the radiative heat source ( $Q_r(t)$ ) acting on the internal structure, the sol-air temperature ( $T_{sa}(t)$ ) acting on the exterior, the convective heat source ( $Q_c(t)$ ) and the outdoor air temperature ( $T_o(t)$ ) both acting on the internal air volume. The radiative source includes solar gains through windows while the convective source includes air-conditioning. Heat gains due to machines, lighting and occupancy can also be included in these two forcing

inputs. Natural ventilation and infiltration are dependent on the outdoor air temperature, while the sol-air temperature accounts *inter alia* for the colour of and radiation on and from exposed surfaces.

At a given time during the day,  $T_{sa,k}(t)$  is determined for each exposed building element  $k$ . A single value for  $T_{sa}(t)$  at that time is then calculated by means of the following weighting equation where  $A_k$  denotes the area and  $R_k$  the thermal resistance from the sol-air node to the interior surface node for each exposed building element  $k$ :

$$T_{sa}(t) = \frac{\sum_k (T_{sa,k}(t) A_k / R_k)}{\sum_k (A_k / R_k)}. \quad (1)$$

There are three resistances in the network, namely  $R_o$ ,  $R_a$  and  $R_v(t)$ . The weighted total resistance ( $R_o$ ) for the exterior shell, calculated from the sol-air node through the shell to the indoor surfaces in terms of the shell area ( $\sum_k A_k$ ), is given by

$$R_o = \frac{\sum_k A_k}{\sum_k (A_k / R_k)}. \quad (2)$$

Note that, unlike the other resistances in the network,  $R_o$  is expressed in terms of the total exposed shell area. This is done to simplify comparisons between the thermal resistances of exterior shells of building zones with different dimensions.

The second resistance in the network is the time-varying ventilation resistance ( $R_v(t)$ ) which is given by  $3.6 / (\text{Vol} \cdot \rho \cdot \text{ach}(t) \cdot c_p)$ , where Vol is the internal volume of the zone, ach(t) the varying air change rate per hour,  $\rho$  the air density and where  $c_p$  is the specific heat of the air at constant pressure. The resistance  $R_v(t)$  can change during the day as infiltration and natural or mechanical ventilation flow rates change.

The remaining resistance ( $R_a$ ) is the resistance between the indoor air and the interior surfaces. Previously [5] this resistance was incorporated in  $R_o$  to give a single value of the total shell resistance ( $R_s$ ) between the outdoor and indoor air. This single value, together with a single value for the active thermal capacity of the building zone, was needed to conform to another semi-empirical method widely used in South Africa at that time [9]. However, for more detailed and theoretically more rigorous analyses, two resistances  $R_o$  and  $R_a$  are needed.

The heat capacity of the indoor air can be simulated by adding a capacitor between the indoor air node (i) and the reference node (r). This capacitor was, however, omitted from the thermal network as its effect is usually negligible [6].

The capacitor ( $\Sigma C$ ) in the network represents the "effective" thermal capacity of the building zone and is expressed per total shell area ( $\sum_k A_k$ ) to simplify comparisons between building zones with different exterior dimensions. The "effective" thermal capacity is that part of the building zone's thermal capacity that is "effective" in storing heat for the indoor air. It consists of contributions from the exposed shell and internal mass which includes interior walls and floors. It is difficult to incorporate all these effects in an appropriate single value for heat storage capability [10]. A procedure to calculate such a value is the main purpose of this paper and will be discussed in detail in the next section.

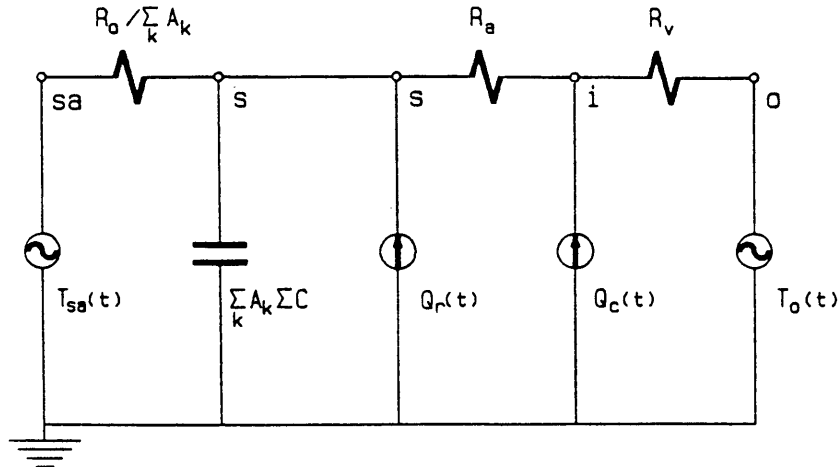


Fig. 1. Simplified thermal network for a building zone.

### 3. SIMULATING HEAT STORAGE EFFECT

#### 3.1. Preamble

It is important that the heat storage effect of the following elements should be accounted for in any simulation of building thermal performance: an unlimited amount of different multi-layered enclosing surfaces; high mass multi-layered floors which are not insulated from the indoor air and high interior mass such as multi-layered partition walls. Furthermore, it must be possible to simulate large variations in and distribution of thermal mass and resistance of the different building elements. All the above-mentioned must preferably be simulated by means of a simplified technique if an efficient tool for designers is to be developed.

A fairly well-known simplified method using a single time constant to describe the heat storage capability of a building is the total thermal time constant method for the complete building (TTTCB) as reported by Givoni [11]. The method as described by Givoni is only applicable to building zones where all the elements of the external shell are nearly identical in construction, placing a restriction on its applicability. Indoor partitions, dividing floors and other interior mass may furthermore only consist of a single material layer.

In two recent papers by Athienitis *et al.* [12, 13], limitations of current simplified tools were highlighted. The noteworthy method proposed by Athienitis *et al.* [12] for eliminating some of these shortcomings is, like all methods, still subject to limitations. Only the heat storage of external surfaces is treated and it is assumed that all the opaque surfaces are made up of an inner lining of storage mass of uniform transport properties and an outer massless insulation.

A very useful thermal design tool was developed by Delsante *et al.* [14] at the CSIRO in Australia. However, Delsante agrees that there is scope for improvement in modelling multi-layered floors which are in contact with the ground and not insulated from the indoor environment. Most simplified methods, e.g. TTTCB [11], ELAN [15], etc. [12] and even the comprehensive TTTC [16] and DEROB [17, 18] methods do not efficiently model the heat storage capability of such floors. Yet, these floors for

low mass, well insulated buildings, e.g. many factories, can significantly reduce the indoor air temperature swing [3]. In climatic regions with large diurnal temperature swings the accurate modelling of ground contact is thus very important as most low-rise buildings can effectively use the ground for heat storage purposes.

Wentzel *et al.* [9] derived equations for the heat storage contribution of a floor in ground contact and for exterior, interior and partition walls. A semi-empirical trial-and-error approach was followed to establish these equations. Through a vast amount of measurements, a correlation equation for the indoor air temperature swings for buildings of varying thermal properties was derived. The procedure was called the CR method and it was shown to be fairly accurate in predicting temperature swings. However, this procedure has certain disadvantages which are described elsewhere [5]. The equations further differ vastly for different mass contributing elements, making them difficult to comprehend. The success, however, of these simplified empirical equations prompted the authors to use the CR equations for the effective heat storage of the building in previous versions of the proposed electrical analogue [3–8]. However, a single empirical constant was always needed to ensure good comparison with measurements. In this paper a single, more cohesive equation for all mass elements, without the need for the above-mentioned empirical constant, is developed.

#### 3.2. New equation for heat storage calculations

It can be shown [14] that the thermal time constant ( $\tau_i$ ) for layer  $i$  of a multi-layered building element is given by the following:

$$\tau_i = (CR_{out})_i, \quad (3)$$

where  $C_i$  is the thermal capacity of layer  $i$  and  $(R_{out})_i$  the thermal resistance from the centre of gravity (node) of the layer up to the sol-air node as shown in Fig. 2.

The total thermal time constant for the whole building zone ( $\tau_b$ ) cannot be obtained by simply averaging the above-mentioned thermal time constants of all the layers across all the areas of its elements. The reason is that the

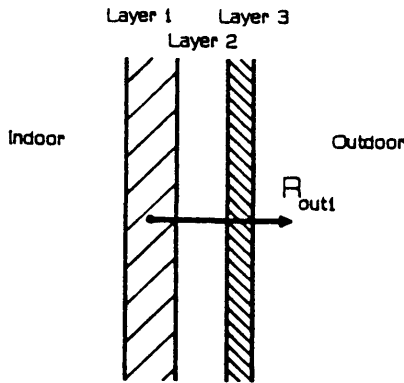


Fig. 2. Multi-layered wall exposed to the outdoor environment.

thermal resistances of the exposed elements may differ considerably, e.g. a brick wall versus a window pane. A simple averaging procedure will only be valid if all the elements of the external shell are nearly identical in construction. As the TTTCB method [11] uses this approach, its predictions may fail when simulating a building with a large variation in and distribution of thermal resistance of exterior elements. It can be shown that the following equation for the total thermal time constant ( $\tau_b$ ) of the whole building zone, consisting of  $n$  layers inside exposed and interior elements, is the correct one:

$$\tau_b = \sum_{i=1,n} (CR_{out})_i \beta_i \quad (4)$$

where  $\beta_i$  is a correction factor which differs for exterior and interior building elements. The value of  $\beta_i$  for each type of element will be discussed in detail in the rest of this section under the special headings of “exterior” and “interior” elements.

When the simplified thermal network in Fig. 1 is used, the total thermal time constant for the whole building, where no ventilation is present, is given by

$$\tau_b = \Sigma CR_o \quad (5)$$

where  $\Sigma C$  is the “effective” heat storage capability of the whole building and  $R_o$  the exterior resistance calculated from the sol-air node through the shell to the indoor surface.

From Eqns (4) and (5) the following equation for  $\Sigma C$  is found:

$$\Sigma C = \sum_{i=1,n} (CR_{out})_i \beta_i / R_o \quad (6)$$

The application of Eqn. (6) to exposed, interior and floor elements will be discussed in more detail in the rest of this section.

**Exposed elements.** It can be shown that the value of  $\beta_i$  for exterior elements, which present parallel heat flow paths between the indoor and outdoor air nodes, is given by  $\beta_i = R_o / R_k$ .  $R_k$  is the thermal resistance of exterior element  $k$ , calculated from the sol-air node up to the interior surface as shown in Fig. 2. With  $\beta_i$  known, Eqn.(6) can now be applied without any difficulty. The contribution of layer 1 in Fig. 2 is, for example, simply given by  $(CR_{out})_1 / R_k$ .

Equation (6) clearly shows an important physical aspect, namely that the mass nearest to the indoor

environment will have the most pronounced effect on it. Furthermore, it is evident from Eqn. (6) that if the thermal resistance ( $R_k$ ) of one of the exterior elements is much larger than the resistance of the rest of the exterior shell, the contribution of that element would be reduced considerably due to the small value of  $\beta_i$ . If this was not the case a very large time constant would result which is not physically correct. This problem is encountered when using the TTTCB method of Ref. [11]. On the other hand, if all the exterior surfaces are identical,  $\beta_i$  will be equal to one and all the elements will contribute fully to the total time constant of the zone. For such a case, simulations by the TTTCB method of Ref. [11] will be correct.

For the CR method [9] the node for  $R_{out}$  was chosen at the interface between the layer under investigation and the next layer between it and the indoor air. However, it is more correct to use a single node at the centre of gravity of a layer as proposed in Eqn. (6). The CR method further does not divide by  $R_k$  but rather by the resistance calculated from the sol-air node up to the interface of the investigated layer and the adjacent layer between it and the outdoor air. This may be the main reason why an empirical constant was needed when using the CR equations for exterior elements in the thermal network.

**Interior elements.** Contributions include intermediate floors in multi-storeyed buildings, interior walls and other high interior mass. At a first glance it may seem that Eqn. (6) and Fig. 3 can be used without adjustment for interior elements. However, when using this approach for the intermediate floor in the well-insulated building shown schematically in Fig. 3, it was found from measurements that the “effective” heat storage was over-estimated by a factor of 2. The reason is that in practice only half of the floor mass is available for storing heat for zone A, while the above-mentioned procedure predicts that all the mass is available for zone A. It must therefore be decided what part of an element between two zones contributes to the “effective” heat storage for the zone under consideration.

This aspect is explained with reference to Fig. 4(a) which shows a multi-layered division floor/wall with three layers between zones A and B. As a single zone approach is used in the thermal network, no heat may be transferred between the zones across the dividing floor/

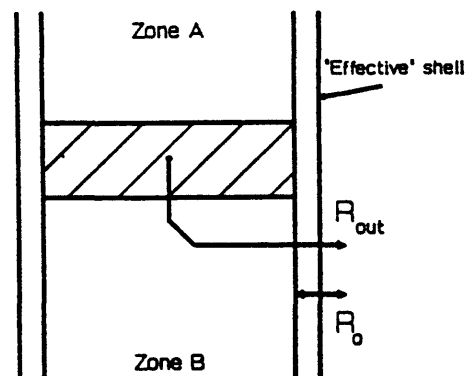


Fig. 3. Multi-layered division wall/floor between zones A and B in a well insulated building.

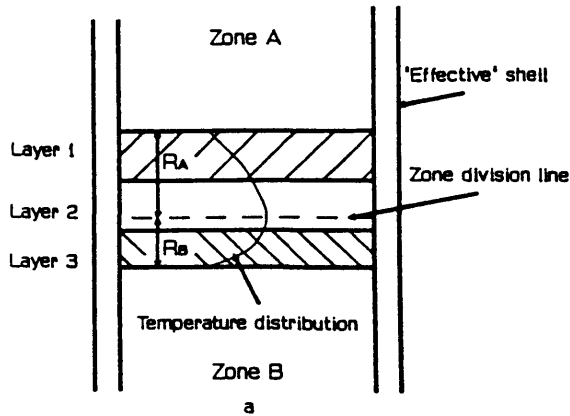


Fig. 4(a). Temperature distribution and zone division line in a multi-layered division wall/floor between zones A and B.

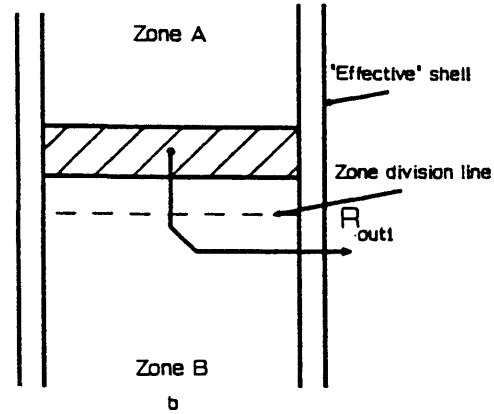


Fig. 4(b). Definition of  $R_{out}$  for division wall/floor between different zones.

wall. This means that heat stored will always be transferred from the floor/wall to both zones. The zero gradient point on the temperature distribution graph given in Fig. 4(a) will determine up to which point heat will be transferred to either zone A or B. The “effective” thermal capacity for such a floor/wall is therefore calculated up to a zone division line situated at the zero gradient point, which is assumed to be fixed for steady and transient state.

The zero gradient point and therefore the zone division line is positioned where the thermal resistance ( $R_A$ ) from the indoor surface of zone A up to the division line is equal to the resistance ( $R_B$ ) from the line up to the indoor surface of zone B as shown in Fig. 4(a). Note that only the mass above the division line contributes to the “effective” thermal capacity for zone A, as heat stored in this area will only be transferred to zone A and not to zone B. This contribution will differ from that for zone B when analysing an asymmetrical division floor/wall.

At this stage it is important to note how  $(R_{out})_i$  in Eqn. (6) is calculated for interior elements. If  $(R_{out})_i$  is taken as the thermal resistance from node  $i$  through the interior mass layers and the zone under investigation (zone A) up to the sol-air node, a layer further away from the indoor air would have a larger “effective” capacity than a layer closer to it. As this is not physically correct, the following method is proposed for the calculation of  $(R_{out})_i$  for interior elements: once the position of the zone division line is established, all mass contributions belonging to zone B should be completely ignored as shown in Fig. 4(b). The value of  $(R_{out})_i$  in Eqn. (6) is then calculated as the thermal resistance from the node under investigation through the adjacent zone B up to the sol-air node [see Fig. 4(b)]. Using the path through zone B rather than through zone A ensures that layers further away from the indoor air in zone A will have a less pronounced effect on it. As a single zone approach is used, it is assumed that the surface coefficients and exterior shell of zone B is the same as that for zone A. No extra information than the information for zone A is therefore needed to calculate  $(R_{out})_i$ .

For certain cases there may be a further complicating factor which warrants further attention. A thermal network, which describes a multi-layered interior wall more

correctly than the very simplified network given in Fig. 1, is presented in Fig. 5(a). Typical temperature swings at the nodes in the wall are also shown in Fig. 5(a), while the wall is schematically given in Fig. 5(b). From the temperature swings ( $dT/dt$ ) in Fig. 5(a) it can be seen that the swing at a node in a layer far removed from the indoor air may become small, *inter alia* due to the high thermal resistance of layers closer to the indoor air. The heat flow due to storage  $C dT/dt$  [3] in the heat transfer equation will thus be negligible ( $dT/dt$  becomes small). As this effect can not be simulated by the simplified single node network in Fig. 1 the “effective” heat capacity is used to compensate for it. A layer where  $dT/dt$  is very small will thus not contribute to the “effective” heat capacity of the building. To account for this the correct value for the correction factor  $\beta_i$  incorporating relevant resistances must be specified in Eqn. (6).

It was reasoned that the above-mentioned effect would *inter alia* depend on how readily heat can be transferred inside the material of the layer under investigation in relation to how easily it is transferred to the indoor surface. Therefore the correction factor for layer 1 in Fig. 5(b) is given by  $(R_{i1}/2)/(R_{i1}/2)$  and for layer 2 by  $(R_{i2}/2)/(R_{i2}/2 + R_{i1})$ . Equation (6) for each layer should now be multiplied by the correction factor for that layer as well as the correction factors for all the layers between the present layer and the indoor surface. This will ensure that mass layer 3 will under no circumstance contribute to the effective heat storage if mass layer 2 did not contribute due to high thermal resistance. The following general equation for the correction factor for a multi-layered interior mass is therefore proposed:

$$\beta_i = \prod_{j=1}^i (R_{ma,j}/R_{i,j}) \quad (7)$$

where  $(R_{ma})_j$  is half of the resistance of the material of layer  $j$  and  $(R_{i,j})$  is the resistance from node  $j$  up to the indoor surface of zone A [see Fig. 5(b)].

It should be noted that the magnitude of the indoor air temperature swing also “influences” the “effective” heat capacity of interior elements. The heat flow due to storage ( $C dT/dt$ ) inside the interior mass will become smaller when the temperature swing ( $C dT/dt$ ) in the interior element becomes smaller. As the indoor air temperature influences the temperature swing inside the

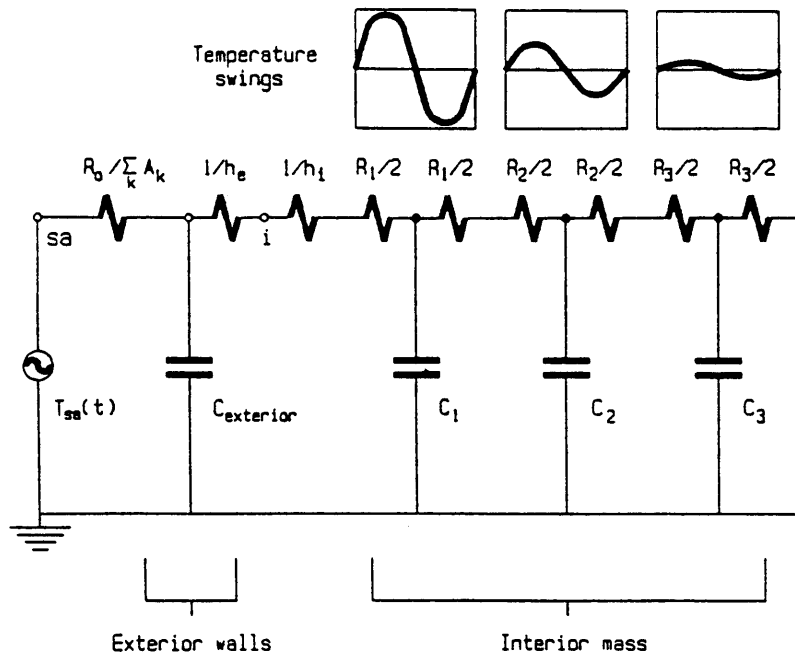


Fig. 5(a). Thermal network for multi-layered interior wall/floor showing typical temperature swings at the different interior mass nodes.

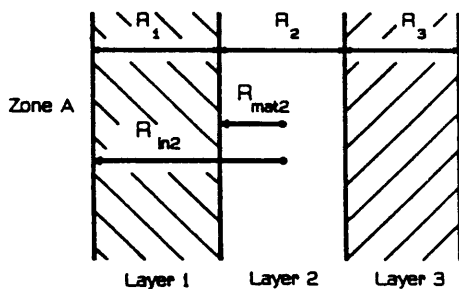


Fig. 5(b). Definition of  $R_{in}$  and  $R_{mat}$  for material layer 2 in multi-layered division wall/floor between two different zones.

element, the heat flow due to storage will become smaller when the indoor air temperature swing becomes smaller. This effect was not incorporated in the present method for passive analysis. It should definitely be considered when the system start-up period of an air-conditioned building is investigated. The interior mass for such a case will progressively become less "effective" as the indoor air temperature swing becomes smaller. More theoretical work is definitely needed regarding the correction factor for interior elements.

The contribution of high mass, such as a partition wall completely inside a zone, is also calculated by means of Eqn. (6). The only difference being that  $R_{in}$  in Eqn. (7) is calculated as the parallel resistance from the node up to the left and right indoor surfaces as shown in Fig. 6, namely  $R_{left} \parallel R_{right}$ . Also note that  $R_{out}$  in Eqn (6) is found by adding the parallel resistance ( $R_{in}$ ) to the resistance from the indoor surface of the partition up to the sol-air node.

Although the CR method [9] does not account for

multi-layered interior elements, it can estimate the storage effect of a single layer element. For such an element the thermal resistance to the outside ( $R_{out}$ ) is approximated as the effective shell resistance ( $R_s$ ) and not as the total resistance from the interior material layer through the indoor air and shell to the sol-air node on the outside of the building [9]. It was found in practice that Eqn. (6) provides a better approximation than the equation used in the CR method and no empirical constant is needed.

The TITCB method as reported by Givoni [11] may have difficulty in treating multi-layered interior elements where high mass is separated from the indoor air by means of high resistance elements such as carpets and acoustic panels. This fact becomes very notable when the exterior shell resistance is small. Equation (30) for the total thermal time constant (TITCB) of interior elements, given in Ref. [11], is used to explain the above. The relevant part of this equation is given here as Eqn. (8):

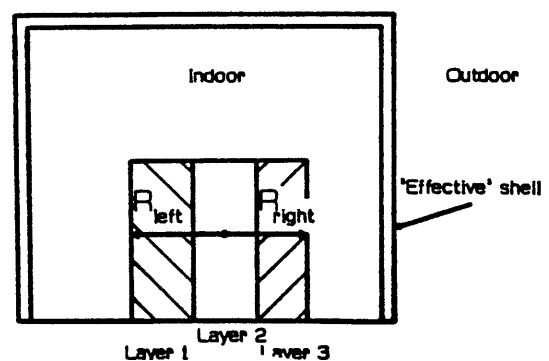


Fig. 6. High mass multi-layered partition wall with  $R_{left}$  and  $R_{right}$  defined.

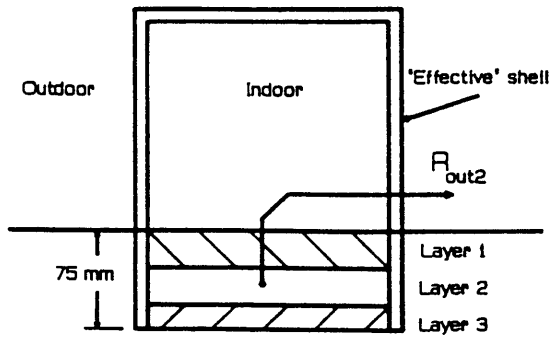


Fig. 7. Multi-layered floor in contact with the ground.

$$TTTCB = 0.5C(\Sigma_k(A_k R_k)/\Sigma_k A_k + R_e + 0.25R_{in}). \quad (8)$$

When the exterior shell resistance is small and the floor is insulated from the indoor air by carpets,  $R_{in}$  is very large and dominates the other terms in parentheses. This will result in a large predicted time constant (TTTCB). However, in practice it was found that the time constant for variations in indoor air temperature is much smaller due to the mass being insulated from the indoor air, therefore the need for the correction factor proposed in Eqn. (7). Furthermore, half of the lumped capacity is always used for TTTCB instead of only the “effective” part as given by the zone division concept.

Another aspect which should be pointed out is that the first term in parentheses in Eqn. (8) is a weighted external resistance, rather than the effective external resistance which is calculated from the relevant resistances in parallel. If, for example, a building zone is extremely well insulated on four sides but very poorly insulated on the others, Eqn. (8) will predict a large time constant (TTTCB) which is not true in practice. Equation (8) is therefore only valid for cases where the exterior elements are nearly identical in thermal resistance. If a building with a large variation in and distribution of thermal properties of the different elements is investigated, the first term should be replaced by an equation for parallel resistances similar to Eqn. (2). Note that the relevant indoor surface coefficients for the different exterior elements should also be accounted for.

**Ground floor elements.** For a building in contact with the ground, the floor and ground contribution is discussed with reference to Fig. 7 which shows a multi-layered floor. For such floors Eqn. (6) can be applied without difficulty if the depth up to which the floor elements contribute to the “effective” heat storage is known. This depth will *inter alia* depend on the resistances of the layers. Based on temperature measurements inside South African buildings, Wentzel *et al.* [9] reasoned that the ground underneath such buildings can contribute to the heat storage capacity of a structure down to a depth of 300 mm below ground level. This depth is deeper than the depth of 200 mm used by the ELAN method [15].

The CR method approximates the thermal resistance to the outside ( $R_{o,w}$ ) only as the effective shell resistance ( $R_e$ ) and not as the total resistance from the floor material layer through the indoor air and shell to the sol-air node

on the outside of the building, as used in Eqn. (6). The CR method further does not divide by  $R_o$  in Eqn. (6) but rather by the resistance calculated from the mass node up to the indoor air node. The above-mentioned aspects coupled with the fairly large empirical depth of 300 mm necessitated the use of an empirical constant in previous versions of the proposed electrical network [3–8].

The empirical constant can be eliminated by employing Eqn. (6) and only calculating the heat storage of layers up to a depth of 75 mm. This depth was arrived at by comparing measured and predicted indoor air temperatures for more than forty cases with floor areas ranging from 9 up to 7700 m<sup>2</sup>. At a certain depth, depending on the resistances of the floor material and the indoor air temperature swing, the temperature swing inside the floor will become negligible. This means that the mass below this point will not contribute to the “effective” heat capacity of the building as the heat storage term  $C dT/dt$  will become negligible. As the simplified single node network in Fig. 1 cannot simulate the fact that  $dT/dt$  becomes zero inside the floor, the calculation of the “effective” heat capacity is used to compensate for it. The “effective” heat capacity is therefore only calculated up to a certain depth, in the present case 75 mm.

High thermal resistance on the floor, such as thick carpets, will reduce the depth where the temperature swing becomes negligible. This effect is accounted for by the correction factor in Eqn. (7). However, the problem of deeper layers contributing more to the effective heat capacity than more shallow layers, as discussed for interior elements, has not yet been fully addressed.

### 3.3. Closure

A single equation for the total “effective” heat capacity ( $\Sigma C$ ) for a single building zone consisting of  $n$  exterior and interior mass layers is given by the following:

$$\Sigma C = \Sigma_{i=1,n}(CR_{out})_i/R_o \cdot \beta_i, \quad (9)$$

where  $\beta_i = R_o/R_k$  for exterior elements and  $\beta_i = \Pi_{j=1,i}(R_{out}/R_{in})_j$  for interior elements. The value of  $C_i$  for interior division floors or walls is found by means of the zone division concept and  $C_i$  for floors in ground contact is found by calculating up to a depth of 75 mm.

Although the equation for the calculation of the “effective” heat storage capability for a building zone was not completely derived from first principles, it will be shown in the next section that it is successful in analysing typical building constructions. This means that the effect of relative position and thermal properties of mass and insulation as well as the fact that a temperature differential exists across the building elements [6] are effectively accounted for. The proposed procedure must not be viewed incorrectly [10] as the traditional lumped-capacity method with its assumptions that the entire mass of a material is equally and completely effective in storing heat and that all this mass is at a constant temperature throughout. The proposed procedure can be viewed as similar to a lumped distributed parameter model which does not suffer from the limitation of the lumped-capacity method, namely that the ratio of mass thermal resistance to external resistance should be small. Note that the limitation is on the above-mentioned ratio and not on

the ratio of thermal inertia to external thermal resistance as often thought [10].

It was found that only one node per layer was needed for conventional building construction when using Eqn. (9). The thickest exterior layer for the cases investigated in the validation study was a 114 mm brick layer in a 360 mm thick wall element, consisting of two layers of bricks, a cavity and plaster on both sides. When using the traditional lumped capacity procedure [19], as most finite difference methods do, at least 10 nodes would be needed in each brick layer.

Necessary future work includes detailed derivation of more theoretically based equations which will more fully define the assumptions and limitations of the procedure.

#### 4. VALIDATION

Ultimately the usefulness of a simulation model as a design tool can only be ascertained by comparing its predictions with experimental results from actual buildings. Predictions for the indoor air temperatures were compared to measurements in order to establish the level of confidence in heat storage calculations and in complete simulations with the simplified network.

It was found that temperature predictions for 62 cases representing a wide range of buildings were within 2°C of measurements for 80% of the time. It is important to note that the accuracy of the Thies Clima thermographs used for temperature measurements is  $\pm 1.5^\circ\text{C}$ . Also note that the authors took great care to include all important types of buildings in the validation process [3]. Buildings included office blocks, shops, schools, residential buildings, townhouses, medium and high mass experimental buildings, low mass well insulated structures with ground contact such as factories, and low mass poorly insulated structures, e.g. agricultural buildings.

The applicability of the procedure for estimating the "effective" heat capacity can be determined by a comparison of predicted and measured indoor air temperature swings, defined as the difference between the maximum and minimum values. Figure 8 presents the measured and predicted swings for all the cases. From

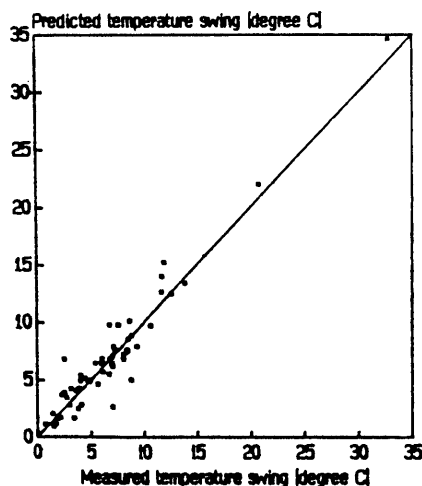


Fig. 8. Comparison between measured and predicted indoor air temperature swings for 62 cases.

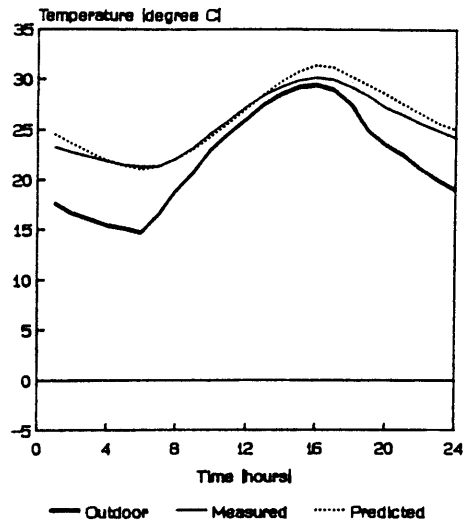


Fig. 9. Outdoor air temperature and measured and predicted indoor air temperatures for low mass, well-insulated factory with uninsulated floor in ground contact.

the large variations in swings, 0.7 to 20.8°C in Fig. 8, it can be deduced that buildings were used which varied significantly in "effective" heat storage capability. For design purposes the correlation between measured and predicted swings should be acceptable. One of the important reasons for the difference between measurements and predictions can be related to the natural ventilation flow rates for buildings with open windows, which were not measured.

Extensive validation of hourly temperature predictions by the complete simulation procedure is given in another paper [3]. In the present paper it is only given for the following cases: a low mass, well-insulated factory with uninsulated floor in ground contact (Fig. 9); a low mass, poorly insulated agricultural building with uninsulated floor in ground contact (Fig. 10); a school of intermediate mass with various interior mass elements (Fig.

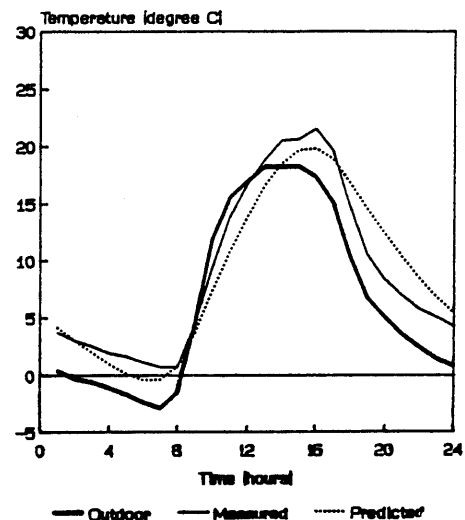


Fig. 10. Outdoor air temperature and measured and predicted indoor air temperatures for low mass, poorly insulated agricultural building with uninsulated floor in ground contact.

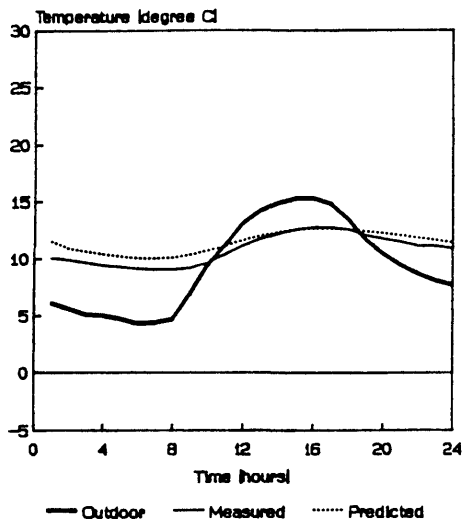


Fig. 11. Outdoor air temperature and measured and predicted indoor air temperatures for school of intermediate mass with various interior mass elements.

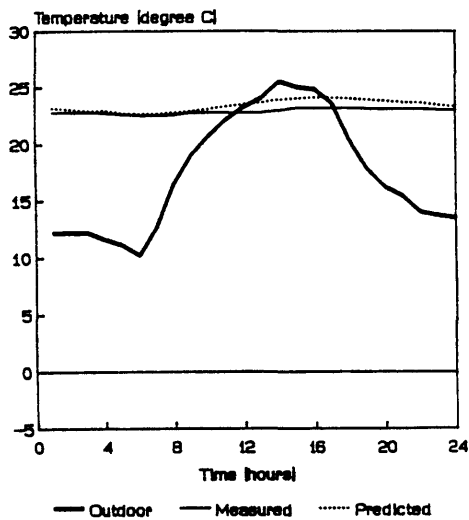


Fig. 12. Outdoor air temperature and measured and predicted indoor air temperatures for high mass office of which five enclosing surfaces are shared with adjacent zones.

11); and a high mass office of which five enclosing surfaces are shared with adjacent zones (Fig. 12). More details of the buildings are given in Table 1. From Figs 9-12 it can be seen that the comparison between predicted

and measured indoor air temperatures is acceptable for design purposes, especially when considering that the IBM(XT) microcomputer running times for the simulations are less than 10 s.

The efficiency of the simulations, which included varying ventilation, internal loads, complex shading devices, direct solar gain and the calculation of sensible energy loads, can *inter alia* be attributed to the following features: the novel treatment of the heat storage of a building, a special treatment of the term describing varying ventilation rates and solving the relevant equations under the assumption that all variables are periodic. For example, if the simulation is performed for a design day, week, month or year, it is assumed that all the previous and following days, weeks, months or years are identical. A closed form solution for the initial value can be found from this periodic assumption. It is therefore not necessary to provide initial conditions or to repeat the simulation for several periods under consideration to eliminate the effect thereof. This fact contributes considerably to the efficiency of calculations.

As the computer program was developed for building designers, who may be computer illiterate, the program was made very user-friendly and data input is very straightforward. For example, the input for each of the above-mentioned buildings used in the validation took in the order of 15 min. The effect of changes to a design can be investigated in less than 30 s.

## 5 SUMMARY AND CONCLUSIONS

A simplified procedure was developed to lump the "effective" heat storage capability of a building zone. The procedure is not based on a rigorous theoretical derivation, but on sound reasoning about the physical problem and on empirical data. Features of the procedure include the ability to efficiently simulate ground contact and multi-layered exterior and interior elements.

The single value for the "effective" heat storage was employed in a simplified thermal network to complete an efficient simulation model of a building zone. Despite its simplicity, the procedure predicted indoor air temperatures within 2°C for 80% of the time for 62 buildings which included office blocks, shops, schools, residential buildings, low mass well-insulated structures in ground contact and low and high mass poorly insulated structures.

Although the thermal model is very simple, the law of

Table 1. Summary of information applicable to building zones used for validation purposes

Type	Factory	Agricultural building	School	Office
Location	Pretoria	Volkstrust	Pretoria	Pretoria
Ground contact	Yes	Yes	No	No
Floor area (m <sup>2</sup> )	7700	750	58	14
Exposed surfaces	4	5	3	1
Exterior colour	Medium/dark	Weathered steel	Medium	Light
ΣC (kJ °C <sup>-1</sup> m <sup>-2</sup> )	204	411	654	3518
R <sub>e</sub> (°C m <sup>2</sup> W <sup>-1</sup> )	0.327	0.050	0.196	0.117
Occupied	Yes	No	No	No

conservation of problems is also applicable here. In order to reduce the complex thermal problem to a simple one, new concepts had to be devised, for example the correction factor ( $\beta$ ), the calculation of  $R_{out}$  for interior elements and the empirical depth of 75 mm for floors in ground contact. All these concepts are, however, based on physical interpretation and were shown to give acceptable results for all the cases that were investigated. It is the authors' view that in general building thermal models should only attempt to provide an economical description of empirical facts. A multitude of detail can easily clutter up the mind, diverting it from the essential.

Future work includes a detailed derivation of a more

theoretically based model which will more fully define the assumptions and limitations of the complete model.

**Acknowledgements**—The authors acknowledge the financial assistance given for the development of the model and the micro-computer program by the following institutions: University of Pretoria, Laboratory for Advanced Engineering, Department of Public Works and Land Affairs, Department of Finance as well as National Energy Council. The program is available from the Centre for Experimental and Numerical Thermoflow at the Department of Mechanical Engineering.

P. H. Joubert did the initial numerical implementation and some of the measurements, while A. C. Leuvenink did most of the programming. The following people also contributed to the project: Prof. D. Holm and L. J. Grobler.

### REFERENCES

1. M. R. Donn, Design tools: panel discussion summaries. Proc. 3rd Int. Congress on Building Energy Management, Vol. 5, pp. 11–15. Lausanne (1987).
2. B. D. Spalding, Chemical reactions in turbulent fluids. *Physico-Chem. Hydrodynamics* 4, 323–336 (1983).
3. E. H. Mathews and P. G. Richards, A tool for predicting hourly air temperatures and sensible energy loads in buildings at sketch design stage. *Energy Build.* 14, 61–80 (1990).
4. P. H. Joubert and E. H. Mathews, Quicktemp—a thermal analysis program for designers of naturally ventilated buildings. *Bldg Envir.* 24, 155–162 (1989).
5. E. H. Mathews, Thermal analysis of naturally ventilated buildings. *Bldg Envir.* 21, 35–39 (1986).
6. E. H. Mathews, The prediction of natural ventilation in buildings. D.Eng. dissertation, University of Potchefstroom, R.S.A. (1985).
7. E. H. Mathews, P. H. Joubert and P. G. Richards, A thermal model of naturally ventilated buildings. Proc. Int. Congress on Progress in Architecture, Construction and Engineering, CSIR, Pretoria, R.S.A., 12p (1987).
8. E. H. Mathews, P. H. Joubert and P. G. Richards, An accessible method to predict the thermal performance of buildings at the design stage. Proc. 13th Nat. Passive Solar Conf., Cambridge, Massachusetts, pp. 21–25 (1988).
9. J. D. Wentzel *et al.*, The prediction of the thermal performance of buildings by the CR method. NBRI Research Report BRR 396, CSIR, Pretoria (1981).
10. S. A. Barakat, Building energy analysis—a look into the future. Proc. 3rd Int. Congress on Building Energy Management, Vol. 1, pp. 90–101. Lausanne (1987).
11. B. Givoni, *Man, Climate and Architecture*, 2nd edn, pp. 414–450. Applied Science, London (1976).
12. A. K. Athienitis, H. F. Sullivan and K. G. T. Hollands, Analytical model, sensitivity analysis and algorithm for temperature swings in direct gain rooms. *Solar Energy* 36, 303–312 (1986).
13. A. K. Athienitis, H. F. Sullivan and K. G. T. Hollands, Discrete Fourier series models for building auxiliary energy loads based on network formulation techniques. *Solar Energy* 39, 203–210 (1987).
14. P. J. Walsh and A. E. Delsante, Calculation of the thermal behaviour of multi-zone buildings. *Energy Build.* 5, 231–242 (1983).
15. M. H. de Wit and H. H. Driessen, ELAN—a computer model for building energy design. *Bldg Envir.* 23, 285–289 (1988).
16. M. E. Hoffman and M. Feldman, Calculation of the thermal response of buildings by the total thermal time constant method. *Bldg Envir.* 16, 71–85 (1981).
17. E. H. Mathews, Empiricism in the thermal analysis of naturally ventilated buildings. *Bldg Envir.* 23, 57–61 (1988).
18. D. Holm, M. J. Vermeulen and J. T. Kemp, Ondersoek na die passiewe ontwerp van lae hoogte kantoorgeboue (Investigation into the passive design of low rise office buildings). Final Report, National Program for Energy Research, CSIR, Pretoria (1986).
19. J. P. Holman, *Heat Transfer*, 6th edn., pp. 133–135. McGraw-Hill, Singapore (1986).
20. J. F. van Straaten, A. J. A. Roux and S. J. Richards, Comparison of the thermal and ventilation conditions in similar houses employing different ventilation schemes. *NBRI Bulletin* No. 13, pp. 5–43. CSIR, Pretoria (1955).
21. J. F. van Straaten, Methods for improving the permanent ventilation in ceiled urban houses of the type NE 51/9. *NBRI Bulletin* No. 15, pp. 65–77, CSIR, Pretoria (1957).
2. T. le Roux *et al.*, Ventilation and thermal considerations in school building design. NBRI Research Report No. 215, CSIR, Pretoria (1965).